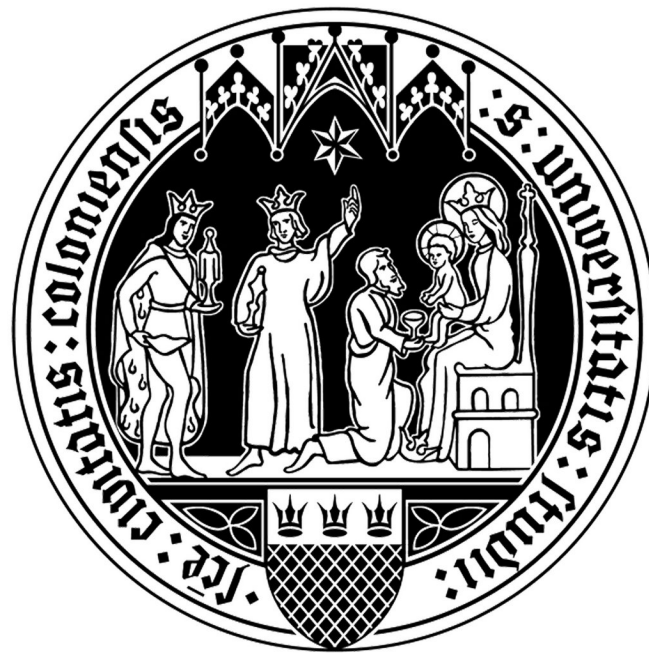

Regulation of mTOR signaling by nutrients and post-translational modifications

Inaugural-Dissertation
zur
Erlangung des Doktorgrades
der Mathematisch-Naturwissenschaftlichen Fakultät
der Universität zu Köln



vorgelegt von
Stephanie de Alcantara Fernandes
aus Barbacena, Brasilien

Köln, 2023

This is a dissertation accepted by the Faculty of Mathematics
and Natural Sciences of the University of Cologne

Berichterstatter: Dr. Constantinos Demetriades
Prof. Dr. Marius Lemberg

Prüfungsvorsitzender: Prof. Dr. Ana García-Sáez

Tag der Disputation: 26.05.2023

*"A discoverer has to be in the right place with the right frame of mind to learn from
the right mistakes."*

Colin Salter, 100 science discoveries that changed the world

Table of contents

Zusammenfassung	6
Abstract	7
Acknowledgements	8
List of figures	11
List of tables	14
Abbreviations	15
1 Introduction	22
1.1 The mTOR complex 1	22
1.1.1 mTORC1 functions	22
1.1.1.1 Protein synthesis	23
1.1.1.2 Autophagy	25
1.1.1.3 Lysosomes	27
1.1.2 mTORC1 regulation	30
1.1.2.1 By growth factors	30
1.1.2.2 By energy	32
1.1.2.3 By amino acids	32
1.1.2.3.1 Lysosomes and the Rag GTPases	32
1.1.2.3.2 Amino acid sensors	34
1.1.2.3.3 Rag-independent mechanisms	36
1.1.2.4 By localization	37
1.1.2.5 By post-translational modifications	38
1.1.2.5.1 Ubiquitination	38
1.1.2.5.2 Regulation of the mTORC1 pathway by ubiquitination	41
1.2 The mTOR complex 2	43
1.2.1 mTORC2 functions	44
1.2.2 mTORC2 regulation	45
1.2.2.1 By growth factors	45
1.2.2.2 By post-translational modifications	45
1.3 Aims of the thesis	47

2 Results	48
Part I: Spatially and Functionally Distinct mTORC1 Entities Orchestrate the Cellular Response to Amino Acid Availability	48
2.1 Cells have basal lysosomal degradative capacity	48
2.2 Lysosomal degradative capacity is tightly linked to mTOR localization and mTORC1 activity towards specific substrates	48
2.3 The Rag GTPases and the lysosomal mTORC1 machinery are required for mTORC1 activity towards lysosomal substrates	59
2.4 Protein synthesis and lysosomal biogenesis programs are controlled by different mTORC1 pools	73
Part II: CYLD is a novel deubiquitinase for mTOR	76
2.5 CYLD interacts with mTOR	76
2.6 CYLD is a DUB for mTOR	76
2.7 CYLD does not affect mTORC1 or mTORC2 complex formation and protein levels of their pathway components	83
2.8 CYLD regulates mTOR activity	83
2.9 CYLD affects protein synthesis downstream of mTORC1	88
3 Discussion	90
3.1 Spatially and Functionally Distinct mTORC1 Entities Orchestrate the Cellular Response to Amino Acid Availability	90
3.2 CYLD is a novel deubiquitinase for mTOR	95
4 Future perspectives	98
5 Materials and methods	101
References	121
Appendix	149
Contributions	149
Erklärung	150

Zusammenfassung

Die mTOR-Signalwege stehen im Zentrum der zellulären Physiologie. Daher ist ihre Dysregulation ein gemeinsames Merkmal vieler Erkrankungen wie Krebs, Neurodegeneration und Alterung. Der mTORC1 (mTOR-Komplex 1) reguliert das Zellwachstum, indem er die Proteinsynthese, die Autophagie und die lysosomale Biogenese steuert. Andererseits ist der mTORC2 (mTOR-Komplex 2) an der Regulierung des Zellüberlebens und der Zellproliferation beteiligt. Der mTOR-Signalweg reagiert auf vorgelagerte Signale, die seine Funktion über die Aktivität wichtiger GTPasen, die seine Lokalisierung regulieren, und über Veränderungen der posttranslationalen Modifikationen (PTM) mehrerer Signalkomponenten steuern.

Insbesondere AAs (Aminosäuren) regulieren mTORC1 über Veränderungen seiner subzellulären Lokalisierung und fördern die Rekrutierung von mTORC1 an die Lysosomen. In den letzten 15 Jahren wurde ein Mechanismus zur Aktivierung von mTORC1 an der lysosomalen Oberfläche beschrieben. Die Gründe für die lysosomale Lokalisierung von mTORC1 und die Frage, ob mTORC1 an verschiedenen subzellulären Orten aktiv ist, ist jedoch noch offen. Mithilfe mehrerer unabhängigen Ansätzen, die lysosomale Funktion zu stören, zeige ich hier, dass die Lokalisierung von mTORC1 an Lysosomen eng mit der lysosomalen Aktivität verbunden ist. Diese Beobachtung deutet darauf hin, dass mTORC1 wahrscheinlich aufgrund des basalen Proteinabbaus im lysosomalen Lumen und der anschließenden Nährstofffreisetzung an Lysosomen zu finden ist. Unerwarteterweise führte die Delokalisierung von mTORC1 weg von den Lysosomen bei AA-Mangel zu einem vollständigen Verlust der TFEB-Phosphorylierung, mit sehr geringen Auswirkungen auf die kanonischen Substrate S6K1 und 4E-BP1. Diese Ergebnisse wurden auch in Zellen bestätigt, denen Rag-GTPasen, Kernkomponenten der lysosomalen mTORC1-Maschinerie, fehlten.

Zu den PTMs gehören in erster Linie Phosphorylierungs- und Ubiquitinierungsvorgänge. Während der erste Vorgang bei der Kontrolle von mTOR-Komplexen bereits gut beschrieben ist, ist der zweite weniger gut verstanden. In den letzten Jahren wurde jedoch festgestellt, dass die Ubiquitinierung mehrerer Komponenten der mTORC1- und mTORC2-Signalwege ebenfalls ein wichtiger Bestandteil ihrer Regulierung ist. mTOR, die katalytische Komponente sowohl von mTORC1 als auch von mTORC2, ist selbst stark ubiquitiniert. Daher ist die Identifizierung von Proteinen, die die Ubiquitinierung von mTOR modulieren können, für das Verständnis der mTOR-Regulierung von großer Bedeutung. In dieser Arbeit habe ich die DUB (Deubiquitinase) CYLD als einen Interaktionspartner von mTOR identifiziert. Bemerkenswerterweise ist CYLD in der Lage, die Ubiquitinierung und Aktivität von mTOR zu modulieren. Insgesamt wurden in meiner Dissertation zwei neue Wege der mTOR-Regulierung aufgezeigt: die räumliche Trennung der mTORC1-Funktionen und eine neue DUB für mTOR.

Abstract

The mTOR (mechanistic target of Rapamycin) signaling pathways are at the center of cellular physiology. As such, their dysregulation is a common characteristic of many conditions, such as cancer, neurodegeneration and aging. mTORC1 (mTOR complex 1) regulates cellular growth by controlling protein synthesis, autophagy and lysosomal biogenesis. On the other hand, mTORC2 (mTOR complex 2) is involved in the regulation of cell survival and proliferation. mTOR signaling responds to upstream cues that control its function via the activity of key GTPases that regulate its localization, and via alterations in PTMs (post-translational modifications) on several signaling components.

In particular, AAs (amino acids) regulate mTORC1 via changes in its subcellular localization, promoting mTORC1 recruitment to lysosomes. Importantly, work over the past 15 years has described a machinery for mTORC1 activation on the lysosomal surface. However, the reasoning for the lysosomal localization of mTORC1 and whether mTORC1 is active in different subcellular locations is an open question. Here, using multiple independent approaches to disrupt lysosomal function, I show that mTORC1 localization to lysosomes is tightly linked to lysosomal activity. This observation indicates that mTORC1 is found at lysosomes likely due to basal protein degradation in the lysosomal lumen and subsequent nutrient release. Unexpectedly, under AA sufficiency, delocalization of mTORC1 from lysosomes led to a complete loss of TFEB phosphorylation, with very mild effects on the canonical substrates S6K1 and 4E-BP1. These findings were also confirmed in cells lacking Rag GTPases, core components in the lysosomal mTORC1 machinery.

PTMs primarily include phosphorylation and ubiquitination events. Although the former is well-described in the control of mTOR complexes, the latter is less well-understood. Nonetheless, work over the recent years established that ubiquitination of several components of the mTORC1 and mTORC2 pathways is also an important part of their regulation. mTOR, the catalytic component of both mTORC1 and mTORC2, is itself heavily ubiquitinated. Hence, the identification of proteins able to modulate mTOR ubiquitination is of great importance to understand mTOR regulation. In this thesis, I identified the DUB (deubiquitinase) CYLD as an interacting partner of mTOR. Strikingly, CYLD is able to modulate mTOR ubiquitination and activity. Overall, my thesis work identified two novel ways of mTOR regulation: the spatial separation of mTORC1 functions and a novel DUB for mTOR.

Acknowledgements

First, I would like to thank my supervisor, Dr. Constantinos Demetriades. I want to thank you for believing in me since the start and throughout the five and a half years of my PhD. You believed in me even when I did not, and for this I will be eternally grateful. I would also like to thank you for supporting me on my choices and for giving me all the skills that I need to succeed in my career. You also taught me how to be a better scientist, a better thinker and also a much better writer, and I am very thankful for that!

I want to thank Prof. Dr. Thomas Langer and Dr. Martin Denzel for being part of my thesis advisory committee, and for giving me valuable feedback during the development of my PhD projects.

Special thanks to Prof. Dr. Marius Lemberg that kindly agreed to be an examiner for this thesis and to Prof. Dr. Ana Garcia-Saéz for being the chair of my disputation. I am also grateful to Dr. Mario Pende that kindly agreed to review my PhD thesis.

I would also like to thank all the MPI core facilities, especially the FACS & Imaging and the Proteomics. Thank you for the support with the work that was done in this thesis.

A huge thanks to the whole CD Lab! Danae, Jiyoung, Nina, Filippo, Andreas, Aish, Peter, Franzi, Laura, Julian, Yoav, Marija and Sabine. In many ways, you all helped me to get here and to finish my PhD. Many of you also helped me a lot personally, through very difficult times in which I did not think I could make it, and for that I am extremely grateful! I also thank you for all the scientific discussions that we had, it was always good to exchange ideas and advance our projects. I am also thankful for all the fun, from the Institute parties to laughing out loud in the lab, that made life much easier.

To the girls' club, Danae, Jiyoung, Nina, Aish and Franzi, thank you very much for everything! Thanks for having my back when I needed, and for being such good company for coffee, for parties, for beers, for trips, and for everything in life!

A big thanks to Danae, your calm and your personality were always comforting. I am above all thankful for your friendship, you helped me a lot through these years and you make life in Germany easier for me. Of course, I am also very grateful for having the opportunity to work with you in very close contact. I am sure that our ability to work together and to listen to each other was what made this project possible!

A gigantic thanks to Jiyoung, you are one of the kindest human beings I know, and to have you as a friend is a true gift for me. Thank you for everything, for your endless support, for infinite coffees and workouts, and for our skill of talking non-stop for 12 hours. I am also very

thankful for your help with the CYLD project, it made a huge difference and we progressed much faster while working together!

Nina, thanks also for helping with the German translations and phone calls, life in this country would not have been possible without your help!

I would also like to thank Andreas, for being very patient while teaching me how to clone. Thank you, Julian, you taught me so many techniques and skills, and I am sure I'm a much better scientist now. Thanks to Laura and Filippo, you also made me a better scientist, but more than this, you both supported me a lot personally over the years and I will take that for life.

Bruna, you made life in Cologne much easier! Thanks for being here, for being my friend and for supporting me unconditionally through all those years. Having you as a friend is one of the best things that happened in my life. Thanks for your understanding and for not giving up on me, this thesis only exists because I had you here!

A big thank you also to my friends from other labs: Rahel, meeting you in my first day in the Institute was the best thing that could have happened! You and Joel helped us so much, in so many ways, and I am very grateful for that. Thanks also to Tania, for having a great shared musical taste and for supporting me in my running endeavors. Thank you also Italian Bruna, you are a very kind person that I am very happy to have as a friend. I am also very thankful to Kavan and Patrick, it was great to be part of the writing club with you, you are both great people. Thank you also to the writing club as a whole, it was a great opportunity to be part of that!

Thanks to the CGA class 2017, it was great to start the PhD journey with you all! Daniel and Paulo, you are my brothers, and I will never forget our time together. Although the PhD time was not the easiest, we had many great moments, and life in Cologne was so much more fun with you. Thank you, Sophie, for the great company over the years and for all the great Wednesday Dinners that helped us keep our sanity for some time. Thanks to Mihaela, you are a very kind person and talking to you was essential to keep me going. Thanks also to Carolina, you were the first person I met at the selection week, and I am very grateful for this long-lasting friendship!

A very big thanks also to the CGA coordinators, in special Dr. Daniela Morick, Julia Zielinski and Jenny Ostermann, you made the PhD journey much easier!

Finally, a very big thanks to the most essential people in my life:

Thank you, mom, you were always my example of dedication and success, and I would have never come this far if it was not for you. Thank you for supporting me throughout my life, for

giving me the freedom to study what I wanted and to follow my own path. You are the best mom in the world!

Dad, although I never had the chance to say this, I want to thank you for showing me how nature is beautiful and amazing and for sparking my love for biology. Also, many thanks for showing me that being a kind and caring person is an essential trait, and this I will take for life.

Many thanks also to my brother, Leon. You inspire me to be a better person! Your personality, your friendship, your companionship, your intelligence, all of those things make me very happy and I am sure I would never have come this far alone. Thanks for existing!

Thanks also to Olivia, I am very grateful for everything you taught me. All the conversations and skills that I learned were essential for me to get here and finish my PhD!

Thank you, Daleska! You were always a sister to me and you will always be. Thanks for supporting me and for being my home away from home. Thanks also to my whole family, tia Miquita, tia Maria Celia, tio Canario, tio Vicente, Lili, Lulu, Kikinha, Pablinho, and also the kids from the new generation. I could only move to Germany and do my PhD because I always had your unconditional support!

Many thanks also to my Brazilian friends: Marina, Joana, Carol, Fernanda, Ricardo, Rodrigo, Nathalia, Skeeter, Anali, Cris, Leticia, Camila e Lucas! Sorry for being so distant since I moved to Germany, but you can be sure that having you in my life made things much easier!

Thanks also to Prof. Dr. Mariz Vainzof, I will never forget everything I learned and how much I grew while I was in your lab. If I managed to finish my PhD here is because I had a good start there.

And finally, to the most important person in my life. Gabriel, without you I would have never made it. Thanks for being my support, for being my partner, for listening to me and for drying my tears and putting up with my crises. Thanks for taking care of the house while I worked through the night, and thanks for understanding my choices, even when they did not make sense. Thanks for moving to Germany with me so I could do my PhD, and thanks for holding on for so long, even when it was not easy for you. Thank you for everything, you are a huge part of my success!

List of figures

Figure 1.1 Schematic representation of autophagosome formation and cargo degradation in lysosomes.	26
Figure 1.2 The mannose-6-phosphate pathway.	28
Figure 1.3 Modes of TSC lysosomal recruitment.	31
Figure 1.4 The mTORC1 regulatory network at the lysosomal surface.	36
Figure 1.5 The NF- κ B pathway activated by TNF α and regulated by CYLD.	40
Figure 1.6 mTOR is a heavily ubiquitinated protein.	41
Figure 2.1 Human cells have basal protein degradation inside lysosomes.	49
Figure 2.2 Mouse cells have basal protein degradation inside lysosomes.	49
Figure 2.3 Blockage of lysosomal function leads to mTORC1 delocalization from lysosomes and substrate-specific changes on its activity.	51
Figure 2.4 Blockage of lysosomal function with ConA leads to mTORC1 delocalization from lysosomes and substrate-specific changes on its activity.	52
Figure 2.5 Blockage of lysosomal function with Chloroquine leads to mTORC1 delocalization from lysosomes and substrate-specific changes on its activity.	53
Figure 2.6 Short-term blockage of lysosomal function leads to mTORC1 delocalization from lysosomes and substrate-specific changes on its activity.	55
Figure 2.7 Blockage of lysosomal function affects mTORC1 activity towards the lysosomal substrate RagC but not of cytosolic substrates.	56
Figure 2.8 Blockage of lysosomal function does not affect levels of mTORC1 upstream regulators.	57
Figure 2.9 Blockage of lysosomal protease activity leads to mTORC1 delocalization from lysosomes and substrate-specific changes on its activity.	58
Figure 2.10 Blockage of lysosomal enzyme trafficking leads to mTORC1 delocalization from lysosomes and substrate-specific changes on its activity.	60
Figure 2.11 Cells lacking the RagA/B GTPases have mTORC1 delocalized from lysosomes and substrate-specific changes on its activity.	62
Figure 2.12 Cells lacking the RagC/D GTPases have mTORC1 delocalized from lysosomes and substrate-specific changes on its activity.	63

Figure 2.13 Mouse cells lacking the RagA/B GTPases have mTORC1 delocalized from lysosomes and substrate-specific changes on its activity.	64
Figure 2.14 Absence of the RagA/B GTPases does not affect cytosolic mTORC1 substrates.	65
Figure 2.15 Phosphorylation of the mTORC1 substrate S6K in HEK293FT cells lacking the Rag GTPases is mTORC1 dependent.	65
Figure 2.16 Phosphorylation of the mTORC2 substrate AKT is unaffected in HEK293FT cells lacking the Rag GTPases.	66
Figure 2.17 LAMTOR1 knockdown phenocopies the loss of Rag GTPases.	66
Figure 2.18 Different mTORC1 components and substrates are localized in distinct cellular compartments.	67
Figure 2.19 MIOS knockdown phenocopies the loss of Rag GTPases.	69
Figure 2.20 Non-lysosomal mTORC1 shows different sensitivity to Serine, Threonine and Cysteine starvation.	70
Figure 2.21 Non-lysosomal mTORC1 does not respond to glucose availability, but has normal response to AAs or AKT inhibition.	71
Figure 2.22 Non-lysosomal mTORC1 is regulated independently of the Golgi machinery.	72
Figure 2.23 Protein synthesis is unaffected in cells lacking RagA/B GTPases.	74
Figure 2.24 Cells lacking RagA/B GTPases show increased nuclear localization of TFEB/TFE3 and activation of their downstream processes.	75
Figure 2.25 The deubiquitinase CYLD interacts with mTOR.	76
Figure 2.26 CYLD deubiquitinates mTOR.	78
Figure 2.27 Catalytically inactive CYLD expression increases mTOR ubiquitination.	79
Figure 2.28 CYLD controls mTOR ubiquitination in mouse cells.	80
Figure 2.29 CYLD deubiquitinates mTOR in vitro.	80
Figure 2.30 CYLD removes K63-linked chains from mTOR.	81
Figure 2.31 CYLD effect on mTOR is independent of its canonical effect on the NF- κ B pathway.	82
Figure 2.32 CYLD does not affect mTORC1 or mTORC2 complex stability.	84
Figure 2.33 CYLD affects mTORC1 and mTORC2 activities.	85
Figure 2.34 CYLD effects on mTORC1 and mTORC2 activities are not specific for	

a stimulus.	87
Figure 2.35 CYLD acts in coordination with known mTORC1 pathway components.	88
Figure 2.36 CYLD affects protein synthesis downstream of mTORC1.	89
Figure 3.1 Model for the spatial separation of mTORC1 functions.	91

List of tables

Table 1 The recipe for Gibco high-glucose DMEM.	101
Table 2 Inorganic components and amino acids used for preparation of custom-made media.	103
Table 3 Antibodies used in this thesis.	104
Table 4 Sequences of PCR oligos used for cloning, restriction sites are underlined and mutations are in bold.	108
Table 5 Sequences of primers used for RT-qPCR (reverse transcription quantitative real-time PCR).	110
Table 6 Sequences of oligos used for sgRNA expression from the pX459 for CRISPR/Cas9 KO cell line generation.	112
Table 7 siRNA sequences for knockdown experiments.	113
Table 8 Experimental work contributions.	149

Abbreviations

mTOR	mechanistic target of Rapamycin
PIKK	PI3K-related protein kinase
et al.	et alia (and others)
mTORC1	mTOR complex 1
mTORC2	mTOR complex 2
RAPTOR	regulatory-associated protein of mTOR
TOS	TOR signaling motifs
mLST8	mammalian lethal with SEC13 protein 8
PRAS40	proline-rich AKT substrate 40 kDa
DEPTOR	DEP-domain-containing mTOR-interacting protein
HEAT	Huntingtin, EF3, PP2A, TOR1
EF3	elongation factor 3
PP2A	protein phosphatase 2A
TOR1	target of Rapamycin kinase 1
FAT	FRAP, ATM, TRRAP
FRAP	mechanistic target of Rapamycin
ATM	serine-protein kinase ATM
TRRAP	transformation/transcription domain-associated protein
FRB	FKBP-Rapamycin-binding
FKBP12	FK506-binding protein 12
AA	amino acid
eIF4F	eukaryotic initiation factor 4F
eIF1	eukaryotic initiation factor 1
eIF1A	eukaryotic initiation factor 1A
eIF3	eukaryotic initiation factor 3
eIF5	eukaryotic initiation factor 5
mRNAs	messenger RNAs
eIF4G	eukaryotic initiation factor 4G
eIF4E	eukaryotic initiation factor 4E
eIF4A	eukaryotic initiation factor 4A
eIF4B	eukaryotic initiation factor 4B
4E-BP1	4E-binding protein 1
S6K1	p70 S6 Kinase 1
TOP	terminal oligopyrimidine tract
LARP1	La-related protein 1
PDK1	phosphoinositide-dependent protein kinase 1
S6	ribosomal protein S6
RSK	p90 ribosomal S6 kinase
MAPK	mitogen-activate protein kinase
PDCD4	programmed cell death protein 4

UBF	upstream binding factor
TIF-1A	transcription initiation factor 1A
MAF1	repressor of RNA polymerase III transcription MAF1 homolog
SKAR	polymerase delta-interacting protein 3
WTAP	Wilms' tumor 1-associating protein
SAM	S-adenosylmethionine
c-MYC	myc proto-oncogenic protein
MXD2	MAX dimerization protein 2
FIP200	200-kDa FAK family kinase-interacting protein
ATG101	autophagy-related protein 101
ULK1	serine/threonine-protein kinase ULK1
ATG13	autophagy-related protein 13
PI3KC3	phosphatidylinositol 3-kinase catalytic subunit type 3
AMBRA1	activating molecule in Beclin1-regulated autophagy protein 1
p115	general vesicular transport factor p115
ATG14	autophagy-related protein 14
ER	endoplasmic reticulum
PM	plasma membrane
PI3P	phosphatidylinositol-3-phosphate
WIPI	WD repeat domain phosphoinositide-interacting proteins
DFCP1	zinc-finger FYVE domain-containing protein 1
ATG12	autophagy-related protein 12
ATG5	autophagy-related protein 5
ATG16L1	autophagy-related protein 16L1
ATG8	autophagy-related 8
MAP1LC3	microtubule-associated proteins 1A/1B light chain
ATG4	autophagy-related protein 4
ATG7	autophagy-related protein 7
ATG3	autophagy-related protein 3
LIRs	LC3-interacting regions
p62/SQSTM1	sequestosome-1
TAX1BP1	tax1-binding protein 1
NBR1	next to BRCA1 gene 1 protein
HUWE1	E3 ubiquitin-protein ligase HUWE1
CTSD	cathepsin D
CLN6	ceroid lipofuscinosis, neuronal, 6
CLN8	ceroid lipofuscinosis, neuronal, 8
GlcNAc	N-Acetylglucosamine
PTase	GlcNAc-1-phosphotransferase
GNPTAB	N-acetylglucosamine-1-phosphotransferase subunits alpha/beta
GNPTG	N-acetylglucosamine-1-phosphotransferase subunit gamma

UCE	N-acetylglucosamine-1-phosphodiester α -N-acetylglucosaminidase
M6P	mannose-6-phosphate
TGN	trans Golgi network
M6PR	M6P receptors
LSDs	lysosomal storage diseases
v-ATPase	vacuolar H ⁺ -ATPase
TFs	transcription factors
bHLH-Zip	basic helix-loop-helix–leucine-zipper
TFEB	transcription factor EB
MiTF	microphthalmia-associated transcription factor
TFE3	transcription factor E3
CLEAR	coordinated lysosomal expression and regulation
ATP6AP1	v-type proton ATPase subunit S1
MCOLN1	mucolipin-1
CLN3	battenin
LAMP1	lysosome-associated membrane glycoprotein 1
LAMP2	lysosome-associated membrane glycoprotein 2
PPT1	palmitoyl-protein thioesterase 1
Calcineurin	serine/threonine-protein phosphatase 2B
RHEB	Ras-homolog enriched in brain
Rags	Ras-related GTP-binding proteins
GFs	growth factors
TSC	tuberous sclerosis complex
TSC1	hamartin
TSC2	tuberin
TBC1D7	TBC1 domain family member 7
GAP	GTPase-activating protein
GTP	guanosine triphosphate
GDP	guanosine diphosphate
AKT	protein Kinase B
PI3K	phosphoinositide 3-kinase
G3BPs	Ras GTPase-activating protein-binding proteins
PIPs	phosphatidylinositol phosphates
IRS-1	insulin receptor substrate 1
GRB10	growth factor receptor-bound protein 10
ERK	extracellular signal-regulated kinase
GSK3 β	glycogen synthase kinase-3 beta
IKK β	inhibitor of nuclear factor kappa-B kinase subunit beta
TNF α	tumor necrosis factor α
CDK1	cyclin-dependent kinase 1

FA	focal adhesion
AMPK	5'-AMP-activated protein kinase
AMP	adenosine monophosphate
GATOR2	GTPase-activating protein activity towards Rags 2
DHAP	dihydroxyacetone phosphate
HK-II	hexokinase-II
LAMTOR	late endosomal/lysosomal adaptor and MAPK and mTOR activator
GEFs	guanine exchange factors
SLC38A9	sodium-coupled neutral amino acid transporter 9
GATOR1	GTPase-activating protein GAP activity towards Rags 1
DEPDC5	DEP domain-containing 5
NPRL2	nitrogen permease regulator-like 2
NPRL3	nitrogen permease regulator-like 3
MIOS	meiosis regulator for oocyte development
WDR24	WD repeat domain 24
WDR59	WD repeat domain59
SEH1L	seh1 like nucleoporin
SEC13	sec13 homolog nuclear pore and COPII coat complex component
KPTN	Kaptein
ITFG2	integrin- α FG-GAP repeat containing 2
SZT2	C12orf66 and seizure threshold 2
FLCN	folliculin
FNIP1/2	FLCN-interacting proteins 1 and 2
LARS	leucyl-tRNA synthetase
CASTOR1/2	cytosolic arginine sensor for mTORC1
TARS2	mitochondrial threonyl-tRNA synthetase 2
ARF1	adenosine diphosphate ribosylation factor-1
PLD1	phospholipase D1
Pib2	phosphatidylinositol 3-phosphate-binding protein 2
R3HCC1	R3H and coiled coil domain-containing protein 1
RAB1A	Ras-related protein Rab-1a
PTMs	post-translational modifications
E1	E1 ubiquitin-activating enzyme
E2	E2 ubiquitin-conjugating enzyme
E3	E3-ubiquitin ligase
DUBs	deubiquitinases
USP	ubiquitin-specific proteases
CYLD	ubiquitin carboxyl-terminal hydrolase CYLD
NF- κ B	nuclear factor kappa B
TNFR	tumor necrosis factor receptor

TRADD	tumor necrosis factor receptor type 1-associated DEATH domain protein
cIAP1/2	cellular inhibitor of apoptosis 1 and 2
RIPK1	receptor-interacting serine/threonine-protein kinase 1
TRAF2	TNF receptor-associated factor 2
TAB2	TGF-beta-activated kinase 1 and MAP3K7-binding protein 2
TAB3	TGF-beta-activated kinase 1 and MAP3K7-binding protein 3
TAK1	transforming growth factor- β -activated kinase 1
IKK α	inhibitor of NF- κ B kinase subunit alpha
NEMO	NF- κ B essential modulator
I κ B	NF- κ B inhibitor
ERK1	mitogen-activated protein kinase 3
ERK2	mitogen-activated protein kinase 1
SCF	SKP, cullin, F-box containing complex
FBXW7	F-box/WD repeat-containing protein 7
FBX8	F-box only protein 8
TRAF6	TNF receptor-associated factor 6
DDB1-CUL4	DNA damage-binding protein1-cullin-4
UCH-L1	ubiquitin carboxyl-terminal hydrolase isozyme L1
OTUD7B	OTU domain-containing protein 7B
RNF7	RING-box protein 2
CUL5	cullin-5
OTUB1	ubiquitin thioesterase OTUB1
UBE3A	ubiquitin-protein ligase E3A
USP32	ubiquitin carboxyl-terminal hydrolase 32
RNF152	E3 ubiquitin-protein ligase RNF152
SKP2	S-phase kinase-associated protein 2
CUL3	cullin-3
KLHL22	Kelch-like protein 22
RING	really interesting new gene
RNF167	E3 ubiquitin-protein ligase RNF167
STAMBPL1	AMSH-like protease
RNF186	E3 ubiquitin-protein ligase RNF186
ROC1	regulator of cullins-1
HERC1	probable E3 ubiquitin-protein ligase HERC1
TRIM31	E3 ubiquitin-protein ligase TRIM31
PAM	E3 ubiquitin-protein ligase MYCBP2
TRIM6	tripartite motif-containing protein 6
RNF152	E3 ubiquitin-protein ligase RNF152
USP4	ubiquitin carboxyl-terminal hydrolase 4
ATXN3	ataxin-3
CHIP	E3 ubiquitin-protein ligase CHIP

KLHL20	Kelch-like protein 20
USP20	ubiquitin carboxyl-terminal hydrolase 20
RICTOR	rapamycin-insensitive companion of mTOR
mSIN1	target of Rapamycin complex 2 subunit MAPKAP1
PROTOR1	proline-rich protein 5
PROTOR2	proline-rich protein 5-like
FOXO	forkhead box proteins
SGK1	serine/threonine-protein kinase SGK1
NDRG1	N-myc downstream-regulated gene 1 protein
PH	pleckstrin-homology
PI(4,5)P ₂	phosphatidylinositol-4,5-bisphosphate
PI(3,4,5)P ₃	phosphatidylinositol-3,4,5- triphosphate
PTEN	phosphatidylinositol 3,4,5-trisphosphate 3-phosphatase and dual-specificity protein phosphatase PTEN
USP9X	probable ubiquitin carboxyl-terminal hydrolase FAF-X
p85	Phosphatidylinositol-3-kinase regulatory subunit
p110	Phosphatidylinositol-4,5-bisphosphate-3-kinase catalytic subunit
FBX12	F-box/LRR-repeat protein 12
HSP70	heat shock 70kDa protein
NEDD4L	E3 ubiquitin-protein ligase NEDD4-like
TTC3	E3 ubiquitin-protein ligase TTC3
MULAN	mitochondrial ubiquitin ligase activator of NF-κB 1
RFP2	E3 ubiquitin-protein ligase TRIM12
BRCA1	breast cancer type 1 susceptibility protein
ZNRF1	E3 ubiquitin-protein ligase ZNRF1
NEDD4	E3 ubiquitin-protein ligase NEDD4
USP1	ubiquitin carboxyl-terminal hydrolase 1
OTUD5	OTU domain-containing protein 5
CUL1	cullin-1
HEK293FT	human embryonic kidney
BafA1	bafilomycin A1
MEFs	murine embryonic fibroblasts
DAPI	4',6-Diamidino-2-phenylindol
ConA	concanamycin A
KO	knockout
WT	wild-type
PepA	pepstatin A
IVK	<i>in vitro</i> kinase assay
siRNAs	small interfering RNAs
HA	hemagglutinin
Lyso-IP	lysosomal immunopurification

GAPDH	glyceraldehyde-3-phosphate dehydrogenase
TMEM192	transmembrane protein 192
GBF1	golgi-specific brefeldin A-resistance guanine nucleotide exchange factor 1
GA	golgicide A
BFA	brefeldin A
GM130	golgin subfamily A member 2
OPP	O-propargyl-puromycin
CHX	cicloheximide
Ub	ubiquitin
SBP	streptavidin-binding peptide
h.e.	high exposure
l.e.	low exposure
ATP	adenosine triphosphate
RHEBL-1	RHEB-like 1
SUnSET	surface sensing of translation
HOPS	homotypic fusion and protein sorting
ESCRT	endosomal sorting complexes required for transport
i.e.,	id est (that is)
°C	degrees celsius
DMEM	Dulbecco's modified eagle medium
FBS	fetal bovine serum
P/S	penicillin-streptomycin
SNP	single nucleotide polymorphism
PCR	polymerase chain reaction
dFBS	dialyzed FBS
MWCO	molecular weight cut-off
PBS	phosphate-buffered saline
cDNA	complementary DNA
RT-qPCR	reverse transcription quantitative real-time PCR
SDS-PAGE	sodium dodecyl sulphate polyacrylamide gel electrophoresis
BSA	bovine serum albumine
RT	room temperature
NaF	sodium fluoride
CHAPS	3-((3-cholamidopropyl) dimethylammonio)-1-propanesulfonate
NEM	N-ethylmaleimide
DTT	dithiothreitol
IPTG	isopropyl-β-D-thiogalactopyranoside
PFA	paraformaldehyde
IF	immunofluorescence
SEM	standard error of the mean

1 Introduction

mTOR (mechanistic target of Rapamycin) is a highly conserved serine/threonine protein kinase that belongs to the PIKK (PI3K-related protein kinase) family (Richardson et al., 2004b). In mammals, it is the catalytic component of two complexes: mTORC1 (mTOR complex 1) and mTORC2 (mTOR complex 2), which have distinct roles (Liu and Sabatini, 2020). Notably, both complexes are dysregulated in several conditions, such as cancer and aging (Liu and Sabatini, 2020).

1.1 The mTOR complex 1

In the context of mTORC1, mTOR is in complex with RAPTOR (regulatory-associated protein of mTOR) (Hara et al., 2002; Kim et al., 2002). RAPTOR acts as a scaffold protein that is necessary for the integrity of the complex. In addition, RAPTOR recognizes some mTORC1 substrates by binding to TOS motifs (TOR signaling motifs) in their sequences (Nojima et al., 2003; Schaim et al., 2003). A second component is mLST8 (mammalian lethal with SEC13 protein 8, also known as GβL) (Kim et al., 2003). mLST8 enhances the binding of RAPTOR to mTOR, however, studies suggest that mLST8 is not required for mTORC1 activity (Guertin et al., 2006; Yang et al., 2013a). Furthermore, mTORC1 has two endogenous inhibitory components: PRAS40 (proline-rich AKT substrate 40 kDa) (Sancak et al., 2007; Vander Haar et al., 2007) and DEPTOR (DEP-domain-containing mTOR-interacting protein) (Peterson et al., 2009), which bind to RAPTOR and mTOR, respectively.

Structurally, mTOR is a protein with three core domains with distinct functions: the HEAT (Huntingtin, EF3 (elongation factor 3), PP2A (protein phosphatase 2A), and yeast TOR1 (target of Rapamycin kinase 1)) repeats, the FAT (FRAP (mechanistic target of Rapamycin), ATM (serine-protein kinase ATM), TRRAP (transformation/transcription domain-associated protein)) domain and the kinase domain (Yip et al., 2010; Yang et al., 2013a; Aylett et al., 2016; Yang et al., 2017). The HEAT repeats are necessary for dimerization of the complex and for the binding of mTOR to RAPTOR (Takahara et al., 2006; Yip et al., 2010; Jain et al., 2014; Aylett et al., 2016), while the FAT domain is an autoinhibitory region (Yang et al., 2017). Furthermore, the kinase domain is where substrate phosphorylation takes place. It is also the site of mLST8 binding (Yip et al., 2010; Aylett et al., 2016; Yang et al., 2017). Additionally, within the kinase domain resides the FRB (FKBP-Rapamycin-binding) sub-domain, which is required for recruitment of substrates to the active kinase site. Importantly, the FKBP12 (FK506-binding protein 12)-Rapamycin complex inhibits mTORC1 by binding to the FRB region (Yip et al., 2010; Aylett et al., 2016; Yang et al., 2017).

1.1.1 mTORC1 functions

Active mTORC1 promotes anabolic processes, such as protein synthesis, tightening favorable conditions to cellular growth. Concomitantly, mTORC1 inhibits catabolic processes, such as autophagy and lysosomal biogenesis.

1.1.1.1 Protein synthesis

By acting as an AA (amino acid)-responsive complex and by controlling mRNA translation, mTORC1 ensures that cells only synthesize proteins when building blocks are available. A major hub for the control of protein synthesis is the eIF4F (eukaryotic initiation factor 4F) complex. eIF4F is necessary for the recruitment of the 43S pre-initiation complex and the initiation factors eIF1 (eukaryotic initiation factor 1), eIF1A (eukaryotic initiation factor 1A), eIF3 (eukaryotic initiation factor 3) and eIF5 (eukaryotic initiation factor 5) to mRNAs (messenger RNAs). The eIF4F complex is composed of the scaffold protein eIF4G (eukaryotic initiation factor 4G), the cap-binding protein eIF4E (eukaryotic initiation factor 4E) and the RNA helicase eIF4A (eukaryotic initiation factor 4A). Furthermore, eIF4B (eukaryotic initiation factor 4B) enhances activity of eIF4A (Merrick and Pavitt, 2018).

mTORC1 coordinates protein synthesis by phosphorylation of its canonical substrates, TOS-containing proteins eukaryotic initiation factor 4E-BP1 (4E-binding protein 1) and S6K1 (p70 S6 Kinase 1) (Burnett et al., 1998; Nojima et al., 2003; Schaim et al., 2003; Fumagalli and Pende, 2022). Importantly, both 4E-BP1 and S6K1 can act on the eIF4F complex.

Regulation of 4E-BP1

As a regulator of 5'-dependent cap translation, 4E-BP1 inhibits this process by binding to eIF4E. mTORC1 phosphorylates 4E-BP1 on multiple sites driving its displacement from eIF4E and releasing its inhibitory function, thereby promoting translation (Hara et al., 1997; Gingras et al., 1999). Importantly, 4E-BP1 is tethered to mTORC1 by two interactions, explaining the hierarchical mode of 4E-BP1 phosphorylation (Bohm et al., 2021). In addition, mTORC1 phosphorylates 4E-BP1 both in its free state and in the eIF4E-bound form. This mode of phosphorylation ensures that all pools of 4E-BP1 are targeted, guaranteeing an efficient translation process (Bohm et al., 2021).

mTORC1 favors translation of TOP (terminal oligopyrimidine tract) mRNAs, which bear a 5' oligopyrimidine sequence downstream of the N⁷-methyl guanosine triphosphate cap, a feature present in many ribosomal mRNAs (Levy et al., 1991; Hsieh et al., 2012; Thoreen et al., 2012). 4E-BP1 is one of the factors that regulate TOP mRNA translation (Hsieh et al., 2012; Thoreen et al., 2012). Nonetheless, mTORC1 also phosphorylates and inactivates a key repressor of this process, LARP1 (La-related protein 1) (Jia et al., 2021). Thus, mTORC1 targets TOP mRNAs via phosphorylation of two distinct substrates.

Regulation of S6K1

Activation of S6K1 occurs via mTORC1-driven phosphorylation (Burnett et al., 1998), in concert with phosphorylation by PDK1 (phosphoinositide-dependent protein kinase 1) (Alessi et al., 1998; Pullen et al., 1998). Active S6K1 in turn phosphorylates distinct downstream substrates.

The best-studied S6K1 target is S6 (ribosomal protein S6). Phosphorylated S6 is suggested to be important for translation of ribosomal genes (Chauvin et al., 2014) and for the translation of short coding sequences (Bohlen et al., 2021). However, mutations in all S6 phospho-sites do not affect translation (Ruvinsky et al., 2005). Thus, the effects downstream of S6 phosphorylation are still unclear. Moreover, although S6K1 is the only responsible kinase for the phosphorylation of S6 at serine 240 and 244 (Roux et al., 2007), both S6K1 and RSK (p90 ribosomal S6 kinase) can phosphorylate serine 235 and 236 (Pende et al., 2004; Roux et al., 2007). These observations suggest that the control of S6 may involve a crosstalk between the mTORC1 and MAPK (mitogen-activate protein kinase) pathways.

In the context of translation initiation, S6K1 phosphorylates and activates eIF4B. eIF4B activation promotes the translation of mRNAs with complex 5' untranslated regions (Holz et al., 2005). S6K1 also phosphorylates additional targets involved in translation, such as the negative regulator of eIF4A, PDCD4 (programmed cell death protein 4) (Dorrello et al., 2006).

S6K1 also activates transcription of ribosomal RNAs by enhancing RNA polymerase I activity via phosphorylation of the regulatory factors UBF (upstream binding factor) (Hannan et al., 2003) and TIF-1A (transcription initiation factor 1A) (Mayer et al., 2004). Likewise, S6K1 also phosphorylates the repressor of RNA polymerase III MAF1 (repressor of RNA polymerase III transcription MAF1 homolog) (Shor et al., 2010). However, a second report suggested that MAF1 is a direct target of mTORC1 (Michels et al., 2010). Hence, the relevance of S6K1-mediated phosphorylation of MAF1 is not clear.

Another process controlled by S6K1 is RNA metabolism. The exon junction complex subunit SKAR (polymerase delta-interacting protein 3; also known as POLDIP3) is phosphorylated by S6K1, increasing the translation efficiency of spliced mRNAs (Richardson et al., 2004a) (Ma et al., 2008). Activation of the S6K1-eIF4B-eIF4A axis promotes an increase in levels of both WTAP (Wilms' tumor 1-associating protein) and of methylated mRNAs. This process is linked to increased transcription of genes involved in cell growth (Cho et al., 2021). Additionally, active mTORC1 supplies methyl groups for RNA methylation via an increase in SAM (S-adenosylmethionine) levels (Villa et al., 2021). Furthermore, the specific activity of the c-MYC (myc proto-oncogenic protein) transcriptional program is also controlled by S6K1 via phosphorylation of the c-MYC suppressor MXD2 (MAX dimerization protein 2) (Huang et al., 2018).

Importantly, the S6K1-mediated control of protein synthesis is tightly linked to cell size. Mice lacking S6K1 have decreased β -cell mass and are smaller than their WT counterparts (Pende et al., 2000; Pende et al., 2004). In line with these findings, muscle deletion of S6K1 does not affect myoblast proliferation, but reduces their size similarly to Rapamycin treatment (Ohanna et al., 2005). Together, these findings show that S6K1, downstream of mTORC1, is an important factor for the regulation of cell mass.

1.1.1.2 Autophagy

Concomitantly with mTORC1 acting as a pro-growth complex, it also inhibits catabolic processes. Macroautophagy, hereafter referred to as autophagy, is the cellular process by which cytoplasmic portions, damaged proteins and organelles are degraded inside lysosomes, promoting the recycling of cellular components (Dikic and Elazar, 2018). Autophagy is in the center of cellular proteostasis. Hence, it is not surprising that autophagy dysregulation is a main feature of aging (Leidal et al., 2018) and of many neurodegenerative diseases in which protein aggregation occurs (Nixon, 2013).

Autophagy induction is coordinated by the initiation complex, formed by FIP200 (200-kDa FAK family kinase-interacting protein), ATG101 (autophagy-related protein 101), ULK1 (serine/threonine-protein kinase ULK1) and ATG13 (autophagy-related protein 13) (Nakatogawa, 2020). The active initiation complex phosphorylates components of PI3KC3 (phosphatidylinositol 3-kinase catalytic subunit type 3; also known as VPS34) complex I (Russell et al., 2013; Park et al., 2016), promoting the nucleation of the phagophore. The PI3KC3 complex I consists of VPS34, Beclin1, AMBRA1 (activating molecule in Beclin1-regulated autophagy protein 1), p115 (general vesicular transport factor p115) and ATG14 (autophagy-related protein 14) (Nakatogawa, 2020). At this stage, both the initiation complex and the PI3KC3 complex I are located at autophagosome precursor membranes. During growth of the phagophore, membranes are recruited from various membrane sources, such as the ER (endoplasmic reticulum), the mitochondria or the PM (plasma membrane) (Nakatogawa, 2020). The active PI3KC3 complex I induces local production of PI3P (phosphatidylinositol-3-phosphate) (Axe et al., 2008; Nascimbeni et al., 2017; Nishimura et al., 2017; Dikic and Elazar, 2018; Nakatogawa, 2020). Next, binding to PI3P brings together WIPI (WD repeat domain phosphoinositide-interacting proteins) proteins and DFCP1 (zinc-finger FYVE domain-containing protein 1) (Dikic and Elazar, 2018). These proteins recruit a complex containing the ATG12 (autophagy-related protein 12), ATG5 (autophagy-related protein 5) and ATG16L1 (autophagy-related protein 16L1) (Dooley et al., 2014). Importantly, the ATG12-ATG5-ATG16L1 complex is part of a key autophagic process: the lipidation of ATG8 (autophagy-related 8) family proteins, such as MAP1LC3 (microtubule-associated proteins 1A/1B light chain), also known as LC3 (Ichimura et al., 2000; Kabeya et al., 2004; Sou et al., 2008). Non-lipidated LC3 (LC3-I) is then converted into lipidated LC3 (LC3-II) via a complex reaction: ATG4 (autophagy-related protein 4) cleaves the C-terminus of LC3, followed by action of ATG7 (autophagy-related protein 7), ATG3 (autophagy-related protein 3) and ATG16L1 as E1-like activating enzyme, E2-like conjugating enzyme and E3-like ligase, respectively, that conjugate phosphatidylethanolamine to LC3 (Nakatogawa, 2020). LC3 lipidation is a requirement for the recruitment of further autophagy proteins, via interaction with LIRs (LC3-interacting regions), as well as for elongation and closure of the phagophore (Nakatogawa et al., 2007). A closed phagophore is named autophagosome, which fuses with lysosomes for degradation of their content. The model for autophagosome formation and degradation of its content in lysosomes is summarized in Figure 1.1. The degradation

products are released to the cytosol via transporters at the lysosomal membrane (Xu and Ren, 2015; Yim and Mizushima, 2020).

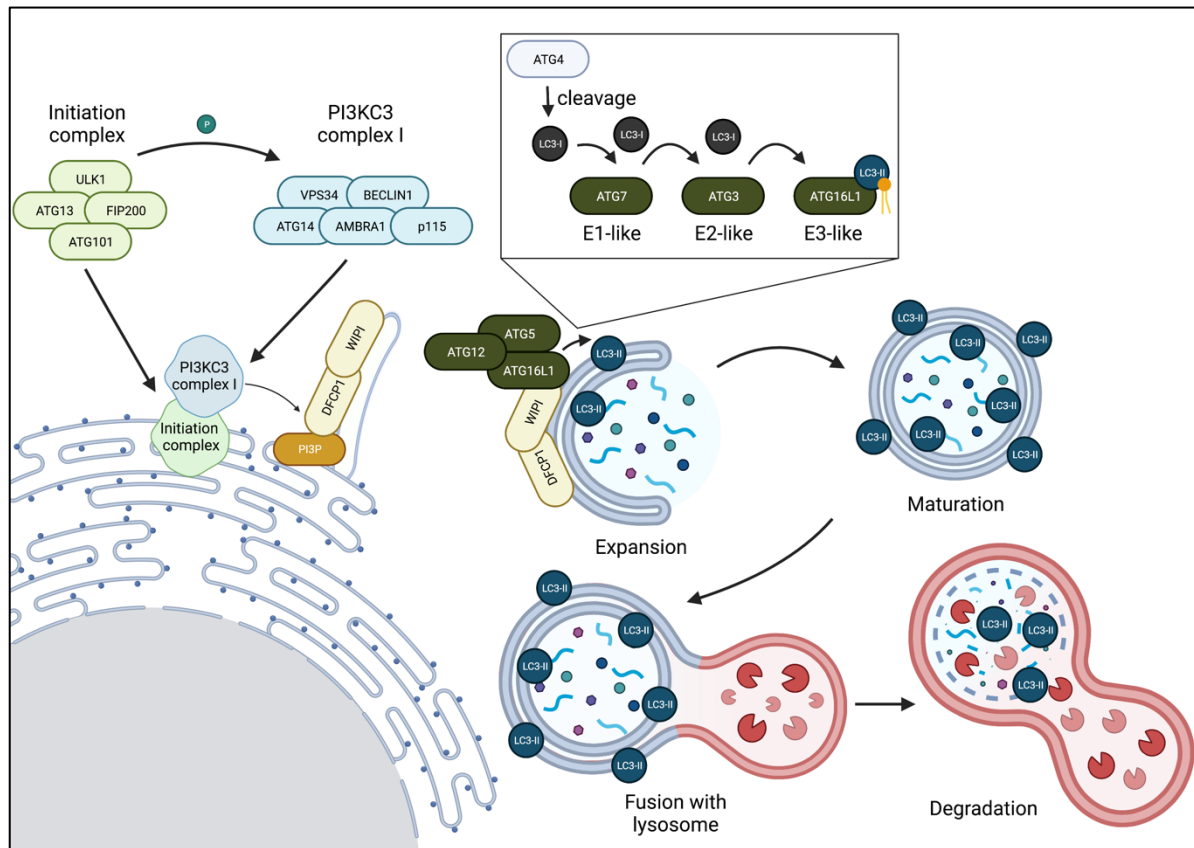


Figure 1.1 Schematic representation of autophagosome formation and cargo degradation in lysosomes. The induction of autophagy starts by the formation of the initiation complex, consisting of ULK1, ATG13, FIP200 and ATG101. The initiation complex phosphorylates components of the PI3KC3 complex I, promoting the production of PI3P at specific sites in the ER. Via binding to PI3P, the proteins DFCP1 and WIPI are recruited to the nucleated vesicle. The DFCP1/WIPI complex recruits the ATG12-ATG5-ATG16L1 complex, promoting the lipidation of LC3-II. In the inset, the LC3-II lipidation reaction is shown: ATG4 cleaves LC3, generating LC3-I, which is substrate for E1 (ATG7), E2 (ATG3), and E3 (ATG16L1)-like conjugating enzymes that add phosphatidylethanolamine to LC3-I, generating LC3-II. The autophagosome matures, fuses with lysosomes and both its content and its inner membrane are degraded. Created with BioRender.com

Autophagy can act non-selectively, by sequestering parts of the cytoplasm, or selectively, targeting specific cargos for degradation (Vargas et al., 2023). Such cargos include damaged organelles or protein aggregates. Importantly, both non-selective and selective autophagy share the same core machinery described above. Yet, selective autophagy has unique properties. For the targeted degradation of cellular components, cargos are commonly marked by attachment of ubiquitin molecules. These marks are recognized by receptor proteins, such as p62/SQSTM1 (sequestosome-1), TAX1BP1 (tax1-binding protein 1) and NBR1 (next to BRCA1 gene 1 protein), which show substrate-specificity (Vargas et al., 2023). Receptor proteins contain a LIR motif, as well as ubiquitin-binding domains, which allow the delivery of marked cargos to the autophagosome (Kirkin and Rogov, 2019).

mTORC1 regulates autophagy in many steps (Rabanal-Ruiz et al., 2017). It phosphorylates and inactivates ULK1 (Kim et al., 2011) and ATG13 (Ganley et al., 2009; Hosokawa et al., 2009), thereby inhibiting autophagy initiation. Moreover, the PI3KC3 complex I, involved in early steps of autophagy, is also targeted by mTORC1 by inhibitory phosphorylation on AMBRA1 (Nazio et al., 2013) and ATG14 (Yuan et al., 2013). Interestingly, AMBRA1 phosphorylation is important for ULK1 protein stability (Nazio et al., 2013). mTORC1 also controls autophagy by phosphorylating WIPI2. This phosphorylation induces the interaction of WIPI2 with the E3 ligase HUWE1 (E3 ubiquitin-protein ligase HUWE1), leading to WIPI2 proteasomal degradation (Wan et al., 2018). On the other hand, autophagy leads to the recycling of cellular components and promotes local release of nutrients at the lysosomal vicinity, thus causing mTORC1 re-activation to restrict excessive autophagy and allow cells to return to their regular growth program (Yu et al., 2010).

1.1.1.3 Lysosomes

Lysosomes are organelles with degradative capacity. Their ability to degrade proteins, carbohydrates and lipids relies on more than 60 acid hydrolases (Ballabio and Bonifacio, 2020). Lysosomal proteases are a class of enzymes that hydrolyze peptide bonds in the lysosomal lumen. Among proteases, cathepsins are the most abundant and are categorized by the amino acid present in their catalytic site. For example, CTSD (cathepsin D) is an aspartic protease (Ruiz-Blazquez et al., 2021). Cathepsins are translated as preprocathepsins in the ER (Hasilik and Neufeld, 1980). The signal peptide from preprocathepsins is co-translationally removed, generating procathepsins (Zaidi et al., 2008). Procathepsins are sorted in the Golgi for delivery to lysosomes (Gieselmann et al., 1983). Importantly, procathepsins are inactive, ensuring that proteolysis does not occur during their trafficking (Richo and Conner, 1991). Once inside lysosomes, cleavage of procathepsins generates active cathepsins. For CTSD, the processing happens by the action of cathepsins B and L (Laurent-Matha et al., 2006). Fully processed cathepsins are active and capable of hydrolyzing their substrates.

Enzyme delivery to lysosomes occurs via the mannose-6-phosphate pathway (Figure 1.2) (Braulke and Bonifacio, 2009). Hydrolases are synthesized and glycosylated by addition of mannose modifications at the ER (Burda and Aebi, 1999; Bai and Li, 2019). There, lysosomal enzymes are recruited by the complex CLN6 (ceroid lipofuscinosis, neuronal, 6) - CLN8 (ceroid lipofuscinosis, neuronal, 8) to be transferred to the Golgi (di Ronza et al., 2018; Bajaj et al., 2020). At the Golgi, GlcNAc (N-Acetylglucosamine)-phosphate is added by the PTase (GlcNAc-1-phosphotransferase) (Li et al., 2022). PTase is an enzymatic complex composed of three subunits (α , β and γ). The transmembrane α and β subunits are encoded by the *GNPTAB* (N-acetylglucosamine-1-phosphotransferase subunits alpha/beta) gene (Kudo et al., 2005), whereas *GNPTG* (N-acetylglucosamine-1-phosphotransferase subunit gamma) encodes the soluble γ subunit (Raas-Rothschild et al., 2000). The modified enzymes are further transported to the trans side of the Golgi, where the uncovering enzyme UCE (N-

acetylglucosamine-1-phosphodiester α -N-acetylglucosaminidase) removes GlcNAc, leaving a M6P (mannose-6-phosphate) mark (Braulke and Bonifacio, 2009). Finally, the enzymes tagged with M6P move to the TGN (trans Golgi network), where the M6P modification is recognized by M6PR (M6P receptors) (Ghosh et al., 2003). Clathrin-coated vesicles then bud off the Golgi and deliver the enzymes to endosomes (Ghosh et al., 2003). Importantly, the enzyme dissociation from the receptor occurs in the acidic pH of late endosomes/lysosomes (Ghosh et al., 2003). The empty receptor is recycled back to the TGN, via retrograde transport from endosomes to Golgi (Bonifacio and Rojas, 2006). Importantly, M6PR also resides at the PM. Hence, the M6P-modified enzymes that are mis-sorted and exocytosed to the extracellular space can be retrieved by the PM-resident M6PR and delivered to lysosomes via the endocytic pathway (Bajaj et al., 2019).

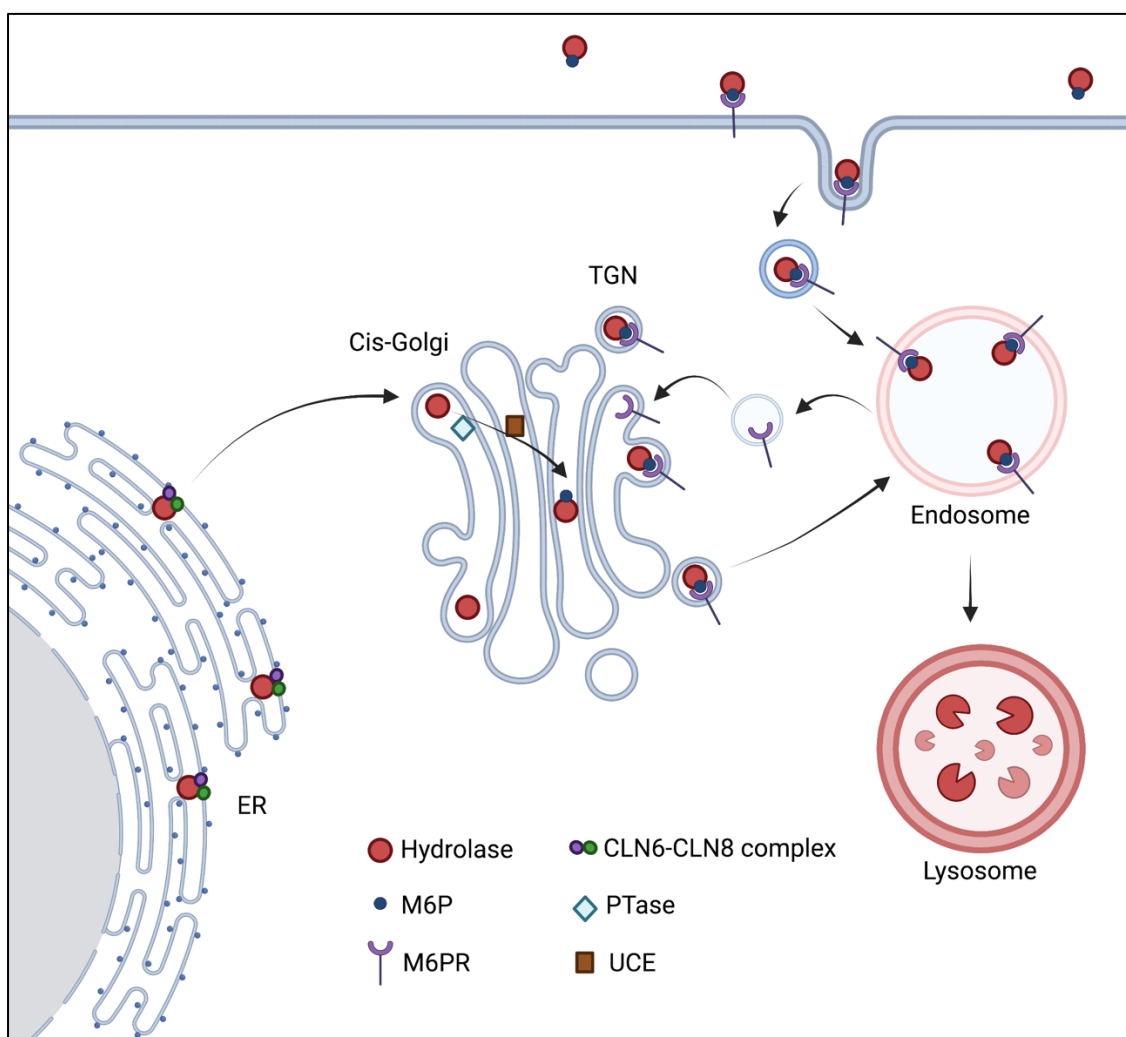


Figure 1.2 The mannose-6-phosphate pathway.

Lysosomal enzymes are synthesized and glycosylated at the ER. There, the enzymes are recognized by the complex CLN6-CLN8 and transported to the Golgi. At the Golgi, the enzymes are marked with mannose-6-phosphate (M6P) by the action of the GlcNAc-1-phosphotransferase (PTase) and the uncovering enzyme (UCE). Modified enzymes are transported to the trans Golgi network (TGN), where M6P is recognized by the mannose-6-phosphate receptor (M6PR). By vesicle transport, enzymes reach endosomes and the M6PRs are recycled back to the Golgi. Alternatively, if lysosomal enzymes

are mis-sorted to the extracellular space, they can be recovered by the action of plasma membrane M6PR. The retrieved enzymes are then transported to endosomes via the endocytic pathway. The enzymes are delivered to lysosomes, where they are cleaved and activated. Created with BioRender.com

Lysosomes have acidic pH. This is a mechanism by which cells safeguard their integrity, allowing the activation of hydrolytic enzymes only in the acidic pH of lysosomes (pH=4.5-5.0) (Ballabio and Bonifacino, 2020). Lysosomal pH is controlled by the v-ATPase (vacuolar(H⁺)-ATPase), a proton pump that transports H⁺ ions to the lysosomal lumen (Mindell, 2012). Importantly, proper lysosomal pH is not only required for activation of acid hydrolases, but it is also essential for the transport of degradation products from the lysosomal lumen to the cytosol via the action of transporters (Xu and Ren, 2015; Rudnik and Damme, 2021). For instance, blockage of lysosomal acidification leads to increased intraluminal concentration of non-essential AAs in lysosomes (Abu-Remaileh et al., 2017).

The importance of lysosomes is emphasized by the existence of more than 70 LSDs (lysosomal storage diseases) (Platt et al., 2018). LSDs can be caused by mutations in genes coding for a number of proteins. For instance, GNPTAB mutations are linked to mucopolipidosis type II and type III (Tiede et al., 2005; Danyukova et al., 2020), highlighting that the correct trafficking of lysosomal enzymes is vital for cellular function. Moreover, mutations causing LSDs are also found in genes coding for lysosomal hydrolases, additional trafficking enzymes, transporters, structural proteins and the v-ATPase (Platt et al., 2018).

mTORC1 controls lysosomal function by targeting TFs (transcription factors) belonging to the microphthalmia family of bHLH-Zip (basic helix-loop-helix-leucine-zipper) TFs (Steingrimsson et al., 2004). It consists of TFEB (transcription factor EB), and the related factors MiTF (microphthalmia-associated transcription factor) and TFE3 (transcription factor E3) (Settembre et al., 2012). TFEB recognizes a 10-base sequence in genes related to lysosomal function, namely CLEAR (coordinated lysosomal expression and regulation) motif (Sardiello et al., 2009; Palmieri et al., 2011). Later on, studies showed that these TFs also target autophagy-related genes (Sardiello et al., 2009; Palmieri et al., 2011; Settembre et al., 2011; Martina et al., 2012). Among TFEB and TFE3 target genes are: subunits of the lysosomal v-ATPase, such as *ATP6AP1* (V-type proton ATPase subunit S1); lysosomal membrane proteins, such as *MCOLN1* (mucopolipin-1), *CLN3* (battenin) and *LAMP1* (lysosome-associated membrane glycoprotein 1); and lysosomal enzymes, such as cathepsins and the lipase *PPT1* (palmitoyl-protein thioesterase 1) (Palmieri et al., 2011; Settembre et al., 2011). In the autophagy pathway, TFEB controls the expression of *MAP1LC3B*, *SQSTM1* and *WIPI* (Palmieri et al., 2011; Settembre et al., 2011). By phosphorylating TFEB, mTORC1 promotes its interaction with 14-3-3 proteins, leading to its cytoplasmic retention (Martina et al., 2012; Roczniak-Ferguson et al., 2012; Martina and Puertollano, 2013). Differently from mTORC1 substrates that contain a TOS-motif for substrate recognition, TFEB is instead recruited to mTORC1 proximity via binding to the lysosomal Rag GTPases (Napolitano et al., 2020; Cui et al., 2023). On the other hand, mTORC1 inactivation

allows for the action of the phosphatase calcineurin (serine/threonine-protein phosphatase 2B) to dephosphorylate TFEB, promoting its nuclear translocation and activation (Medina et al., 2015). In sum, mTORC1 acts to repress the transcriptional regulation of autophagy and lysosomal biogenesis, ensuring that catabolic processes are inactive during growth-promoting conditions.

1.1.2 mTORC1 regulation

mTORC1 is tightly regulated by extracellular cues, ensuring that cells only promote cell growth when they have available building blocks and energy to make macromolecules. Most of the known machinery that regulates mTORC1 converges on two small GTPases: RHEB (Ras-homolog enriched in brain) and Rags (Ras-related GTP-binding proteins). RHEB is a small GTPase that acts as an indispensable mTORC1 activator at the lysosomal surface. On the other hand, Rags are lysosomal proteins that promote mTORC1 lysosomal recruitment, where it can meet its direct activator RHEB (Liu and Sabatini, 2020).

1.1.2.1 By growth factors

The regulation of mTORC1 by GFs (growth factors) is largely mediated by TSC (tuberous sclerosis complex) (Tee et al., 2002). TSC is composed by three components, TSC1 (hamartin), TSC2 (tuberin) and TBC1D7 (TBC1 domain family member 7) (Dibble et al., 2012; Yang et al., 2021). TSC1 and TSC2 are mutated in the disease TSC, which is characterized by the development of multiple benign tumors, hinting to its function in the mTORC1 pathway (Huang and Manning, 2008). TSC2 acts as a GAP (GTPase-activating protein) for RHEB. They interact on the lysosomal surface (Menon et al., 2014), leading to RHEB inactivation by the conversion of RHEB-GTP (guanosine triphosphate) to RHEB-GDP (guanosine diphosphate). Inactivation of RHEB consequently leads to mTORC1 inactivation (Garami et al., 2003; Tee et al., 2003b). Importantly, TSC2 is regulated by AKT (protein Kinase B), which is directly controlled by GF availability (Inoki et al., 2002; Manning et al., 2002; Tee et al., 2003a). When GFs are present, they bind to their receptor at the cell surface and promote the activation of PI3K (phosphoinositide 3-kinase) and PDK1, leading to AKT activation (Hoxhaj and Manning, 2020). Active AKT phosphorylates TSC2, promoting its dissociation from lysosomes where RHEB resides. When TSC is displaced from lysosomes, RHEB stays in its GTP-loaded state, activating mTORC1 (Menon et al., 2014; Demetriades et al., 2016a). The activation of mTORC1 by RHEB occurs via binding of the latter to the FAT domain of mTOR, inducing conformational changes that release mTORC1 inhibition (Yang et al., 2017). Additional tethering mechanisms were recently uncovered. TSC is recruited to lysosomes by the G3BPs (Ras GTPase-activating protein-binding proteins) – independently of their canonical role in stress granules – via their interaction with the lysosomal proteins LAMP1/2 (Prentzell et al., 2021). Furthermore, the TSC component TSC1 binds directly to lysosomal PIPs (phosphatidylinositol phosphates), inducing TSC lysosomal localization and RHEB inactivation (Fitzian et al., 2021). The TSC complex can also be recruited to lysosomes upon AA starvation, which will be introduced in section 1.1.2.3. All mechanisms of TSC recruitment

are summarized in Figure 1.3. The way via which the different lysosomal TSC tethers act in concert is not clear to date.

GFs also control mTORC1 via the AKT-mediated phosphorylation of PRAS40, releasing its endogenous inhibitory function in the mTORC1 complex. Interestingly, S6K1 phosphorylates and inhibits IRS-1 (insulin receptor substrate 1). This phosphorylation event fine-tunes the activation of the pathway by GFs via a negative feedback loop (Harrington et al., 2004; Shah et al., 2004). Finally, mTORC1 also induces a negative feedback loop on the GF signaling branch by phosphorylating GRB10 (growth factor receptor-bound protein 10), a protein that binds and inactivates the insulin receptor (Yu et al., 2011).

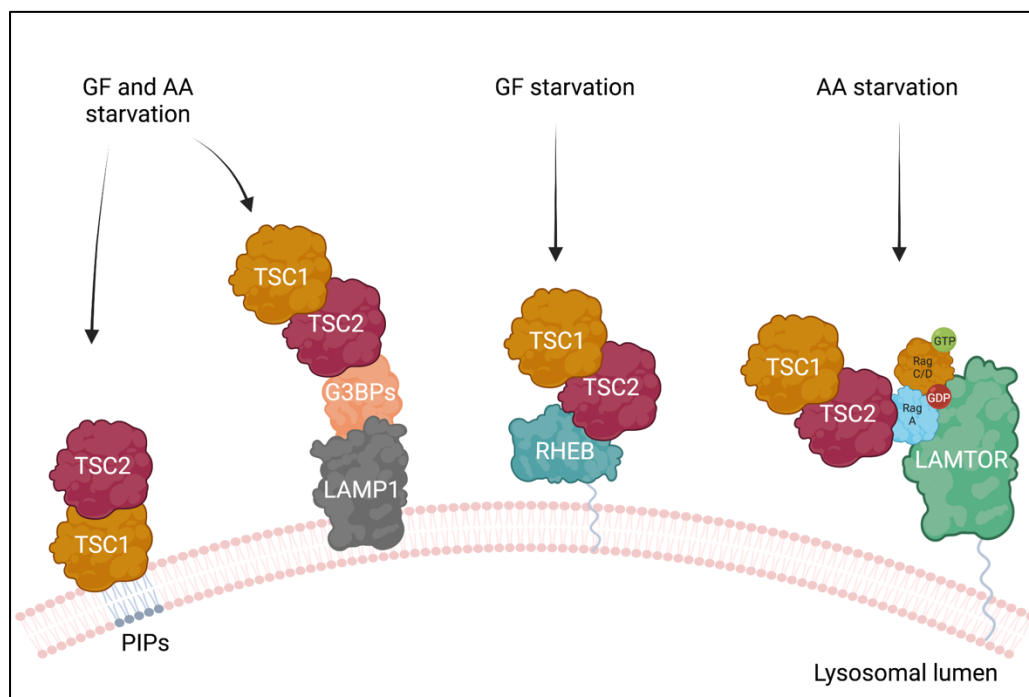


Figure 1.3 Modes of TSC lysosomal recruitment.

In response to GF starvation, TSC can be recruited to lysosomes by binding to lysosomal PIPs, via interaction with the G3BPs or by direct binding to RHEB. On the other hand, upon AA starvation, TSC can also be recruited to the lysosomal surface by binding to G3BPs or by direct binding of TSC2 to RagA-GDP. Created with BioRender.com

Different branches of GF signaling also act through TSC. Both ERK (extracellular signal-regulated kinase) and RSK phosphorylate TSC2, leading to TSC inhibition (Roux et al., 2004; Ma et al., 2005). TSC2 is also phosphorylated by GSK3 β (glycogen synthase kinase-3 beta), a component on the Wnt signaling pathway, promoting mTORC1 activity (Inoki et al., 2006). Another component of the complex, TSC1, is also directly phosphorylated by IKK β (inhibitor of nuclear factor kappa-B kinase subunit beta), making the complex responsive to TNF α (tumor necrosis factor α) stimulation (Lee et al., 2008). TSC1 is also phosphorylated by CDK1 (cyclin-dependent kinase 1), coupling cell growth to cell cycle control (Astrinidis et al., 2003).

By its central action in converging multiple GF signaling cues to mTORC1, TSC is strongest mTORC1 negative regulator.

Additionally, GF receptors were shown to cluster in FA (focal adhesion) sites. Interestingly, mTORC1 is clustered and active in these specific regions (Rabanal-Ruiz et al., 2021). This compartment seems to be essential for mTORC1 activity. Further studies are required to shed light to the regulation of mTORC1 in FAs and to investigate whether this depends on the known machinery components, such as TSC and RHEB.

1.1.2.2 By energy

As cell growth is one of the most energy consuming cellular processes, mTORC1 activity is also modulated by energy sufficiency. The main component of the cellular energy sensing machinery is AMPK (5'-AMP-activated protein kinase). AMPK binds AMP (adenosine monophosphate) molecules that signal energy shortage. An increase in AMP is observed when cells undergo nutrient or glucose starvation, or in low oxygen conditions (Herzig and Shaw, 2018). Thus, in such settings, AMPK signals to inactivate mTORC1, coordinating the communication between energy availability and cell growth. AMPK regulates mTORC1 via direct phosphorylation and activation of TSC2, thereby inhibiting mTORC1 (Inoki et al., 2003). AMPK also phosphorylates RAPTOR, promoting its sequestration via association with 14-3-3 proteins (Gwinn et al., 2008). In addition, AMPK phosphorylates and inactivates the GATOR2 (GTPase-activating protein activity towards Rags 2) complex, a direct positive regulator of mTORC1 (Dai et al., 2023). GATOR2 is a complex that acts via the Rag GTPases, indicating that the Rags are important for glucose sensing. In agreement, mice that either lack RagA or have constitutively active RagA show insensitivity to glucose starvation (Efeyan et al., 2013; Efeyan et al., 2014).

Independently of AMPK, glucose availability also signals to mTORC1 via the glycolysis intermediate DHAP (dihydroxyacetone phosphate) (Orozco et al., 2020). Low glucose levels are also directly sensed by mTORC1 via the glycolytic enzyme HK-II (hexokinase-II) (Roberts et al., 2014). However, the direct sensors for such metabolites are still uncharacterized.

1.1.2.3 By amino acids

AAs are one of the strongest stimuli that can activate mTORC1. As early as the 90s, studies identified the regulators of protein synthesis, S6K1 and 4E-BP1, as responsive to AA sufficiency (Blommaart et al., 1995; Hara et al., 1998). Later on, the Rag GTPases were found as a converging hub for the AA-mediated control of mTORC1 activity (Kim et al., 2008; Sancak et al., 2008).

1.1.2.3.1 Lysosomes and the Rag GTPases

The Rag GTPases form obligate heterodimers, with RagA or B binding RagC or D (Sekiguchi et al., 2001). Although the Rag GTPases reside on lysosomes, they do not harbor a lipid-

signal that allows lysosomal anchorage. Instead, they are tethered via interaction with the LAMTOR (late endosomal/lysosomal adaptor and MAPK and mTOR activator) complex (also known as Ragulator) (Sancak et al., 2010). AA sufficiency induces activation of the Rag dimers, with RagA or B binding to GTP and RagC or D binding to GDP (Kim et al., 2008; Sancak et al., 2008; Shen et al., 2017; Lawrence et al., 2018). The active Rag GTPases interact with RAPTOR to promote lysosomal mTORC1 recruitment. Structural work described that RAPTOR has a “claw” that recognizes the active state of the Rag GTPases (Sancak et al., 2008; Anandapadamanaban et al., 2019; Rogala et al., 2019). Nonetheless, the interaction between RAPTOR and the Rag GTPases is not sufficient to promote mTORC1 activation. Instead, the interaction induces mTORC1 lysosomal recruitment, allowing mTORC1 to encounter its direct activator RHEB. In agreement with this model, RHEB depletion inhibits mTORC1 activation by AAs without affecting its lysosomal localization, highlighting the existence of two branches: the lysosomal recruitment by Rag GTPases and the activation by RHEB (Sancak et al., 2008; Sancak et al., 2010). The importance of the Rag GTPases is highlighted by the observation that RagA knockout mice die in the embryonic day E10.5 (Efeyan et al., 2014). Additionally, mice harboring a constitutively active RagA mutant die neonatally, being unable to inactivate mTORC1 and activate autophagy (Efeyan et al., 2013). These findings emphasize that AA sensing by mTORC1 is essential for organismal survival.

Over the years, a large number of regulators of the Rag GTPases were identified. In the control of small GTPases, GEFs (guanine exchange factors) or GAPs promote either GTP-binding or GTP hydrolysis, respectively. The LAMTOR complex was the first identified GEF for RagA/B and their interaction relies both on AA-sufficiency and v-ATPase binding (Bar-Peled et al., 2012). Later on, SLC38A9 (sodium-coupled neutral amino acid transporter 9), an AA transporter that resides on the lysosomal surface, was identified as a RagA GEF (Shen and Sabatini, 2018). Conversely, GATOR1 (GTPase-activating protein (GAP) activity towards Rags 1), a trimeric complex consisting of DEPDC5 (DEP domain-containing 5), NPRL2 (nitrogen permease regulator-like 2), and NPRL3 (nitrogen permease regulator-like 3), was described as a GAP for RagA, promoting GTP hydrolysis upon AA insufficiency (Bar-Peled et al., 2013; Shen et al., 2018). GATOR1 acts downstream of a positive regulatory complex termed GATOR2, comprised of MIOS (meiosis regulator for oocyte development), WDR24 (WD repeat domain 24), WDR59 (WD repeat domain 59), SEH1L (seh1 like nucleoporin) and SEC13 (sec13 homolog nuclear pore and COPII coat complex component). GATOR2 likely regulates mTORC1 activity by ubiquitinating NPRL2, an event needed for GATOR1 inhibition (Jiang et al., 2023). GATOR1 lysosomal recruitment occurs via interaction with KICSTOR, a complex comprised of the proteins KPTN (Kaptin), ITFG2 (integrin- α FG-GAP repeat containing 2) and SZT2 (C12orf66 and seizure threshold 2), allowing its interaction with both the Rag GTPases and GATOR2 (Peng et al., 2017; Wolfson et al., 2017). Additionally, the protein SH3BP4 (SH3 domain-binding protein 4) is a Rag GTPase negative regulator. It acts by interacting with inactive Rag GTPases upon AA starvation to prevent their activation (Kim et al., 2012).

The complex FLCN (folliculin) – FNIP1/2 (FLCN-interacting proteins 1 and 2) was described as a GAP for RagC/D (Petit et al., 2013; Tsun et al., 2013). RagC/D, in the active Rag GTPase dimer, is GDP-bound. Hence, the FLCN-FNIP complex acts as a positive regulator of mTORC1 in response to AAs. Upon starvation, FLCN is recruited to the lysosomal surface. However, the lysosomal FLCN complex adopts a conformation in which its GAP activity is abrogated (Lawrence et al., 2019). Upon AA stimulation, SLC38A9 acts to destabilize the lysosomal FLCN complex, promoting FLCN GAP activity (Fromm et al., 2020). Rag C/D has a unique role in the phosphorylation of some mTORC1 targets, such as TFEB. In the Birt-Hogg-Dubé syndrome, a disease where FLCN is mutated, TFEB is particularly affected (Napolitano et al., 2020). Later work demonstrated that RagD is specifically needed for TFEB phosphorylation (Gollwitzer et al., 2022). Interestingly, TFEB itself is recruited by the Rag GTPases, and recent work showed the existence of a megacomplex containing mTORC1-TFEB-Rag-LAMTOR complex (Cui et al., 2023). In addition, TFEB nuclear translocation, achieved in response to mTORC1 inactivation, feeds back to mTORC1 by inducing RagD expression (Di Malta et al., 2017). An additional feedback mechanism occurs through the mTORC1-dependent phosphorylation of RagC, which is necessary for full mTORC1 activation (Yang et al., 2019). Finally, in the presence of AAs, LARS (leucyl-tRNA synthetase), a second GAP for RagD, controls its activation (Han et al., 2012). Collectively, the Rag GTPases constitute one of the main cellular hubs in a complex network of mTORC1 activation by AAs.

Importantly, the inactivation of mTORC1 upon AA starvation also occurs via the Rag GTPases. As described in previous sections, TSC is the main negative regulator of the pathway. As such, TSC is recruited to the lysosomal surface in the absence of AAs by direct binding to inactive RagA (Demetriades et al., 2014). Moreover, the mechanisms of TSC recruitment by binding to lysosomal PIPs and binding to G3BPs are also relevant upon AA starvation, as shown in Figure 1.3.

1.1.2.3.2 Amino acid sensors

After the discovery of the Rag GTPases, several studies unraveled a complex network of AA sensors that signal to activate mTORC1 (Figure 1.4).

v-ATPase

The response of mTORC1 to AA availability relies on the control of the lysosome-anchored Rag GTPases. The canonical role of the v-ATPase is in lysosomal acidification; however, the v-ATPase is also a core AA sensing component. It transduces the presence of lysosomal luminal AAs to mTORC1 activation via interaction with the LAMTOR complex and further activation of the Rag GTPases (Zoncu et al., 2011; Bar-Peled et al., 2012).

Arginine sensing

SLC38A9, a neutral amino acid transporter, is a lysosomal arginine sensor that can bind arginine and activate mTORC1 via the v-ATPase-LAMTOR complex axis (Jung et al., 2015; Rebsamen et al., 2015; Wang et al., 2015; Wyant et al., 2017a). Interestingly, SLC38A9 is important for the arginine-dependent release of leucine from lysosomes, highlighting the crosstalk between AAs that signal for mTORC1 activation (Wyant et al., 2017a). Additionally, arginine can be sensed by CASTOR1/2 (cytosolic arginine sensor for mTORC1). Upon arginine depletion, the CASTOR proteins interact with and inhibit GATOR2, leading to mTORC1 inactivation. When arginine is present, it binds to CASTOR1/2, releasing the inhibition of GATOR2 and activating mTORC1 (Chantranupong et al., 2016; Saxton et al., 2016a).

Leucine sensing

GATOR2 is also the converging point of leucine sensing. Similar to the CASTOR proteins, SESTRIN proteins bind and inactivate GATOR2 upon leucine deprivation (Chantranupong et al., 2014; Parmigiani et al., 2014). Leucine binds to SESTRIN2, releasing its inhibitory function on GATOR2 (Saxton et al., 2016b; Wolfson et al., 2016). Interestingly, SESTRINs were primarily found as stress response proteins (Budanov et al., 2002), and later on were also identified to negatively regulate mTORC1 via the AMPK-TSC2 axis (Budanov and Karin, 2008). These findings indicate that SESTRINs are part of a broader cellular response.

Additionally, leucine also activates mTORC1 via its aminoacyl-tRNA synthetase, LARS, a GAP for RagD (Han et al., 2012). An alternative sensing mechanism for leucine was proposed based on a metabolic derivative of leucine catabolism, expanding the spectrum of possible signaling cues. More specifically, the end product of leucine metabolism, acetyl-coenzyme A, signals leucine availability via RAPTOR acetylation, leading to mTORC1 activation (Son et al., 2019).

Methionine sensing

As observed for leucine, methionine sensing occurs via a metabolic product of its catabolism. SAM is a methionine-derived compound that functions as a methyl group donor. In contrast to leucine and arginine sensors, SAM does not signal via GATOR2. Instead, SAM binds to the protein SAMTOR (S-adenosylmethionine sensor upstream of mTORC1; also known as C7orf60), releasing the interaction of SAMTOR with GATOR1 and KICSTOR to promote mTORC1 activation (Gu et al., 2017).

Threonine sensing

Independently of the GATOR components, threonine was found to signal its sufficiency via TARS2 (mitochondrial threonyl-tRNA synthetase 2). Threonine binding to TARS2 stimulates RagC-GTP hydrolysis and GTP loading of RagA, promoting mTORC1 activation (Kim et al., 2021). However, since TARS2 does not have GEF domains, it is unlikely that it acts directly on RagA, raising the question whether TARS2 might signal through an unknown GEF.

Other AAs

As for leucine and methionine that signal to activate mTORC1 via their downstream metabolites, glutamine is able to activate mTORC1 in a Rag-dependent manner via α -ketoglutarate, a product of glutaminolysis, which also depends on the presence of leucine (Duran et al., 2012).

In addition to the aforementioned AAs, alanine, histidine, serine and valine are AAs that activate mTORC1 through the Rag GTPases (Kobayashi et al., 2014; Dyachok et al., 2016; Meng et al., 2020). Additionally, an intricate network of proteins coordinates AA-dependent activation of mTORC1: certain AAs are required for priming the complex for activation by others (Dyachok et al., 2016). Finally, additional AA sensors for the remaining AAs known to activate the pathway are likely to emerge with future investigations.

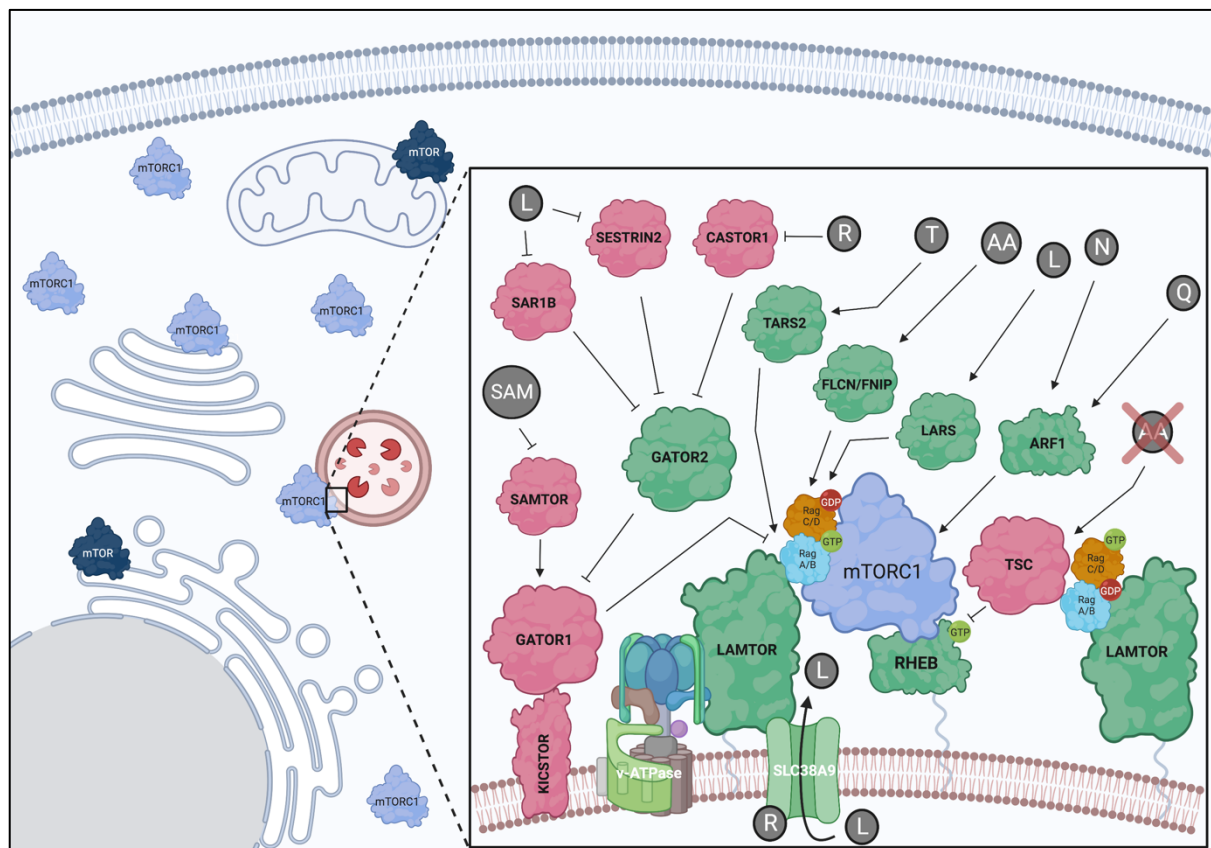


Figure 1.4 The mTORC1 regulatory network at the lysosomal surface.

Positive mTORC1 regulators shown in green and negative regulators shown in red. For more details, see section 1.1.2.3. Additional mTOR locations are also depicted. Adapted from Fernandes and Demetriades, 2021. Created with BioRender.com

1.1.2.3.3 Rag-independent mechanisms

Although most of the regulation of mTORC1 by AAs was described to occur via the Rag GTPases, a growing body of evidence has established the existence of Rag-independent mechanisms of mTORC1 activation. Of note, RagA/B knockout cardiomyocytes have impaired lysosomal function, with little change in the phosphorylation of mTORC1 substrates,

such as 4E-BP1 (Kim et al., 2014). Similar findings are observed in zebrafish RagA mutants, as well as in Rag knockout or knockdown cells (Demetriades et al., 2014; Efeyan et al., 2014; Kim et al., 2014; Jewell et al., 2015; Shen et al., 2016). Interestingly, glutamine re-addition acts independently of the Rag GTPases, although still relying on lysosomal localization of mTORC1 and v-ATPase activity (Jewell et al., 2015). Furthermore, the GTPase ARF1 (adenosine diphosphate ribosylation factor-1) mediates the localization and activation of mTORC1 at the lysosomes in a Rag-independent manner (Jewell et al., 2015). Additionally, glutamine-induced activation of mTORC1 signals via PLD1 (phospholipase D1), an enzyme linked to both mTOR complex stability and activity (Toschi et al., 2009; Yoon et al., 2011). Both PLD1 and α -ketoglutarate can also act via ARF1, supporting the evidence of ARF1-mediated mTORC1 activation (Bernfeld et al., 2018). However, further work is required to establish how α -ketoglutarate acts in concert in both a Rag-dependent and independent way (Duran et al., 2012; Bernfeld et al., 2018). Importantly, the mechanism of glutamine signaling to mTORC1 is conserved in yeast, where it signals independently of the Gtr proteins, the Rag orthologs (Stracka et al., 2014). Nonetheless, the candidate glutamine sensor in yeast, the protein Pib2 (phosphatidylinositol 3-phosphate-binding protein 2) (Ukai et al., 2018), is not conserved in humans, and the closest related proteins Phafin1 or R3HCC1 (R3H and coiled coil domain-containing protein 1) did not affect glutamine signaling to mTORC1 (Meng et al., 2020).

Apart from glutamine, asparagine is also capable of activating mTORC1 in Rag-depleted cells via an ARF1-dependent mechanism (Meng et al., 2020). However, to date, the mechanism of ARF1 action towards mTORC1 is unclear and further studies are needed to elucidate its precise function in mTORC1 activation. Although most of the aforementioned studies propose a lysosome-centric view of mTORC1 regulation, RAB1A (Ras-related protein Rab-1a), a GTPase involved in trafficking and a resident Golgi protein, acts in a Rag-independent manner to activate mTORC1 (Thomas et al., 2014). Furthermore, previous reports indicate that Rag GTPase-null cells have diffusely localized mTORC1 with only moderate impairment of mTORC1 activity, hinting to the involvement of other locations in mTORC1 activation (Efeyan et al., 2014; Kim et al., 2014; Jewell et al., 2015; Demetriades et al., 2016a; Shen et al., 2016). Collectively, those findings suggest that the regulation of mTORC1 by AAs is broader than currently thought and involves more players than those involved in the lysosomal AA sensing machinery that center around the Rag GTPases.

1.1.2.4 By localization

Even though most of the described activation of mTORC1 takes place on lysosomes, (Sancak et al., 2010), mTOR, its regulators and substrates are also found in other cellular compartments (Betz and Hall, 2013). Remarkably, mTOR itself is found on other organelles, such as Golgi, mitochondria and the ER (Schieke et al., 2006; Liu and Zheng, 2007; Ramanathan and Schreiber, 2009; Yadav et al., 2013; Gosavi et al., 2018). The Golgi is particularly relevant, since two Golgi proteins are mTORC1 substrates (Nuchel et al., 2021; Kaeser-Pebernard et al., 2022). mTORC1 is also found at FAs, a location recognized as a

hub for mTORC1 activation by GF and AAs (Rabanal-Ruiz et al., 2021). Additionally, many of the mTORC1 regulators and substrates are not exclusively lysosomal. RHEB, the indispensable mTORC1 activator, is enriched in many endomembranes, such as the Golgi, ER and peroxisomes (Buerger et al., 2006; Hanker et al., 2010; Yadav et al., 2013; Zhang et al., 2013; Gosavi et al., 2018; Hao et al., 2018; Angarola and Ferguson, 2019). TSC2, the main negative regulator of the pathway, is also found at the cytosol and peroxisomes (van Slegtenhorst et al., 1998; Nellist et al., 1999; Zhang et al., 2013). ARF1 and RAB1A are primarily involved in vesicle trafficking in the Golgi (Thomas et al., 2014; Jewell et al., 2015). Moreover, the mTORC1 substrates S6K1 and 4E-BP1 are cytoplasmic components that regulate translation, raising the possibility that active mTORC1 may localize in the cytoplasm to phosphorylate them (Holz et al., 2005; Zhou et al., 2015; Ahmed et al., 2019). Finally, the main requirement for mTORC1 activation is its encounter with RHEB. Considering that RHEB is enriched in multiple endomembranes, it is likely that mTORC1 activation can happen at additional subcellular locations, besides the lysosomal surface.

1.1.2.5 By post-translational modifications

As described in the previous sections, the mTORC1 pathway depends on events that occur at specific subcellular locations. In addition to localization, mTORC1 regulation also relies on PTMs (post-translational modifications) (Yin et al., 2021). Of note, a PTM that is predominant in mTORC1 pathway components is phosphorylation. For instance, GF signaling to mTORC1 requires phosphorylation of TSC2 by AKT (Inoki et al., 2002; Manning et al., 2002). Additionally, glucose signals partially by RAPTOR phosphorylation (Gwinn et al., 2008). mTOR is also subject to many phosphorylation events (Chiang and Abraham, 2005; Acosta-Jaquez et al., 2009; Ekim et al., 2011), albeit with less clear effects. Furthermore, mTORC1 itself is a kinase complex, hence, phosphorylation of its downstream substrates is the outcome of mTORC1 activation. Nonetheless, additional PTMs are also relevant for mTORC1 regulation. Over the recent years, ubiquitination was shown to control several factors in the mTORC1 pathway (Jiang et al., 2019; Sun et al., 2020).

1.1.2.5.1 Ubiquitination

Ubiquitin is a 76 amino-acid-long protein that is attached to certain targets as a PTM. Ubiquitination is a modification that occurs via formation of a covalent bond between the C-terminal glycine residue of ubiquitin and the amino group of a lysine residue of a substrate (Kliza and Husnjak, 2020). Ubiquitin can be attached as a monoubiquitin, where one molecule is added to a substrate. However, ubiquitin itself contains seven lysines, key residues that can be further ubiquitinated for the formation of ubiquitin chains. Ubiquitin can also form linear chains, which originate from consecutive ubiquitin molecules binding to the N-terminus of a ubiquitin molecule. Importantly, each of these modifications elicit a different response. For instance, the most common ubiquitin chain found in cells is the K48-linked, related to degradation of proteins via the proteasome system (Swatek and Komander, 2016). The second most common chain type is the K63-linked, which is a non-degradative modification that controls signaling pathways (Chen and Sun, 2009).

The addition of ubiquitin molecules to a target occurs via a cascade involving three classes of enzymes. E1 (E1 ubiquitin-activating enzyme) first binds and activates ubiquitin. Next, ubiquitin is transferred to the E2 (E2 ubiquitin-conjugating enzyme). The E3 (E3-ubiquitin ligase) then binds both the substrate and the E2 and transfers ubiquitin to the substrate (Komander and Rape, 2012). To date, two E1s, around 30 E2s and approximately 600 E3s have been identified (Kliza and Husnjak, 2020). Importantly, the large number of E3s reflects their substrate specificity. Notably, ubiquitination is a reversible modification. Hence, the termination of the signal that was initiated by ubiquitin addition is of equal relevance. The removal of ubiquitin molecules is catalysed by a class of enzymes called DUBs (deubiquitinases). Around 100 DUBs exist, with different modes of action. Some DUBs act directly by recognition of the chain type that is attached to a given protein, instead of recognizing the substrate protein itself (Mevisen and Komander, 2017). However, a DUB family called USP (ubiquitin-specific proteases) is known for their ability to engage in protein-protein interactions with their substrates (Mevisen and Komander, 2017). Intriguingly, most members of this family do not possess chain specificity (Faesen et al., 2011; Mevisen and Komander, 2017). One exception is the USP family member CYLD (ubiquitin carboxyl-terminal hydrolase CYLD), which can engage both in protein-protein interactions (Brummelkamp et al., 2003; Kovalenko et al., 2003; Trompouki et al., 2003; Saito et al., 2004) and specifically cleave K63-linked or linear ubiquitin chains (Komander et al., 2008; Komander et al., 2009).

CYLD is a tumor suppressor gene that is mutated in cylindromatosis, a disease characterized by benign skin tumors (Bignell et al., 2000). The CYLD enzyme is a DUB that negatively regulates the NF- κ B pathway, a key regulator of the inflammatory response (Figure 1.5) (Brummelkamp et al., 2003; Kovalenko et al., 2003; Trompouki et al., 2003). In the canonical NF- κ B (nuclear factor kappa B) pathway, TNF α binds to the TNFR (tumor necrosis factor receptor). This leads to the recruitment of the TNFR signaling complex, composed of TRADD (tumor necrosis factor receptor type 1-associated DEATH domain protein), cIAP1/2 (cellular inhibitor of apoptosis 1 and 2), RIPK1 (receptor-interacting serine/threonine-protein kinase 1) and TRAF2 (TNF receptor-associated factor 2) (Harhaj and Dixit, 2012). At this stage, TRAF2 is ubiquitinated and it recruits cIAP1/2 that further ubiquitinates RIPK1 (Bertrand et al., 2008; Mace et al., 2010; Zheng et al., 2010). RIPK1 ubiquitination is a platform for the ubiquitin-binding protein TAB2 (TGF-beta-activated kinase 1 and MAP3K7-binding protein 2), which together with TAB3 (TGF-beta-activated kinase 1 and MAP3K7-binding protein 3) recruits TAK1 (transforming growth factor- β -activated kinase 1) (Kanayama et al., 2004; Bertrand et al., 2008). TAK1 is a kinase that phosphorylates IKK β , a component of the IKK complex, promoting its activation (Wang et al., 2001; Adhikari et al., 2007). The IKK complex contains the catalytic subunits IKK α (inhibitor of NF- κ B kinase subunit alpha) and IKK β , and the regulatory subunit NEMO (NF- κ B essential modulator; also known as IKK γ). NEMO is also heavily ubiquitinated. This modification is important for the recruitment of the IKK complex to the proximity of the TNFR signaling complex (Ea et al., 2006). The active IKK complex

phosphorylates I κ B (NF- κ B inhibitor), a signal that induces its ubiquitination and proteasomal degradation. I κ B degradation allows for the nuclear translocation of NF- κ B components, inducing an inflammatory transcriptional program (Harhaj and Dixit, 2012; Wang et al., 2012). In this pathway, CYLD is essential, as it removes K63-linked ubiquitin chains from TRAF2 and NEMO to terminate the NF- κ B pathway activation (Brummelkamp et al., 2003; Kovalenko et al., 2003; Trompouki et al., 2003). Importantly, CYLD has also been linked to deubiquitination of proteins that are not in the NF- κ B pathway, such as AKT (Lim et al., 2012; Yang et al., 2013b) and ERK1 (mitogen-activated protein kinase 3) and ERK2 (mitogen-activated protein kinase 1) (Zhu et al., 2021), indicating that CYLD likely has a broader role in cells.

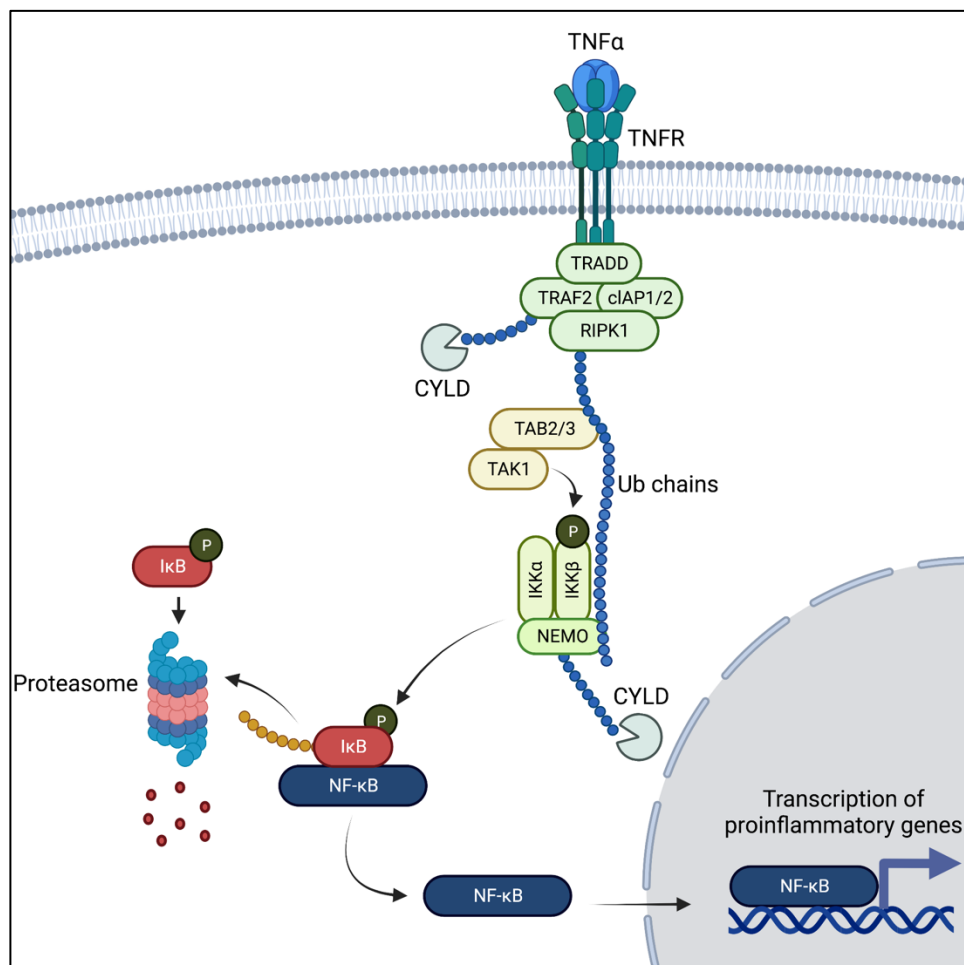


Figure 1.5 The NF- κ B pathway activated by TNF α and regulated by CYLD.

TNF α binds to its receptor at the plasma membrane. TRADD, TRAF2, cIAP1/2 and RIPK1 (the TNFR signaling complex) are recruited and RIPK1 is ubiquitinated. TAB2/3 act by binding to ubiquitinated RIPK1, further recruiting TAK1. TAK1 phosphorylates and activates IKK β , while NEMO interacts with ubiquitinated RIPK1 to bring the complexes in proximity. NEMO ubiquitination is necessary for its activity as a regulatory component of the IKK complex. Active IKK phosphorylates I κ B, which is targeted for proteasomal degradation. Without I κ B, NF- κ B translocates to the nucleus and promotes the transcription of proinflammatory genes. CYLD acts as a negative regulator of the pathway by removing ubiquitin chains on TRAF2 and NEMO. Blue circles represent K63-linked ubiquitin chains, yellow circles represent K48-linked chains. Created with BioRender.com

1.1.2.5.2 Regulation of the mTORC1 pathway by ubiquitination

The mTORC1 pathway is regulated by ubiquitination in many steps, both by degradative and regulatory ubiquitination events.

Ubiquitination of mTORC1 core components

mTOR is heavily ubiquitinated, with many ubiquitination sites across the protein (Figure 1.6). mTOR ubiquitination by the SCF (SKP, cullin, F-box containing complex)/FBXW7 (F-box/WD repeat-containing protein 7) or SCF/FBX8 (F-box only protein 8) ligase is linked to its degradation (Mao et al., 2008; Wang et al., 2017b). Additionally, upon AA stimulation, the E3 ubiquitin ligase TRAF6 (TNF receptor-associated factor 6) together with the adaptor protein p62, attaches K63-linked ubiquitin chains on mTOR. This ubiquitination event is important for mTOR lysosomal recruitment and activation (Linares et al., 2013b). Moreover, mTOR is ubiquitinated by the E3 ligase PARKIN, which is important for the maintenance of mTORC1 activity upon mitochondrial stress (Park et al., 2014). Altogether, these studies point to an important function of ubiquitin in the regulation of the mTOR protein. Nonetheless, although certain E3 ligases that participate in such reactions are known, no DUB was identified to act on mTOR to date.

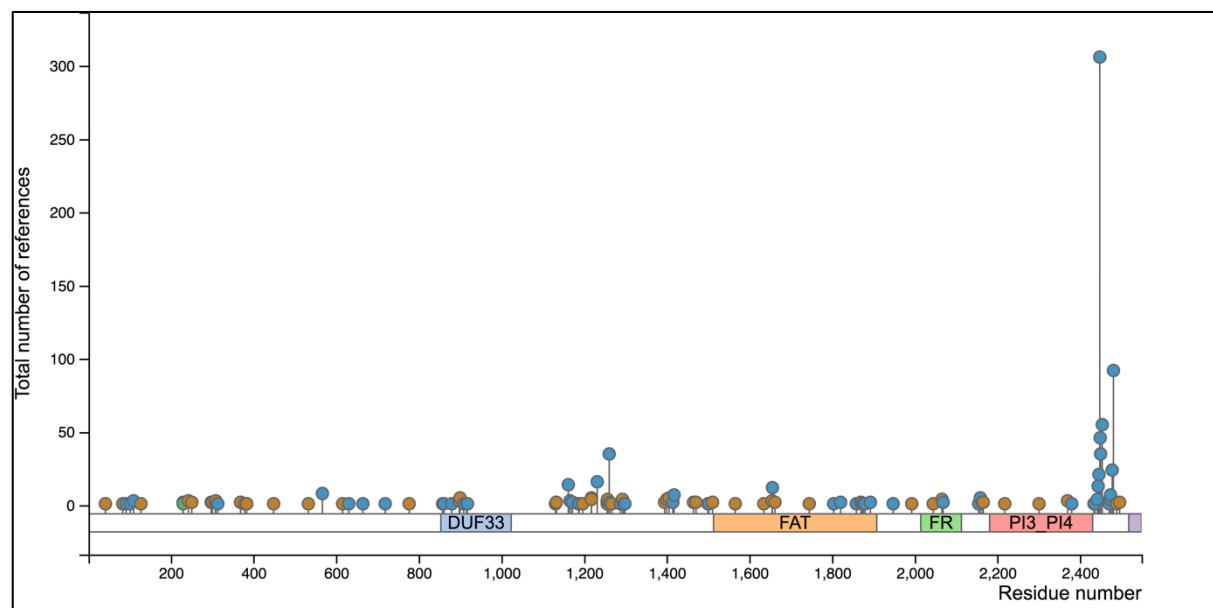


Figure 1.6 mTOR is a heavily ubiquitinated protein.

In the x-axis are the residue numbers, with the mTOR domains depicted in different colors. The y-axis is the total number of references in which each site was identified. Circles in orange are ubiquitination sites, in blue are phosphorylation sites and in green acetylation sites. Figure obtained from <https://www.phosphosite.org>.

Unlike for mTOR, both ligases and DUBs are known to act on other components of mTORC1. RAPTOR is ubiquitinated by the E3 ligase TRAF2, which is necessary for mTORC1 activity (Ye et al., 2021), and by DDB1-CUL4 (DNA damage-binding protein1-cullin-4) complex. Importantly, the latter ubiquitination event is counteracted by the DUB UCH-L1 (ubiquitin

carboxyl-terminal hydrolase isozyme L1) to control mTORC1 stability (Hussain et al., 2013). mLST8 is also ubiquitinated by TRAF2, weakening the interaction with mTORC2 and promoting instead mTORC1 formation. OTUD7B (OTU domain-containing protein 7B) removes such ubiquitin chains, favoring mTORC2 formation (Wang et al., 2017a). Finally, the inhibitory subunit of mTORC1, DEPTOR, is targeted for degradation by several Ub ligases. For instance, SCF (Duan et al., 2011; Gao et al., 2011; Zhao et al., 2011), SCF/RNF7 (RING-box protein 2) (Tan et al., 2016) and CUL5 (cullin-5) (Antonioli et al., 2014) are E3s that attach degradative ubiquitin signals to DEPTOR when mTORC1 is activated by different signals. When mTORC1 becomes inactive, the DUB OTUB1 (ubiquitin thioesterase OTUB1) (Zhao et al., 2018) acts on DEPTOR to promote its stabilization.

Ubiquitination of components of the AA sensing machinery

Many components of the mTORC1 AA sensing machinery are regulated by ubiquitination. LAMTOR1 is targeted for degradation by UBE3A (ubiquitin-protein ligase E3A) (Sun et al., 2018) and stability of the LAMTOR complex is also dictated by proteasomal degradation of LAMTOR3 (de Araujo et al., 2013). More recently, the DUB USP32 (ubiquitin carboxyl-terminal hydrolase 32) was shown to act on LAMTOR1, promoting its interaction with the v-ATPase (Hertel et al., 2022). RagA is ubiquitinated by RNF152 (E3 ubiquitin-protein ligase RNF152) upon acute AA starvation, promoting its association with GATOR1 and mTORC1 inactivation (Deng et al., 2015). Likewise, via RagA interaction with GATOR1, prolonged AA availability induces a negative feedback loop by the action of the E3 ligase SCF/SKP2 (S-phase kinase-associated protein 2) (Jin et al., 2015). Similarly, the GATOR1 component DEPDC5 is targeted for degradation by CUL3 (cullin-3)/KLHL22 (Kelch-like protein 22) when AAs are available (Chen et al., 2018a). Interestingly, GATOR2 has three components that contain RING (really interesting new gene) domains, common in E3 ligases. In the presence of leucine, the GATOR2 component WDR24 ubiquitinates and inactivates the GATOR1 component NPRL2 (Jiang et al., 2023). Importantly, ubiquitination is also a key event in the regulation of the AA sensors SESTRIN2 and CASTOR1. Upon leucine starvation, SESTRIN2 is ubiquitinated by RNF167 (E3 ubiquitin-protein ligase RNF167), which promotes its interaction with GATOR2, leading to its inhibition. Upon leucine binding, SESTRIN2 is deubiquitinated by STAMBPL1 (AMSH-like protease), releasing GATOR2 to activate mTORC1 (Wang et al., 2022). SESTRIN2 stability is also regulated by ubiquitination via RNF186 (E3 ubiquitin-protein ligase RNF186) (Lear et al., 2019). However, it is not clear how these two modes of SESTRIN2 ubiquitination work in concert. In a tumorigenic context, CASTOR1 ubiquitination by RNF167 is increased, leading to its degradation and further mTORC1 activation (Li et al., 2021). In sum, ubiquitination is a key modification in the control of the mTORC1 AA sensing machinery.

Ubiquitination of upstream regulators

One of the best-understood ubiquitination events on the mTORC1 signaling pathway is the control of TSC complex stability. TSC2 is a highly ubiquitinated protein, and many ligases act to promote its degradation. For instance, the ligases DDB1-CUL4-ROC1 (regulator of cullins-

1) (Hu et al., 2008), HERC1 (probable E3 ubiquitin-protein ligase HERC1) (Chong-Kopera et al., 2006), TRIM31 (E3 ubiquitin-protein ligase TRIM31) (Guo et al., 2018), PAM (E3 ubiquitin-protein ligase MYCBP2) (Han et al., 2008) and TRIM6 (tripartite motif-containing protein 6) (Liu et al., 2020) are all reported to ubiquitinate TSC2. However, it is not clear how they act in a concerted manner. TSC1 is also ubiquitinated, both for degradation (Guo et al., 2018; Liu et al., 2020; Ko et al., 2021) and in a K63-linked manner to control its interaction with TSC2 (Ko et al., 2021). Finally, the third component of the complex, TBC1D7 is also ubiquitinated and degraded (Madigan et al., 2018). Markedly, early reports hinted to the stabilization of TSC2 protein levels by its binding to TSC1 (Benvenuto et al., 2000). This effect is likely because TSC1 acts by preventing the interaction of TSC2 with E3 ligases (Chong-Kopera et al., 2006; Han et al., 2008).

Downstream of TSC is RHEB, an additional mTORC1 regulator that is controlled by ubiquitination. RHEB is ubiquitinated by RNF152 (E3 ubiquitin-protein ligase RNF152), promoting its binding to the TSC complex (Deng et al., 2019). Upon GF stimulation, RHEB is a substrate of the DUB USP4 (ubiquitin carboxyl-terminal hydrolase 4), promoting its release from TSC (Deng et al., 2019). In conditions of AA sufficiency, RHEB is ubiquitinated, facilitating its binding to mTOR. Upon AA starvation, the DUB ATXN3 (ataxin-3) is recruited to the lysosomal surface to deubiquitinate RHEB, participating in the mTORC1 inactivation (Yao et al., 2020).

Ubiquitination of mTORC1 substrates

mTORC1 substrates are not only regulated by phosphorylation, but also by ubiquitination. Phosphorylated TFEB is targeted by CHIP (E3 ubiquitin-protein ligase CHIP), leading to its degradation (Sha et al., 2017). In response to AA starvation, the autophagy protein AMBRA1 is dephosphorylated and interacts with the ligase TRAF6. This interaction induces ULK1 ubiquitination and stabilization (Nazio et al., 2013). Autophagy induction triggers ULK1 autophosphorylation, leading to recruitment of the E3 ligase CUL3-KLHL20 (Kelch-like protein 20), driving ULK1 to degradation in order to limit autophagy initiation (Liu et al., 2016). On the other hand, USP20 (ubiquitin carboxyl-terminal hydrolase 20) acts to deubiquitinate and stabilize ULK1 (Kim et al., 2018). Therefore, the observation that not only mTORC1 components and regulators are ubiquitinated, but also some of its substrates, highlights the crosstalk between different PTMs in controlling signaling pathways.

1.2 The mTOR complex 2

mTORC2 shares mTOR, mLST8 and DEPTOR as common subunits with mTORC1 (Liu and Sabatini, 2020). Nonetheless, mTORC2 has additional unique components. Instead of RAPTOR, its defining subunit is RICTOR (rapamycin-insensitive companion of mTOR) (Jacinto et al., 2004; Sarbassov et al., 2004), a scaffolding protein that binds to the mTOR HEAT domain. RICTOR interacts with mSIN1 (target of Rapamycin complex 2 subunit MAPKAP1), a protein required for mTORC2 substrate phosphorylation and complex formation (Frias et al., 2006; Jacinto et al., 2006; Yang et al., 2006). RICTOR also binds to

PROTOR1 (proline-rich protein 5) and PROTOR2 (proline-rich protein 5-like), although the function of this interaction is unclear (Pearce et al., 2007; Woo et al., 2007). As for mTORC1, mTORC2 dimerization is also important for its function (Chen et al., 2018b; Stuttfeld et al., 2018). Importantly, the structural positioning of RICTOR and mSIN1 renders mTORC2 insensitive to Rapamycin (Chen et al., 2018b; Stuttfeld et al., 2018).

1.2.1 mTORC2 functions

mTORC2 regulates cell survival and cell proliferation via phosphorylating members of the AGC kinase family.

Regulation of AKT

AKT is a protein kinase that regulates cell survival, metabolism and cell proliferation. Its activity is mainly mediated by the downstream phosphorylation of FOXO (forkhead box proteins) and GSK3, key molecules in the regulation of the aforementioned cellular processes (Manning and Toker, 2017). mTORC2 phosphorylates AKT on serine 473, in the AKT hydrophobic motif (Sarbasov et al., 2005). Moreover, the mTORC2-induced AKT phosphorylation acts by disrupting AKT autoinhibition (Chu et al., 2018). However, RICTOR or mSIN tissue-specific knockouts do not fully abrogate AKT activity (Jacinto et al., 2006; Moore et al., 2011; Hagiwara et al., 2012; Fu and Hall, 2020). These findings suggest that mTORC2-mediated AKT phosphorylation is required for its activity in a context specific manner. Additionally, full AKT activation requires phosphorylation on threonine 308 by PDK1 (Alessi et al., 1997). AKT also phosphorylates mSIN1, establishing a positive feedback loop to mTORC2 (Yang et al., 2015). Furthermore, AKT is also an important factor in the activation of mTORC1 by GFs, via phosphorylation of TSC2, establishing a link between mTORC1 and mTORC2 (Inoki et al., 2002).

Regulation of SGK1

mTORC2 also phosphorylates SGK1 (serine/threonine-protein kinase SGK1) in its hydrophobic motif, promoting its kinase activity. SGK1 has similar targets to AKT, such as the FOXO proteins, and it is also involved in cell proliferation and survival. Importantly, in mouse fibroblasts lacking Rictor, mSin1 or mLst8, SGK1 activity is abolished (Garcia-Martinez and Alessi, 2008). This is also confirmed by the lack of NDRG1 (N-myc downstream-regulated gene 1 protein) phosphorylation, a target of SGK1, which directly reflects the activation status of mTORC2 (Garcia-Martinez and Alessi, 2008). Importantly, SGK1 binding to mTORC2 induces a conformational change that is not seen upon binding to AKT, indicating that mTORC2 might have different modes of action in a substrate-specific way (Yu et al., 2022).

1.2.2 mTORC2 regulation

1.2.2.1 By growth factors

The best characterized stimulus that activates mTORC2 is GF availability. A study that used phosphorylated AKT on serine 473 as a reporter, showed that mTORC2 is mainly active at the PM (Ebner et al., 2017). mSIN1 contains a PH (pleckstrin-homology) domain, characterized for its phosphoinositide-binding activity. Upon GF stimulation, PI3K phosphorylates PI(4,5)P₂ (phosphatidylinositol-4,5-bisphosphate) at the PM, generating PI(3,4,5)P₃ (phosphatidylinositol-3,4,5-trisphosphate). The PH domain of mSIN1 binds to PI(3,4,5)P₃, releasing the mTORC2 autoinhibition and allowing AKT phosphorylation (Gan et al., 2011; Liu et al., 2015). The reverse reaction from PI(3,4,5)P₃ to PI(4,5)P₂ is catalyzed by PTEN (phosphatidylinositol 3,4,5-trisphosphate 3-phosphatase and dual-specificity protein phosphatase PTEN), fine-tuning GF signaling (Fu and Hall, 2020).

1.2.2.2 By post-translational modifications

As described in the previous sections, mTORC2 participates in a signaling pathway regulated by multiple phosphorylation events. However, as for mTORC1, many components of the mTORC2 pathway are also regulated by ubiquitination.

Ubiquitination of mTORC2 core components

RICTOR is ubiquitinated and degraded via the proteasome by action of the SCF/FBXW7 ligase (Koo et al., 2015). Intriguingly, this ubiquitination event is induced by RICTOR phosphorylation by GSK3, creating a phospho-degron that is recognized by the aforementioned ligase (Koo et al., 2015). GSK3 is a target of AKT, and this mechanism likely contributes to a feedback loop comprised of both phosphorylation and ubiquitination events. Recently, RICTOR ubiquitination was shown as a determinant of the formation of mTORC2. RICTOR deubiquitination is regulated by the DUB USP9X (probable ubiquitin carboxyl-terminal hydrolase FAF-X). Deubiquitinated RICTOR has increased interaction with mTOR (Wrobel et al., 2020). Importantly, the expression of USP9X was induced in the presence of GFs, connecting GF availability to mTORC2 assembly (Wrobel et al., 2020). As described in section 1.1.2.5.2, an additional determinant of mTORC2 assembly is the ubiquitination status of mLST8 (Wang et al., 2017a). Hence, further studies are required to reconcile these findings. Moreover, other common components of mTORC1 and mTORC2 are mTOR and DEPTOR, and their ubiquitination status is relevant for their function, as discussed in section 1.1.2.5.2.

Ubiquitination of mTORC2 upstream regulators

PI3K is a complex formed by p85 (phosphatidylinositol-3-kinase regulatory subunit) and the p110 (phosphatidylinositol-4,5-bisphosphate-3-kinase catalytic subunit). Non-phosphorylated p85 is ubiquitinated by SCF/FBX12 (F-box/LRR-repeat protein 12) and targeted to degradation (Kuchay et al., 2013). p85 is also targeted for degradation by the E3 ligase complex HSP70 (heat shock 70kDa protein)/CHIP (Ko et al., 2014), as well as by the non-degradative and activating ubiquitination by TRAF6 (Hamidi et al., 2017). The subunit p110

is targeted by NEDD4L (E3 ubiquitin-protein ligase NEDD4-like) for degradation, decreasing PI3K activity (Wang et al., 2016).

Ubiquitination of mTORC2 substrates

AKT promotes cell survival and proliferation, thus, disturbances in its activity are linked to the development of many cancers. For this reason, AKT activity is tightly regulated in cells. To limit AKT activation, cells employ mechanisms in which active, double phosphorylated AKT (on threonine 308 and serine 473), is targeted to degradation (Jiang et al., 2019). Many E3 ligases act on AKT, such as TTC3 (E3 ubiquitin-protein ligase TTC3) (Suizu et al., 2009), MULAN (mitochondrial ubiquitin ligase activator of NF- κ B 1) (Bae et al., 2012), RFP2 (E3 ubiquitin-protein ligase TRIM12) (Joo et al., 2011), BRCA1 (breast cancer type 1 susceptibility protein) (Xiang et al., 2008), CHIP (Su et al., 2011) and ZNRF1 (E3 ubiquitin-protein ligase ZNRF1) (Wakatsuki et al., 2011). The existence of many E3s acting on the same target might hint to tissue and cell-type specificity of such E3s. In addition, AKT is also ubiquitinated with K63-linked chains by TRAF6 (Yang et al., 2009), NEDD4 (E3 ubiquitin-protein ligase NEDD4) (Fan et al., 2013) and SCF/SKP2 (Chan et al., 2012), modifications that are important for AKT activation in response to different stimuli. Furthermore, in many cancer settings, other ligases act to ubiquitinate AKT in response to specific GFs, amplifying AKT activity (Li et al., 2013; Zhang et al., 2017). K63-linked polyubiquitination on AKT is removed by CYLD, USP1 (ubiquitin carboxyl-terminal hydrolase 1) and OTUD5 (OTU domain-containing protein 5), terminating the signal for AKT activation (Lim et al., 2012; Yang et al., 2013b; Yin et al., 2019; Goldbraikh et al., 2020).

SGK1 activity is controlled by degradative ubiquitination. SGK1 is targeted for degradation by the E3 ligases NEDD4L (Zhou and Snyder, 2005) and CHIP (Belova et al., 2006). Additionally, RICTOR associates with CUL1 (cullin-1) to form a functional E3 ligase complex that ubiquitinates and targets SGK1 for degradation (Gao et al., 2010). This mechanism shows that besides the action of mTORC2 on SGK1, the mTORC2 component RICTOR can also regulate SGK1 via controlling its levels.

Many studies over the years have established an essential role for ubiquitination of mTOR pathway components, regulators and substrates. However, the lack of DUBs for some proteins, such as mTOR, show that the network of ubiquitin regulators in the mTOR pathways likely is more complex than what is currently known.

1.3 Aims of the thesis

mTOR is a protein kinase present in two distinct complexes: mTORC1 and mTORC2. These regulate processes essential for cellular homeostasis, such as growth, survival and proliferation. Therefore, dysregulation of the activity of either complex is linked to conditions, such as cancer, neurodegeneration and aging (Liu and Sabatini, 2020; Fernandes and Demetriades, 2021; Querfurth and Lee, 2021). Thus, understanding how mTOR is regulated in cells is essential for advancing our understanding about disease etiology, as well as for the development of more targeted therapeutic approaches. In the context of this thesis, I aimed to shed light on the cell biology of mTOR regulation.

Aim 1: Exploring the relationship between the subcellular localization of mTORC1 and its activity towards various substrates and cellular processes

AAs are the strongest stimulus that activates mTORC1. According to the current consensus in the field, AAs regulate mTORC1 exclusively on lysosomes, from where mTOR is supposed to control the phosphorylation of all of its substrates and to regulate all cellular functions. Although work over the past 15 years described the existence of numerous regulators of the mTORC1 lysosomal AA sensing machinery, the reason why mTORC1 activity is specifically regulated on lysosomes by exogenous nutrients remains an open question. Hence, I aimed to investigate the teleonomy of the localization of mTORC1 to lysosomes.

Despite the described regulation of mTORC1 on lysosomes, a large body of evidence suggests that the full picture is likely more complex: mTOR itself and several of its regulators are also found in other subcellular locations (Betz and Hall, 2013). Given that mTORC1 is not exclusively present on lysosomes, I additionally aimed to investigate whether mTORC1 is active elsewhere. Furthermore, mTORC1 substrates reside in distinct subcellular locations: for instance, TFEB is found on lysosomes, whereas S6K1 and 4E-BP1 are cytosolic proteins. These observations suggest that mTORC1 is likely active also away from lysosomes. Therefore, I further aimed to explore the relationship between mTORC1 localization and its activity towards its different substrates.

Aim 2: Investigating the regulation of mTOR by ubiquitination

The mTOR-related pathways are heavily regulated by PTMs, such as phosphorylation and ubiquitination, on multiple signaling components. Over the previous years, several studies showed that the mTOR kinase, mTORC1 and mTORC2 components, as well as many of their regulators are ubiquitinated (Jiang et al., 2019). As described above, mTOR is a protein whose levels and activation by AAs is modified by the addition of ubiquitin chains. Notably, although four E3 ligases that attach ubiquitin chains to mTOR have been reported in the literature, no DUB enzyme that reverses mTOR ubiquitination is known to date. Thus, in the second part of this thesis, I aimed to identify the DUB for mTOR.

2 Results

Part I: Spatially and Functionally Distinct mTORC1 Entities Orchestrate the Cellular Response to Amino Acid Availability

2.1 Cells have basal lysosomal degradative capacity

According to the current consensus and previous data from our group and others, a large fraction of mTORC1 is found at the lysosomal surface in the presence of AAs. To investigate whether the lysosomal localization of mTORC1 is dependent on lysosomal activity and on the consequent nutrient release from lysosomes, I sought to determine whether cells cultured in the presence of AAs have basal lysosomal degradation. HEK293FT (Human embryonic kidney) cells were treated with the v-ATPase inhibitor BafA1 (Bafilomycin A1), a drug that blocks lysosomal acidification, consequently blocking lysosomal activity. To investigate whether BafA1 treatment leads to changes in lysosomal degradative capacity, I assessed the levels of known autophagy markers, which are proteins that are delivered and degraded at the lysosomes in the last step of autophagy. BafA1 treatment led to accumulation of the autophagosome marker LC3B, as well as of the autophagic adaptor protein p62, observed by immunofluorescence (Figure 2.1a-d). Furthermore, BafA1 treatment induced the accumulation of the autophagy adaptors TAX1BP1 and NBR1, as well as of the lipid-conjugated form of LC3B, LC3B-II (Figure 2.1e). Taken together, these data indicate that, even in the presence of exogenous AAs, HEK293FT cells show basal protein degradation inside lysosomes. Importantly, MEFs (murine embryonic fibroblasts) also display an increase in LC3B upon BafA1 treatment (Figure 2.2), highlighting that this process is not specific for a cell type or species.

2.2 Lysosomal degradative capacity is tightly linked to mTOR localization and mTORC1 activity towards specific substrates

2.2.1 Lysosomal function is required for mTOR lysosomal localization and TFEB phosphorylation

Since cells have basal lysosomal function, I aimed to understand whether lysosomal activity contributes to the mTORC1 localization at lysosomes. I focused on the condition where cells are basally cultured in the presence of AAs. However, to evaluate if distinct treatment strategies impact the pathway differently, I also assessed mTORC1 localization and activity during AA starvation or add-back conditions. In the presence of AAs, either basal or add-back conditions, a fraction of mTOR colocalizes with LAMP2, a lysosomal marker, while another fraction shows diffuse cytosolic localization (Figure 2.3a-b). Importantly, treatment with BafA1 led to delocalization of mTOR from lysosomes in all conditions tested (Figure 2.3a-b), supporting the hypothesis that mTOR lysosomal localization requires proper lysosomal function.

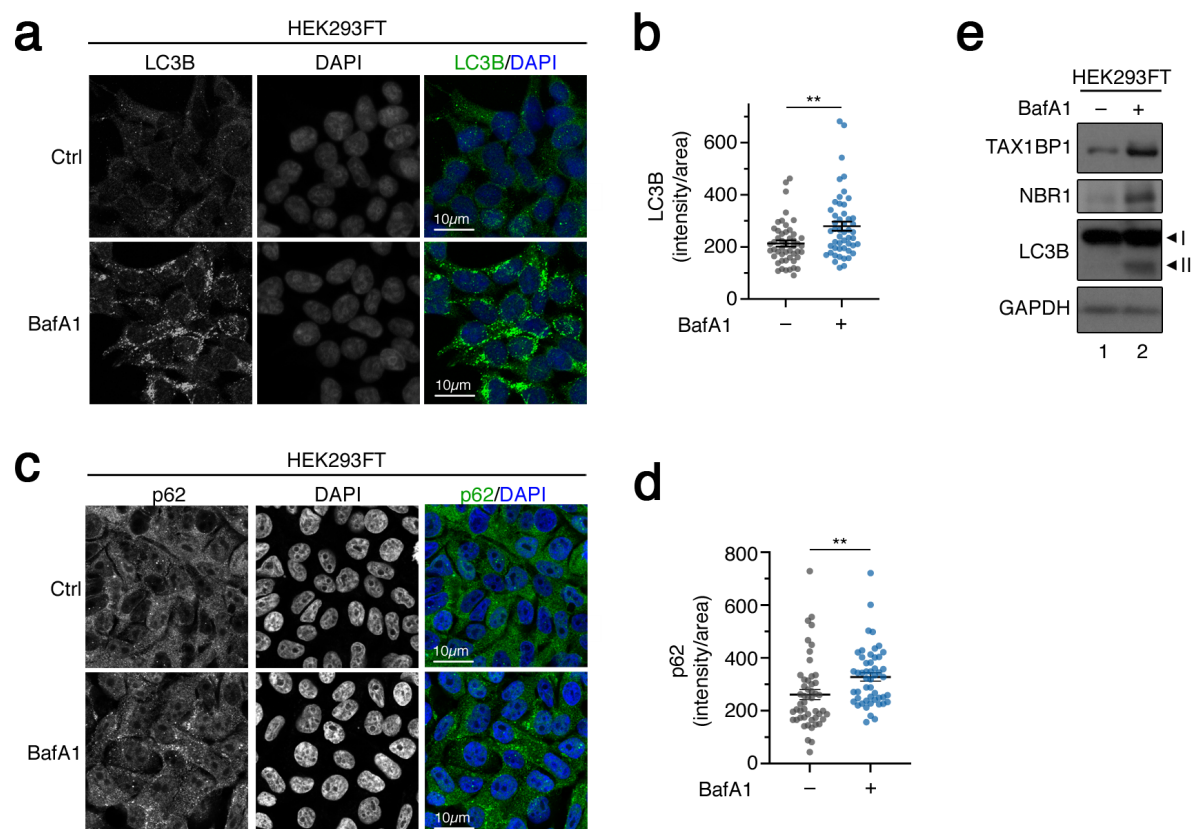


Figure 2.1 Human cells have basal protein degradation inside lysosomes.

(a-b) HEK293FT cells stained for LC3B and DAPI (4',6-Diamidino-2-phenylindol) in the presence or absence of BafA1. LC3B signal intensity is quantified in (b) from 50 cells of 5 different fields.

(c-d) HEK293FT cells stained for p62 and DAPI in the presence or absence of BafA1. p62 signal intensity is quantified in (d) from 50 cells of 5 different fields.

(e) Western blots from HEK293FT lysates treated with BafA1, probed with the indicated antibodies and GAPDH as a loading control. Arrowheads indicate different forms of a protein. Scale bars: 10µm. Data in (b) and (d) are shown as mean ± SEM, ** p<0.01.

Data shown are representative of 3 independent biological replicates. Arrowheads indicate different forms of a protein. Scale bars: 10µm. Data in (b) and (d) are shown as mean ± SEM, ** p<0.01.

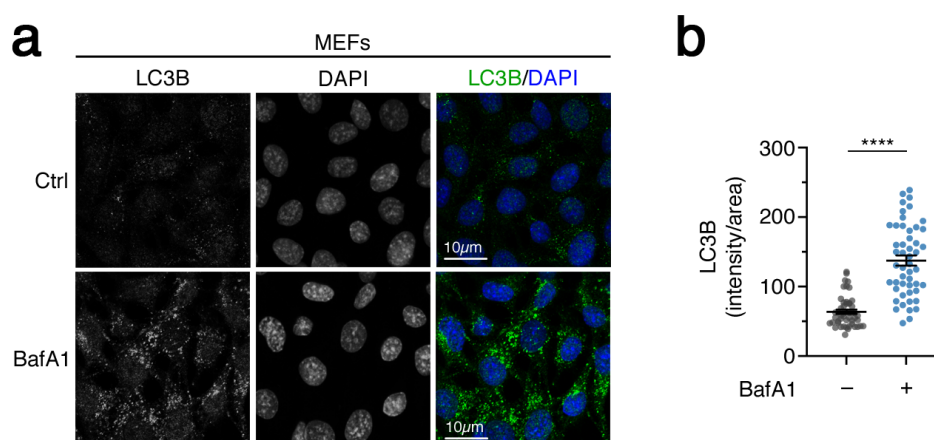


Figure 2.2 Mouse cells have basal protein degradation inside lysosomes.

(a-b) MEF cells stained for LC3B and DAPI, treated with BafA1. LC3B signal intensity is quantified in (b) from 50 cells of 5 different fields.

Data shown are representative of 3 independent biological replicates. Scale bars: 10µm. Data in (b) is shown as mean ± SEM, **** p<0.0001.

Next, I investigated whether the changes in mTOR lysosomal localization are reflected in mTORC1 activity towards its substrates TFEB, S6K and 4E-BP1. Surprisingly, BafA1 treatment led to complete loss of TFEB phosphorylation in all conditions. On the contrary, phosphorylation of S6K and 4E-BP1 was unaffected by BafA1 treatment in cells basally cultured with AAs (Figure 2.3c). During AA starvation, their phosphorylation decreased as expected (Figure 2.3c). However, and in line with a previous report (Fedele and Proud, 2020), BafA1 treatment in the add-back condition led to a partial reduction in the phosphorylation of S6K and 4E-BP1 (Figure 2.3c). These data indicate that, after a period of starvation, cells require lysosomal function for the acute re-activation of mTORC1 towards these substrates.

To further examine if lysosomal activity is required for mTOR localization at lysosomes and for substrate-specific changes on mTORC1 activity, I used two additional inhibitors of lysosomal acidification: ConA (Concanamycin A) and Chloroquine. Similar to BafA1, ConA is an inhibitor of v-ATPase activity that leads to alkalinization of lysosomes and inhibition of lysosomal activity. Accordingly, treatment with ConA led to delocalization of mTOR from lysosomes (Figure 2.4a-b) and abrogation of TFEB phosphorylation in all conditions (Figure 2.4c). Interestingly, the decrease of S6K and 4E-BP1 phosphorylation upon starvation of AAs was partially blunted by ConA (Figure 2.4c), indicating that this drug might affect mechanisms of mTORC1 inactivation. Additionally, ConA also induced a partial decrease on the re-phosphorylation of S6K and 4E-BP1 in the add-back condition (Figure 2.4c). Because the v-ATPase was shown to be part of the AA sensing machinery that is required for mTORC1 activation at the lysosomes (Zoncu et al., 2011), I sought to interfere with lysosomal function in a v-ATPase-independent manner. HEK293FT cells were treated with Chloroquine, an agent that sequesters protons inside lysosomes, causing lysosomal alkalinization and changes in lysosomal function. As with the aforementioned treatments, Chloroquine induced delocalization of mTOR from lysosomes (Figure 2.5a-b) and complete loss of TFEB phosphorylation (Figure 2.5c). On the other hand, Chloroquine had a partial effect on S6K and 4E-BP1 phosphorylation in basal conditions (Figure 2.5c), which might be due to the higher concentrations and consequent toxicity of Chloroquine in comparison to BafA1 and ConA. Furthermore, as with BafA1 and ConA, Chloroquine treatment led to a decrease in S6K and 4E-BP1 in the add-back condition (Figure 2.5c). Overall, these results show that cells require lysosomal function for maintaining mTOR lysosomal localization and mTORC1 activity towards TFEB in all conditions. On the contrary, the mTORC1 substrates S6K and 4E-BP1 are regulated differently: their phosphorylation is unaffected by changes in lysosomal activity under exogenous AA sufficiency, but is partially reduced during re-addition of AAs after starvation.

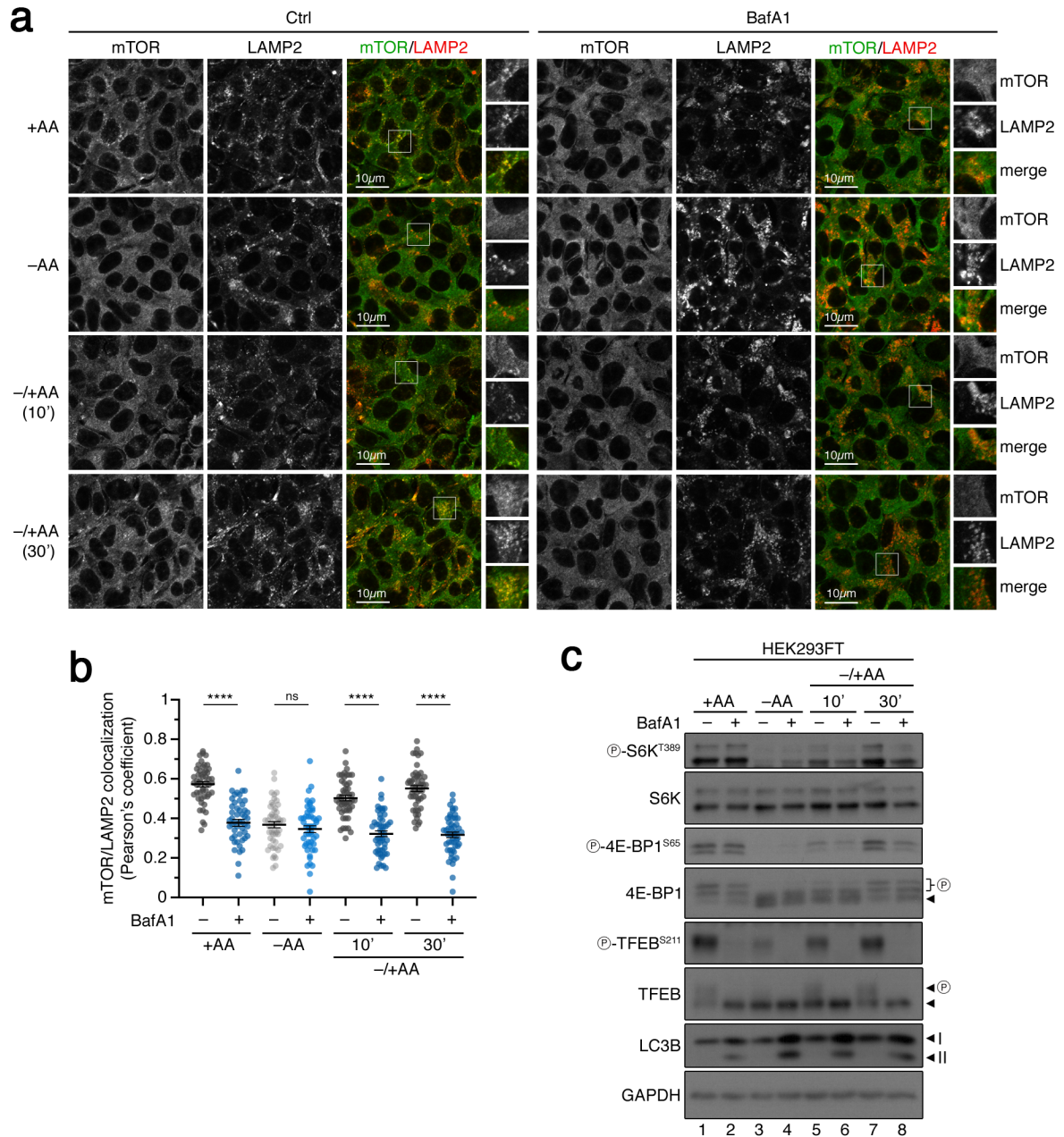


Figure 2.3 Blockage of lysosomal function leads to mTORC1 delocalization from lysosomes and substrate-specific changes on its activity.

(a-b) HEK293FT cells stained for mTOR and LAMP2 (lysosomal marker) in the presence or absence of BafA1, treated with media containing or lacking AAs, in basal (+AA), starvation (-AA) or add-back (-/+AA) conditions. mTOR colocalization with LAMP2 quantified in (b) from 50 cells of 5 different fields. (c) Western blots from HEK293FT lysates in the presence or absence of BafA1 treated with media containing or lacking AAs, in basal (+AA), starvation (-AA) or add-back (-/+AA) conditions, probed with the indicated antibodies and GAPDH as a loading control.

Data shown are representative of 3 independent biological replicates. Arrowheads indicate different forms of a protein, P: phosphorylated form. Scale bars: 10µm. Data in (b) is shown as mean ± SEM, **** p<0.0001, ns non-significant.

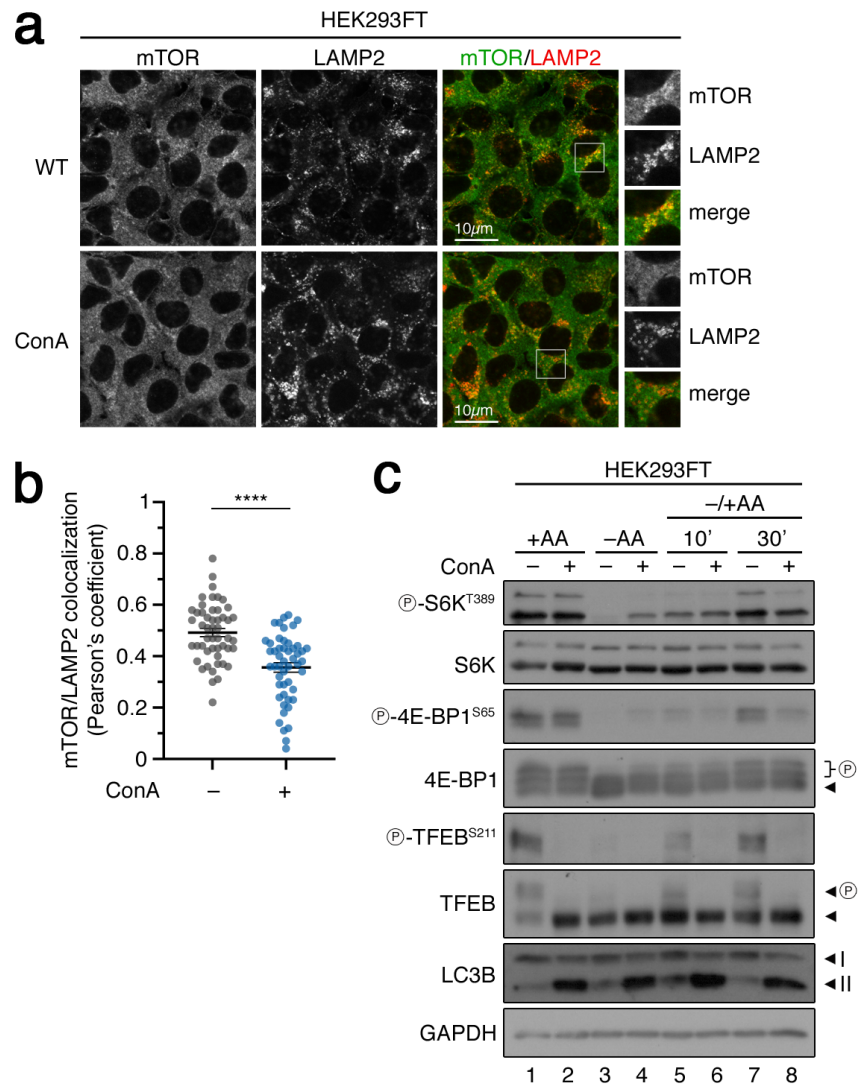


Figure 2.4 Blockage of lysosomal function with ConA leads to mTORC1 delocalization from lysosomes and substrate-specific changes on its activity.

(a-b) HEK293FT cells stained for mTOR and LAMP2 (lysosomal marker) in the presence or absence of ConA. mTOR colocalization with LAMP2 quantified in (b) from 50 cells of 5 different fields.

(c) Western blots from HEK293FT lysates in the presence or absence of ConA treated with media containing or lacking AAs, in basal (+AA), starvation (-AA) or add-back (-/+AA) conditions, probed with the indicated antibodies and GAPDH as a loading control.

Data shown are representative of 3 independent biological replicates. Arrowheads indicate different forms of a protein, P: phosphorylated form. Scale bars: 10µm. Data in (b) is shown as mean ± SEM, **** p<0.0001.

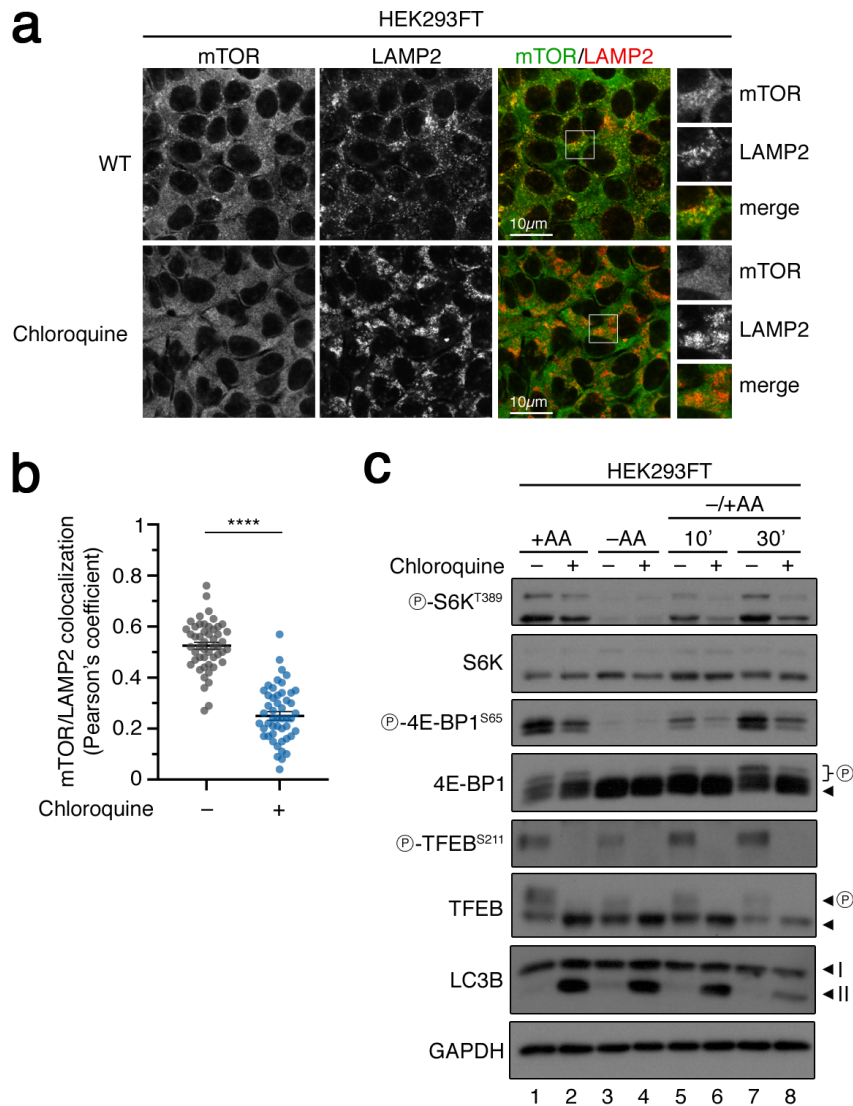


Figure 2.5 Blockage of lysosomal function with Chloroquine leads to mTORC1 delocalization from lysosomes and substrate-specific changes on its activity.

(a-b) HEK293FT cells stained for mTOR and LAMP2 (lysosomal marker) in the presence or absence of Chloroquine. mTOR colocalization with LAMP2 quantified in (b) from 50 cells of 5 different fields.

(c) Western blots from HEK293FT lysates in the presence or absence of Chloroquine treated with media containing or lacking AAs, in basal (+AA), starvation (-AA) or add-back (-/+AA) conditions, probed with the indicated antibodies and GAPDH as a loading control.

Data shown are representative of 3 independent biological replicates. Arrowheads indicate different forms of a protein, P: phosphorylated form. Scale bars: 10µm. Data in (b) is shown as mean ± SEM, **** p<0.0001.

2.2.2 BafA1 has a rapid and specific effect towards lysosomal mTORC1 substrates

Considering that BafA1 treatment induces changes in phosphorylation of TFEB but not in S6K/4E-BP1 in basal conditions, I next evaluated whether changes in the latter might happen in different time points than what is needed for observing changes in TFEB. To analyze the effect of BafA1 over time, I first treated cells from two to eight hours and observed that as

early as at two hours, mTOR is delocalized from lysosomes (Figure 2.6a-b). Subsequently, I evaluated the phosphorylation of mTORC1 substrates upon BafA1 treatment from one to eight hours. TFEB phosphorylation was diminished as early as at two hours, and largely abolished from four hours onwards (Figure 2.6c-e). Strikingly, phosphorylation of S6K and 4E-BP1 was unaffected in all time points tested (Figure 2.6c-d). Taken together, our results point to the requirement of lysosomal function and mTOR lysosomal localization for the phosphorylation of TFEB, but not of the S6K and 4E-BP1 substrates in basal conditions.

One major feature of TFEB is the requirement of lysosomal recruitment for its phosphorylation by mTORC1. To evaluate whether other mTORC1 substrates that have the same subcellular localization behave in a similar manner to TFEB, I established an experimental setup to assess RagC phosphorylation, another known lysosome localized protein. First, I checked whether RagC lysosomal localization was preserved upon BafA1 treatment. Importantly, no changes in RagC localization were observed (Figure. 2.7a-b). To analyze the phosphorylation status of RagC, I made use of an antibody that differentially recognizes the phosphorylated from the non-phosphorylated form of RagC (RagC antibody #5466). I treated HEK293FT cells with Torin1, a potent mTOR inhibitor, and probed for RagC using the aforementioned antibody. Importantly, RagC immunoblotting showed increased signal upon mTOR inhibition (Figure 2.7c), confirming the detection of unphosphorylated RagC in an mTOR-dependent manner. RagC phosphorylation status was further evaluated in the presence or absence of BafA1 during basal, starvation or add-back of AAs, and the non-phosphorylated form of RagC was more abundant in all samples treated with BafA1 (Figure 2.7d). Collectively, these data show that phosphorylation of RagC, a second lysosomal mTORC1 substrate, is also diminished by alterations in lysosomal function and mTOR lysosomal localization.

To further confirm that S6K and 4E-BP1 are not affected by BafA1 treatment, I assessed phosphorylation of S6, a protein that is directly phosphorylated by S6K, as well as another phosphorylation site on 4E-BP1, and I did not observe changes upon BafA1 treatment (Figure 2.7e). To test whether the persistent mTORC1 activity in BafA1-treated cells is restricted towards S6K and 4E-BP1, I additionally assessed phosphorylation of other mTORC1 substrates that are also cytoplasm-resident proteins, such as ULK1 and GRB10. Importantly, they were only mildly affected by BafA1 treatment, unlike TFEB that showed complete loss of phosphorylation (Figure 2.7e). mTORC1 activity is tightly regulated by a variety of upstream signaling components, some of which act as positive regulators, such as AKT and RHEB, while others as negative regulators, like PTEN, TSC1 or TSC2. To assess whether changes in the expression of positive or negative regulators could explain the sustained activity of mTORC1 towards cytosolic substrates, I investigated how protein levels are affected upon BafA1 treatment and observed no consistent changes (Figure 2.8). Therefore, our findings support a model whereby lysosomal function and mTOR lysosomal localization are not required for mTORC1 activity towards cytosolic substrates in basal culture conditions.

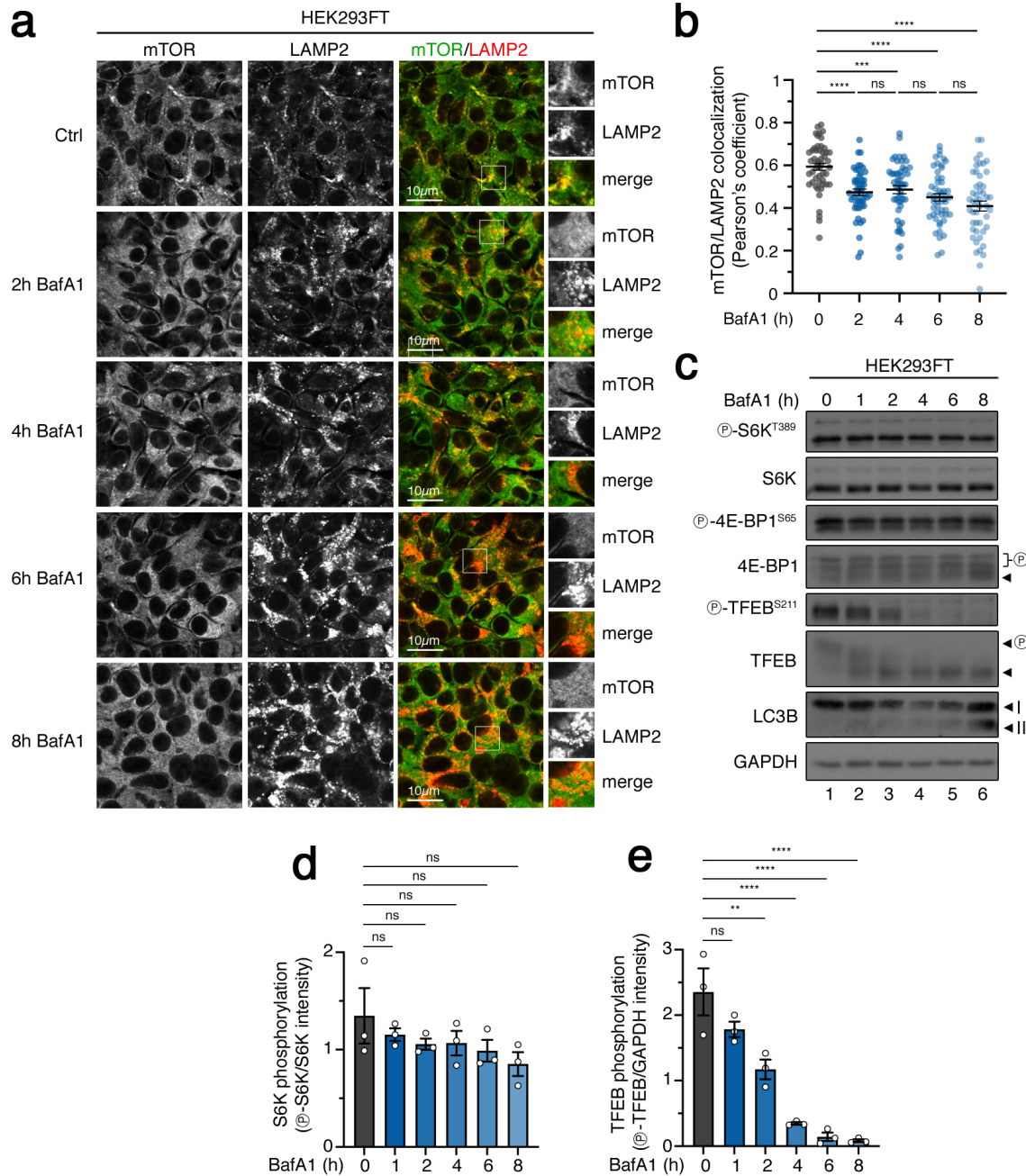


Figure 2.6 Short-term blockage of lysosomal function leads to mTORC1 delocalization from lysosomes and substrate-specific changes on its activity.

(a-b) HEK293FT cells stained for mTOR and LAMP2 (lysosomal marker) in the presence or absence of BafA1, treated for the indicated times. mTOR colocalization with LAMP2 quantified in (b) from 50 cells of 5 different fields.

(c-e) Western blots from HEK293FT lysates treated with BafA1 for the pointed times, probed with the indicated antibodies and GAPDH as a loading control. Quantification of mTORC1 activity (d) p-S6K^{T389}/S6K and (e) p-TFEB^{S211}/GAPDH, n=3.

Data shown are representative of 3 independent biological replicates. Arrowheads indicate different forms of a protein, P: phosphorylated form. Scale bars: 10µm. Data in (b), (d) and (e) are shown as mean ± SEM, ** p<0.01, *** p<0.001, **** p<0.0001, ns non-significant.

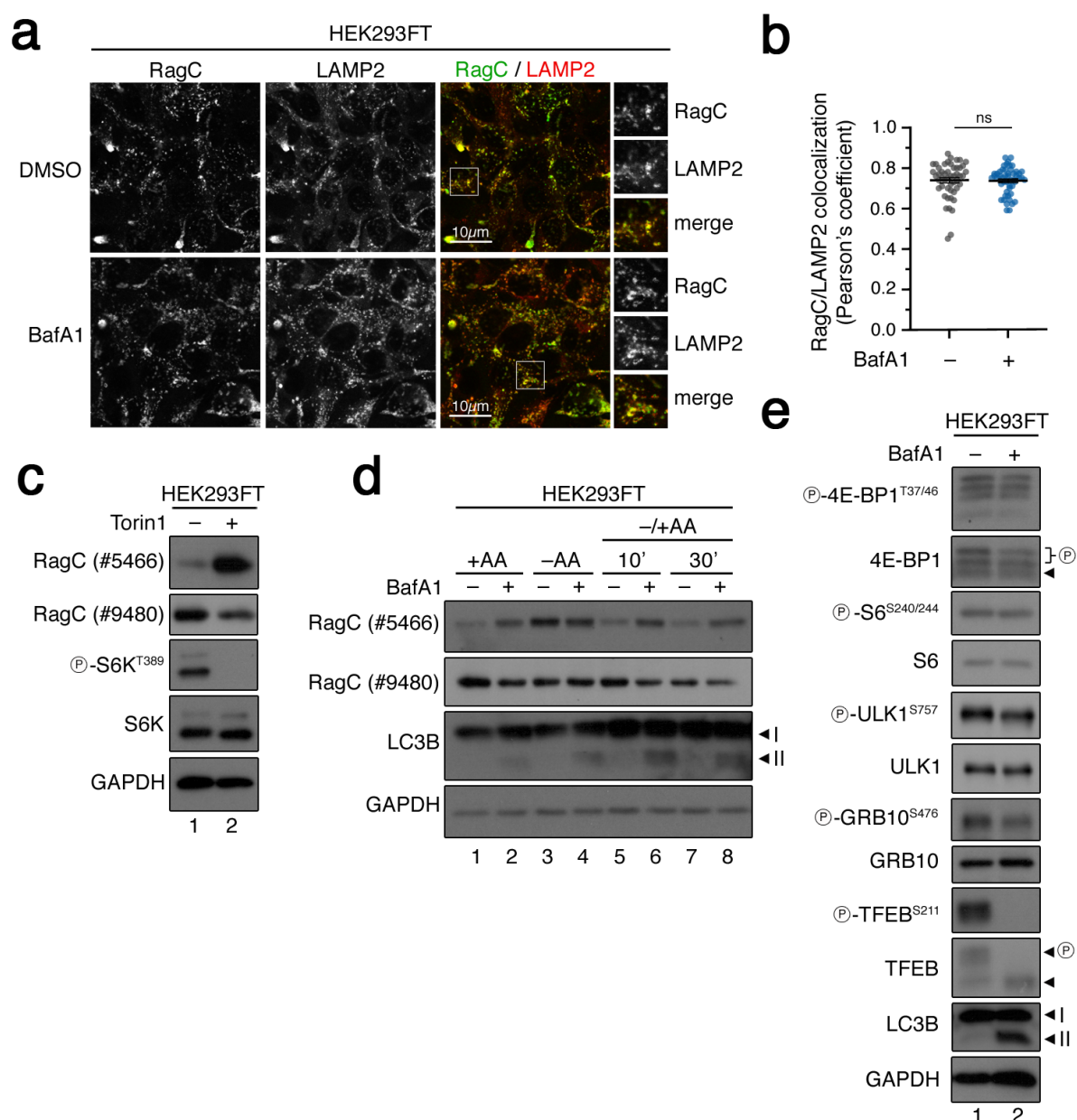


Figure 2.7 Blockage of lysosomal function affects mTORC1 activity towards the lysosomal substrate RagC but not of cytosolic substrates.

(a-b) HEK293FT cells stained for RagC and LAMP2 (lysosomal marker) in the presence or absence of BafA1, treated for the indicated times. RagC colocalization with LAMP2 quantified in (b) from 50 cells of 5 different fields.

(c) Western blots from HEK293FT lysates treated with Torin1, probed with the indicated antibodies and GAPDH as a loading control. RagC (#5466) refers to the RagC antibody sensitive to RagC phosphorylation status.

(d) Western blots from HEK293FT lysates in the presence or absence of BafA1 treated with media containing or lacking AAs, in basal (+AA), starvation (-AA) or add-back (-/+AA) conditions, probed with the indicated antibodies and GAPDH as a loading control.

(e) Western blots from HEK293FT lysates treated with BafA1, probed with the indicated antibodies and GAPDH as a loading control.

Data shown are representative of 3 independent biological replicates. Arrowheads indicate different forms of a protein, P: phosphorylated form. Scale bars: 10 μ m. Data in (b) is shown as mean \pm SEM, ns non-significant.

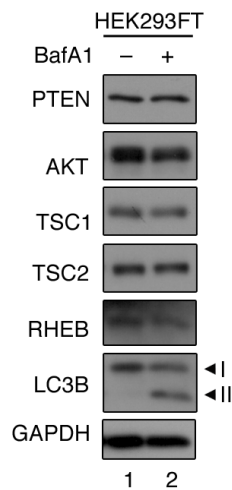


Figure 2.8 Blockage of lysosomal function does not affect levels of mTORC1 upstream regulators. Western blots from HEK293FT lysates treated with BafA1, probed with the indicated antibodies and GAPDH as a loading control.

Data shown are representative of 3 independent biological replicates. Arrowheads indicate different forms of a protein.

2.2.3 AA production in lysosomes is required for mTOR lysosomal localization and TFEB phosphorylation

Lysosomes are degradative organelles that can recycle different types of nutrients, such as lipids, carbohydrates and AAs. Among all nutrients, AAs are known as the most robust activators of mTORC1. Hence, we aimed to understand whether the effects of blocking lysosomal function on mTORC1 could be related to a decrease in AA production in lysosomes. We treated HEK293FT cells with a combination of PepA (Pepstatin A) and E64, compounds that directly inhibit the activity of lysosomal proteases. Importantly, treated cells displayed delocalization of mTOR from lysosomes (Figure 2.9a-b), as well as a strong decrease of TFEB phosphorylation. Concerning S6K and 4E-BP1 phosphorylation, no effect was observed under basal conditions, whereas their phosphorylation was blunted upon AA re-addition (Figure 2.9c). Taken together, these data show that AA production in lysosomes derived from protein degradation is essential for mTOR localization at lysosomes and the subsequent TFEB phosphorylation.

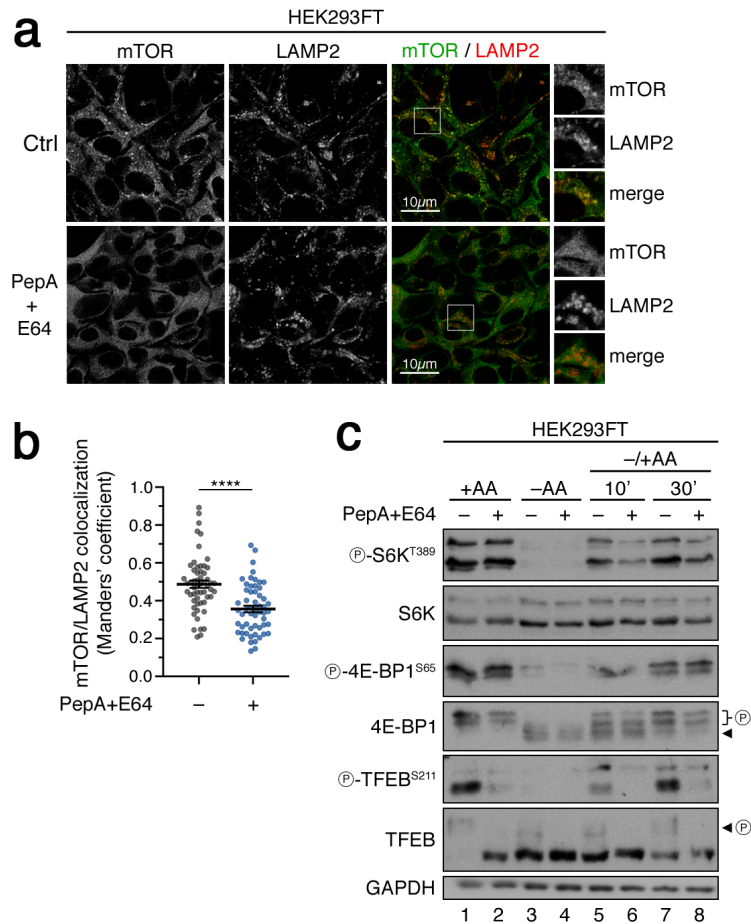


Figure 2.9 Blockage of lysosomal protease activity leads to mTORC1 delocalization from lysosomes and substrate-specific changes on its activity.

(a-b) HEK293FT cells stained for mTOR and LAMP2 (lysosomal marker) in the presence or absence of PepA+E64. mTOR colocalization with LAMP2 quantified in (b) from 50 cells of 5 different fields.

(c) Western blots from HEK293FT lysates in the presence or absence of PepA+E64 treated with media containing or lacking AAs, in basal (+AA), starvation (-AA) or add-back (-/+AA) conditions, probed with the indicated antibodies and GAPDH as a loading control.

Data shown are representative of 3 independent biological replicates. Arrowheads indicate different forms of a protein, P: phosphorylated form. Scale bars: 10µm. Data in (b) is shown as mean ± SEM, **** p<0.0001.

2.2.4 Loss of lysosomal enzyme trafficking mimics blockage of lysosomal function

The ability of lysosomes to degrade intracellular nutrients and components arise from the presence of specific catabolic enzymes at the lysosomal lumen. Lysosomal enzymes are delivered to these organelles via a complex trafficking mechanism from ER to the Golgi and from there to lysosomes. One of the major steps of lysosomal enzyme sorting at the Golgi is the attachment of a M6P modification that targets enzymes for correct delivery. The GNPTAB enzyme is one of the core components of the M6P pathway. To evaluate whether the loss of enzyme delivery to lysosomes would elicit similar effects to what I observed upon pharmacological blockage of lysosomal activity, I generated HEK293FT GNPTAB KO (knockout) cells. First, I characterized two different GNPTAB KO clones, and observed a

strong decrease in overall M6P signal and processing of CTSD (Figure 2.10a). In addition, I also detected extracellular release of the pro-form of CSTD (Figure 2.10b). Together, our data show that GNPTAB KO cells demonstrate lysosomal enzyme mis-sorting. Next, I investigated whether mTORC1 signaling is affected in these cells. While TFEB phosphorylation is completely lost in GNPTAB KOs, no changes in the phosphorylation status of S6K were detected (Figure 2.10a). To better understand whether the observed changes were due to differential localization of mTOR, I performed immunofluorescence experiments that revealed complete loss of mTOR lysosomal localization (Figure 2.10c-d). Collectively, our results indicate that correct lysosomal enzyme delivery is required for lysosomal localization of mTOR and activity towards phosphorylation of TFEB.

2.3 The Rag GTPases and the lysosomal mTORC1 machinery are required for mTORC1 activity towards lysosomal substrates

2.3.1 Rag GTPase deficiency leads to loss of mTOR lysosomal localization and TFEB phosphorylation

Cells have evolved an extensive machinery at lysosomes to recruit and activate mTORC1, centered around the heterodimeric Rag GTPases that are responsible for the direct recruitment of the complex on the lysosomal surface. To further dissect the lysosomal vs non-lysosomal localization and activation of mTORC1, we generated HEK293FT cells lacking the RagA/B GTPases (RagA/B KO). As expected, RagA/B KO cells do not have lysosomal mTOR (Figure 2.11a-b). Importantly, RagA/B KO cells lack TFEB and TFE3 phosphorylation (Figure 2.11c). Furthermore, phosphorylation of S6K and 4E-BP1 was largely unaffected during basal conditions (Figure 2.11c), resembling the phenotype of cells with lysosomal dysfunction. However, during starvation, S6K and 4E-BP1 phosphorylation was partially maintained, which was previously shown to be due to a lower recruitment of the mTORC1 inactivation machinery (Demetriades et al., 2014). Additionally, phosphorylation of the aforementioned substrates was also compromised during AA add-back, in line with the well-established role of Rag GTPases in the acute reactivation of mTORC1 (Kim et al., 2008; Sancak et al., 2008) (Figure 2.11c). In addition, IVKs (*in vitro* kinase assays) with immunopurified mTORC1 from WT (wild-type) or RagA/B KO cells, assessing phosphorylation of the substrate 4E-BP1, confirmed that mTORC1 activity is unaffected by loss of the RagA/B GTPases (Figure 2.11d).

To confirm that our observations are due to the lack of the RagA/B GTPases and not a secondary effect of the loss of these proteins, we transiently re-expressed WT RagA, a constitutively active RagA mutant (Q66L) or an inactive RagA mutant (T21N) in RagA/B KO cells. Remarkably, transfection of the active mutant of RagA fully rescued TFEB phosphorylation, while it only mildly increased S6K phosphorylation (Figure 2.11e).

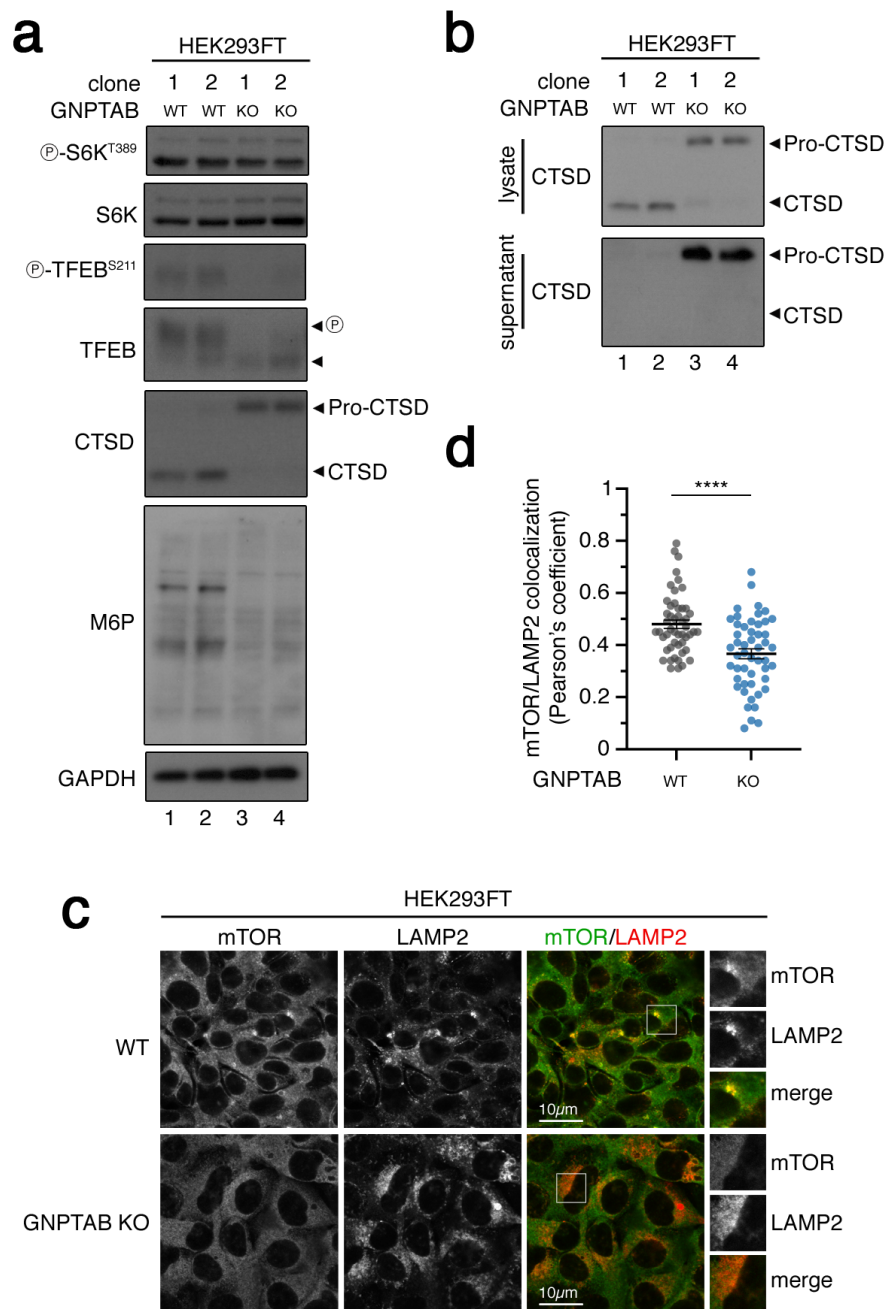


Figure 2.10 Blockage of lysosomal enzyme trafficking leads to mTORC1 delocalization from lysosomes and substrate-specific changes on its activity.

(a) Western blots from different lysates from HEK293FT WT and GNPTAB KO clones, probed with the indicated antibodies and GAPDH as a loading control.

(b) Western blots from different HEK293FT WT and GNPTAB KO lysates and supernatants, probed with the indicated antibody.

(c-d) HEK293FT WT and GNPTAB KO cells stained for mTOR and LAMP2 (lysosomal marker). mTOR colocalization with LAMP2 quantified in (d) from 50 cells of 5 different fields.

Data shown in (c), (d) and (e) are representative of 3 independent biological replicates. Arrowheads indicate different forms of a protein, P: phosphorylated form. Scale bars: 10µm. Data in (d) is shown as mean ± SEM, **** p<0.0001.

We further addressed the question of possible cellular changes because of RagA/B GTPase loss by generating cells lacking RagC/D. As for RagA/B KO cells, HEK293FT RagC/D KO cells also have non-lysosomal mTOR (Figure 2.12a-b) and loss of TFEB and TFE3 phosphorylation (Figure 2.12c). In addition, we solidified our findings by assessing the effects of RagA/B loss in MEFs, which confirmed that the requirement of the RagA/B GTPases for mTOR localization (Figure 2.13a-b) and activity towards TFEB and TFE3, but not S6K or 4E-BP1 (Figure 2.13c), is not cell-type or species specific.

As observed for blockage of lysosomal function, also RagA/B KO cells show no changes in phosphorylation of S6, downstream of S6K, as well as of additional cytosolic substrates, such as ULK1 and GRB10 (Figure 2.14), highlighting the differential requirement of the lysosomal machinery for phosphorylation of lysosomal vs non-lysosomal substrates. Furthermore, we show that the S6K phosphorylation observed in Rag-deficient cells is mTOR-dependent by treating cells with the mTOR inhibitor Torin1, which led to a full loss of phospho-S6K (Figure 2.15). Finally, RagA/B KO (Figure 2.16a) or RagC/D KO (Figure 2.16b) cells had no differences in mTORC2 activity, showing that the loss of the Rag GTPases affect specifically mTORC1.

The Rag GTPases are tethered to lysosomes via interactions with the LAMTOR complex. Hence, we aimed to remove the RagA/B GTPases from lysosomes without affecting their levels, via knocking down the LAMTOR1 component of the LAMTOR complex. In agreement with our results in Rag GTPase KO cells, knock down of LAMTOR1 leads to delocalization of mTOR from lysosomes (Figure 2.17a-b) as well as loss of TFEB phosphorylation (Figure 2.17c-d).

Using multiple pharmacological and genetic approaches we separate mTOR localization from mTORC1 activity towards different substrates. Based on our immunofluorescence experiments, I hypothesize that mTORC1 components in different locations might encounter substrates that reside in distinct cellular compartments. To test the lysosomal and non-lysosomal presence of mTORC1 using an independent biochemical method, we first generated WT or RagA/B KO cells that stably express HA (hemagglutinin)-tagged lysosomal transmembrane protein TMEM192 (transmembrane protein 192) or FLAG-tagged TMEM192 as a negative control. Next, based on the established protocol for lysosomal isolation (Lyso-IP; lysosomal immunopurification) (Abu-Remaileh et al., 2017), we set up a modified Lyso-IP protocol that allowed us to retrieve both lysosomal and non-lysosomal fractions. We successfully isolated intact lysosomes, as seen by the presence of LAMP2 and CTSD in the lysosome-enriched fraction, as well as the non-lysosomal fraction, assessed by the presence of the cytosolic protein GAPDH (glyceraldehyde-3-phosphate dehydrogenase) (Figure 2.18a). As expected, the mTORC1 components mTOR and RAPTOR do not localize to lysosomes in RagA/B KO cells (Figure 2.18a). Remarkably, we observed that in both WT and RagA/B KO cells a large proportion of mTOR and RAPTOR is localized at the non-lysosomal fraction (Figure 2.18a). We next assessed localization of the substrates S6K and TFEB. TFEB

is found in both fractions, as expected by the dynamic nature of its phosphorylation (Figure 2.18b). On the contrary, S6K is exclusively non-lysosomal (Figure 2.18b). These data show that S6K and mTORC1 co-exist in non-lysosomal fractions, which likely allow the maintenance of S6K phosphorylation even when mTORC1 is away from the lysosomal surface.

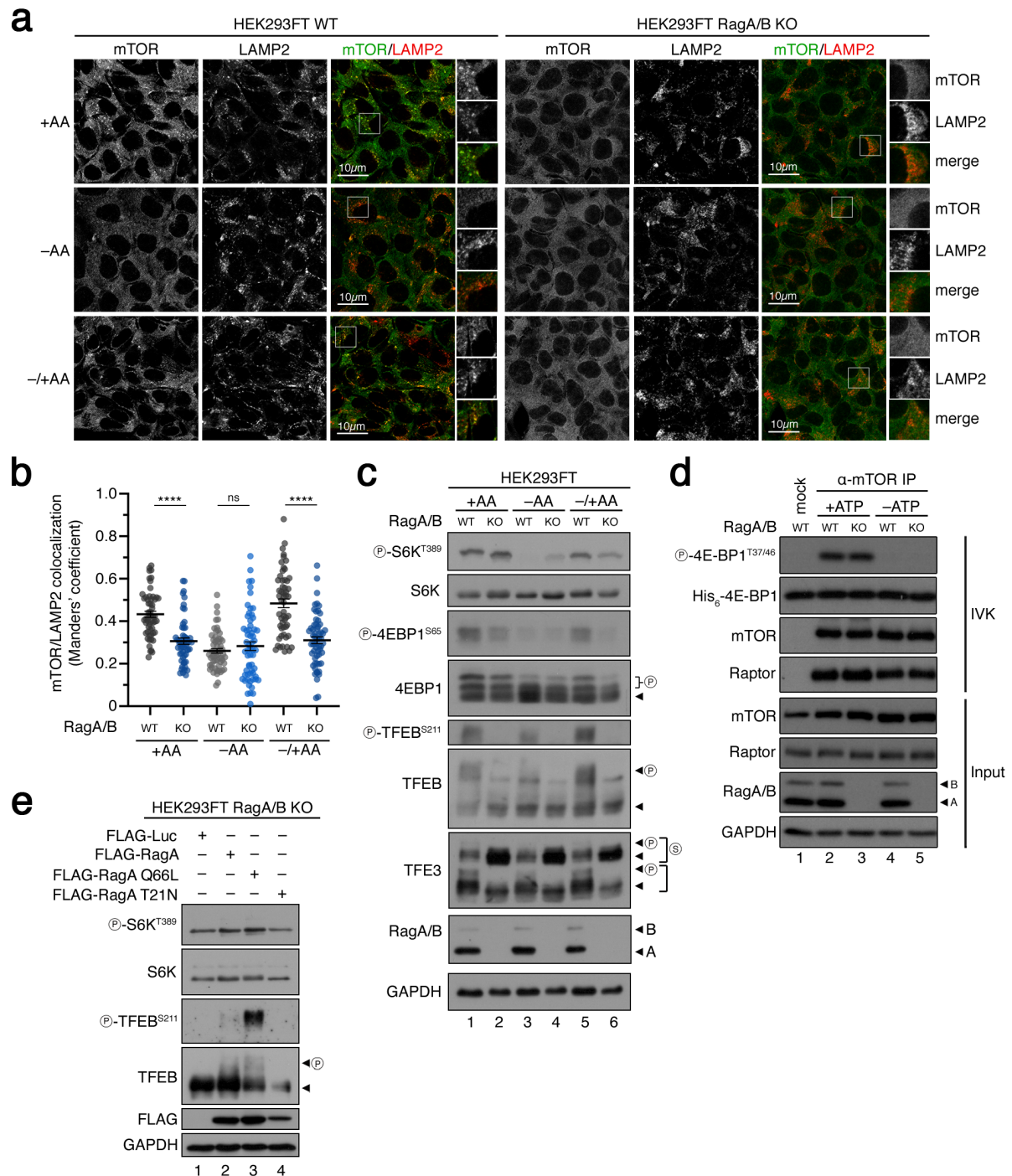


Figure 2.11 Cells lacking the RagA/B GTPases have mTORC1 delocalized from lysosomes and substrate-specific changes on its activity.

(a-b) HEK293FT WT and RagA/B KO cells stained for mTOR and LAMP2 (lysosomal marker), treated with media containing or lacking AAs, in basal (+AA), starvation (-AA) or add-back (-/+AA) conditions. mTOR colocalization with LAMP2 quantified in (b) from 50 cells of 5 different fields.

(c) Western blots from HEK293FT WT and RagA/B KO lysates treated with media containing or lacking AAs, in basal (+AA), starvation (–AA) or add-back (–/+AA) conditions, probed with the indicated antibodies and GAPDH as a loading control.

(d) Western blots from IVKs with mTORC1 purified from HEK293FT WT and RagA/B KO with 4EBP1 as substrate, probed with the indicated antibodies and GAPDH as a loading control.

(e) Western blots from HEK293FT RagA/B KO lysates transfected with the indicated plasmids, probed with the indicated antibodies and GAPDH as a loading control.

Data are representative of 3 independent biological replicates. Arrowheads indicate different forms of a protein, P: phosphorylated form. Scale bars: 10µm. Data in (b) is shown as mean ± SEM, **** p<0.0001, ns non-significant.

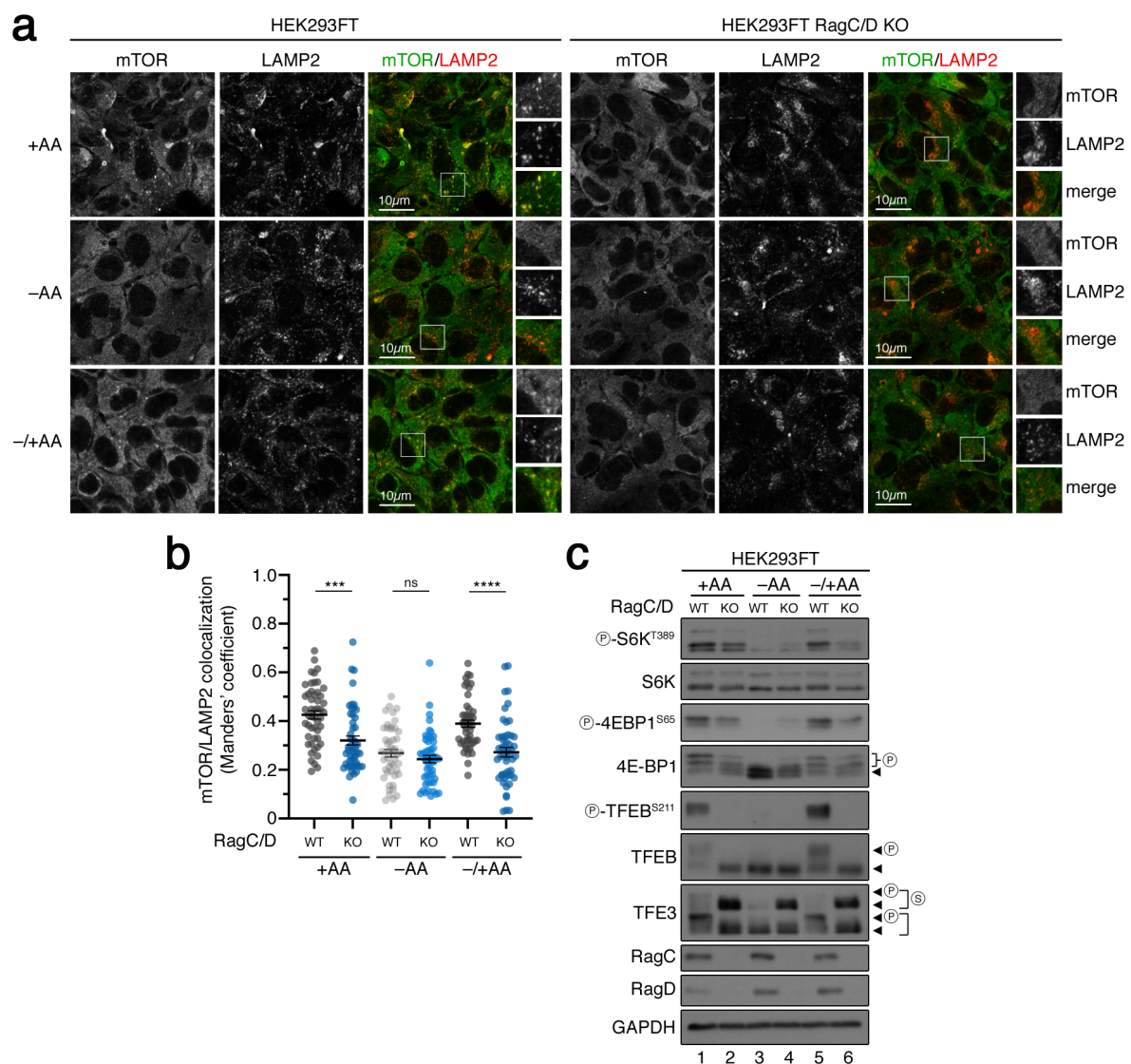


Figure 2.12 Cells lacking the RagC/D GTPases have mTORC1 delocalized from lysosomes and substrate-specific changes on its activity.

(a-b) HEK293FT WT and RagC/D KO cells stained for mTOR and LAMP2 (lysosomal marker), treated with media containing or lacking AAs, in basal (+AA), starvation (–AA) or add-back (–/+AA) conditions. mTOR colocalization with LAMP2 quantified in (b) from 50 cells of 5 different fields.

(c) Western blots from HEK293FT WT and RagC/D KO lysates treated with media containing or lacking AAs, in basal (+AA), starvation (–AA) or add-back (–/+AA) conditions, probed with the indicated antibodies and GAPDH as a loading control.

Data are representative of 3 independent biological replicates. Arrowheads indicate different forms of a protein, P: phosphorylated form. Scale bars: 10µm. Data in (b) is shown as mean ± SEM, **** p<0.0001, ns non-significant.

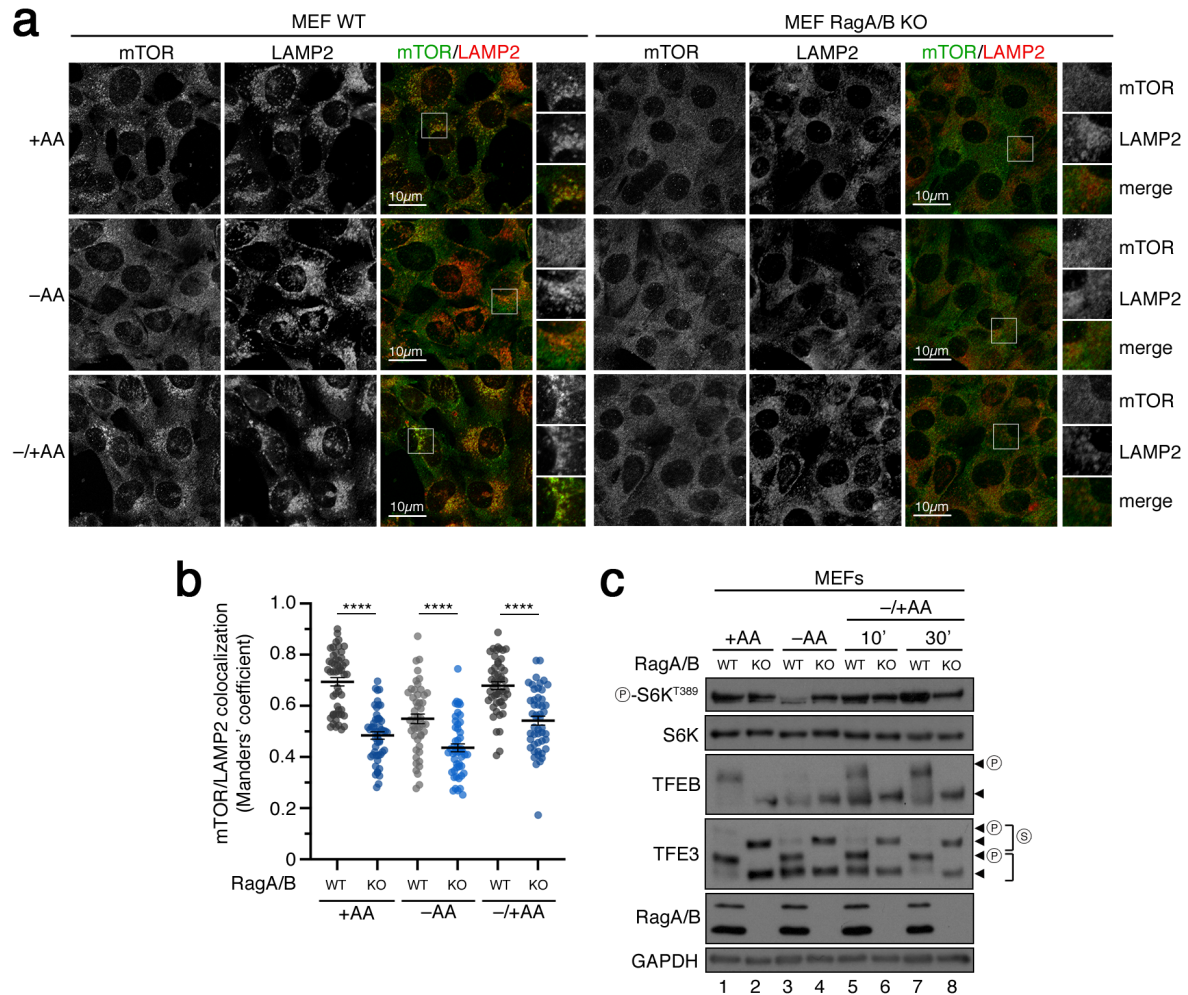


Figure 2.13 Mouse cells lacking the RagA/B GTPases have mTORC1 delocalized from lysosomes and substrate-specific changes on its activity.

(a-b) MEF WT and RagA/B KO cells stained for mTOR and LAMP2 (lysosomal marker), treated with media containing or lacking AAs, in basal (+AA), starvation (–AA) or add-back (–/+AA) conditions. mTOR colocalization with LAMP2 quantified in (b) from 50 cells of 5 different fields.

(c) Western blots from MEF WT and RagA/B KO lysates treated with media containing or lacking AAs, in basal (+AA), starvation (–AA) or add-back (–/+AA) conditions, probed with the indicated antibodies and GAPDH as a loading control.

Data are representative of 3 independent biological replicates. Arrowheads indicate different forms of a protein, P: phosphorylated form. Scale bars: 10µm. Data in (b) is shown as mean ± SEM, **** p<0.0001, ns non-significant.



Figure 2.14 Absence of the RagA/B GTPases does not affect cytosolic mTORC1 substrates.
 Western blots from HEK293FT WT and RagA/B KO lysates, probed with the indicated antibodies and GAPDH as a loading control.
 Data shown are representative of 3 independent biological replicates.

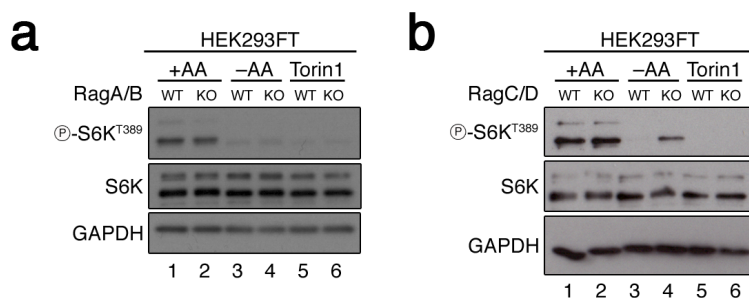


Figure 2.15 Phosphorylation of the mTORC1 substrate S6K in HEK293FT cells lacking the Rag GTPases is mTORC1 dependent.
 (a) Western blots from HEK293FT WT and RagA/B KO lysates treated with media containing or lacking AAs, in basal (+AA) or starvation (-AA) conditions, or treated with Torin1, probed with the indicated antibodies and GAPDH as a loading control.
 (b) Western blots from HEK293FT WT and RagC/D KO lysates treated with media containing or lacking AAs, in basal (+AA) or starvation (-AA) conditions, or treated with Torin1, probed with the indicated antibodies and GAPDH as a loading control.
 Data are representative of 3 independent biological replicates.

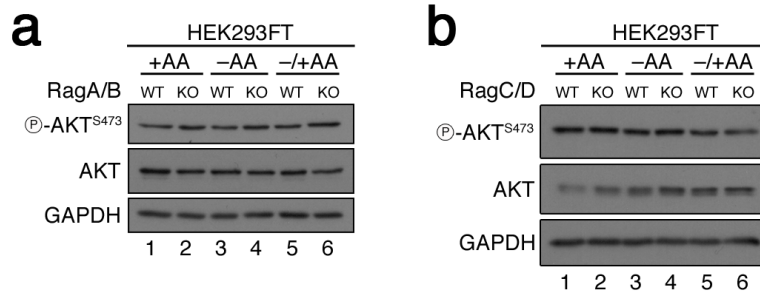


Figure 2.16 Phosphorylation of the mTORC2 substrate AKT is unaffected in HEK293FT cells lacking the Rag GTPases.

(a) Western blots from HEK293FT WT and RagA/B KO lysates treated with media containing or lacking AAs, in basal (+AA) or starvation (-AA) conditions, or treated with Torin1, probed with the indicated antibodies and GAPDH as a loading control.

(b) Western blots from HEK293FT WT and RagC/D KO lysates treated with media containing or lacking AAs, in basal (+AA) or starvation (-AA) conditions, or treated with Torin1, probed with the indicated antibodies and GAPDH as a loading control.

Data are representative of 3 independent biological replicates.

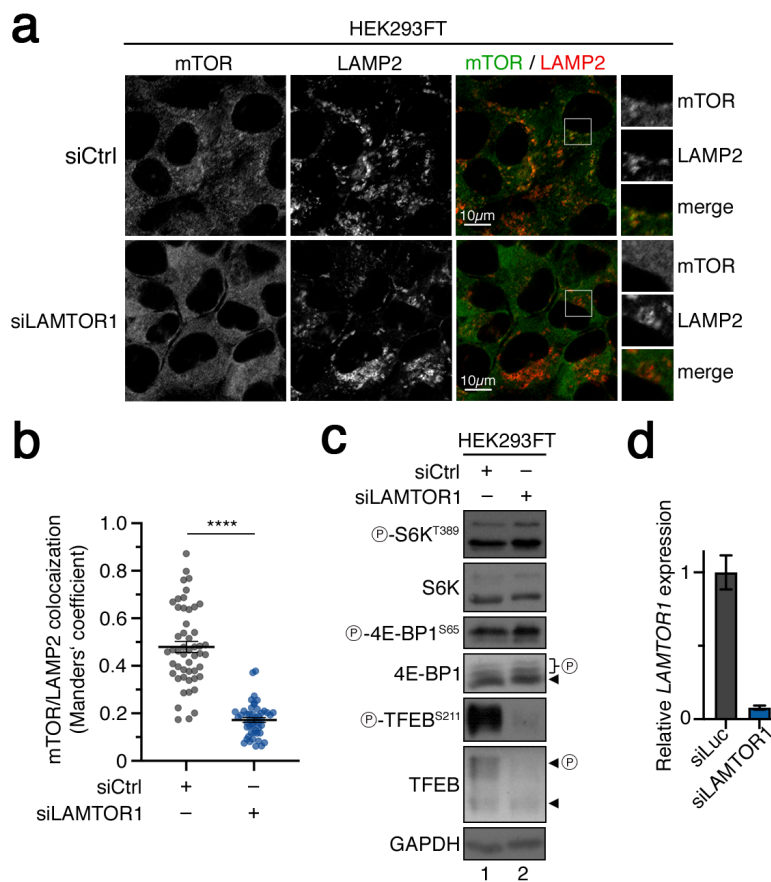


Figure 2.17 LAMTOR1 knockdown phenocopies the loss of Rag GTPases.

(a-b) HEK293FT cells transiently transfected with siRNAs (small interfering RNAs) targeting LAMTOR1 or a control RNAi duplex, stained for mTOR and LAMP2 (lysosomal marker). mTOR colocalization with LAMP2 quantified in (b) from 50 cells of 5 different fields.

(c) Western blots from HEK293FT lysates of cells transiently transfected with siRNAs targeting LAMTOR1 or a control RNAi duplex, probed with the indicated antibodies and GAPDH as a loading control.

(d) LAMTOR1 expression levels of HEK293FT cells transiently transfected with siRNAs targeting LAMTOR1 or a control RNAi duplex.

Data shown are representative of 3 independent biological replicates. Arrowheads indicate different forms of a protein, P: phosphorylated form. Scale bars: 10µm. Data in (b) is shown as mean \pm SEM and data in (d) is shown as mean \pm SD, **** $p < 0.0001$.

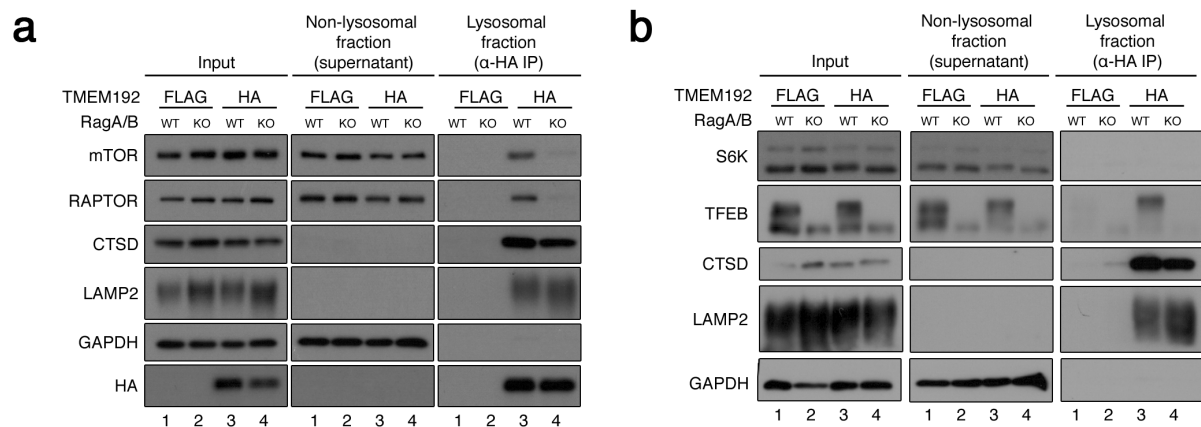


Figure 2.18 Different mTORC1 components and substrates are localized in distinct cellular compartments.

(a) Lyso-IP experiment in HEK293FT WT and RagA/B KO cells expressing either HA-TMEM192 or the control construct FLAG-TMEM192. Intact lysosomes were immunopurified in native conditions with anti-HA beads and the resulting lysosomal and non-lysosomal fractions, as well as the input, were analyzed by immunoblotting with the indicated antibodies to assess localization of mTORC1 components.

(a) Lyso-IP experiment in HEK293FT WT and RagA/B KO cells expressing either HA-TMEM192 or the control construct FLAG-TMEM192. Intact lysosomes were immunopurified in native conditions with anti-HA beads and the resulting lysosomal and non-lysosomal fractions, as well as the input, were analyzed by immunoblotting with the indicated antibodies to assess localization of mTORC1 substrates.

Data are representative of 3 independent biological replicates.

2.3.2 Non-lysosomal mTORC1 activity has distinct sensitivity to specific AAs, independently of the canonical AA sensing machinery

Our findings show that non-lysosomal mTORC1 is capable of responding to changes in extracellular AA levels, since cells with only non-lysosomal mTORC1 still respond to AA starvation. Hence, I aimed to understand whether canonical AA sensors would be able to regulate non-lysosomal mTORC1. For instance, leucine and arginine are AAs that activate mTORC1 via pathways that converge on the positive regulator GATOR2 complex. Therefore, I knocked down MIOS, a component of the GATOR2 complex, to test whether this is involved in the activation of cytoplasmic mTORC1 by exogenous AAs. Although MIOS knock down decreased mTOR lysosomal localization (Figure 2.19a-b) and TFEB phosphorylation (Figure 2.19c), likely due to inactivation of the Rag GTPases, it did not affect basal phosphorylation

of S6K or 4E-BP1 (Figure 2.19c). Thus, despite the fact that GATOR2 is a complex that also localizes to the cytoplasm, it regulates the activity of lysosomal mTORC1.

To further investigate which AAs are relevant for the activation of non-lysosomal mTORC1, we treated WT or RagA/B KO HEK293FT cells with media lacking different AA groups, based on their biochemical properties. In WT cells, mTORC1 activity was downregulated in response to starvation of hydrophobic (methionine, leucine, isoleucine, glycine, valine; '–MLIGV') or positively-charged (histidine, arginine, lysine; '–HRK') AAs, whereas RagA/B KO cells did not respond to these treatments (Figure 2.20a-b). On the other hand, only RagA/B KO cells responded to starvation of serine, threonine and cysteine ('–STC') (Figure 2.20c-d). Importantly, in Rag A/B KO cells, starvation of each of the three AAs serine, threonine or cysteine was sufficient to downregulate mTORC1 activity (Figure 2.20e-f), indicating that each of these AAs is important to sustain non-lysosomal mTORC1 activity. Overall, our results demonstrate that non-lysosomal mTORC1 responds to different AAs, for which the sensing mechanisms remain to be elucidated.

Because mTORC1 activity is responsive to additional stimuli apart from AA availability, I aimed to understand whether cells with exclusively non-lysosomal mTOR are capable of responding to such signaling cues. First, I assessed whether HEK293FT RagA/B KO cells respond to glucose starvation and re-addition. WT cells were able to downregulate mTORC1 activity upon glucose deprivation and re-activate mTORC1 upon glucose re-addition (Figure 2.21a). On the contrary, RagA/B KO cells were insensitive to glucose removal (Figure 2.21a), likely due to previously described Rag-dependent mechanisms of glucose sensing (Efeyan et al., 2014; Dai et al., 2023). Next, I evaluated if RagA/B KO cells are able to respond to GF signaling. For this purpose, I treated WT and RagA/B KO HEK293FT cells with an AKT inhibitor, since AKT is a key node in the transmission of GF availability to mTORC1. Interestingly, RagA/B KO cells downregulated mTORC1 to the same extent as WT cells in response to AKT inhibition (Figure 2.21b). Taken together, our findings indicate that non-lysosomal mTORC1 is still responsive to AAs and GFs, but not to glucose.

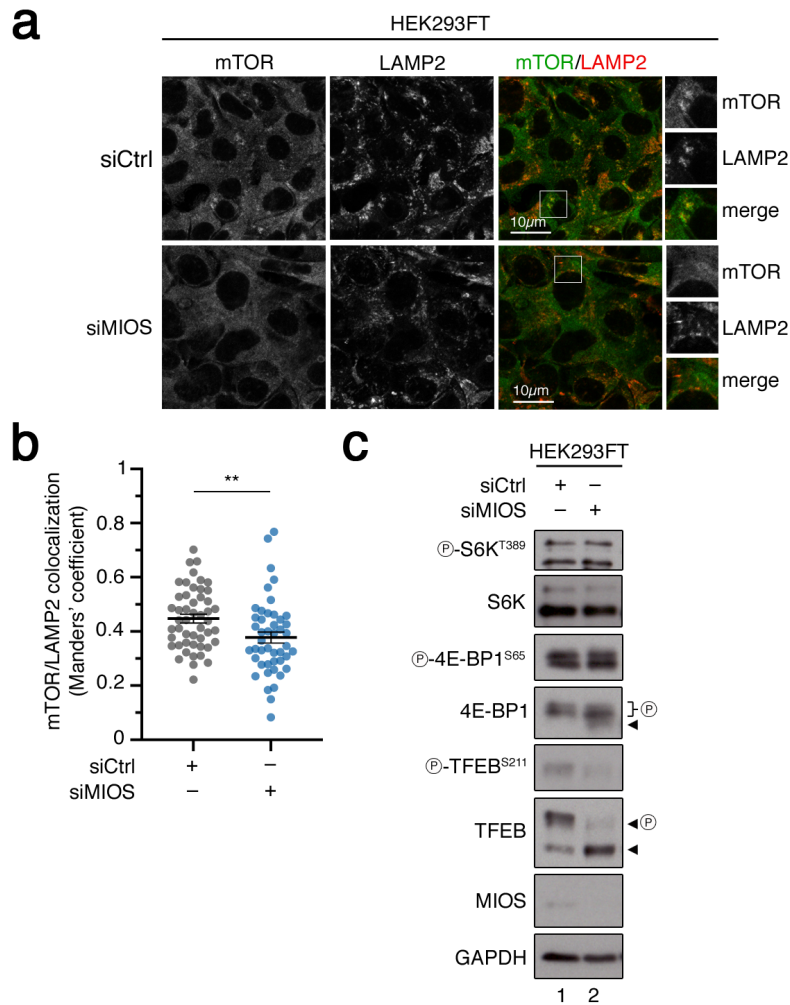


Figure 2.19 MIOS knockdown phenocopies the loss of Rag GTPases.

(a-b) HEK293FT cells transiently transfected with siRNAs targeting MIOS or a control RNAi duplex, stained for mTOR and LAMP2 (lysosomal marker). mTOR colocalization with LAMP2 quantified in (b) from 50 cells of 5 different fields.

(c) Western blots from HEK293FT lysates of cells transiently transfected with siRNAs targeting MIOS or a control RNAi duplex, probed with the indicated antibodies and GAPDH as a loading control.

Data shown are representative of 3 independent biological replicates. Arrowheads indicate different forms of a protein, P: phosphorylated form. Scale bars: 10µm. Data in (b) is shown as mean \pm SEM, ** $p < 0.01$.



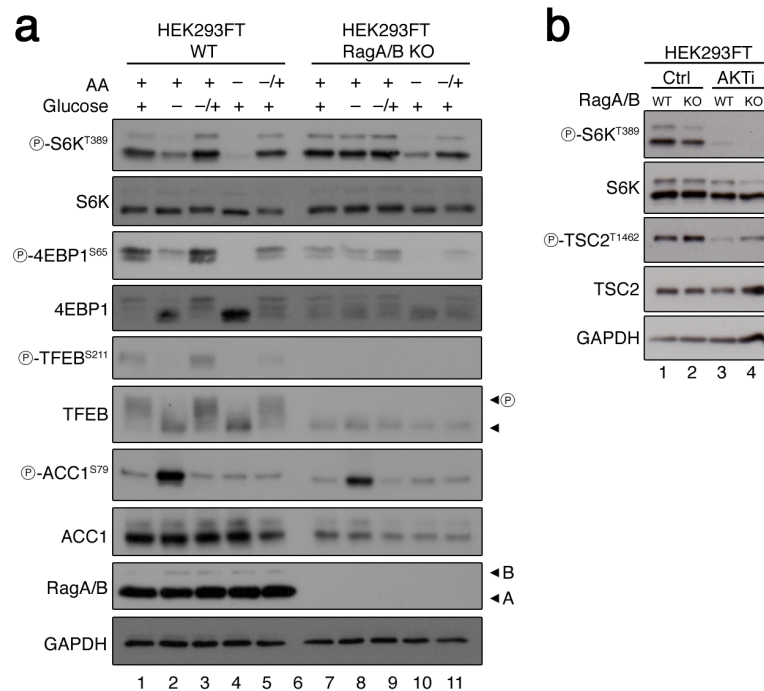


Figure 2.21 Non-lysosomal mTORC1 does not respond to glucose availability, but has normal response to AAs or AKT inhibition.

(a) Western blots from HEK293FT WT and RagA/B KO lysates treated with media containing or lacking AAs, or media containing or lacking glucose, in basal (+), starvation (-) or add-back (-/+) conditions probed with the indicated antibodies and GAPDH as a loading control.

(b) Western blots from HEK293FT WT and RagA/B KO lysates treated with AKT inhibitor, probed with the indicated antibodies and GAPDH as a loading control.

Data are representative of 3 independent biological replicates.

2.3.3 Previously described Rag-independent mechanisms are not involved in the regulation of non-lysosomal mTORC1

Previous studies suggested that glutamine and asparagine signal to re-activate mTORC1 after AA starvation via a Rag-independent mechanism mediated by the ARF1 GTPase, a Golgi-resident protein (Jewell et al., 2015; Meng et al., 2020). Given that non-lysosomal mTORC1 is active in the absence of the Rag GTPases, we investigated whether ARF1 could be the main regulator of this mTORC1 pool. Knockdown of ARF1 in HEK293FT RagA/B KO cells did not affect the phosphorylation of S6K and 4E-BP1 in basal conditions (Figure 2.22a-b). Furthermore, treatment of HEK293FT WT or RagA/B KO cells with GA (golgicide A) or BFA (brefeldin A), two inhibitors of the ARF1 GEF, GBF1 (golgi-specific brefeldin A-resistance guanine nucleotide exchange factor 1), did not affect the phosphorylation of any mTORC1 substrate (Figure 2.22c), although Golgi morphology was severely affected as expected (Figure 2.22d).

An additional previously described Rag-independent mechanism involves the ER-to-Golgi trafficking protein RAB1A, which was suggested to bind and regulate mTORC1 at the Golgi (Thomas et al., 2014). As mentioned above, Golgi disruption did not affect non-lysosomal

mTORC1 activity towards S6K and 4E-BP1 (Figure 2.22d). Moreover, knock down of RAB1A in WT or RagA/B KO HEK293FT cells had no effect on the phosphorylation of S6K or 4E-BP1 (Figure 2.22e). Intriguingly, RAB1A knock down led to a decrease in TFEB phosphorylation (Figure 2.22e), likely via its canonical trafficking role that can impair enzyme delivery to lysosomes. Overall, our results suggest that cytoplasmic mTORC1 is not regulated through any of the Rag-independent mechanisms that were described so far, and is independent from Golgi morphology and Golgi-residing GTPases.

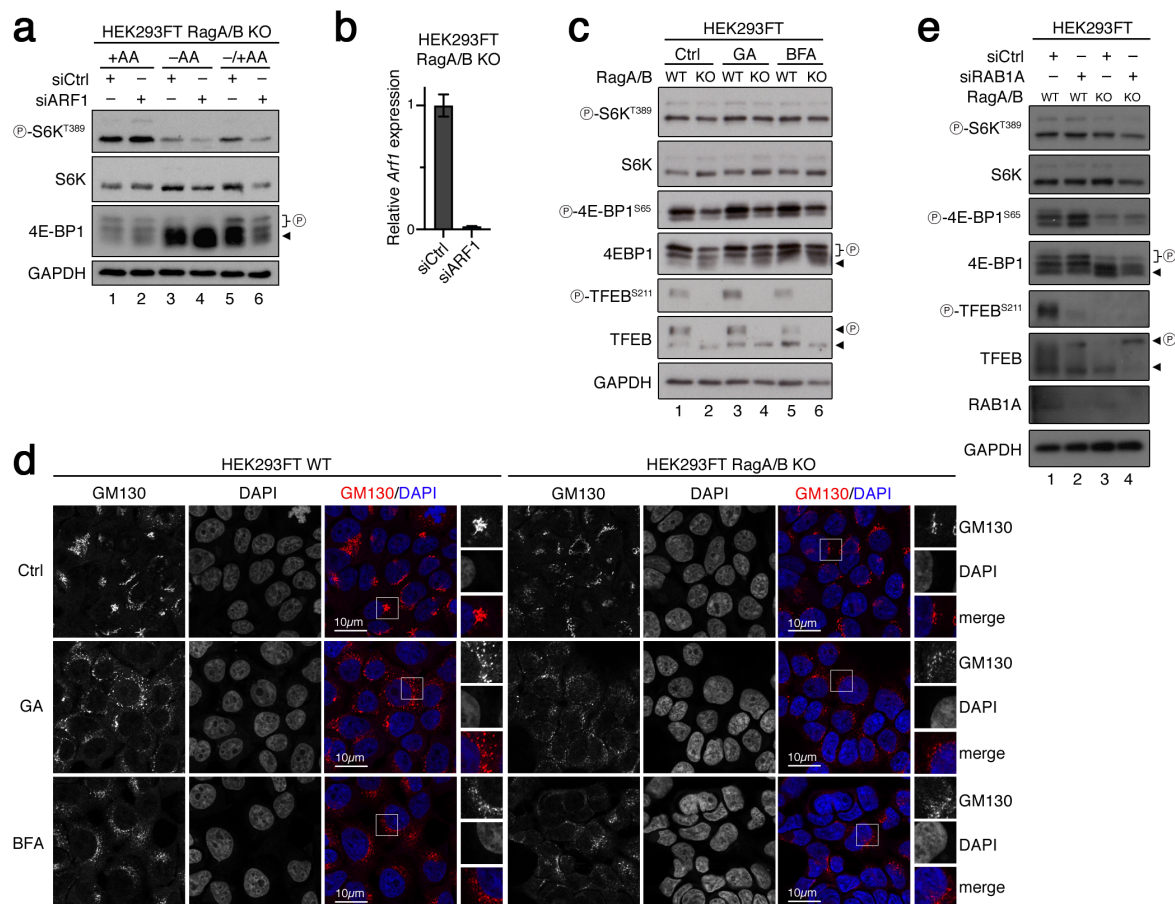


Figure 2.22 Non-lysosomal mTORC1 is regulated independently of the Golgi machinery.

(a) Western blots from HEK293FT RagA/B KO lysates of cells transiently transfected with siRNAs targeting ARF1 or a control RNAi duplex, probed with the indicated antibodies and GAPDH as a loading control.

(b) ARF1 expression levels of HEK293FT cells transiently transfected with siRNAs targeting ARF1 or a control RNAi duplex.

(c) Western blots from HEK293FT WT and RagA/B KO lysates treated with GA or BFA, probed with the indicated antibodies and GAPDH as a loading control.

(d) HEK293FT cells WT and RagA/B KO treated with GA or BFA, stained for GM130 (golgin subfamily A member 2) and DAPI.

(e) Western blots from HEK293FT WT or RagA/B KO lysates of cells transiently transfected with siRNAs targeting RAB1A or a control RNAi duplex, probed with the indicated antibodies and GAPDH as a loading control.

Data shown are representative of 3 independent biological replicates. Arrowheads indicate different forms of a protein, P: phosphorylated form. Scale bars: 10µm. Data in (b) is shown as mean ± SD.

2.4 Protein synthesis and lysosomal biogenesis programs are controlled by different mTORC1 pools

Our results showed that distinct mTORC1 locations are relevant for different categories of substrates in cells cultured in the presence of AAs: non-lysosomal mTORC1 controls cytosolic substrates, such as S6K and 4E-BP1, whereas lysosomal mTORC1 is relevant for lysosomal substrates, such as TFEB. Because S6K and 4E-BP1 are involved in the regulation of translation, we used a modified puromycin incorporation assay, the OPP (O-propargyl-puromycin) assay, to investigate whether *de novo* protein synthesis is affected in cells that contain only non-lysosomal mTORC1. Consistently with the phosphorylation status of S6K and 4E-BP1 being largely unaffected in RagA/B deficient cells, no changes in protein synthesis were observed (Figure 2.23).

In contrast to S6K and 4E-BP1, phosphorylation of lysosomal substrates such as TFEB and TFE3 is abolished in RagA/B-null cells. In agreement with the lack of TFEB and TFE3 phosphorylation, HEK293FT RagA/B KO cells show increased nuclear localization of these two transcription factors (Figure 2.24a-d) and, as a consequence, increased transcription of their targets related to lysosome biogenesis and autophagy (Figure 2.24e). As expected, the higher expression of TFEB/TFE3 targets led to an increase in lysosome abundance, assessed by LysoTracker staining (Figure 2.24f-g), as well as of autophagosome abundance, as observed by LC3B staining (Figure 2.24h-i).

In sum, our work establishes the existence of a lysosomal pool of mTORC1 that localizes at the lysosomal surface in response to the release of freshly produced AAs inside lysosomes. The lysosomal pool is relevant for the control of lysosomal substrates and subsequent control of lysosome and autophagosome biogenesis. At the same time, we describe the existence of a non-lysosomal/cytoplasmic pool of mTORC1, which is responsive to a subset of exogenous AAs, and is relevant for the phosphorylation of cytosolic substrates and the downstream control of protein synthesis.

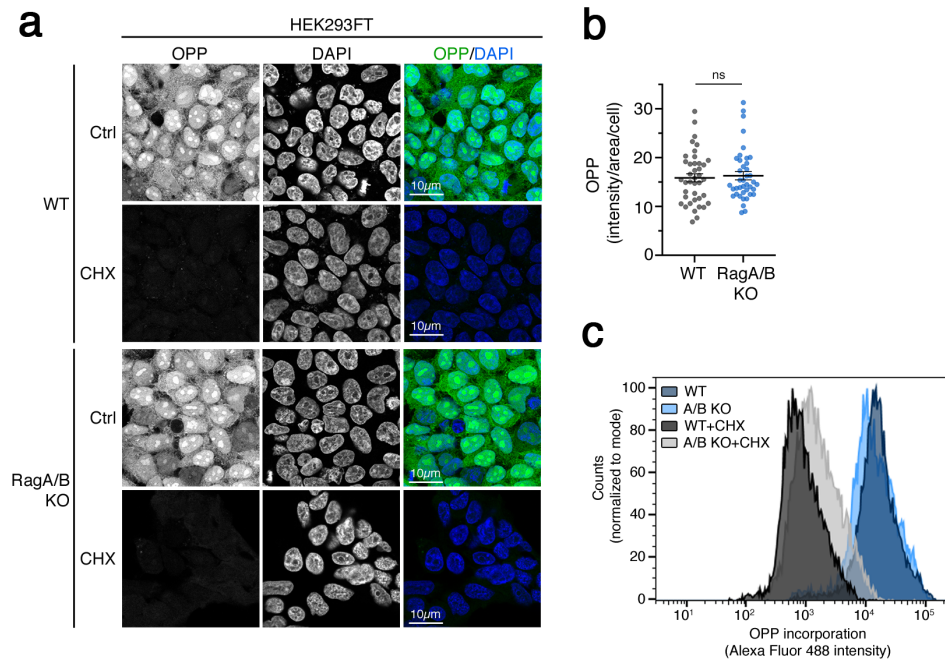


Figure 2.23 Protein synthesis is unaffected in cells lacking RagA/B GTPases.

(a-b) De novo protein synthesis assessed by OPP incorporation in HEK293FT WT and RagA/B KO, nuclei stained with DAPI. CHX (cicloheximide) was used as a negative control. Quantification of OPP signal in (b) from 50 cells of 5 different fields.

(c) De novo protein synthesis assessed by OPP incorporation in HEK293FT WT and RagA/B KO via flow cytometry. $n_{WT} = 9306$, $n_{ABKO} = 9317$, $n_{WT+CHX} = 9572$, $n_{ABKO+CHX} = 8869$.

Data shown are representative of 3 independent biological replicates. Scale bars: 10 μ m. Data in (b) is shown as mean \pm SEM, ns non-significant.

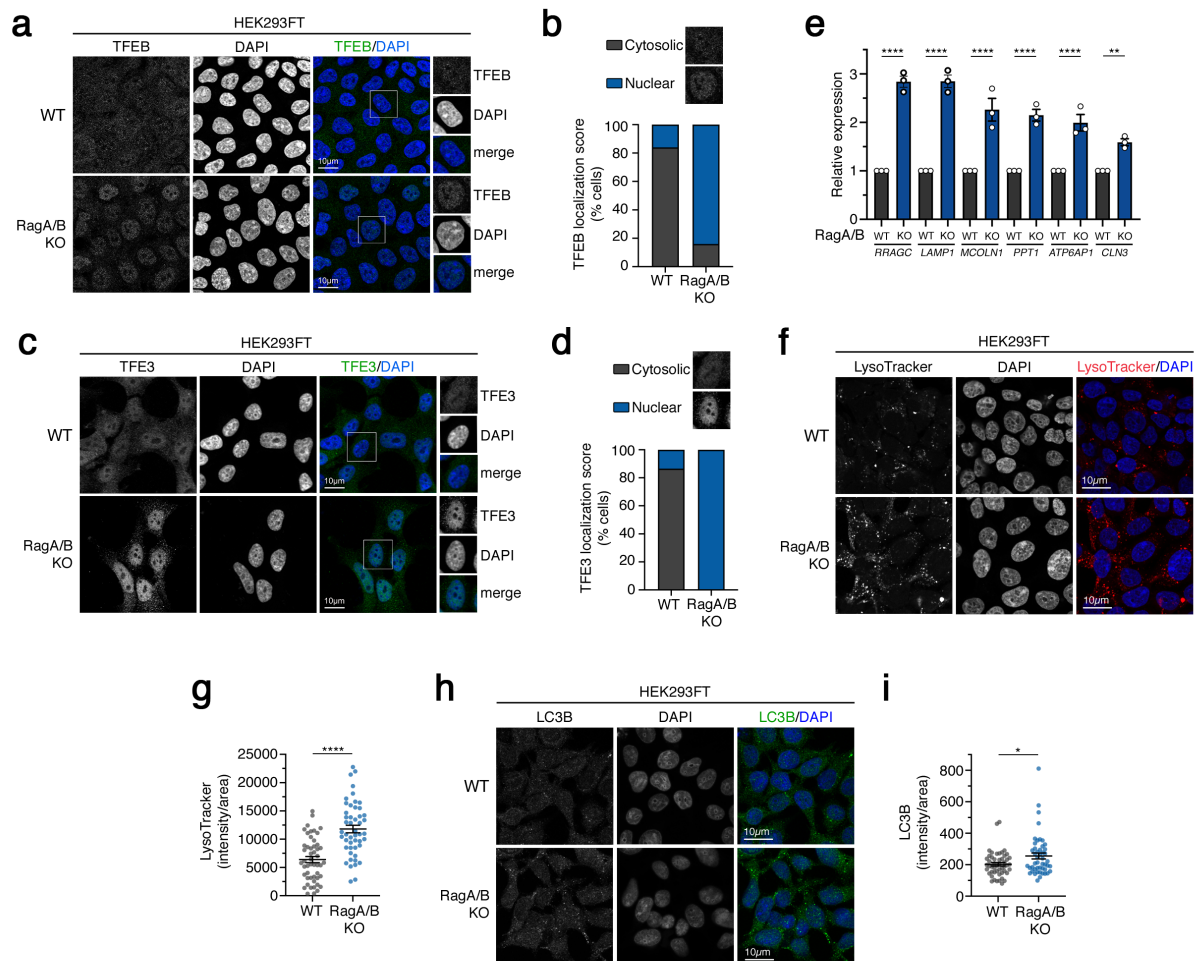


Figure 2.24 Cells lacking RagA/B GTPases show increased nuclear localization of TFEB/TFE3 and activation of their downstream processes.

(a-b) HEK293FT WT and RagA/B KO cells stained for TFEB and DAPI. Scoring of nuclear or cytosolic TFEB localization in (b), as indicated by the example images, $n_{WT} = 65$ cells, $n_{ABKO} = 102$ cells.

(c-d) HEK293FT WT and RagA/B KO cells stained for TFE3 and DAPI. Scoring of nuclear or cytosolic TFE3 localization in (d), as indicated by the example images, $n_{WT} = 52$ cells, $n_{ABKO} = 52$ cells.

(e) Expression levels of TFEB/TFE3 target genes in HEK293FT WT or RagA/B KO cells.

(f-g) HEK293FT WT and RagA/B KO cells stained with LysoTracker and DAPI. LysoTracker signal intensity quantified in (g) from 50 cells of 5 different fields.

(h-i) HEK293FT WT and RagA/B KO cells stained with LC3B and DAPI. LC3B signal intensity quantified in (i) from 50 cells of 5 different fields.

Data shown are representative of 3 independent biological replicates. Scale bars: 10 μ m. Data in (c), (g) and (i) are shown as mean \pm SEM, * $p < 0.05$, ** $p < 0.01$, **** $p < 0.0001$.

Part II: CYLD is a novel deubiquitinase for mTOR

2.5 CYLD interacts with mTOR

mTOR is ubiquitinated by the E3 ligase TRAF6 (Linares et al., 2013a). Ubiquitination is a reversible process; hence, DUBs are of equal importance for the control of signaling pathways. Notably, no DUB for mTOR has been identified so far. Based on the current knowledge, the DUB CYLD is described to counteract TRAF6 towards some of its substrates (Yang et al., 2013b). Hence, I aimed to determine whether CYLD could be a DUB for mTOR. For CYLD to remove ubiquitin molecules from mTOR, they need to be in close contact. Thus, to investigate whether CYLD interacts with mTOR, I expressed a FLAG-tagged CYLD construct in HEK293T CYLD knockout cells (CYLD KO). By performing anti-FLAG immunoprecipitation, I could detect mTOR being co-immunoprecipitated with FLAG-tagged CYLD (Figure 2.25a). Likewise, in HEK293T WT cells, CYLD co-precipitated with SBP (streptavidin binding peptide)-tagged mTOR in streptavidin affinity precipitation experiments (Figure 2.25b). In sum, I show that CYLD and mTOR interact.

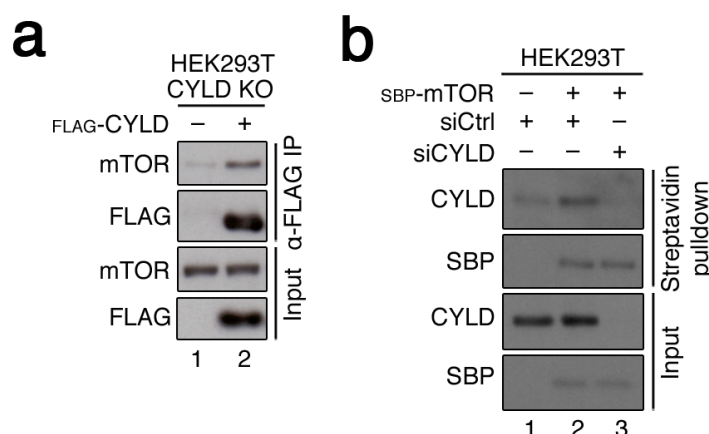


Figure 2.25 The deubiquitinase CYLD interacts with mTOR.

(a) Western blots from FLAG immunoprecipitation experiments in HEK293T WT and CYLD KO, expressing a FLAG-tagged CYLD construct, probed with the indicated antibodies.

(b) Western blots from streptavidin pulldown experiments in HEK293T cells transiently transfected with siRNAs targeting CYLD or a control RNAi duplex and expressing an SBP-tagged mTOR construct, probed with the indicated antibodies.

Data are representative of 2 independent biological replicates.

2.6 CYLD is a DUB for mTOR

2.6.1 CYLD regulates mTOR ubiquitination

Since CYLD interacts with mTOR, I aimed to determine if CYLD is capable of modulating mTOR ubiquitination. First, I knocked down CYLD in HEK293T cells expressing FLAG-tagged mTOR and HA-tagged ubiquitin (Ub). By immunopurifying mTOR and assessing HA levels, I observed an increase in mTOR ubiquitination upon CYLD knockdown (Figure 2.26a-b). To test whether the Ub signal I observed originates from mTOR itself or from an mTOR-interacting protein, I used a His₆-tagged mTOR construct. Next, I performed His pulldown

under very stringent lysis conditions. In this setup, where no protein-protein interactions are expected to be present, mTOR ubiquitination is still observed and is increased when CYLD is knocked down (Figure 2.26c-d). Therefore, I established that CYLD can modulate the ubiquitination status of mTOR.

To confirm that CYLD is a DUB for mTOR and to rule out possible off-target effects of the CYLD siRNAs, I evaluated the effect of expressing a catalytically inactive CYLD construct (FLAG-CYLD^{C601S}). I immunopurified mTOR from HEK293T cells expressing FLAG-tagged mTOR and HA-tagged Ub together with FLAG-tagged CYLD^{C601S}. Previous reports suggest that the CYLD^{C601S} mutant acts as dominant negative (Tauriello et al., 2010; Yang et al., 2013c). Accordingly, I observed an increase in mTOR ubiquitination in cells expressing FLAG-tagged CYLD^{C601S} (Figure 2.27a-b). Importantly, the same effect of CYLD on mTOR ubiquitination was also observed in MEFs that stably express FLAG-tagged mTOR and bear the catalytically inactive CYLD^{R932X} mutant (CYLD Δ 932) (Figure 2.28a-b). This result highlights that the effect of CYLD on mTOR is not cell-type- or species-specific. Finally, I performed *in vitro* DUB assays with mTOR immunopurified from HEK293T cells. Addition of recombinant CYLD lowered mTOR ubiquitination (Figure 2.29a-b), showing that CYLD can directly remove ubiquitin molecules from mTOR. In sum, using five independent ways to perturb CYLD function, I could confirm that CYLD acts as a DUB for mTOR.

2.6.2 CYLD regulates K63-linked ubiquitin chains on mTOR

Ubiquitin can be attached to a protein either as mono-ubiquitin or in the form of different ubiquitin chains. Importantly, each type of ubiquitination can elicit different downstream effects. CYLD is a DUB that is described to act mostly on K63-linked ubiquitin chains (Komander et al., 2008). To assess if K63-linked chains on mTOR are modulated by CYLD, I evaluated mTOR ubiquitination in the presence of ubiquitin constructs that cannot form K63-linked chains (Ub^{K63R}), or the other most common form of ubiquitin chain, K48-linked (Ub^{K48R}). Importantly, expressing HA-tagged Ub^{K63R} greatly diminished mTOR ubiquitination and completely ablated the CYLD effect (Figure 2.30). Intriguingly, expressing the HA-tagged Ub^{K48R} construct led to an increase in mTOR ubiquitination, with a further enhancement when CYLD is knocked down (Figure 2.30). This observation might indicate that by not allowing the formation of K48-linked chains, more molecules are available to form K63-chains. Together, these results suggest that CYLD modulates K63-linked chains on mTOR.

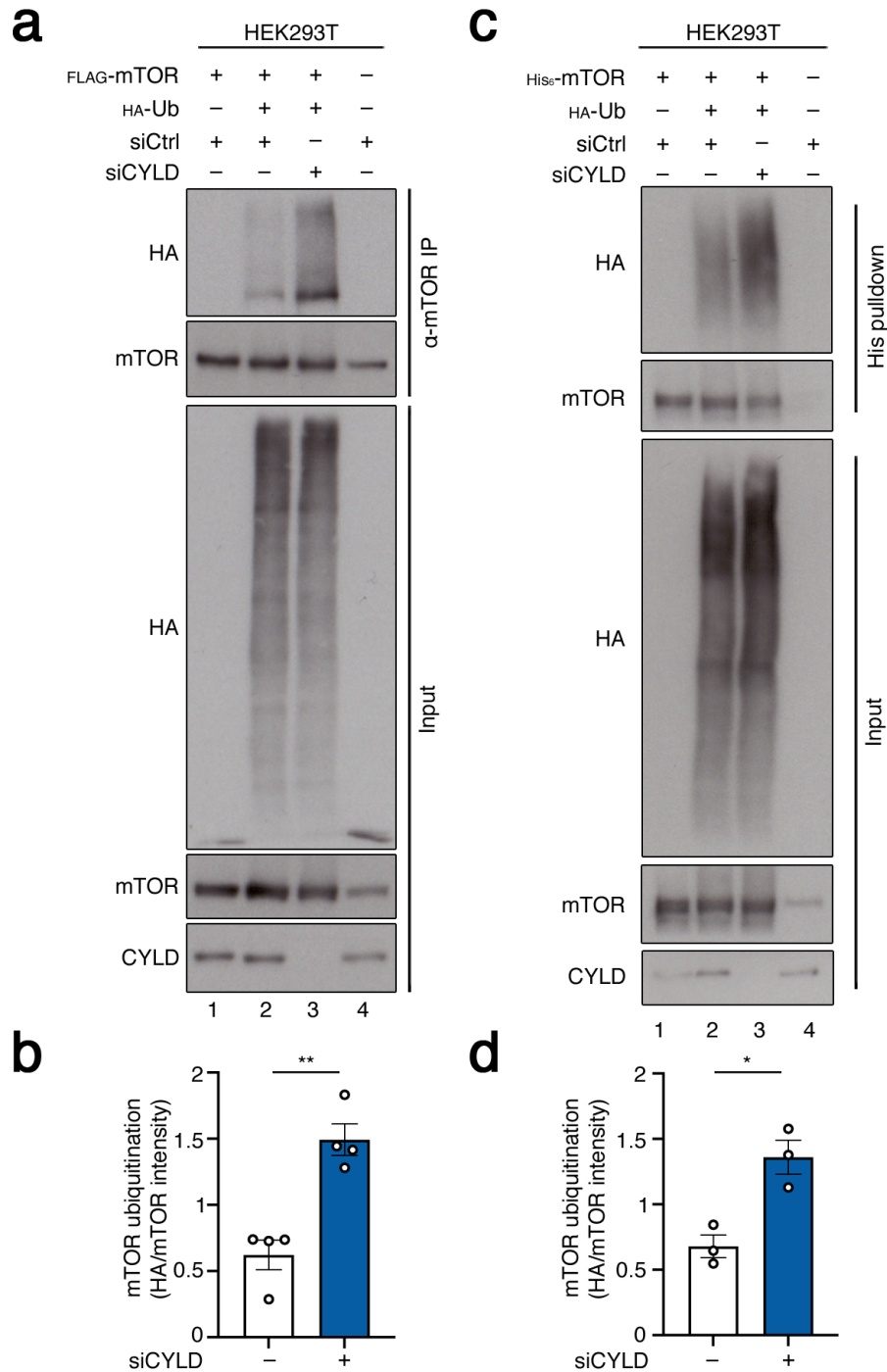


Figure 2.26 CYLD deubiquitinates mTOR.

(a-b) Western blots from mTOR immunoprecipitation experiments in HEK293T cells transiently transfected with siRNAs targeting CYLD or a control RNAi duplex, expressing FLAG-tagged mTOR and HA-tagged Ub constructs, probed with the indicated antibodies. (b) Quantification of mTOR ubiquitination, HA/mTOR signal ratio, n=4.

(c-d) Western blots from His-tag affinity precipitation experiments in HEK293T cells transiently transfected with siRNAs targeting CYLD or a control RNAi duplex, expressing His₆-tagged mTOR and HA-tagged Ub constructs, probed with the indicated antibodies. (d) Quantification of mTOR ubiquitination, HA/mTOR signal ratio n=3.

Data in (b) and (d) are shown as mean \pm SEM, * p<0.05, ** p<0.01.

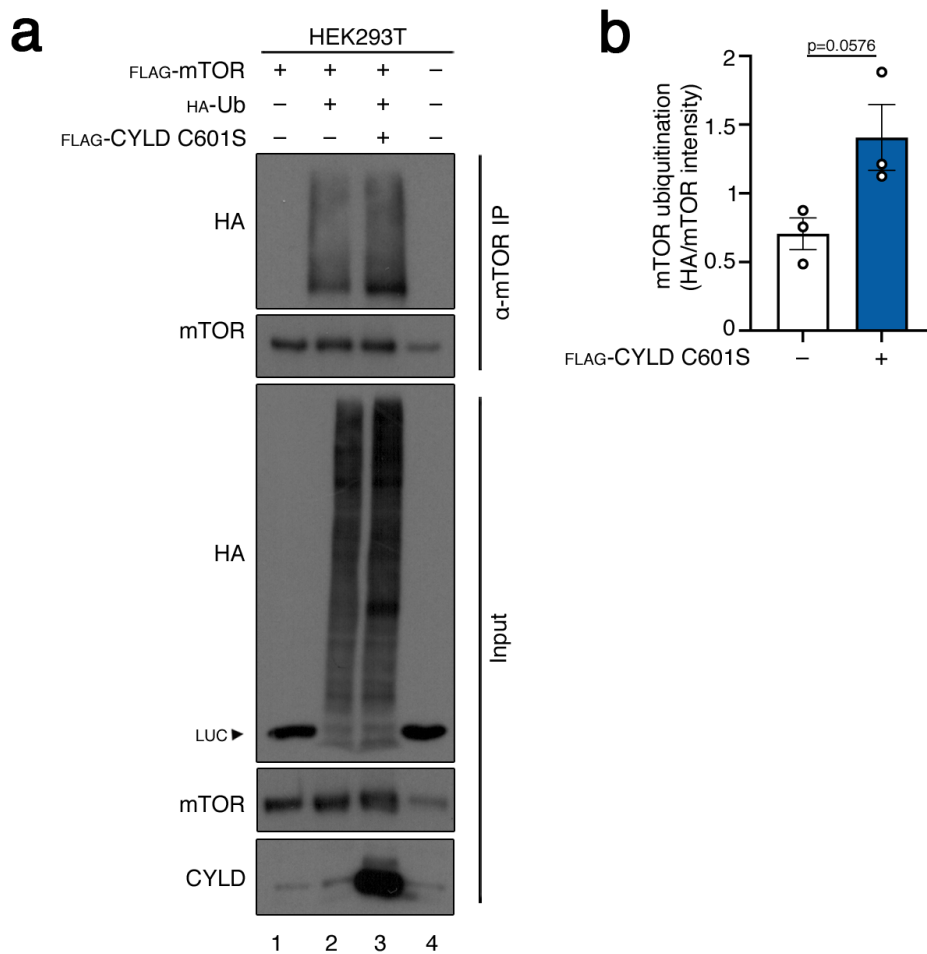


Figure 2.27 Catalytically inactive CYLD expression increases mTOR ubiquitination.

(a-b) Western blots from mTOR immunoprecipitation experiments in HEK293T cells expressing FLAG-tagged catalytically inactive CYLD (C601S), FLAG-tagged mTOR and HA-tagged Ub constructs, probed with the indicated antibodies. (b) Quantification of mTOR ubiquitination, HA/mTOR signal ratio $n=3$.

Data in (b) is shown as mean \pm SEM.

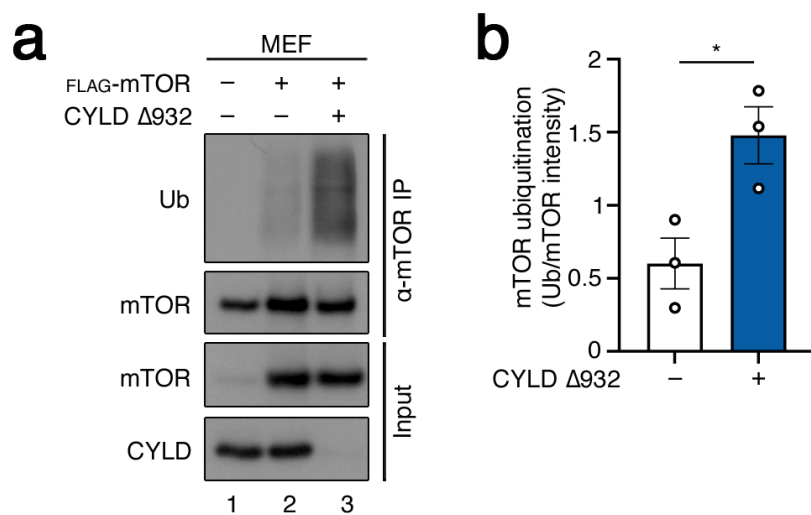


Figure 2.28 CYLD controls mTOR ubiquitination in mouse cells.

(a-b) Western blots from mTOR immunoprecipitation experiments in MEF WT or CYLD $\Delta 932$ cells stably expressing FLAG-tagged mTOR, probed with the indicated antibodies. (b) Quantification of mTOR ubiquitination, endogenous Ub/mTOR signal ratio $n=3$.

Data in (b) is shown as mean \pm SEM, * $p<0.05$.

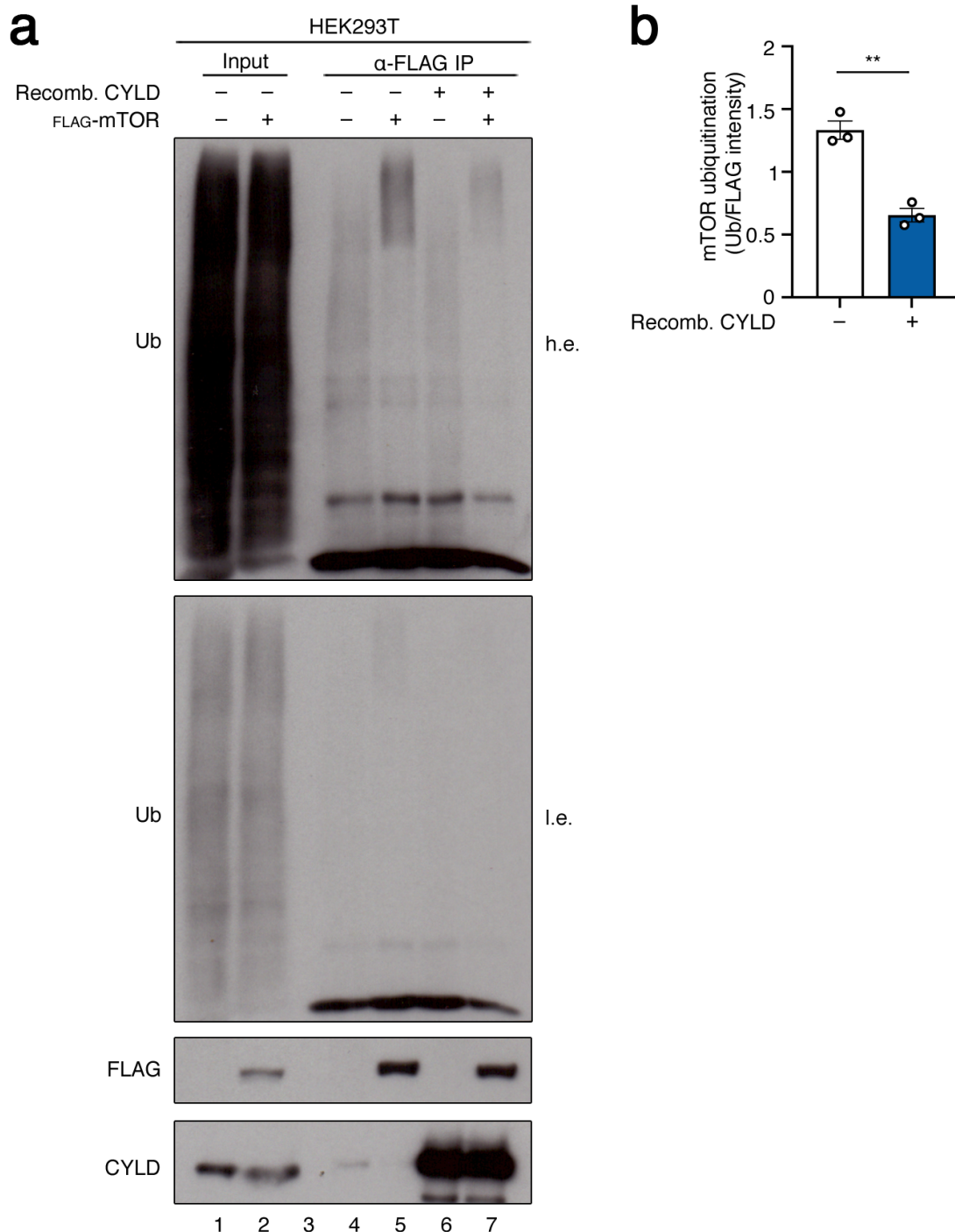


Figure 2.29 CYLD deubiquitinates mTOR *in vitro*.

(a-b) Western blots from an *in vitro* DUB assay in HEK293T cells expressing FLAG-tagged mTOR; FLAG immunoprecipitation was performed and 200ng of recombinant CYLD was added to lysates for

60 minutes; probed with the indicated antibodies. (b) Quantification of mTOR ubiquitination, endogenous Ub/FLAG signal ratio n=3. h.e. high exposure, l.e. low exposure. Data in (b) is shown as mean \pm SEM, ** p<0.01.

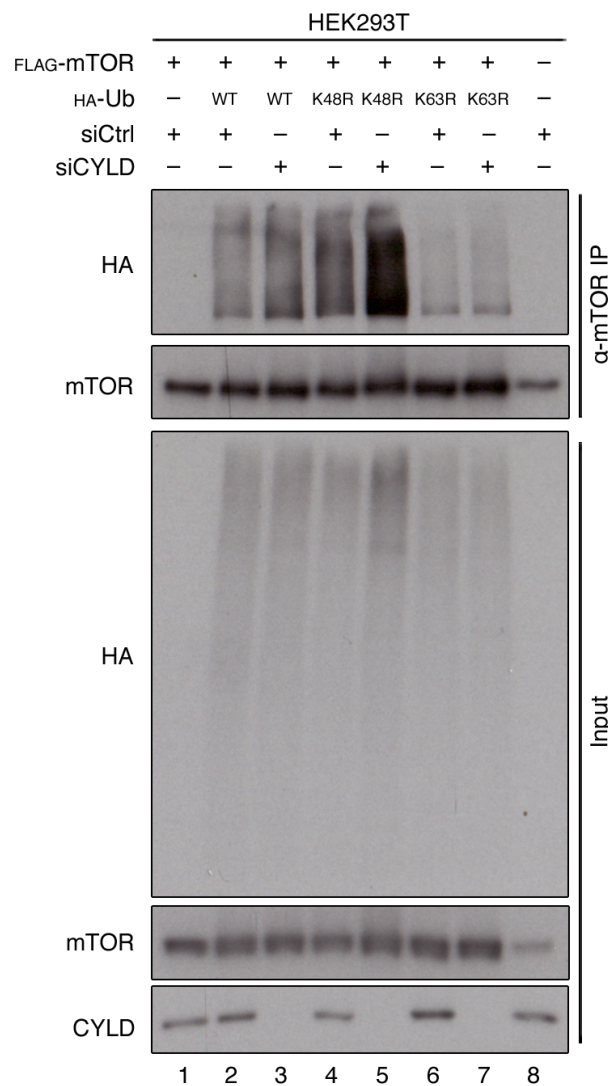


Figure 2.30 CYLD removes K63-linked chains from mTOR.

Western blots from mTOR immunoprecipitation experiments in HEK293T cells transiently transfected with siRNAs targeting CYLD or a control RNAi duplex, expressing FLAG-tagged mTOR and HA-tagged Ub WT, K48R or K63R constructs, probed with the indicated antibodies.

Data are representative of 3 independent biological replicates.

2.6.3 CYLD regulates mTOR ubiquitination independently of its canonical role on NF- κ B

The best-described role of CYLD is in the regulation of multiple components of the NF- κ B pathway. To evaluate whether the CYLD effect on mTOR is due to changes in NF- κ B activation, we knocked down IKK β , the core component of NF- κ B pathway, alone or in combination with CYLD. First, we investigated whether the loss of IKK β and CYLD elicit the expected effects on NF- κ B activity. IKK β knockdown led to a small drop in NF- κ B activity, as

assessed by a Luciferase reporter assay (Figure 2.31a). On the contrary, CYLD knockdown increased NF- κ B activity. Importantly, knockdown of both CYLD and IKK β had an intermediate effect (Figure 2.31a). Overall, I confirmed that the loss of CYLD and IKK β affect NF- κ B activity as previously described. Next, we investigated the effects of down-regulated IKK β and CYLD levels on mTOR ubiquitination. IKK β knockdown alone did not alter mTOR ubiquitination. In agreement with IKK β not affecting mTOR ubiquitination, knocking down both CYLD and IKK β did not influence the CYLD effect on mTOR ubiquitination (Figure 2.31b). Together, our findings show that CYLD regulates mTOR ubiquitination independently of its role in NF- κ B signaling.

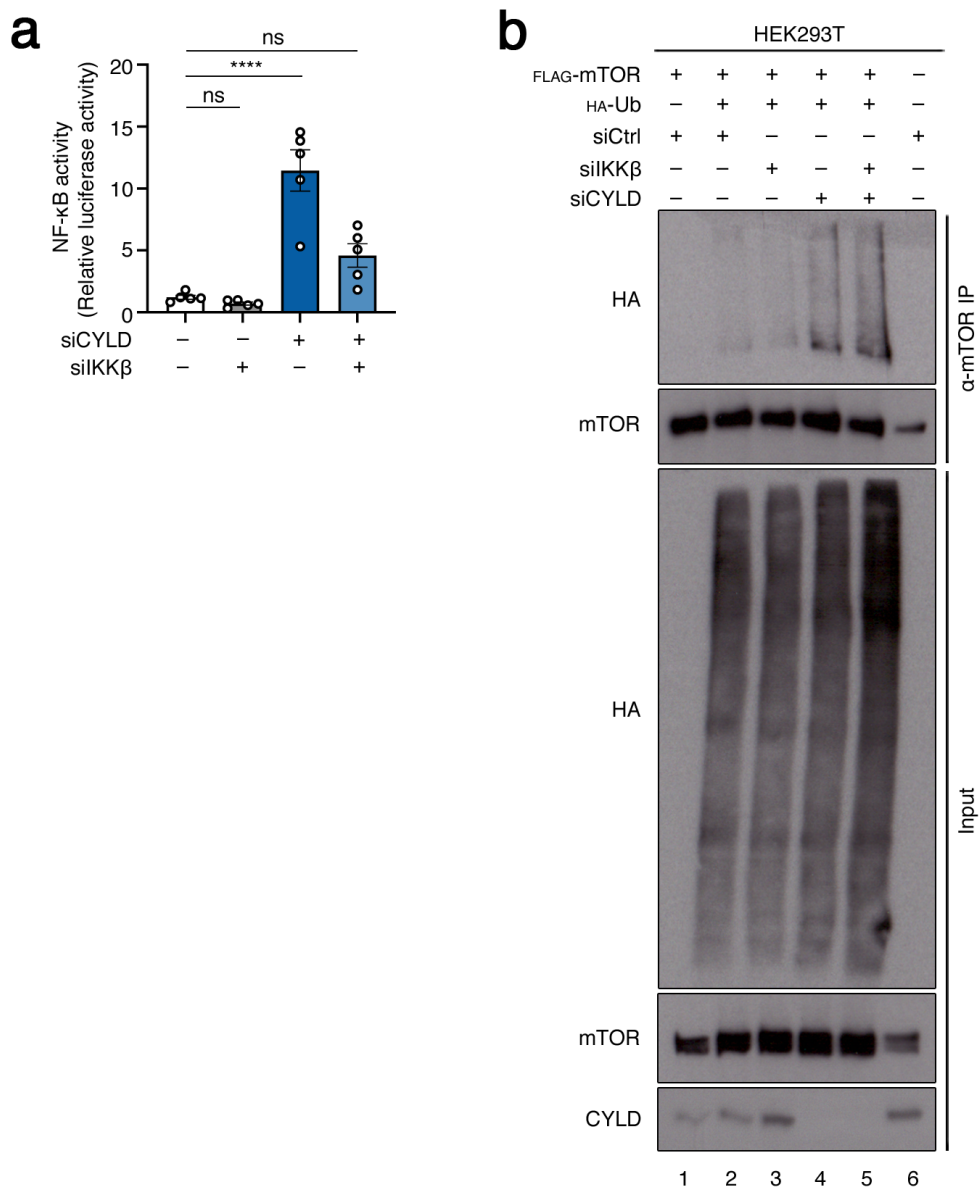


Figure 2.31 CYLD effect on mTOR is independent of its canonical effect on the NF- κ B pathway.

(a) Luciferase activity assay in HEK293T cells transiently expressing an NF- κ B firefly luciferase reporter construct, transfected with siRNAs targeting CYLD, IKK β or a control RNAi duplex, n=5.

(b) Western blots from mTOR immunoprecipitation experiments in HEK293T cells transiently transfected with siRNAs targeting CYLD, IKK β or a control RNAi duplex, expressing FLAG-tagged mTOR and HA-tagged Ub constructs, probed with the indicated antibodies. Data is representative of 3 independent biological replicates.

Data in (a) is shown as mean \pm SEM, **** $p < 0.0001$, ns non-significant.

2.7 CYLD does not affect mTORC1 or mTORC2 complex formation and protein levels of their pathway components

CYLD loss increases mTOR ubiquitination. Importantly, the ubiquitination status of a protein can influence protein-protein interactions. Thus, I hypothesized that the increased activity of mTOR complexes could be due to increased interactions between mTOR and components of complex 1 and complex 2. To assess mTOR complex formation, I knocked down CYLD and immunoprecipitated mTOR, evaluating its interaction with RAPTOR, RICTOR and mLST8. No major changes were observed in complex formation upon CYLD loss (Figure 2.32a).

Another well-known function of ubiquitination is to target proteins for degradation, commonly via the addition of K48-linked ubiquitin chains. Hence, I investigated whether CYLD loss affects protein levels of mTOR itself or of mTORC1 and mTORC2 pathway components. To evaluate if protein levels change due to ubiquitin-driven degradation, I knocked down CYLD in the presence or absence of the proteasome inhibitor MG132. Importantly, mTOR levels were unchanged upon CYLD knockdown. The lack of differences in mTOR levels is consistent with the current knowledge that CYLD does not act on K48-linked chains. Furthermore, no change in protein levels of any of the other mTORC1 and mTORC2 components was observed, except for RHEB (Figure 2.32b). Although RHEB levels are decreased upon CYLD knockdown, its levels are not rescued by proteasomal inhibition (Figure 2.32b). These data indicate that RHEB might be modulated by CYLD in a way that does not involve its proteasomal degradation. Taken together, these observations show that CYLD does not affect protein levels of the majority of known mTORC1 and mTORC2 pathway components.

2.8 CYLD regulates mTOR activity

2.8.1 CYLD regulates mTORC1 and mTORC2 activities

The data presented above show that CYLD controls the ubiquitination status of mTOR. Hence, I asked whether the increased mTOR ubiquitination upon CYLD loss causes changes in the activity of mTOR complexes. CYLD knockdown in HEK293T led to increased phosphorylation of the mTORC1 substrates, S6K and 4E-BP1 (Figure 2.33a-b), and the mTORC2 substrates, AKT and NDRG1 (Figure 2.33a-c). Importantly, changes in the phosphorylation status of mTORC1 substrates were fully mTOR-dependent, since treatment with the mTOR inhibitor Torin1 abolished the CYLD effect (Figure 2.33d-e). Similarly, the effect of CYLD loss on mTORC2 substrates was largely mTOR-dependent (Figure 2.33d-f). Nonetheless, CYLD knockdown rendered cells partially resistant to Torin1 treatment towards

mTORC2 substrates (Figure 2.33d-f). Since Torin1 is an ATP (adenosine triphosphate)-competitive inhibitor, it is unexpected that CYLD loss interferes with its action. These results show that CYLD controls both mTORC1 and mTORC2 activities.

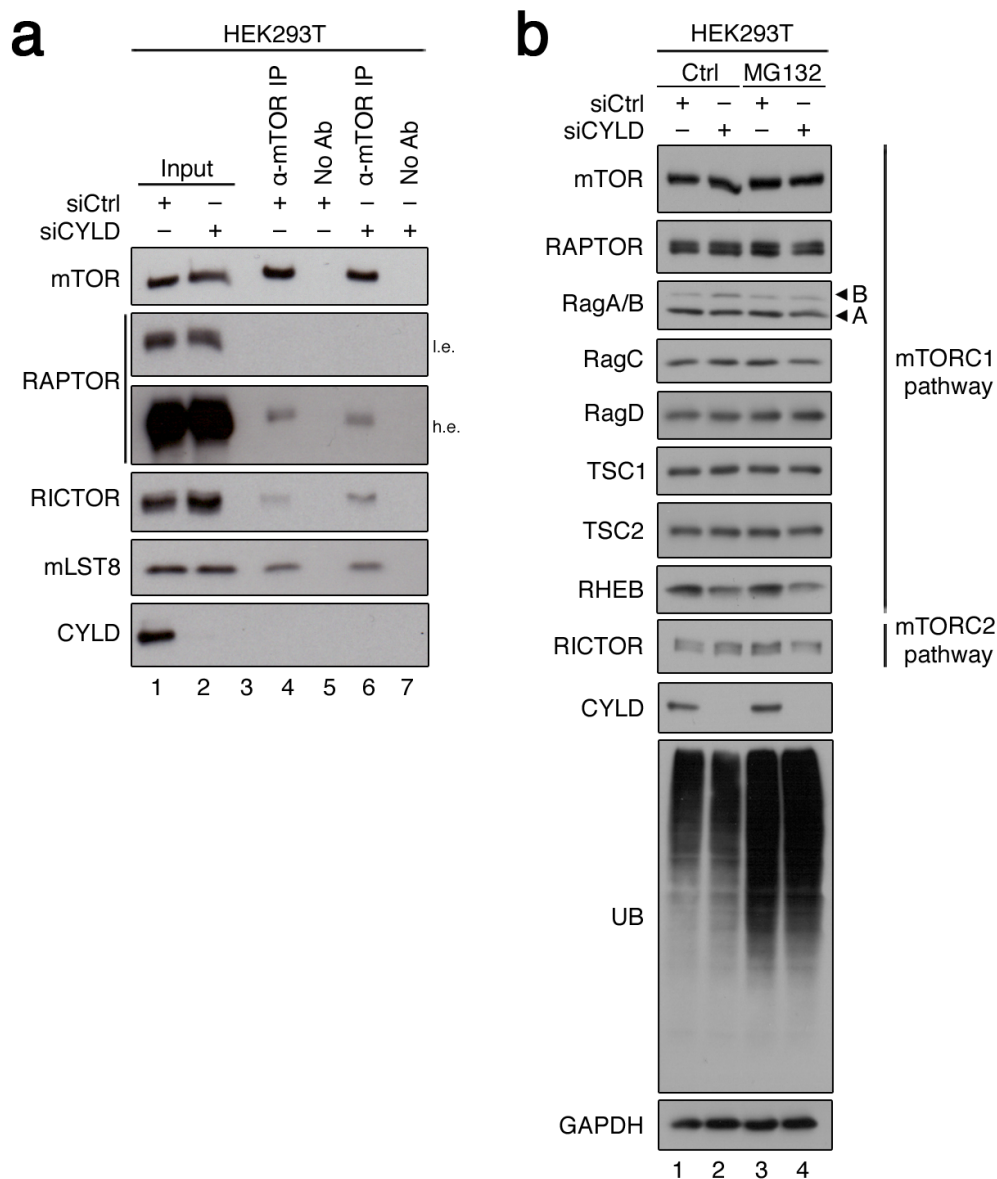


Figure 2.32 CYLD does not affect mTORC1 or mTORC2 complex stability.

(a) Western blots from mTOR immunoprecipitation experiments in HEK293T cells transiently transfected with siRNAs targeting CYLD or a control RNAi duplex, probed with the indicated antibodies.

(b) Western blots from HEK293T lysates of cells transiently transfected with siRNAs targeting CYLD or a control RNAi duplex, treated with the proteasomal inhibitor MG132, probed with the indicated antibodies.

Data are representative of 3 independent biological replicates.

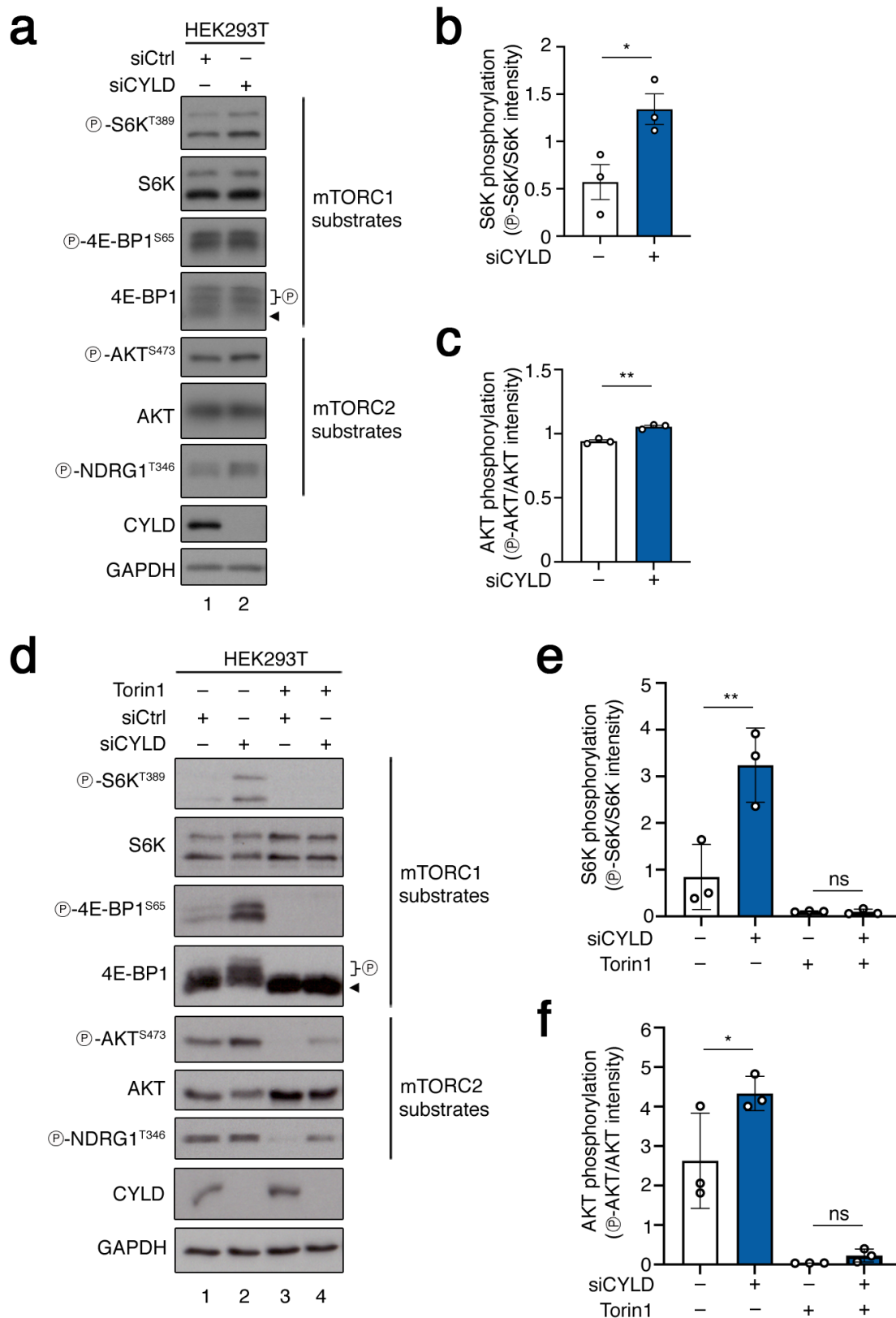


Figure 2.33 CYLD affects mTORC1 and mTORC2 activities.

(a-c) Western blots from HEK293T lysates of cells transiently transfected with siRNAs targeting CYLD or a control RNAi duplex, probed with the indicated antibodies and GAPDH as a loading control (b) Quantification of mTORC1 activity p-S6K^{T389}/S6K and (c) mTORC2 activity pAKT^{S473}/AKT n=3.

(d-f) Western blots from HEK293T lysates of cells transiently transfected with siRNAs targeting CYLD or a control RNAi duplex, treated with Torin1, probed with the indicated antibodies and GAPDH as a loading control (e) Quantification of mTORC1 activity p-S6K^{T389}/S6K and (f) mTORC2 activity pAKT^{S473}/AKT n=3.

Data in (b), (c), (e) and (f) are shown as mean \pm SEM, * p<0.05, ** p<0.01, ns non-significant.

2.8.2 CYLD is a broad regulator of mTOR

One major feature of mTOR complexes is their ability to respond to changes in environmental conditions, such as availability of AAs, glucose and GFs. Thus, I hypothesized that CYLD might modulate mTOR ubiquitination and activity in response to a specific stimulus. To test this hypothesis, I performed different starvation experiments, removing factors that are known to signal to mTOR. AA starvation led to decreased mTORC1 activity regardless of CYLD (Figure 2.34a). Next, I evaluated whether the CYLD effect on mTORC1 activity was maintained during glucose starvation. Importantly, CYLD knockdown increased mTORC1 activity, even in the absence of glucose (Figure 2.34b-c). GFs are known to signal to both mTORC1 and mTORC2. Considering that both mTOR complexes are affected by CYLD, I investigated the cellular response to GF starvation upon CYLD loss. Remarkably, CYLD knockdown increased phosphorylation of mTORC1 and mTORC2 substrates even in the absence of GFs (Figure 2.34d-f). Collectively, the partial resistance of cells to both glucose and GF starvation demonstrates that CYLD does not act to convey a specific stimulus to regulate mTORC1 activity. Instead, CYLD apparently has a broader effect on the activity of the two mTOR complexes.

2.8.3 CYLD acts in coordination with known mTORC1 pathway components

The mTORC1 pathway is tightly regulated by the negative upstream regulators, TSC1 and TSC2, and the positive regulator, RHEB. Thus, we aimed to understand if the CYLD effect on mTORC1 activity requires the aforementioned regulators. As expected, knockdown of TSC1 and TSC2 increased mTORC1 activity (Figure 2.35). On the other hand, knockdown of RHEB had no effect (Figure 2.35), likely due to the compensatory role of RHEBL-1 (RHEB-like 1) (Angarola and Ferguson, 2019). Importantly, combined knockdown of CYLD with TSC1 or TSC2 did not have an additive effect (Figure 2.35), presumably because TSC is the strongest known negative regulator of mTORC1. Hence, the complex is likely already maximally activated upon TSC loss. Moreover, combined knockdown of RHEB and CYLD abrogated the CYLD-mediated increase in mTORC1 activity (Figure 2.35). Overall, these data indicate that CYLD knockdown does not affect the mTORC1 response to loss of its upstream regulators.

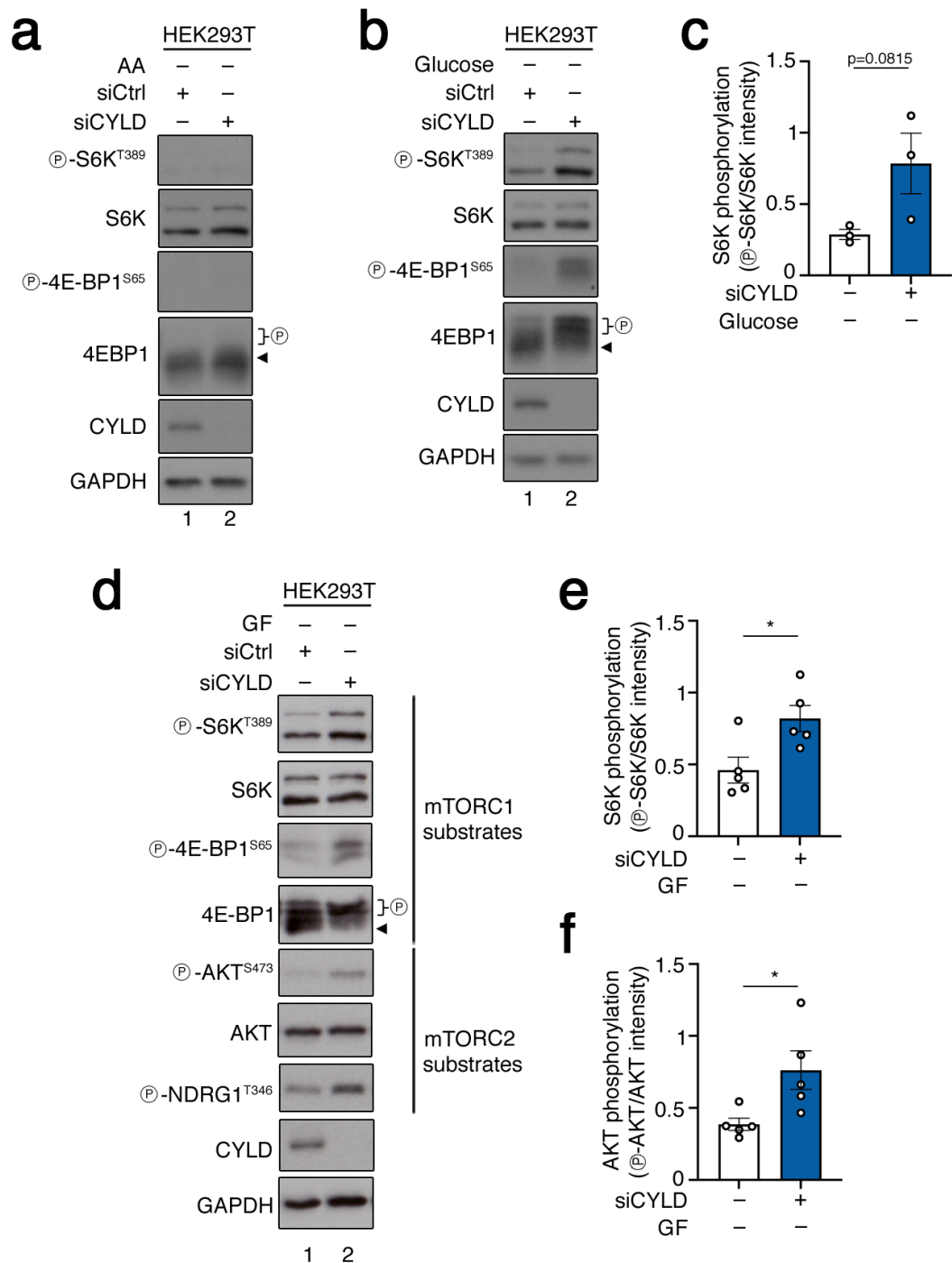


Figure 2.34 CYLD effects on mTORC1 and mTORC2 activities are not specific for a stimulus.

(a) Western blots from HEK293T lysates of cells transiently transfected with siRNAs targeting CYLD or a control RNAi duplex, cultured in media lacking AAs for one hour, probed with the indicated antibodies and GAPDH as a loading control.

(b-c) Western blots from HEK293T lysates of cells transiently transfected with siRNAs targeting CYLD or a control RNAi duplex, cultured in media lacking Glucose for one hour, probed with the indicated antibodies and GAPDH as a loading control (c) Quantification of mTORC1 activity p-S6K^{T389}/S6K n=2.

(d-f) Western blots from HEK293T lysates of cells transiently transfected with siRNAs targeting CYLD or a control RNAi duplex, cultured in media lacking GFs for 16 hours, probed with the indicated

antibodies and GAPDH as a loading control (e) Quantification of mTORC1 activity p-S6K^{T389}/S6K and (f) mTORC2 activity pAKT^{S473}/AKT n=5.
Data in (c), (e) and (f) are shown as mean \pm SEM, * p<0.05.

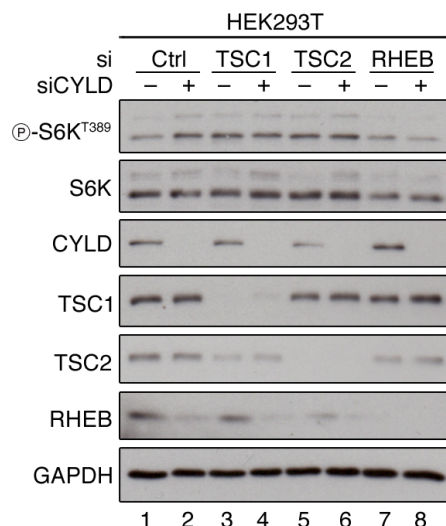


Figure 2.35 CYLD acts in coordination with known mTORC1 pathway components.

Western blots from HEK293T lysates of cells transiently transfected with siRNAs targeting CYLD, TSC1, TSC2, RHEB or a control RNAi duplex, probed with the indicated antibodies.
Data are representative of 3 independent biological replicates.

2.9 CYLD affects protein synthesis downstream of mTORC1

The observation that CYLD loss increases mTORC1 activity led us to investigate whether the processes regulated downstream of mTORC1 are affected accordingly. One of the major functions of mTORC1 is to control protein synthesis, via phosphorylation of the key translation regulators S6K and 4E-BP1. Hence, we performed a SUnSET (surface sensing of translation) assay to monitor *de novo* protein synthesis. Consistently with the upregulation of S6K and 4E-BP1 phosphorylation, CYLD knockdown increased incorporation of puromycin into nascent polypeptide chains (Figure 2.36a-b), indicating increased translation rate. Importantly, this effect was abolished by Torin1 treatment (Figure 2.36a-b), showing that the observed effects on translation are mTOR-dependent. Furthermore, puromycin incorporation was fully blocked by treatment with the translation inhibitor CHX (Figure 2.36a-b). In sum, our findings suggest that CYLD controls protein synthesis via mTORC1.

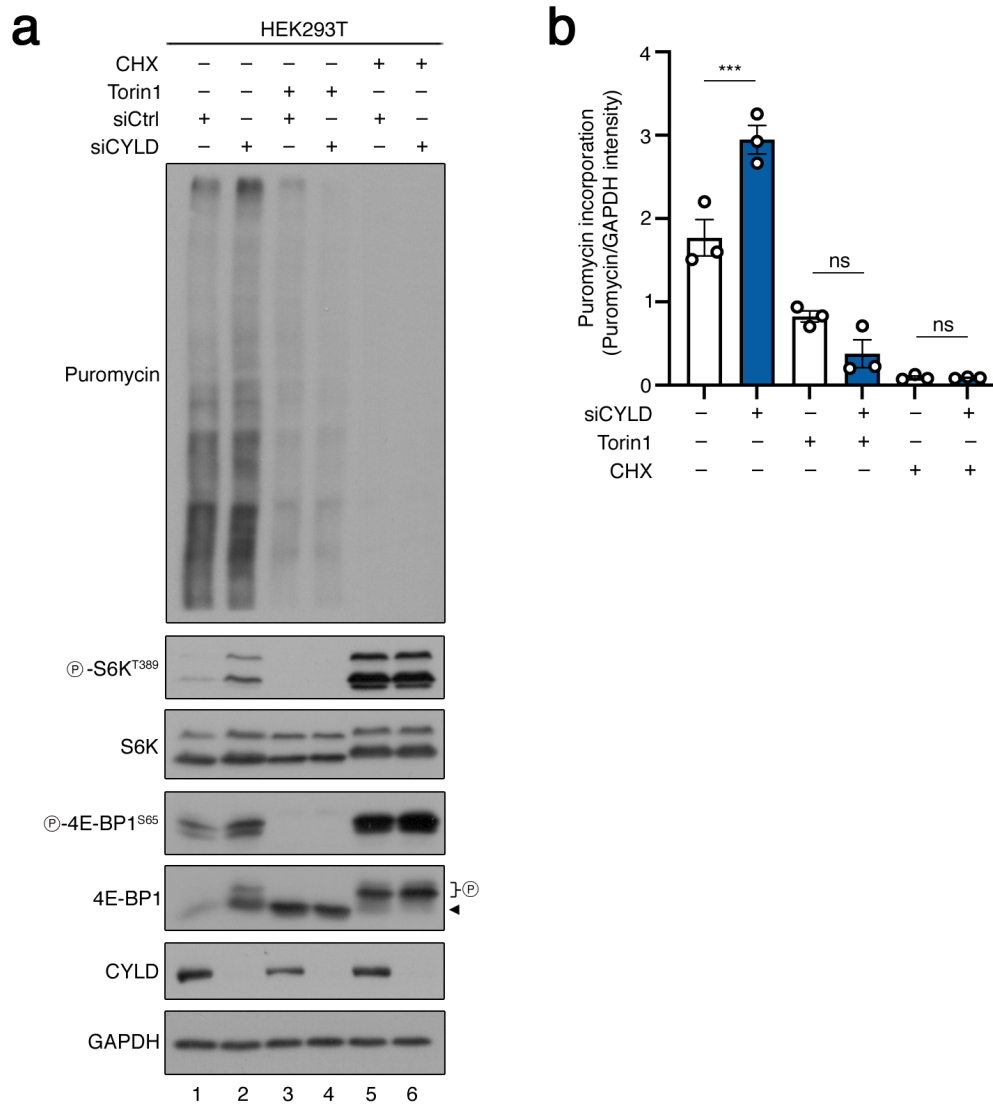


Figure 2.36 CYLD affects protein synthesis downstream of mTORC1.

(a-b) Western blots from HEK293T lysates of cells transiently transfected with siRNAs targeting CYLD or a control RNAi duplex, treated with Torin1 or CHX, probed with the indicated antibodies. (b) Quantification of Puromycin incorporation Puromycin/GAPDH, $n=3$.

Data in (b) is shown as mean \pm SEM, *** $p<0.001$, ns non-significant.

3 Discussion

The findings shown in this thesis shed light on new ways of mTOR regulation. First, I explored the reasoning for mTOR localization at the lysosomal surface. Within this project, I demonstrate that function and activity of lysosomes are required for mTOR lysosomal localization. Strikingly, although localization is tightly connected to lysosomal function, phosphorylation of mTORC1 substrates was selectively affected. These observations elucidate how spatial compartmentalization of mTORC1 functions is achieved. Second, the observation that mTOR is a heavily ubiquitinated protein prompted me to search for novel ubiquitin modulators that act on mTOR. I identified CYLD as a novel DUB for mTOR, controlling its ubiquitination status and the activity of both mTORC1 and mTORC2.

3.1 Spatially and Functionally Distinct mTORC1 Entities Orchestrate the Cellular Response to Amino Acid Availability

The reason for mTORC1 localization at the lysosomes has remained elusive since its discovery around 15 years ago (Kim et al., 2008; Sancak et al., 2008). In the majority of studies in the field, most experiments to evaluate the regulation of mTORC1 by AAs are performed using a protocol of starvation and acute AA re-addition. In this setup, it is intuitive that mTORC1 is regulated at the lysosomal surface. Lysosomes are the central degradative organelles in the cell. Hence, upon starvation, this organelle becomes the main source of cellular nutrient supply. Upon short-term AA re-addition, mTORC1 would be in close proximity to the center of nutrient release. This allows the complex to sense lysosome-derived AAs while cells take enough AAs up to replenish the cellular nutrient pool. However, in the context of constant supply of exogenous AAs, lysosomal localization of mTORC1 is somehow counter-intuitive. Importantly, in this thesis, by using multiple ways of disrupting lysosomal activity, I established that mTORC1 lysosomal localization requires functional lysosomes. I also show that cells cultured in the presence of exogenous AAs have active lysosomal degradation, as reported previously (Musiwaro et al., 2013). With these findings, I provide evidence to support the hypothesis that a fraction of mTORC1 is lysosomal because of local AA release. Furthermore, I also show that cells contain a non-lysosomal pool of mTORC1. Strikingly, during exogenous AA sufficiency, non-lysosomal mTORC1 remains active towards its canonical substrates, S6K and 4E-BP1. On the contrary, the lysosomal substrate TFEB is severely affected by the loss of mTORC1 localization to lysosomes. Along the same line, the importance of functional lysosomes for TFEB phosphorylation was also demonstrated by assessing changes in the trafficking of cargo to lysosomes. Previous studies showed that inhibition of trafficking to lysosomes either via i) mutations in the HOPS (homotypic fusion and protein sorting) complex that is essential for fusion of lysosomes with endosomes and autophagosomes (van der Welle et al., 2021), or ii) loss of the ESCRT-I (endosomal sorting complexes required for transport) complex, which is required for degradation of lysosomal membrane proteins (Wrobel et al., 2022), selectively affected TFEB phosphorylation. Together, the data presented here suggest a model (Figure 3.1) in which lysosomal-derived AAs are important for mTORC1 lysosomal localization and TFEB phosphorylation. On the

other hand, non-lysosomal mTORC1 responds to extracellular AAs and is required for phosphorylation of S6K and 4E-BP1.

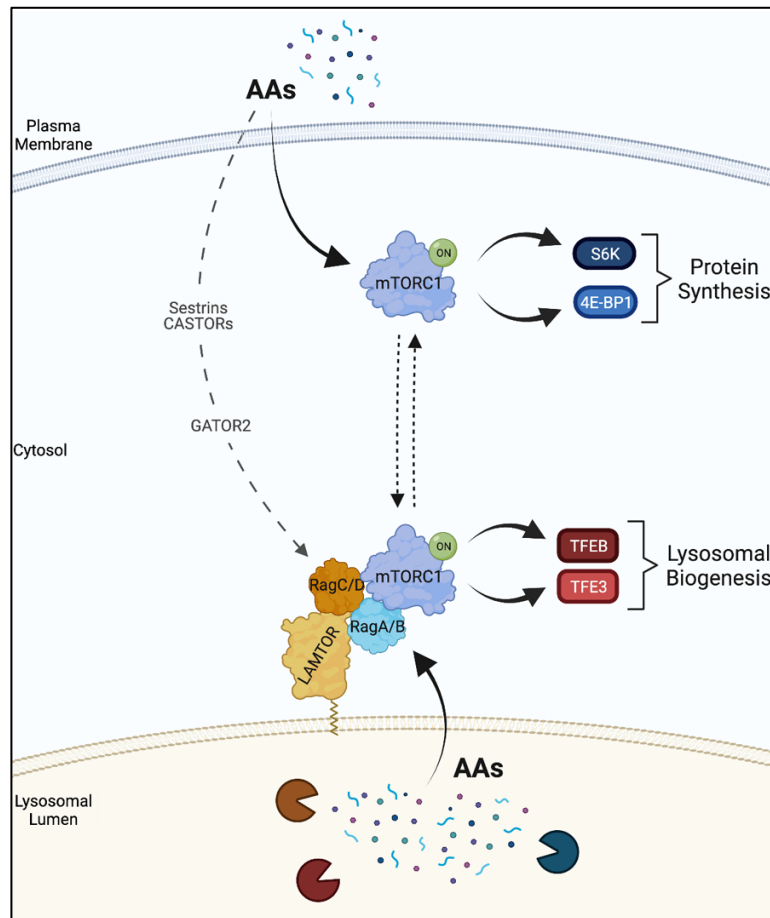


Figure 3.1 Model for the spatial separation of mTORC1 functions.

AAs derived from protein degradation in lysosomes are important for the regulation of lysosomal mTORC1. This pool of mTORC1 is responsible for the phosphorylation of the substrates TFEB and TFE3. On the other side, mTORC1 that is non-lysosomal is responsive to extracellular AAs, and is relevant for the regulation of the substrates S6K and 4E-BP1. Created with BioRender.com

Previous work showed that inhibition of lysosomal acidification led to decreased mTORC1 lysosomal localization (Zoncu et al., 2011). By using the widely-established protocol of 50-minutes AA starvation and 10-minutes AA re-addition, the authors claim that the delocalization of mTORC1 is coupled to decreased mTORC1 activity towards S6K and 4E-BP1 (Zoncu et al., 2011). However, I now show that this coupling is only relevant after starvation and re-addition. Upon constant AA supply, v-ATPase inhibition delocalizes mTORC1 from lysosomes without affecting its activity towards the canonical substrates S6K and 4E-BP1.

Under normal diet conditions, cells and tissues have available AAs through food intake and further nutrient distribution via the blood stream (Felig et al., 1973; Broer and Broer, 2017). Additionally, even during short term starvation, AA levels in the plasma do not immediately drop (Felig et al., 1969). Thus, it is reasonable to assume that in most conditions, mTORC1

is regulated primarily by exogenous AAs. In addition, the physiological existence of a starvation/re-addition protocol is harder to establish. Although there are specific scenarios where cells can be starved, such as in solid tumors (Sutherland, 1988; Leprivier et al., 2013; Pan et al., 2022), the specific re-addition of AAs is harder to assess. Nonetheless, one of the examples where a change in nutrient status can be observed is during development and birth. The human placenta is mature around embryonic day E35 (Hemberger et al., 2020). Hence, nutrient levels might change from early to late developmental stages. Additionally, in mammals, the nutrient supply is cut after birth until feeding occurs. Importantly, in this specific case, autophagy is essential (Kuma et al., 2004). In this thesis, I show that the Rag GTPases are required for the starvation/re-addition response, as well as for TFEB phosphorylation. TFEB is a transcription factor involved in the transcription of lysosome-biogenesis- and autophagy-related genes. Hence, in the post-birth scenario, where autophagy is essential, the Rag GTPases become key mTORC1 regulators. Strikingly, mice with constitutively active RagA die neonatally because they cannot activate autophagy (Efeyan et al., 2013), supporting a key role for the Rag GTPases in the post-birth period.

In previous studies, changes in mTOR lysosomal localization did not always correlate with a drop in S6K and 4E-BP1 phosphorylation (Averous et al., 2014; Demetriades et al., 2014; Jewell et al., 2015; Manifava et al., 2016). Furthermore, mTOR and other mTORC1 components (Drenan et al., 2004; Schieke et al., 2006; Liu and Zheng, 2007; Betz and Hall, 2013; Yadav et al., 2013; Zhou et al., 2015; Manifava et al., 2016; Gosavi et al., 2018; Lawrence et al., 2018; Nuchel et al., 2021) as well as many of the known mTORC1 regulators, such as RHEB, TSC, the Rags, ARF1 and RAB1A (van Slegtenhorst et al., 1998; Nellist et al., 1999; Buerger et al., 2006; Hanker et al., 2010; Yadav et al., 2013; Thomas et al., 2014; Jewell et al., 2015; Manifava et al., 2016; Hao et al., 2018; Lawrence et al., 2018; Angarola and Ferguson, 2019) are not exclusively lysosomal proteins. This large body of evidence suggests that mTORC1 is likely not an exclusively lysosomal complex.

Recent work has established the Golgi as a major location for mTORC1 regulation: besides the localization of mTORC1 components and regulators at this cellular compartment (Liu and Zheng, 2007; Gosavi et al., 2018; Hao et al., 2018; Nuchel et al., 2021), two Golgi proteins were recently identified as mTORC1 substrates (Nuchel et al., 2021; Kaeser-Pebernard et al., 2022). These studies have established that mTORC1 is involved in the control of Golgi architecture and protein secretion. Together, the existence of a Golgi-residing mTORC1 pool and the control of Golgi-related functions expands the understanding of mTORC1 regulation. Importantly, it shows that mTORC1 is likely active in different locations.

Remarkably, strengthening the findings that mTORC1 is not only regulated by the lysosomal machinery, Rag knockout mice do not phenocopy mTOR or RAPTOR loss. RagA knockout mice die around embryonic day E10.5 (Efeyan et al., 2014). Similarly, LAMTOR2 and GATOR2 knockout mouse embryos that mimic Rag loss, die around E10.5 (Teis et al., 2006; Jiang et al., 2023). On the other hand, mTOR and RAPTOR knockout mice die earlier in

development, around day E3.5 and E6.5, respectively (Gangloff et al., 2004; Murakami et al., 2004; Guertin et al., 2006). Importantly, MEFs isolated from RagA-null animals have persistent mTORC1 activity, assayed by phosphorylation of S6K and 4E-BP1, even though they completely lose mTORC1 lysosomal localization (Efeyan et al., 2014). Furthermore, in mouse models that lack both RagA and RagB, mTORC1 activity towards S6K and 4E-BP1 is only slightly reduced in MEFs and cardiomyocytes (Kim et al., 2014; Jewell et al., 2015). Thus, in the absence of the Rag GTPases, mTORC1 can still be active towards its canonical substrates. In combination with the data presented in this thesis, it is likely that the Rag GTPases are largely not required for the control of S6K and 4E-BP1 during AA sufficiency.

In most of the aforementioned studies, the interpretation of why Rag GTPase KO cells have sustained mTORC1 activity was related to cellular adaptation to Rag loss. However, I show here that approaches that are shorter in time elicit the same effect on S6K and 4E-BP1: knock down of components that mimic Rag loss, such as knockdown of LAMTOR1 or MIOS, and use of multiple drugs that disrupt lysosomal activity, as BafA1, ConA, Chloroquine and PepA+E64. Moreover, knockout of GNPTAB, a protein that is unrelated to the Rag GTPases, also shows persistent S6K and 4E-BP1 phosphorylation. Taken together, the data presented here indicate that the sustained mTORC1 activity towards S6K and 4E-BP1 in Rag-null cells is not due to cellular adaptation.

The Rag GTPases have evolved as part of the lysosomal machinery to regulate mTORC1. Thus, the reason for unaffected mTORC1 activity towards S6K and 4E-BP1 in Rag-null mice is not known. I propose in this thesis that the Rag GTPases are necessary for mTORC1 activity in a substrate-specific manner. Importantly, the studies that assessed the effects of Rag-loss did not evaluate the phosphorylation status of TFEB. Hence, I speculate that the lethality observed in Rag KO animals is likely due to differences in TFEB regulation. During development, mammals have a steady supply of nutrients via placental delivery (Remesar et al., 1980; Desforges and Sibley, 2010; Hemberger et al., 2020). Importantly, in mice, an early placenta is observed from day E9.5 (Hemberger et al., 2020), which is before the death of Rag-null embryos. Therefore, having a constantly active catabolic machinery even in the presence of nutrients could be deleterious during development, when cells need to divide and grow. An alternative explanation is that Rag KO cells display partial resistance to starvation and a defective response to AA re-addition. Thus, it is possible that during the transitional phase between early embryogenesis and placental formation (Hemberger et al., 2020), cells are exposed to different concentrations of nutrients. In this case, Rag-null embryos would be unable to properly regulate mTORC1.

One important difference between the outcome of the approaches I used in this work was the response to starvation. Chloroquine and PepA+E64 treatments did not affect the starvation response. However, treatment with BafA1 and ConA as well as knockout of the Rag GTPases, led to blunted starvation. In Rag KO cells, TSC cannot be recruited to the lysosomal surface, hence the blunted starvation response (Demetriades et al., 2014;

Demetriades et al., 2016b). However, later studies expanded the machinery for lysosomal TSC recruitment. First, G3BPs were recognized as a second tether for TSC at the lysosomes by their binding to the lysosomal proteins LAMP1/2 (Prentzell et al., 2021). Second, the TSC component TSC1 was found to bind directly to lysosomal PIPs (Fitzian et al., 2021). This observation indicates that the TSC complex can also be directly tethered to lysosomes. Hence, it is possible that altering v-ATPase activity by BafA1 or ConA would affect one of these recruitment mechanisms directly or indirectly. One possibility is that changes in the degradation capacity of lysosomes by v-ATPase blockage could lead to differences in nutrient availability, such as of lipids. If lipid composition of the lysosomal membrane is altered, lysosomal PIPs and, hence, recruitment of TSC by this mechanism could be affected. Nonetheless, all mechanisms described above are lysosome-centered. Therefore, I can speculate that either lysosomal TSC can control non-lysosomal mTOR, or that similar mechanisms exist elsewhere.

AAs are the strongest regulators of mTORC1, albeit not the only stimulus that can activate the complex. In this thesis, I show that non-lysosomal mTORC1 responds to fluctuations in AA availability. Importantly, RagA/B KO cells that contain only non-lysosomal mTORC1 also respond to blockage of the GF signaling branch. In contrast, I show that Rag-null cells do not starve for glucose, showing that non-lysosomal mTORC1 cannot sense glucose availability. Importantly, mice that lack the RagA GTPase also show insensitivity to glucose withdrawal (Efeyan et al., 2014). Likewise, mice with constitutively active RagA also display glucose insensitivity (Efeyan et al., 2013). This phenotype is accompanied by increased localization of mTOR to the lysosomal surface even in the absence of glucose (Efeyan et al., 2013). In addition, a recent report proposed that AMPK controls GATOR2, a direct positive regulator of the Rag GTPases, to signal glucose availability to mTORC1 (Dai et al., 2023). Thus, I confirm that glucose signaling to mTORC1 requires the Rag GTPases and lysosomal localization of mTORC1.

Finally, I observed TFEB phosphorylation being fully dependent on lysosomes and the lysosomal mTORC1 machinery. In agreement, previous studies described the requirement of RagC and/or RagD for TFEB phosphorylation (Napolitano et al., 2020; Gollwitzer et al., 2022; Cui et al., 2023), as well as of the RagC/D GAP complex FLCN/FNIP (Lawrence et al., 2019). Importantly, no changes on S6K and 4E-BP1 phosphorylation were observed under the same conditions. Moreover, TSC loss, a condition where mTORC1 is hyperactive, has opposing effects on different substrates: although S6K and 4E-BP1 are indeed hyperphosphorylated, TFEB phosphorylation is completely lost (Alesi et al., 2021; Asrani et al., 2022). Finally, work in yeast has also established a separation between phosphorylation of Sch9, the homologue for S6K, and autophagy regulators (Hatakeyama et al., 2019). Altogether, this body of work corroborates the idea that distinct mTORC1 substrates are regulated differently. In this thesis, by using multiple approaches to uncouple mTOR localization and activity, I showed that this is likely caused by the existence of different mTORC1 pools.

3.2 CYLD is a novel deubiquitinase for mTOR

mTOR is a heavily ubiquitinated protein. Nonetheless, most of the work that described the regulation of mTOR-related pathways focused on the role of phosphorylation (Yin et al., 2021). However, in the past years, studies started evaluating the effects of other PTMs on mTOR. By focusing on ubiquitination, E3 ligases that attach ubiquitin chains on mTOR were identified. The E3 ligase SCF/FBXW7 acts directly on mTOR to promote its degradation (Mao et al., 2008). Furthermore, K63-linked chains are attached to mTOR upon AA sufficiency by the combined action of the adaptor protein p62 and the E3 ligase TRAF6 (Linares et al., 2013a). Mitochondrial stress has also been linked to mTOR ubiquitination by PARKIN (Park et al., 2014). Nonetheless, ubiquitin is a reversible modification. The termination of the signal that was initiated by ubiquitin addition is of equal relevance for the control of signaling pathways. To date, no DUB that removes ubiquitin molecules from mTOR has been identified. Although the DUB USP9X was described to modulate mTOR activity (Agrawal et al., 2012), no evidence to support direct action on mTOR ubiquitination is present. Hence, in this thesis, I describe for the first time that CYLD is a DUB for mTOR.

In agreement with CYLD functioning as an mTOR regulator, previous work showed that Cyld and mTOR interact in mouse hippocampal lysates (Colombo et al., 2021). Moreover, hippocampal homogenates from *Cyld*^{-/-} mice showed increased mTORC1 activity (Colombo et al., 2021). On the contrary, CYLD overexpression in the heart led to a decreased phosphorylation of the mTORC1 substrate S6K (Qi et al., 2020). Together, these studies support my findings that CYLD is involved in the regulation of mTOR signaling. Nonetheless, although they observe changes in mTOR signaling, they did not unravel the mechanisms involved in this regulation. Here, I show that mTOR ubiquitination is regulated by CYLD, and that this effect is important for mTOR activity.

Remarkably, most of the components of the mTORC1 and mTORC2 pathways are known to be ubiquitinated. For instance, RAPTOR ubiquitination has been described to control mTORC1 stability (Hussain et al., 2013). DEPTOR, the inhibitory subunit of both mTOR complexes, is targeted to degradation by the ubiquitin-proteasomal system when the complex is activated (Gao et al., 2011). Additionally, ubiquitination of mLST8 is one of the driving factors to direct the formation of mTORC2 over mTORC1 (Wang et al., 2017a). Besides ubiquitination of direct components of the complex, many mTORC1 regulators are also heavily modulated by ubiquitin. RHEB ubiquitination is known to be involved in its activation by GFs (Deng et al., 2019) and enhances its binding to mTOR in the presence of AAs (Yao et al., 2020). LAMTOR1 ubiquitination favors activation of the Rag GTPases (Hertel et al., 2022). RagA itself is also ubiquitinated, which impacts its interaction with the negative regulator GATOR1 (Deng et al., 2015; Jin et al., 2015). The stability of the TSC complex is also known to be regulated by ubiquitination. Importantly, the interaction between different TSC components was shown to prevent their degradation (Chong-Kopera et al., 2006; Han et al., 2008; Hu et al., 2008; Zheng et al., 2008; Mohan et al., 2016; Guo et al., 2018; Madigan et al., 2018). Ubiquitination of AA sensors, such as Sestrin2 and CASTOR, is also important

for their activity (Lear et al., 2019; Li et al., 2021). Thus, it becomes clear that ubiquitination is a PTM of extreme relevance for mTOR signaling pathways. My work adds to this body of knowledge by identifying a novel player in the regulation of mTOR ubiquitination.

In 2008, a study on the structure of CYLD showed preferential activity towards the removal of K63-linked chains (Komander et al., 2008). In agreement with this study, the effect of CYLD loss on mTOR ubiquitination was abolished by co-expressing a ubiquitin mutant that cannot form K63-linked chains. Nonetheless, I observed that in the absence of K48-linked chains, the CYLD effect on mTOR is enhanced. It is possible that cells that express the ubiquitin K48R mutant mostly forms K63 chains, which would explain the enhancement of the CYLD effect. In contrast, WT ubiquitin allows for the formation of both K48 and K63-linked chains, therefore less ubiquitin molecules are available to form K63-linked chains. A second possibility is that K48 chains affect the generation of K63-linked chains. Importantly, CYLD regulation is known to be modulated by the existence of complex ubiquitin chains, formed by the branching of K63- and K48-linked chains. In the NF- κ B pathway, K48 branches are added on K63 chains. This phenomenon protects substrates from the DUB activity of CYLD (Ohtake et al., 2016). Finally, the modulation of complex chains was also observed by a study in which the authors demonstrated that CYLD can act on the tumor suppressor p53 (Fernandez-Majada et al., 2016). Additionally, CYLD is also known to act directly in linear ubiquitin chains (Komander et al., 2009). Nevertheless, my experiments show that the CYLD effect is fully K63-dependent, indicating that CYLD does not act on linear ubiquitin chains on mTOR. In sum, my work shows that K63 ubiquitin chains are the major modifications modulated by CYLD on mTOR.

The best studied role of CYLD is in the regulation of the NF- κ B pathway (Brummelkamp et al., 2003; Kovalenko et al., 2003; Trompouki et al., 2003; Sun, 2010). Intriguingly, components of the NF- κ B pathway, mainly from the IKK complex, signal to mTORC1 and mTORC2. IKK signals to mTORC1 via phosphorylation of TSC1 (Lee et al., 2007) and to mTORC2 via interaction with RICTOR (Xu et al., 2013). Hence, because mTOR is affected by CYLD, I investigated whether the effect that CYLD has on NF- κ B and the effects of the latter on mTOR are disconnected. In this thesis, I showed that CYLD modulates mTOR ubiquitination directly and independently of the NF- κ B pathway.

I demonstrate here that CYLD acts directly on mTOR by showing that i) it binds to mTOR, ii) it regulates its ubiquitination directly and iii) it changes the status of mTOR activation. However, CYLD is known to affect ubiquitination of other proteins too. Of relevance, AKT is one of the proteins that is regulated by CYLD (Lim et al., 2012; Yang et al., 2013b). Intriguingly, CYLD knockdown rendered mTORC2 partially resistant to Torin1 treatment. I speculate here that this is likely due to the action that CYLD has on AKT directly. Importantly, AKT feeds back to mTORC2 (Yang et al., 2015). Hence, although mTOR kinase activity is inhibited by Torin1, the constant feedback from AKT to activate mTORC2 might be responsible for the remaining phosphorylation of both AKT itself and NDRG1. An additional

possibility is that ubiquitination-induced conformational changes might influence Torin1 binding to mTOR in the context of mTORC2. I can also not exclude that CYLD acts on the phosphatases that remove phosphorylation of mTORC2 substrates. Thus, although CYLD acts directly on mTOR, it is also part of an intricate network of ubiquitin regulation.

mTOR complexes are known to be activated in the presence of positive signals from the cellular environment, such as the presence of AAs, GFs or glucose. Interestingly, ubiquitination of both mTOR itself and components of the pathway have been shown to take place in response to AA or GF sufficiency (Linares et al., 2013a; Deng et al., 2019; Yao et al., 2020). Hence, I hypothesized that CYLD activity towards mTOR might be responsive to such cues. However, CYLD still enhanced mTORC1 activity when either GFs or glucose were absent, but not during AA starvation. These findings indicate that CYLD does not act to convey a specific stimulus to mTOR. Instead, it suggests that CYLD has a broader action on mTOR signaling. Of note, the partial resistance to starvation was only observed in settings where the starvation does not fully abolish phosphorylation of mTOR substrates. Thus, I speculate that CYLD increases mTOR activity during starvation whenever there is some mTOR activity left.

Besides regulatory ubiquitination, this PTM also has an important role in protein degradation. By evaluating levels of proteins in the mTORC1 and mTORC2 pathways upon CYLD loss, I showed that most of them are unaffected. This observation is in agreement with the action of CYLD in the regulation of K63-linked chains, linear and complex ubiquitin chains that are not related to degradative signals (Komander et al., 2008; Komander et al., 2009; Ohtake et al., 2016). One exception was RHEB, whose levels drop upon CYLD knockdown. Although lysosomal RHEB is known to undergo proteasome-mediated degradation (Yao et al., 2020), blockage of this system with MG132 did not rescue RHEB levels. Additionally, lower RHEB levels cannot explain the observed increase in mTORC1 activity. Together, these findings suggest that RHEB is not being degraded by the proteasomal system upon CYLD loss. Instead, RHEB might undergo ubiquitination that is also modulated by CYLD. Since ubiquitination increases the molecular weight of proteins, hyper-ubiquitinated RHEB might run in a gel at a higher size. Thus, it is possible that the lower levels of RHEB upon CYLD loss are instead reflected in an up-shift of RHEB that I was not able to observe in my experimental conditions for unclear reasons.

Finally, I show that the effects of CYLD on mTOR are translated to increased protein synthesis. Importantly, this effect requires mTOR activity. Thus, I conclude that CYLD acts as a DUB for mTOR, modulating its ubiquitination status, its activity and its downstream functions.

4 Future perspectives

In the past years, nutritional interventions were developed to increase healthspan. Importantly, many of these are centered around mTORC1 inhibition (Fernandes and Demetriades, 2021). The regulation of mTORC1 activity differs depending on the nutritional strategy, i.e., constant nutrient supply vs starvation/re-addition. Thus, to evaluate the efficacy of nutritional interventions, it is necessary to understand how different diets affect mTORC1. Additionally, different AAs regulate different mTORC1 pools, opening up the possibility of tailored diets for specific inhibition of certain subsets of mTOR complexes.

Aging is accompanied by a dysregulation in protein synthesis, autophagy and lysosomal activity (Fernandes and Demetriades, 2021). Thus, it is vital to assess which downstream functions of mTORC1 are targeted by anti-aging interventions. In this thesis, I show that loss of lysosomal activity or Rag depletion leads to mTORC1 inactivation towards TFEB, but not towards S6K and 4E-BP1. Hence, if a therapeutic approach aims to lower translation rates, it is not advantageous to interfere with lysosomes or with the Rag GTPases. In contrast, these approaches induce TFEB nuclear translocation. Of note, nuclear TFEB is associated with increased lifespan in *C. elegans* and mice (Lapierre et al., 2013; Silvestrini et al., 2018). Therefore, these findings indicate that for development of anti-aging interventions, mTORC1 activity should be evaluated in a substrate-specific manner.

Availability of many AAs is communicated to mTORC1 via the action of AA sensors. To date, most AA sensors are known to signal to mTORC1 via the Rag GTPases. Hence, it is not surprising that sensors for serine, threonine and cysteine, AAs that signal to non-lysosomal mTORC1, are not well known. The only sensor identified for this class of AAs is TARS2, a sensor for threonine (Kim et al., 2021). However, this study was based on the action of TARS2 upon threonine re-addition. Likewise, serine was described as an AA that signals via the Rag GTPases, albeit using a similar protocol of re-addition (Meng et al., 2020). Thus, further research is required to determine which are the key regulators that signal AA sufficiency to non-lysosomal mTORC1. Importantly, Rag KO cells could be used as a model for the identification of such regulators.

Although I focused on AAs that signal to mTORC1 in a Rag-independent way, this thesis described that the effect of hydrophobic (methionine, leucine, isoleucine, glycine, valine) or positively-charged (histidine, arginine, lysine) AAs on mTORC1 is mostly Rag-dependent. This observation is in agreement with the mechanism of methionine, leucine and arginine sensing. The AA sensors for these three AAs signal to activate mTORC1 via the Rag GTPases (Han et al., 2012; Jung et al., 2015; Rebsamen et al., 2015; Wang et al., 2015; Chantranupong et al., 2016; Saxton et al., 2016a; Saxton et al., 2016b; Wolfson et al., 2016; Gu et al., 2017; Wyant et al., 2017b; Chen et al., 2021). Hence, it is possible that Rag-null cells cannot sense whether methionine, leucine and arginine are available. Furthermore, isoleucine, glycine, valine, histidine and lysine are AAs for which no sensors are known. According to the

observations made in this thesis, I hypothesize that these AAs are regulated via the Rag GTPases.

v-ATPase inhibition decreases mTOR lysosomal localization and activity towards TFEB. Interestingly, a recent study showed that mTOR kinase inhibition is, in turn, needed for the assembly of the v-ATPase at the lysosomal surface (Ratto et al., 2022). Thus, it is possible that upon mTOR inhibition, cells enhance lysosomal v-ATPase assembly to rescue mTORC1 lysosomal localization.

Notably, in certain LSDs, such as Pompe disease or cystinosis, the induction of a TFEB-mediated transcriptional program is beneficial (Medina et al., 2011; Spampinato et al., 2013; Rega et al., 2016; Gatto et al., 2017). However, here I show that TFEB dephosphorylation is observed in GNPTAB KO cells, which are a model for the LSDs mucopolipidosis type II and III (Tiede et al., 2005; Danyukova et al., 2020). Hence, the constant lysosomal biogenesis induced by nuclear TFEB might lead to a futile cycle in which more lysosomes are generated, without being loaded with lysosomal enzymes. In the same manner, many diseases are caused by deficiencies in the v-ATPase (Colacurcio and Nixon, 2016; Bagh et al., 2017; Song et al., 2020). As I described in this thesis, v-ATPase inhibition leads to loss of TFEB phosphorylation. As a consequence, more lysosomes that cannot be properly acidified would also produce a futile cycle. In these settings, induction of TFEB activity might be deleterious. Further research is needed to evaluate whether removing TFEB from the nucleus is beneficial for the aforementioned diseases. As observed for the model of tuberous sclerosis, overexpression of FLCN or RagC was able to restore TFEB phosphorylation and cytosolic localization (Alesi et al., 2021; Asrani et al., 2022). Intriguingly, treatment with Rapamycin also rescued TFEB phosphorylation in TSC-deficient cells (Asrani et al., 2022). Therefore, these approaches are good candidates for treating diseases in which constant activation of TFEB might be damaging.

In addition to identifying a spatial separation of mTOR localization and function, in this thesis I identified CYLD as a DUB for mTOR. Importantly, CYLD modulates mTOR ubiquitination and activity. Yet, it is unclear how changes in mTOR ubiquitination lead to changes in its activation. Ubiquitination is a signaling modification that affects kinase activity by several mechanisms. One example is by modifying the interaction of a kinase with its regulators. For instance, in the NF- κ B pathway, the ubiquitination of RIPK1 is important for the recruitment of the ubiquitin-binding protein, TAB2 that further recruit TAK1 (Kanayama et al., 2004). TAK1 phosphorylates IKK β , which leads to activation of the NF- κ B-dependent transcriptional program. Hence, CYLD-mediated mTOR ubiquitination might change mTOR interaction with its regulators. Although this is a plausible explanation for the effect of CYLD on mTOR activity, mTORC1 binds to different upstream regulators than mTORC2. Since both complexes are affected by CYLD, this mechanism likely does not explain the increase in mTOR activity upon CYLD loss. Ubiquitination is also relevant for the oligomerization of kinase complexes, as it occurs in the activation of Receptor-interacting serine/threonine-protein kinase 2 (RIPK2)

(Hasegawa et al., 2008). Importantly, dimerization of both mTORC1 and mTORC2 were reported previously (Takahara et al., 2006; Yip et al., 2010; Jain et al., 2014; Aylett et al., 2016). Accordingly, an interesting hypothesis is that CYLD-mediated changes in mTOR ubiquitination modulate dimerization of mTOR complexes. Finally, ubiquitination can induce conformational changes in enzymes (Sagar et al., 2007). This might facilitate binding to substrates or ATP, modifying kinase activity. Thus, additional research is required to elucidate the reason for changes in mTOR activity upon CYLD loss.

The mTOR protein consists of domains with defined functions. Ubiquitination sites on mTOR have been described in the HEAT repeats, both by TRAF6 (Linares et al., 2013a) and by SCF/FBXW7 (Mao et al., 2008). Moreover, PARKIN ubiquitinates mTOR in the kinase domain (Park et al., 2014). Importantly, the described ubiquitination events on mTOR evoke different cellular responses. Hence, the investigation of which ubiquitination site on mTOR is modulated by CYLD might shed light on how this DUB regulates mTOR activity.

CYLD mutations are found in cylindromatosis. This disease is characterized by benign skin tumors, called cylindromas (Sun, 2010). Although other proteins and pathways are affected by CYLD, it is possible that mTOR dysregulation is an important contributor for the disease phenotype. mTORC1, as a central regulator of cell growth, contributes to tumor development (Kim et al., 2017). Likewise, mTORC2 is an important regulator of cell proliferation, a process often dysregulated in cancerous cells (Kim et al., 2017). Furthermore, both complexes are essential for skin homeostasis (Ding et al., 2016). Thus, mTOR inhibitors might be beneficial for the treatment of cylindromatosis. Rapamycin is used in the clinic as an mTORC1 inhibitor (Li et al., 2014). Importantly, its efficacy in topical application was tested for the treatment of TSC (Lin et al., 2022), making it an attractive drug to treat cylindromas. Additionally, treatment of cylindromatosis patients with Torin1 might be effective, since this drug has an inhibitory effect on both mTORC1 and mTORC2. Nonetheless, it would be necessary to understand the partial resistance of mTORC2 to Torin1 upon CYLD deficiency. Because Torin1 is a strong and specific inhibitor of mTOR, it is unlikely that CYLD loss makes cells resistant to its action.

5 Materials and methods

Cell culture

Cells were grown at 37 °C, 5% CO₂. HEK293FT (human female embryonic kidney) cells (#R70007, Invitrogen) and immortalized MEFs (mouse embryonic fibroblasts) were cultured in full media, consisting of high-glucose DMEM (Dulbecco's modified eagle medium) (#41965-039, Gibco), supplemented with 10% FBS (fetal bovine serum) (#F7524, Sigma; #S1810, Biowest) and 1x P/S (penicillin-streptomycin) (#15140-122, Gibco). For cell passaging or seeding, cells were incubated with 0.25% Trypsin (#25200-056, Gibco) at RT (room temperature) for five minutes to detach cells from the cell culture flasks. Trypsin was inactivated by addition of fresh full media.

Wild-type control and RagA/B KO immortalized MEFs were a kind gift of Prof. Dr. Kun-Liang Guan (described in (Jewell et al., 2015)). Wild-type control and CYLD^{R932X} (CYLD Δ 932) immortalized MEFs were a kind gift of Prof. Dr. Manolis Pasparakis (described in (Welz et al., 2011)). HEK293T and HEK293T CYLD KO cells were a kind gift of Prof. Dr. George Mosialos. The identity of the HEK293FT cells was validated by the Multiplex human Cell Line Authentication test (Multiplexion GmbH), which uses a SNP (single nucleotide polymorphism) typing approach, and was performed as described at www.multiplexion.de. All cell lines were regularly tested for Mycoplasma contamination, using a PCR (polymerase chain reaction)-based approach and were confirmed to be Mycoplasma-free.

Cell culture treatments

For AA starvation, custom-made starvation media were formulated according to the Gibco recipe for high-glucose DMEM (table 1), omitting either all AAs or specific AA groups, as indicated in the figures. The lists of components used for the starvation media are summarized in table 2. The media were filtered through a 0.22 μ m filter device and tested for proper pH (pH 7.4) and osmolality before use. For the respective AA-replete (+AA) treatment media, commercially available high-glucose DMEM was used. All treatment media were supplemented with 10% dFBS (dialyzed FBS) and 1x P/S. For this purpose, FBS was dialyzed against 1x PBS (phosphate-buffered saline) through a 3,500 MWCO (molecular weight cut-off) dialysis tubing to remove all AAs that FBS might contain. For basal (+AA) conditions, the culture media were replaced with +AA treatment media 60-90 minutes before lysis or fixation. For amino-acid starvation (-AA), culture media were replaced with starvation media for one hour. For AA add-back experiments, cells were first starved as described above and then starvation media were replaced with +AA treatment media for 10 or 30 minutes.

Table 1 The recipe for Gibco high-glucose DMEM.

Components	Molecular Weight	Concentration (mg/L)	mM
Amino Acids			
Glycine	75.0	30.0	0.4

L-Arginine hydrochloride	211.0	84.0	0.39810428
L-Cystine 2HCl	313.0	63.0	0.20127796
L-Glutamine	146.0	584.0	4.0
L-Histidine hydrochloride-H ₂ O	210.0	42.0	0.2
L-Isoleucine	131.0	105.0	0.8015267
L-Leucine	131.0	105.0	0.8015267
L-Lysine hydrochloride	183.0	146.0	0.7978142
L-Methionine	149.0	30.0	0.20134228
L-Phenylalanine	165.0	66.0	0.4
L-Serine	105.0	42.0	0.4
L-Threonine	119.0	95.0	0.79831934
L-Tryptophan	204.0	16.0	0.078431375
L-Tyrosine disodium salt dihydrate	261.0	104.0	0.39846742
L-Valine	117.0	94.0	0.8034188
Vitamins			
Choline chloride	140.0	4.0	0.028571429
D-Calcium pantothenate	477.0	4.0	0.008385744
Folic Acid	441.0	4.0	0.009070295
Niacinamide	122.0	4.0	0.032786883
Pyridoxine hydrochloride	206.0	4.0	0.019417476
Riboflavin	376.0	0.4	0.0010638298
Thiamine hydrochloride	337.0	4.0	0.011869436
i-Inositol	180.0	7.2	0.04
Inorganic Salts			
Calcium Chloride (CaCl ₂) (anhyd.)	111.0	200.0	1.8018018
Ferric Nitrate (Fe(NO ₃) ₃ ·9H ₂ O)	404.0	0.1	2.4752476E-4
Magnesium Sulfate (MgSO ₄) (anhyd.)	120.0	97.67	0.8139166
Potassium Chloride (KCl)	75.0	400.0	5.3333335
Sodium Bicarbonate (NaHCO ₃)	84.0	3700.0	44.04762
Sodium Chloride (NaCl)	58.0	6400.0	110.344826
Sodium Phosphate monobasic (NaH ₂ PO ₄ ·H ₂ O)	138.0	125.0	0.9057971
Other Components			
D-Glucose (Dextrose)	180.0	4500.0	25.0

Table 2 Inorganic components and amino acids used for preparation of custom-made media.

Supplier	Name	Catalog number
Inorganic components		
Applichem	CaCl ₂ ·2H ₂ O	A1873
Sigma	Iron(III) nitrate nonahydrate	F8508
Sigma	Magnesium sulfate heptahydrate	13142
Roth	Potassium Chloride	6781.1
Sigma	Sodium bicarbonate	S5761
Sigma	Sodium chloride	31434
Roth	Sodium dihydrogen phosphate monohydrate	K300.2
Applichem	D-Glucose	A1422
Amino acids		
Sigma	L-Arginine	A8094
Sigma	L-Cystin	30200
Sigma	L-Glutamine	49419
Sigma	L-Histidine	H8000
Sigma	L-Isoleucine	I2752
Sigma	L-Leucine	L8912
Sigma	L-Lysine Hydrochloride	L5626
Sigma	L-Methionine	M9625
Sigma	L-Phenylalanine	P5482
Sigma	L-Proline	P0380
Alfa Aesar	L-Serine	J62187
Sigma	L-Threonine	T8625
Sigma	L-Tryptophan	T0254
Applichem	L-Tyrosine	A1677
Sigma	L-Valine	V0500

For glucose starvation (-Glucose), cells were cultured for one hour in DMEM without Glucose (#11966025, Gibco) supplemented with 10% dFBS and 1x P/S. For basal glucose conditions (+Glucose), the culture media was replaced with DMEM high-glucose, supplemented with 10% dFBS and 1x P/S one hour before lysis. For glucose add-back experiments, cells were first starved for glucose as described and media was replaced with +Glucose media for an extra hour. For growth factor starvation (-GF), cells were cultured for 16 hours in high-glucose DMEM supplemented with 1x P/S, without FBS.

For both BafA1 (#BML-CM110-0100, Enzo) and ConA (#C9705, Sigma) treatments, the drug was added to a final concentration of 100 nM in the media for six hours before lysis or fixation, unless otherwise stated in the figure legends. Chloroquine (#C6628, Sigma) was added to the media to a final concentration of 50 μ M for six hours. Treatment with E64 (#2935.1, Roth) and PepA (#P5318, Sigma) to block lysosomal protease activity was performed by adding a combination of E64 (25 μ M) and PepA (50 μ M) in the media for 16 hours before lysis or fixation, and in the last 90 minutes before lysis the AA add-back protocol was conducted. For experiments including treatments with +AA and –AA media, BafA1, ConA, Chloroquine or E64+PepA were also kept in the treatment media. To inhibit mTOR kinase activity, Torin1 (#14379, Cell Signaling Technology) was added in the media to a final concentration of 250 nM for one hour. Akt inhibition was achieved by addition of the Akt inhibitor VIII (#ENZ-CHM125, Enzo) in the culture media for 30 minutes (final concentration of 10 μ M). GA (#345862, Sigma) and BFA (#BUF075, Biorad) were added in the culture media at final concentrations of 10 μ M and 10 μ g/ml, respectively, for one hour. MG132 (#M7449, Sigma) was added to the media in a final concentration of 10 μ M for four hours, in order to inhibit proteasomal activity.

Antibodies

A list of all antibodies and concentrations used in this thesis is found in Table 3.

The H4B4 and ABL-93 antibodies against LAMP2, were obtained from the Developmental Studies Hybridoma Bank, created by the NICHD of the NIH and maintained at The University of Iowa, Department of Biology. H4B4 was deposited to the DSHB by August, J.T. / Hildreth, J.E.K. (DSHB Hybridoma Product H4B4). ABL-93 was deposited to the DSHB by August, J.T. (DSHB Hybridoma Product ABL-93).

Table 3 Antibodies used in this thesis.

Antibody	Dilution	Supplier	Catalog Number
Rabbit monoclonal anti-phospho-p70 S6 Kinase (Thr389) (D5U1O)	1:1,000 (WB)	Cell Signaling Technology	97596
Rabbit polyclonal anti-S6 Kinase	1:1,000 (WB)	Cell Signaling Technology	9202
Rabbit monoclonal anti-phospho-TFEB (Ser211) (E9S8N)	1:1,000 (WB)	Cell Signaling Technology	37681
Rabbit polyclonal anti-TFEB (for human TFEB)	1:1,000 (WB); 1:200 (IF)	Cell Signaling Technology	4240
Rabbit polyclonal anti-TFEB (for mouse TFEB)	1:1,000 (WB)	Bethyl Laboratories	A303-673A
Rabbit polyclonal anti-TFE3	1:1,000 (WB); 1:200 (IF)	Cell Signaling Technology	14779

Rabbit polyclonal anti-phospho-Akt (Ser473)	1:1,000 (WB)	Cell Signaling Technology	9271
Rabbit polyclonal anti-Akt	1:1,000 (WB)	Cell Signaling Technology	9272
Rabbit monoclonal anti-phospho-4E-BP1 (Ser65) (D9G1Q)	1:1,000 (WB)	Cell Signaling Technology	13443
Rabbit polyclonal anti-phospho-4E-BP1 (Thr37/46)	1:1,000 (WB)	Cell Signaling Technology	9459
Rabbit polyclonal anti-4E-BP1	1:1,000 (WB)	Cell Signaling Technology	9452
Rabbit monoclonal anti-phospho-NDRG1 (Thr346) (D98G11)	1:1,000 (WB)	Cell Signaling Technology	5482
Rabbit monoclonal anti-mTOR (7C10)	1:1,000 (WB); 1:200 (IF)	Cell Signaling Technology	2983
Rabbit monoclonal anti-LC3B (D11) XP	1:1,000 (WB); 1:200 (IF)	Cell Signaling Technology	3868
Rabbit polyclonal anti-SQSTM1/p62	1:1,000 (WB); 1:200 (IF)	Cell Signaling Technology	5114
Rabbit monoclonal anti-TAX1BP1 (D1D5)	1:1,000 (WB)	Cell Signaling Technology	5105
Mouse monoclonal anti-NBR1 (4BR)	1:500 (WB)	Santa Cruz Biotechnology	sc-130380
Rabbit monoclonal anti-TSC1 (D43E2)	1:1,000 (WB)	Cell Signaling Technology	6935
Rabbit polyclonal anti-TSC2	1:3,000 (WB)	Cell Signaling Technology	4308
Rabbit polyclonal anti-phospho-Tuberin/TSC2 (Thr1462)	1:1,000 (WB)	Cell Signaling Technology	3611
Rabbit monoclonal anti-MIOS (D12C6)	1:1,000 (WB)	Cell Signaling Technology	13557
Rabbit monoclonal anti-RAPTOR (24C12)	1:1,000 (WB)	Cell Signaling Technology	2280
Rabbit monoclonal anti-RICTOR (D16H9)	1:1,000 (WB)	Cell Signaling Technology	9476
Rabbit monoclonal anti-RagA (D8B5)	1:1,000 (WB)	Cell Signaling Technology	4357
Rabbit monoclonal anti-RagC (D8H5)	1:1,000 (WB); 1:200 (IF)	Cell Signaling Technology	9480
Rabbit monoclonal anti-RagC (D31G9)	1:1,000 (WB)	Cell Signaling Technology	5466

Rabbit polyclonal anti-RagD	1:1,000 (WB)	Cell Signaling Technology	4470
Rabbit polyclonal anti-CathepsinD	1:1,000 (WB)	Cell Signaling Technology	2284
Rat monoclonal anti-HA (3F10)	1:1,000 (WB)	Roche	11867423001
Rabbit monoclonal anti-GAPDH (14C10)	1:3,000 (WB)	Cell Signaling Technology	2118
Mouse monoclonal anti- α -Tubulin	1:3,000 (WB)	Sigma-Aldrich	T9026
Rat monoclonal anti-LAMP2 (ABL-93)	1:200 (IF)	Developmental Studies Hybridoma Bank	ABL-93
Mouse monoclonal anti-LAMP2 (H4B4)	1:500 (WB); 1:200 (IF)	Developmental Studies Hybridoma Bank	H4B4
Rabbit monoclonal anti-phospho-S6 ribosomal protein (Ser240/244) (D68F8)	1:1,000 (WB)	Cell Signaling Technology	5364
Rabbit monoclonal anti-phospho-S6 ribosomal protein (Se235/236) (D57.2.2E)	1:1,000 (WB)	Cell Signaling Technology	4858
Mouse monoclonal anti-S6 ribosomal protein (52D2)	1:1,000 (WB)	Cell Signaling Technology	2317
Rabbit monoclonal anti-phospho-ULK (Ser757) (D7O6U)	1:1,000 (WB)	Cell Signaling Technology	14202
Rabbit monoclonal anti-ULK (D8H5)	1:1,000 (WB)	Cell Signaling Technology	8054
Rabbit monoclonal anti-phospho-GBR10 (Ser476) (D4E6)	1:1,000 (WB)	Cell Signaling Technology	11817
Rabbit polyclonal anti-GRB10	1:1,000 (WB)	Proteintech	23591-1-AP
Rabbit monoclonal anti-PTEN (D4.3)	1:1,000 (WB)	Cell Signaling Technology	9188
Mouse monoclonal anti-RHEB (B-12)	1:500 (WB)	Santa Cruz Biotechnology	sc-271509

Rabbit polyclonal anti-phospho-ACC1 (Ser79)	1:1,1000 (WB)	Cell Signaling Technology	3661
Rabbit polyclonal anti-ACC1	1:1,1000 (WB)	Proteintech	21923-1AP
Rabbit polyclonal anti-M6P	1:1,000 (WB)	ABCD Antibodies	AG949
Rabbit polyclonal anti-RAB1A	1:1,000 (WB)	Proteintech	11671-1-AP
Mouse monoclonal anti-GM130 (35)	1:150 (IF)	BD Biosciences	610822
Rabbit monoclonal anti-CYLD (D1A10)	1:1,000 (WB)	Cell Signaling Technology	8462
Rabbit polyclonal anti-FLAG	1:1,000 (WB)	Cell Signaling Technology	2368
Mouse monoclonal anti-SBP (SB19-C4)	1:1000 (WB)	Santa Cruz Biotechnology	sc-101595
Mouse monoclonal anti-Ubiquitin (P4D1)	1:500 (WB)	Santa Cruz Biotechnology	sc-8017
Mouse monoclonal anti-Puromycin (4G11)	1:1000 (WB)	Merck	MABE342

mRNA isolation and cDNA synthesis

Total mRNA was isolated from HEK293FT cells using a standard TRIzol/chloroform-based method (#15596018, Thermo Fisher Scientific), according to manufacturer's instructions. The concentration of the RNA was measured using a Nanodrop spectral photometer. For cDNA (complementary DNA) synthesis, 2 µg of mRNA was transcribed to cDNA using the RevertAid H Minus Reverse Transcriptase kit (#EP0451, Thermo Fisher Scientific) according to manufacturer's instructions.

PCRs, plasmids and molecular cloning

PCRs performed for cloning were done using the Phusion High-Fidelity DNA polymerase (#M0530, New England BioLabs), according to manufacturer's instructions. For PCRs in which the starting material was cDNA, a 1:10 cDNA dilution was used as template. For plasmid templates, 20 ng of DNA was used. The primers used for PCR amplification are described in Table 4.

Table 4 Sequences of PCR oligos used for cloning, restriction sites are underlined and mutations are in bold.

PCR oligos for cloning	
4EBP1-For- NcoI	5' T <u>Accatgg</u> CGTCCGGGGGCAGCAGCTGCAGCCAGACCCCA 3'
4EBP1-Rev- NotI	5' GAAT <u>gcggccgc</u> CTTTAAATGTCCATCTCAAACCTGTGA 3'
Ub-For- EcoRI	5' GAA <u>Agaattc</u> CCGAACCGACAGTCGGTCTCTTCAC 3'
Ub-Rev- Acc65I	5' GCC <u>ggtacc</u> TAACCAAGTTCCTCTTTCAGAGGTT 3'
Ub-K48R-For	5' TGCTGGG aga CAGCTGGAAGATGGACGC 3'
Ub-K48R- Rev	5' GCGTCCATCTTCCAGCTG tct CCCAGCA 3'
Ub-K63R-For	5' CATCCAG aga GAGTCCACCCTGCACC 3'
Ub-K63R- Rev	5' GGTGCAGGGTGGACTC tct CTGGATG 3'
HIS-For- HindIII	5' GCC <u>aagctt</u> ATGCATCATCATCATCATCTTGGAACCGGACCTGCC GCCGCCA 3'
HIS-Rev- NheI	5' CCTTCCACTCCTATGAGG <u>ctagc</u> TATGGCCAAGATGCCACC 3'
SBP-For- KpnI	5' TATA <u>aggtacc</u> GCCACCATGGACGAGAAGACCACTGG 3'
SBP-Rev- BamHI	5' ATAT <u>ggatcc</u> TGGTTCACGTTGACCTTGTG 3'
mTOR-For- NotI	5' TATA <u>gcggccgc</u> ATGCTTGGAACCGGACCTGC 3'
mTOR-Rev- AgeI	5' ATAT <u>accggt</u> TTACCAGAAAGGGCACCAGC 3'
FLAG- APEX2-for- SfiI	5' TATA <u>ggcctctgaggcc</u> GCCACCATGGACTACAAAGACGATGAC GACAAGAAGTCTTACCCAACTGTGAG 3'

APEX2-rev- NheI	5' ATATG <u>ctagc</u> GCCTCCGCCTCCCCCGGCATCAG CAAACCCAAGCTC 3'
mTOR-Rev- Sall	5' ATAT <u>gtcgac</u> TTACCAGAAAGGGCACCAGC 3'
pITR-FLAG- mTOR-For- NotI	5' GACGATGACGACAAG <u>gccggccgc</u> ACTTGGAAACCGGACCT 3'

For all cloning reactions, PCR products were cleaned to remove primers and components of the PCR reaction using the NucleoSpin Gel and PCR Clean-up kit (#740609.250, Macherey-Nagel). PCR products and vectors were digested using restriction enzymes purchased from Fermentas/Thermo Scientific as detailed below. Vector ends were dephosphorylated using the quick CIP enzyme (#M0525, New England BioLabs), as described in the manufacturer's instructions. Inserts and vectors were ligated using the T4 DNA ligase protocol (#M0202, New England BioLabs). Cloned constructs were transferred into NEB-5-alpha Competent *E. coli* (#C2987, New England BioLabs) via chemical transformation. Single colonies were picked, grown in LB (Luria-Bertani broth; #L3022, Sigma) liquid medium with 100 µg/ml ampicillin (#A9518, Sigma). The plasmid DNA was retrieved by plasmid purification with the NucleoSpin Plasmid kit (#740588.250, Macherey-Nagel). The integrity of all constructs was verified by sequencing.

The pSpCas9(BB)-2A-Puro (PX459) V2.0 plasmid was a gift from Feng Zhang (Addgene plasmid #62988) and described in (Ran et al., 2013). The pLJC6-3xHA-TMEM192 and pLJC6-2xFLAG-TMEM192 plasmids (Wyant et al., 2017b) were obtained from Addgene (plasmids #104434 and #104435; deposited by the Sabatini lab). The pcDNA3-FLAG-hRagA Q66L and pcDNA3-FLAG-hRagA T21N generation is described in (Demetriades et al., 2014). The pRK5-HA-Ubiquitin-WT plasmid (Lim et al., 2005) was obtained from Addgene (plasmid #17608; deposited by the Ted Dawson lab). The pcDNA3-FLAG-mTOR (Vilella-Bach et al., 1999) was also obtained from Addgene (plasmid #26603; deposited by the Jie Chen lab). The pcDNA3-FLAG-CYLD and pcDNA3-FLAG-CYLD-C601S, described in (Trompouki et al., 2003), as well as the vector with a luciferase gene under the control of three NF-κB binding sites (3x κBL) and the control pRL-null, described in (Mitchell and Sugden, 1995) were a kind gift from Dr. George Mosialos.

The pETM-11-4E-BP1 vector used to express His₆-tagged 4E-BP1 in bacteria was generated by PCR-amplifying human 4E-BP1 from cDNA, using the primers described in table 4 and cloned in the NcoI-NotI restriction sites of pETM-11. For generation of the K48R and K63R ubiquitin mutants, ubiquitin was amplified from the pRK5-HA-Ubiquitin-WT plasmid with the primers described in table 4, using the mutagenic oligos to introduce the desired mutations. In brief, a first PCR was done using the ubiquitin forward primer with the mutagenic reverse

primer, and a second reaction was set up with the mutagenic forward primer and the ubiquitin reverse primer. Next, 50 ng of each cleaned product were used as templates for a reaction with the ubiquitin forward and reverse primers. Final products were cloned back into the pRK5-HA-Ubiquitin-WT using the EcoRI and Acc65I restriction sites. The pcDNA4/T0/SBP-mTOR construct was generated by Dr. Julian Nuechel, in brief, the SBP tag was amplified from the pIRES-Str-KDEL-ManII-SBP-GFP (obtained from Addgene, plasmid #65252) using the oligos described in table 4. The SBP tag was cloned into pcDNA4/T0/Myc-His6 using the KpnI/BamHI restriction sites, resulting in a new pcDNA4/T0/SBP vector. mTOR was amplified from pcDNA3-FLAG-mTOR and cloned in frame into the pcDNA4/T0/SBP vector using the NotI/AgeI sites. For the generation of the His₆-tagged mTOR construct, a PCR reaction was set with an oligo containing the His₆-tag and the initial mTOR sequence. The product was inserted back into the original pcDNA3-FLAG-mTOR, using the HindIII and NheI restriction sites. By using these sites, the FLAG-tag is removed, resulting in a pcDNA3-His₆-mTOR. The pITR-TTP-FLAG-mTOR was generated by removing the APEX sequence from a pITR-TTP-APEX-mTOR generated by Dr. Julian Nuechel. In brief, the APEX tag was amplified using the oligos described in table 4 from the pITR-TTP-hGRASP55-APEX2-Myc6xHis (Nuchel et al., 2021), and inserted into the pITR-TTP1 using the SfiI/NheI sites. mTOR was then amplified using the mTOR-for-NotI oligo, in conjunction with the mTOR-rev-Sall. mTOR was cloned into the NotI/XhoI sites of the pITR-TTP-FLAG-APEX2 vector. For generation of the pITR-TTP-FLAG-mTOR, the tags were removed using the sites SfiI and NotI. The FLAG tag was inserted back using the same restriction sites via oligo annealing with the sequences:

5' aggccGCCACCATGGACTACAAAGACGATGACGACAAGgc 3'

5' ggccgcCTTGTCGTCATCGTCTTTGTAGTCCATGGTGGCggcctcag 3'

Following the insertion of the FLAG tag, the second ATG that precedes the mTOR sequence was removed by PCR amplifying a part of the FLAG tag and the beginning of the mTOR sequence as described in table 4, using the same reverse oligo used to clone the His₆-tagged mTOR construct. The resulting insert was cloned back into the pITR-TTP-FLAG-mTOR using the NotI and NheI restriction sites.

Quantitative real-time PCR

The cDNAs were diluted 1:10 in nuclease-free water and 4 µl of diluted cDNA were used per reaction, consisting of 5 µl 2x Maxima SYBR Green/ROX qPCR master mix (#K0223, Thermo Fisher Scientific) and 1 µl primer mix (2.5 µM of forward and reverse primers). Reactions were done in technical triplicates in a StepOnePlus Real-Time PCR system (Applied Biosystems). Relative gene expression was calculated by the $2^{-\Delta\Delta C_t}$ method, with RPL13a as an internal control, and normalized to the expression of the gene in the respective siCtrl or WT sample. All qPCR primers used in this study are listed in Table 5.

Table 5 Sequences of primers used for RT-qPCR (reverse transcription quantitative real-time PCR).

RT-qPCR gene-specific oligos	
RRAGC_for	5' ACTGCCGACCTTGGAACC 3'

RRAGC_rev	5' GGGAAGTGTCTGTTGCAATGT 3'
LAMP1_for	5' TGGGCGTCTCTAATGTCTGC 3'
LAMP1_rev	5' CAGGATCACCCCGAATGTCA 3'
MCOLN1_for	5' CTATCATGTGAAGTTCCGCTC 3'
MCOLN1_rev	5' GTCACAAACATGTCGTCCC 3'
PPT1_for	5' CTCTCAGTACGTTGCCCTCTG 3'
PPT1_rev	5' ACTGTAGGCCAGTGGGATTTG 3'
ATP6AP1_for	5' TTCTAACCTAGAGAATGCCCTG 3'
ATP6AP1_rev	5' AGAGTGCTGACTGCATACC 3'
CLN3_for	5' TGGACAGTGTTC AAGGGTC 3'
CLN3_rev	5' GTCCCTGGTTAATGAAATACTCG 3'
LAMTOR1_for	5' CAAAGCTCTCAATGGAGCC 3'
LAMTOR1_rev	5' AATGATGTTGCTGGCTGTC 3'
ARF1_for	5' GCCAGTGCCTTCCACCTGTC 3'
ARF1_rev	5' GCCTCGTTCACACGCTCTCTG 3'
RPL13a_for	5' CCGCCCTACGACAAGAAA 3'
RPL13a_rev	5' AGGCGCCCCAGATAGG 3'

Plasmid DNA transfections

Plasmid DNA transfections in HEK293FT cells were performed using Effectene transfection reagent (#301425, QIAGEN), according to the manufacturer's instructions. For plasmid transfections in MEFs, the ViaFect Transfection Reagent was used (#E4981, Promega), as described in the manufacturer's protocol.

Generation of stable cell lines

For the generation of stable cell lines expressing HA-tagged TMEM192 (lyso-IP lines) or FLAG-tagged TMEM192 (negative control lines for HA lyso-IPs), WT HEK293FT cells were transfected using the respective expression vectors. Forty-eight hours post-transfection, cells were selected with 3 µg/ml puromycin (#A11138-03, Thermo Fisher Scientific). Single-cell clones that express similar TMEM192 levels were used in lyso-IP experiments. Stable cell lines in MEF WT and CYLD^{R932X} (CYLD Δ932) were generated by using a doxycycline-inducible transposon system (Kowarz et al., 2015). The pITR-TTP-FLAG-mTOR construct was transfected in a 10:1 ratio with the transposase containing pCMV-Trp vector. Selection with puromycin was performed as described above. A polyclonal population was used for further experiments. Expression of the mTOR construct was induced with 250 ng/ml of doxycycline (#D9891, Sigma) for four hours before cell lysis.

Generation of knockout cell lines

The HEK293FT RagA/B KO, RagC/D KO, HEK293FT HA-TMEM192 RagA/B KO and FLAG-TMEM192 RagA/B KO cell lines were generated by Dr. Peter Gollwitzer using the pX459-based CRISPR/Cas9 method, as described in (Ran et al., 2013). In the same manner, I generated the HEK293FT GNPTAB KO. The sgRNAs sequences are described in table 6. The sgRNA expression vectors were generated by cloning the DNA oligonucleotides into the BbsI restriction sites of the pX459 vector (#62988, Addgene). An empty vector was used to generate matching control cell lines. In brief, transfected cells were selected with 3 µg/ml puromycin 48 hours post-transfection. Single-cell clones were generated by single cell sorting and clones were validated by immunoblotting.

Table 6 Sequences of oligos used for sgRNA expression from the pX459 for CRISPR/Cas9 KO cell line generation.

sgRNAs	
RagA-gRNA-5UTR-s	5' caccgATTACATTGCTCGCGACACC 3'
RagA-gRNA-5UTR-as	5' aaacGGTGTCTCGCGAGCAATGTAATc 3'
RagB-gRNA-5UTR-s	5' caccgCTGCCTATTCTCATCGCCTA 3'
RagB-gRNA-5UTR-as	5' aaacTAGGCGATGAGAATAGGCAGc 3'
RagB-gRNA-3CDS-s	5' caccgTACATCCAACACTTATGTGA 3'
RagB-gRNA-3CDS-as	5' aaacTCACATAAGTGTTGGATGTAc 3'
RagC-gRNA-5CDS-s	5' caccgATCGGCCGCGCCGTAAGTGC 3'
RagC-gRNA-5CDS-as	5' aaacGCAGTTACGGCGCGGCCGATc 3'
RagC-gRNA-3UTR-s	5' caccgTAGTCTGAATCCCAGCGTCG 3'
RagC-gRNA-3UTR-as	5' aaacCGACGCTGGGATTCAGACTAc 3'
RagD-gRNA-5UTR-s	5' caccgTGAATCCTCCGCCGGCGGGC 3'
RagD-gRNA-5UTR-as	5' aaacGCCCCGCCGGCGGAGGAGTCAc 3'
RagD-gRNA-3UTR-s	5' caccgAGATTGGAGCTACAAGCTCC 3'
RagD-gRNA-3UTR-as	5' aaacGGAGCTTGTAGCTCCAATCTc 3'
GNPTAB-gRNA-exon7-s	5' caccgTTGCATTAGCACTAATCCA 3'
GNPTAB-gRNA-exon7-as	5' aaacTGGATTAGTGCTAATGCAAc 3'

Gene silencing experiments

Transient knockdown of LAMTOR1, MIOS, ARF1, RAB1A, CYLD, IKKβ, TSC1, TSC2 and RHEB was performed using pools of 4 siGENOME gene-specific siRNAs (Horizon Discoveries). The siRNA sequences are described in Table 7. An siRNA duplex targeting the *R. reniformis* luciferase gene (RLuc) (#P-002070-01-50, Horizon Discoveries) was used as control. Transfections were performed with 20 nM siRNA and the Lipofectamine RNAiMAX

transfection reagent (#13778075, Thermo Fisher Scientific) in 12-well plates, according to the manufacturer's instructions. After 72 hours, cells were harvested or fixed and knockdown efficiency was verified by immunoblotting or quantitative real-time PCR.

Table 7 siRNA sequences for knockdown experiments.

Target	Sequences
LAMTOR1	5' GGAGCUGGUUGUACAGUUU 3'
	5' UACCAAAGCUCUCA AUGGA 3'
	5' GCAGCAGCCUGACCCAUUG 3'
	5' AAGAGGAGCUGGUUGUACA 3'
MIOS	5' ACACUGCGAUUACAGCUAA 3'
	5' AAACAAAGUUGCAGUACGU 3'
	5' GGAGUGGGUUGGAUAAGCA 3'
	5' CAAUGGCUUUAUCGGGUUA 3'
ARF1	5' GACCACCAUUCCCACCAUA 3'
	5' ACAGAGAGCGUGUGAACGA 3'
	5' CGGCCGAGAUCACAGACAA 3'
	5' ACGUGGAAACCGUGGAGUA 3'
RAB1A	5' GAACAAUCACCUCCAGUUA 3'
	5' CAAUCAAGCUUCAAUAUG 3'
	5' GGAAACCAGUGCUAAGAAU 3'
	5' CAGCAUGAAUCCCGAAUAU 3'
CYLD	5' CGAAGAGGCUGAAUCAUAA 3'
	5' GAACAGAUUCCACUCUUUA 3'
	5' GAACUCACAUGGUCUAGAA 3'
	5' GGACAUGGAUAACCCUAUU 3'
IKBKB (IKK β)	5' GGAAGUACCUGAACCAGUU 3'
	5' CCAAUAAUCUUAACAGUGU 3'
	5' GGAUUCAGCUUCUCCUAAA 3'
	5' GUGGUGAGCUUAAUGAAUG 3'
TSC1	5' GAAGAUGGCUAUUCUGUGU 3'
	5' CGACACGGCUGAUAAACUGA 3'
	5' CGGCUGAUGUUGUAAAUA 3'
	5' GGACAGGAUUAACGAAUAU 3'

TSC2	5' GCAUUAUAUCUCUUACCAUA 3'
	5' CCAAUGUCCUCUUGUCUUU 3'
	5' UCACCAGGCUCAUCAAGAA 3'
	5' GGAAUGUGGCCUCAACAAU 3'
RHEB	5' CCUCAGACAUACUCCAUAAG 3'
	5' GCAAAUUGUUGGAUAUGGU 3'
	5' UUACAAAGUUGAUCACAGU 3'
	5' CCAAGAAUUUUAUCGGCAU 3'

Protein secretion

For protein secretion experiments, HEK293FT cells were cultured in serum-free media for 16 hours. Supernatants were collected and centrifuged (five minutes, 2000 x g, 4 °C) to remove dead cells and debris. Cleared supernatants were concentrated using 3 kDa cut-off concentrator tubes (#516-0227P, VWR), according to the manufacturer's instructions. Laemmli loading buffer (1x final concentration; 6x Laemmli sample buffer composition: 350mM Tris-HCl pH 6.8, 12.8% SDS, 50% glycerol (#15523, Sigma), 600mM DTT (dithiothreitol; #A1101, AppliChem), 0.12% bromophenol blue (#T116.1, Roth)) was added to the concentrated supernatants and samples were boiled at 95 °C for five minutes before loading into SDS-PAGE gels.

Cell lysis and immunoblotting

Cells at around 90% of confluence were treated as indicated in the figures, washed once with serum-free DMEM, and lysed in ice-cold Triton lysis buffer (50 mM Tris pH 7.5, 1% Triton X-100 (#A4975, AppliChem), 150 mM NaCl (#31434, Sigma), 50 mM NaF (sodium fluoride; #A3904, AppliChem), 2 mM Na-vanadate (#S6508, Sigma), 0.011 gr/ml beta-glycerophosphate (#G9422, Sigma), supplemented with 1x PhosSTOP phosphatase inhibitors (#04906837001, Roche) and 1x cOmplete protease inhibitors (#11836153001, Roche)), for 10 minutes on ice. Samples were clarified by centrifugation (14,000 rpm, 15 minutes, 4 °C) and supernatants transferred to a new tube. Protein concentration was determined using a Protein Assay Dye Reagent (#5000006, Bio-Rad). Normalized samples were boiled at 95 °C for five minutes in 1x Laemmli sample buffer.

Standard SDS-PAGE (sodium dodecyl sulphate polyacrylamide gel electrophoresis) was used to separate proteins by their molecular size. The addition of SDS, an anionic detergent, denatures and adds a negative charge to proteins. Electrophoresis was performed at 25 mA per gel using a 1x running buffer (25 mM Tris (#T1503, Sigma), 250 mM glycine (#G8898, Sigma) and 0.1% SDS (#A1112, AppliChem)). To determine the molecular weight of proteins, a protein marker was loaded to each gel (PAGE ruler plus, #26620, Thermo Fischer). Proteins were then transferred to nitrocellulose membranes (#10600002 or #10600001, Amersham) in a blotting chamber with ice-cold 1x transfer buffer (25 mM Tris, 192 mM glycine, 20%

methanol (#32212, Honeywell)) at 300 mA for one hour and 15 minutes. Membranes were stained with 0.2% Ponceau solution (#33427-01, Serva) to confirm equal loading. Membranes were blocked with 5% skim milk powder (#42590, Serva) in PBS-T (1x PBS, 0.1% Tween-20 (#A1389, AppliChem)) for one hour at RT, washed three times for 10 minutes with PBS-T and incubated with primary antibodies (in PBS-T, 5% BSA (bovine serum albumine; #10735086001, Roche)) rotating overnight at 4 °C. All antibodies and dilutions used are summarized in table 3. The next day, membranes were washed three times for 10 minutes with PBS-T and incubated with appropriate HRP-conjugated secondary antibodies (1:10000 in PBS-T, 5% milk) for one hour at RT. Signals were detected by enhanced chemiluminescence (ECL), using the ECL Western Blotting Substrate (#W1015, Promega); or SuperSignal West Pico PLUS (#34577, Thermo Scientific) and SuperSignal West Femto Substrate (#34095, Thermo Scientific) for weaker signals. Immunoblot images were captured on films (#28906835, GE Healthcare; #4741019289, Fujifilm). Quantification of immunoblots was performed using the GelAnalyzer software (www.gelalyzer.com).

Lysosomal purification (Lyso-IP) assays

To biochemically isolate intact lysosomes and associated proteins, we developed a modified lyso-IP method, based on the protocol previously described by the Sabatini group (Abu-Remaileh et al., 2017). Our method allows for the additional assessment of the non-lysosomal fractions. In brief, cells were seeded on a 15cm dish until they reached 80-90% confluency, washed 2x with ice-cold PBS and scraped in 1 ml ice-cold PBS, containing 1x PhosSTOP phosphatase inhibitors and 1x cOmplete protease inhibitors. Cells were then pelleted by centrifugation (1,000 x g, two minutes, 4 °C) and resuspended in 1 ml ice-cold PBS containing phosphatase and protease inhibitors. For input samples, 25 µl of the cell suspension were transferred in a new tube and lysed by the addition of 125 µl of Triton lysis buffer on ice for 10 minutes. Lysed input samples were then cleared by centrifugation (14,000 x g, 15 minutes, 4 °C) and the supernatant was transferred to new tubes containing 37.5 µl of 6x Laemmli sample buffer and boiled for five minutes at 95 °C. For the lysosomal and non-lysosomal fractions, the remaining cell suspension was homogenized with 20 strokes in pre-chilled 2 ml hand dounce homogenizers kept on ice. The homogenate was cleared by centrifugation (1,000 x g, two minutes, 4 °C) and incubated with 100 µl pre-washed Pierce anti-HA magnetic beads (#88837, Thermo Fisher Scientific) on a nutating mixer for three minutes at RT. After incubation with the beads, the supernatant was transferred to a new tube and centrifuged at high speed (20,000 x g, 10 minutes, 4 °C) to remove membranes and other organelles and retrieve the non-lysosomal fraction. Twenty-five microliters of the cleared supernatant were transferred in a new tube, mixed with 125 µl Triton lysis buffer, and incubated for 10 minutes on ice. Next, 37.5 µl 6x Laemmli sample buffer was added and samples were boiled. For the lysosomal fraction, beads were washed three times with ice-cold PBS containing 1x PhosSTOP phosphatase inhibitors and 1x cOmplete protease inhibitors using a DynaMag spin magnet (#12320D, Invitrogen). After the last wash, lysosomes were eluted from the beads by addition of 50 µl Triton lysis buffer and incubation

for 10 minutes of ice. Isolated lysosomes were then transferred to a new tube, 12.5 μ l 6x Laemmli sample buffer was added and samples were boiled.

Immunoprecipitation

For immunoprecipitation experiments, cells were lysed in Triton lysis buffer. For the assessment of mTORC1 complex stability, CHAPS lysis buffer (50 mM Tris pH 7.5, 0.3% CHAPS ((3-((3-cholamidopropyl) dimethylammonio)-1-propanesulfonate)) (#A1099, Applichem), 150 mM NaCl, 50 mM NaF, 2 mM Na-vanadate, 0.011 gr/ml beta-glycerophosphate), supplemented with 1x PhosSTOP phosphatase inhibitors and 1x cOmplete protease inhibitors) was used. For all experiments in which ubiquitination of mTOR was assessed, the lysis buffer was supplemented with 10 mM NEM (N-ethylmaleimide; #E3876, Sigma) as a deubiquitinase inhibitor. For the pulldown of FLAG-tagged proteins, lysates were incubated with 20 μ l slurry of anti-FLAG M2 affinity gel (Sigma, #A2220) previously equilibrated with IP wash buffer (lysis buffer without inhibitors), rotating for two hours at 4 °C. Samples were washed four times with IP wash buffer. For the immunoprecipitation of mTOR, 1 μ l of antibody was added to lysates and samples were incubated rotating for three hours at 4 °C. After that, 30 μ l of protein A agarose beads (#11134515001, Roche) previously equilibrated with IP wash buffer were added to the samples, which were incubated with rotation for an extra hour at 4 °C, followed by four washes with IP wash buffer. Beads were then boiled for six minutes in 2x Laemmli sample buffer. Samples were analyzed by immunoblotting as indicated in the figures.

SBP pulldown

Cells transfected with the pcDNA4/T0/SBP-mTOR construct were lysed 48 hours post-transfection in Triton lysis buffer. After lysis, samples were incubated for two hours at 4 °C with 30 μ l slurry of streptavidin-sepharose beads (#GE17-5113-01, Sigma) previously equilibrated with IP wash buffer. Samples were washed four times with IP wash buffer. Beads were then boiled for six minutes in 2x Laemmli sample buffer.

His-tag pulldown

For the pulldown of His₆-tagged mTOR, cells were lysed in 300 μ l of binding buffer (1x PBS, 8 M Urea (#15604, Sigma), 10 mM Imidazole (#A1073, Applichem), 300 mM NaCl). Lysates were sonicated four times for 15 seconds with 15 second breaks. The samples were then subjected to three freeze-thaw cycles (from liquid N₂ to 37 °C), followed by a centrifugation of 13,000 rpm for five minutes at RT. Fifty μ l of lysates were kept for the input, and 12.5 μ l of 6x Laemmli sample buffer were added. The remaining volume of sample was incubated with 100 μ l of slurry of Ni-NTA (nickel-nitriloacetic acid; #1018244, Qiagen) beads previously equilibrated with binding buffer for two hours at 4 °C. Beads were then washed five times with binding buffer, followed by two washes with binding buffer containing 30 mM imidazole. Beads were then boiled for six minutes in 2x Laemmli sample buffer.

Production of recombinant His₆-tagged 4E-BP1 protein in bacteria

Recombinant His₆-tagged 4E-BP1 protein was produced by transforming *E. coli* BL21 RP electrocompetent bacteria with the pETM-11-4E-BP1 vector, according to standard procedures. In brief, protein expression was induced with IPTG (isopropyl- β -D-thiogalactopyranoside; #A1008, Applichem) for three hours at 30 °C, and His₆-4E-BP1 was purified using Ni-NTA agarose and eluted with 250 mM imidazole.

mTORC1 kinase activity assays

In vitro mTORC1 kinase assays were developed based on previous reports (Sancak et al., 2007; Mahoney et al., 2018), using endogenous mTORC1 complexes immunopurified from HEK293FT WT or RagA/B KO cells. Cells of a near-confluent 10 cm dish were lysed in CHAPS IP buffer for 10 minutes on ice. Samples were clarified by centrifugation (14,000 rpm, 15 minutes, 4 °C), supernatants were collected and a portion was kept as input material. The remaining supernatants were further used for immunoprecipitation by incubation with 2 μ l of anti-mTOR antibody for three hours rotating at 4 °C, followed by incubation with 30 μ l of pre-washed Protein A agarose bead slurry for an additional hour rotating at 4 °C. Beads were then washed four times with IP wash buffer and once with kinase wash buffer (25 mM HEPES pH 7.4 (#A3724, Applichem), 20 mM KCl (#6878.1, Roth)), and excess liquid was removed with a Hamilton syringe. Kinase reactions were prepared by adding 10 μ l 3x kinase assay buffer (75 mM HEPES/KOH pH 7.4 (#60377, Sigma), 60 mM KCl, 30 mM MgCl₂ (#1.058.330.250, Merck)) to the beads. Reactions were started by adding 10 μ l of kinase assay start buffer (25 mM HEPES/KOH pH 7.4, 140 mM KCl, 10 mM MgCl₂), supplemented with 500 μ M ATP and 35 ng of recombinant His₆-4E-BP1 substrate. Reactions lacking ATP were used as negative controls. All reactions were incubated at 30 °C for 30 minutes, and stopped by the addition of in 2x Laemmli sample buffer and boiling for six minutes at 95 °C. Samples were run in SDS-PAGE and the mTORC1-mediated phosphorylation on 4E-BP1^{T37/46} was detected by immunoblotting.

DUB assay

Cells transfected with pcDNA3-FLAG-mTOR were lysed 48 hours post-transfection with Triton lysis buffer without NEM. mTOR immunoprecipitation was performed as described above. After the four washes with IP washing buffer, one wash with 50 mM Tris pH 7.5 was performed. Subsequently, 200 ng of recombinant CYLD (#E556, Boston Biochem) in 10 μ l of DUB reaction buffer (50 mM Tris pH 7.5, 5 mM DTT) were added to the beads. Samples were incubated at 37 °C for one hour. The reaction was terminated by addition of 2x Laemmli sample buffer and boiling for six minutes at 95 °C.

Immunofluorescence and confocal microscopy

Cells were seeded on glass coverslips (coated with fibronectin (#A8350, Applichem)), treated as described in the figure legends, and fixed with 4% PFA (paraformaldehyde) in 1x PBS (10 minutes, RT), followed by two permeabilization/washing steps with PBT (1x PBS,

0.1% Tween-20). Cells were blocked in BBT (1x PBS, 0.1% Tween-20, 1% BSA) for 45 minutes at RT. All dilutions and catalogue numbers for primary antibodies used for IF (immunofluorescence) are described in Table 3. Staining with anti-mTOR, anti-LAMP2, anti-RagC or anti-GM130 primary antibodies was performed in BBT for two hours at RT. Staining with anti-TFEB or anti-TFE3 antibodies was performed by incubation for 16 hours at 4 °C. After staining with primary antibodies, cells were washed three times with PBT. Next, cells were stained with highly cross-adsorbed fluorescent secondary antibodies (Donkey anti-rabbit Alexa Fluor 488, Donkey anti-mouse TRITC; both from Jackson ImmunoResearch) diluted 1:200 in BBT for one hour. Nuclei were stained with DAPI (#A1001, VWR) (1:2000 in PBT) for five minutes and coverslips were washed three times with PBT solution. Coverslips were mounted on glass slides with Fluoromount-G (#00-4958-02, Invitrogen).

For LC3B and p62 staining, cells were fixed with 100% methanol for 15 minutes at -20 °C, permeabilized with 0.1% Triton-X 100 for five minutes and blocked for one hour in LC3B blocking solution (1x PBS, 5% FBS, 0.3% Triton X-100). Coverslips were incubated overnight at 4 °C with anti-LC3B or anti-p62 antibody in LC3B staining solution (1x PBS, 1% BSA, 0.3% Triton X-100). Slides were washed three times in 1x PBS, incubated with Donkey anti-rabbit Alexa Fluor 488 (Jackson ImmunoResearch) (1:500, in 1x PBS, 1% BSA, 0.3% Triton X-100) for one hour at RT. Coverslips were washed twice with 1x PBS, stained with DAPI (1:2000 in 1x PBS) and mounted on glass slides with Fluoromount-G.

All images were captured on an SP8 Leica confocal microscope (TCS SP8 X or TCS SP8 DLS, Leica Microsystems) using a 40x oil objective lens. Image acquisition was performed using the LAS X software (Leica Microsystems). Images from single channels are shown in grayscale, whereas in merged images, Alexa Fluor 488 is shown in green, TRITC in red and DAPI in blue.

LysoTracker staining

For LysoTracker staining experiments, cells were seeded in fibronectin-coated coverslips and grown until they reached 80-90% confluency. Lysosomes were stained by the addition of 100 nM LysoTracker Red DND-99 (#L7528, Invitrogen) in full media for one hour. Cells were fixed with 4% PFA in PBS for 10 minutes at RT, followed by permeabilization with PBT solution (1x PBS, 0.1% Tween-20). Nuclei was stained with DAPI (1:2000 in PBT) for 10 minutes. Coverslips were mounted on slides using Fluoromount-G. All images were captured on an SP8 Leica confocal microscope (TCS SP8 X or TCS SP8 DLS, Leica Microsystems) using a 40x oil objective lens. Image acquisition was performed using the LAS X software (Leica Microsystems).

Quantification of colocalization

Colocalization analysis in confocal microscopy experiments was performed as in (Demetriades et al., 2016a; Fitzian, 2021), using the Coloc2 plugin of the Fiji software (Schindelin et al., 2012). An average of 50 cells from five independent representative different

images captured from each experiment was used and Manders' colocalization coefficient (MCC) with automatic Costes thresholding (Manders et al., 1993; Costes et al., 2004; Dunn et al., 2011) was calculated in individual cells. In cases where lysosomal size and morphology were altered, which are reflected in signal intensity, Pearson's correlation coefficient (PCC) was used, since PCC is independent of signal levels and background (Dunn et al., 2011). The area corresponding to the cell nucleus was excluded from the cell region of interest (ROI) to prevent false-positive colocalization due to automatic signal adjustments. MCC and PCC show how much of the signal of interest (mTOR or RagC) overlaps with a second signal (LAMP2).

Quantification of LC3B, p62 and LysoTracker intensities

Staining intensity was calculated using the Fiji software. ROIs were determined for approximately 50 cells per condition over 5 independent representative images and integrated density was calculated, representing the sum of the values of all pixels in the given ROI. Exact numbers of individual cells analysed per experiment are indicated in the figure legends.

Scoring of TFEB/TFE3 localization

Subcellular localization of TFEB and TFE3 was analyzed by scoring the distribution of signal in the cytoplasm and the nucleus. Five independent fields were analysed per experiment. Exact numbers of individual cells analysed per experiment are indicated in the figure legends.

Luciferase assay

Cells were transfected with the siRNAs targeting CYLD and IKK β either alone or in combination. The next day, 700 μ l of the media was removed from the cells and 400 μ l of fresh media was added to each well. Cells were then transfected with Effectene as described above, with 200 ng of the 3x κ BL construct and 100 ng of the control pRL-null. Forty-eight hours later, the luciferase assay was performed with the Dual Luciferase Assay Reporter System (#E1910, Promega), as described in the manufacturer's instructions. The reporter activity is calculated by dividing the signal from the Firefly luciferase by the signal from the Renilla luciferase.

OPP assay

To test de novo protein synthesis, OPP incorporation assays were performed using the Click-iT Plus OPP Protein Synthesis Assay kit (#C10456, Thermo Fisher Scientific), according to the manufacturer's instructions. In brief, cells were seeded in fibronectin-coated coverslips until they reached 80-90% confluence. Control samples were treated with 100 μ M CHX (#239765, Sigma) for four hours to block translation before fixation. Click-iT OPP component A (20 μ M) was added to the media for 30 minutes, cells were fixed for 10 minutes at RT with 4% PFA, and washed twice with PBT. Next, cells were incubated with Click-iT Plus OPP

reaction cocktail for 30 minutes at RT protected from light, followed by one wash with Click-iT Reaction Rinse Buffer and DAPI staining as described for immunofluorescence. All samples were imaged on an SP8 Leica confocal microscope (TCS SP8 X or TCS SP8 DLS, Leica Microsystems) using a 40x oil objective lens. Image acquisition was performed using the LAS X software (Leica Microsystems).

For cytometry-based detection of protein translation levels, 1×10^6 cells were used per condition. Cells were incubated with 20 μ M of Click-iT OPP component A for one hour, harvested and centrifuged for three minutes, 1,400 rpm at RT. Samples were fixed with ice-cold 70% ethanol, incubated on ice for 30 minutes, washed once with 1x PBS, followed by two washes with 1x PBS, 0.3% BSA and permeabilization with 0.1% Saponin (#47036, Sigma) in 1x PBS, 0.3% BSA at RT for 10 minutes. Cells were then centrifuged for three minutes, 1,400 rpm at RT. The supernatant was removed and cells were incubated with Click-iT Plus OPP reaction cocktail for 30 minutes. Next, cells were washed twice with 1x PBS, 0.3% BSA. Alexa Fluor 488 signal was detected with a FITC filter in a BD LSR Fortessa™ Cell Analyzer flow cytometer (BD Biosciences) and further analysed in the FlowJo™ v10 software (TreeStar).

SUnSET assay

Cells were treated with Torin1 for 16 hours, CHX for four hours or with DMSO as a control. In the last 30 minutes of the treatments, puromycin (10 μ g/ml) was added to the culture media. Cells were lysed as described above and lysates were subjected to SDS-PAGE for detection of puromycin incorporation into nascent polypeptide chains. Protein synthesis rates were determined by quantification of total puromycin signal divided by GAPDH, using the GelAnalyzer software.

Statistical analysis

Statistical analysis and presentation of quantification data was performed using GraphPad Prism (version 9.1.0). Data in graphs shown as mean \pm SEM. Significance was calculated using Student's t-test (for pairwise comparisons) or one-way ANOVA with post hoc Holm-Sidak test (pairwise comparisons in experiments with more than two conditions). Sample sizes (n) and significance values are indicated in figure legends (* $p < 0.05$, ** $p < 0.01$, *** $p < 0.005$, **** $p < 0.001$, ns non-significant).

References

- Abu-Remaileh, M., Wyant, G.A., Kim, C., Laqtom, N.N., Abbasi, M., Chan, S.H., et al. (2017). Lysosomal metabolomics reveals V-ATPase- and mTOR-dependent regulation of amino acid efflux from lysosomes. *Science* 358(6364), 807-813. doi: 10.1126/science.aan6298.
- Acosta-Jaquez, H.A., Keller, J.A., Foster, K.G., Ekim, B., Soliman, G.A., Feener, E.P., et al. (2009). Site-specific mTOR phosphorylation promotes mTORC1-mediated signaling and cell growth. *Mol Cell Biol* 29(15), 4308-4324. doi: 10.1128/MCB.01665-08.
- Adhikari, A., Xu, M., and Chen, Z.J. (2007). Ubiquitin-mediated activation of TAK1 and IKK. *Oncogene* 26(22), 3214-3226. doi: 10.1038/sj.onc.1210413.
- Agrawal, P., Chen, Y.T., Schilling, B., Gibson, B.W., and Hughes, R.E. (2012). Ubiquitin-specific peptidase 9, X-linked (USP9X) modulates activity of mammalian target of rapamycin (mTOR). *J Biol Chem* 287(25), 21164-21175. doi: 10.1074/jbc.M111.328021.
- Ahmed, A.R., Owens, R.J., Stubbs, C.D., Parker, A.W., Hitchman, R., Yadav, R.B., et al. (2019). Direct imaging of the recruitment and phosphorylation of S6K1 in the mTORC1 pathway in living cells. *Scientific Reports* 9. doi: ARTN 3408 10.1038/s41598-019-39410-z.
- Alesi, N., Akl, E.W., Khabibullin, D., Liu, H.J., Nidhiry, A.S., Garner, E.R., et al. (2021). TSC2 regulates lysosome biogenesis via a non-canonical RAGC and TFEB-dependent mechanism. *Nat Commun* 12(1), 4245. doi: 10.1038/s41467-021-24499-6.
- Alessi, D.R., James, S.R., Downes, C.P., Holmes, A.B., Gaffney, P.R., Reese, C.B., et al. (1997). Characterization of a 3-phosphoinositide-dependent protein kinase which phosphorylates and activates protein kinase B α . *Curr Biol* 7(4), 261-269. doi: 10.1016/s0960-9822(06)00122-9.
- Alessi, D.R., Kozlowski, M.T., Weng, Q.P., Morrice, N., and Avruch, J. (1998). 3 Phosphoinositide-dependent protein kinase 1 (PDK1) phosphorylates and activates the p70 S6 kinase in vivo and in vitro. *Current Biology* 8(2), 69-81. doi: Doi 10.1016/S0960-9822(98)70037-5.
- Anandapadamanaban, M., Masson, G.R., Perisic, O., Berndt, A., Kaufman, J., Johnson, C.M., et al. (2019). Architecture of human Rag GTPase heterodimers and their complex with mTORC1. *Science* 366(6462), 203-210. doi: 10.1126/science.aax3939.
- Angarola, B., and Ferguson, S.M. (2019). Weak membrane interactions allow Rheb to activate mTORC1 signaling without major lysosome enrichment. *Mol Biol Cell* 30(22), 2750-2760. doi: 10.1091/mbc.E19-03-0146.
- Antonoli, M., Albiero, F., Nazio, F., Vescovo, T., Perdomo, A.B., Corazzari, M., et al. (2014). AMBRA1 interplay with cullin E3 ubiquitin ligases regulates autophagy dynamics. *Dev Cell* 31(6), 734-746. doi: 10.1016/j.devcel.2014.11.013.
- Asrani, K., Woo, J., Mendes, A.A., Schaffer, E., Vidotto, T., Villanueva, C.R., et al. (2022). An mTORC1-mediated negative feedback loop constrains amino acid-induced FLCN-Rag activation in renal cells with TSC2 loss. *Nat Commun* 13(1), 6808. doi: 10.1038/s41467-022-34617-7.
- Astrinidis, A., Senapedis, W., Coleman, T.R., and Henske, E.P. (2003). Cell cycle-regulated phosphorylation of hamartin, the product of the tuberous sclerosis complex 1 gene, by cyclin-dependent kinase 1/cyclin B. *J Biol Chem* 278(51), 51372-51379. doi: 10.1074/jbc.M303956200.

- Averous, J., Lambert-Langlais, S., Carraro, V., Gourbeyre, O., Parry, L., B'Chir, W., et al. (2014). Requirement for lysosomal localization of mTOR for its activation differs between leucine and other amino acids. *Cell Signal* 26(9), 1918-1927. doi: 10.1016/j.cellsig.2014.04.019.
- Axe, E.L., Walker, S.A., Manifava, M., Chandra, P., Roderick, H.L., Habermann, A., et al. (2008). Autophagosome formation from membrane compartments enriched in phosphatidylinositol 3-phosphate and dynamically connected to the endoplasmic reticulum. *J Cell Biol* 182(4), 685-701. doi: 10.1083/jcb.200803137.
- Aylett, C.H., Sauer, E., Imseng, S., Boehringer, D., Hall, M.N., Ban, N., et al. (2016). Architecture of human mTOR complex 1. *Science* 351(6268), 48-52. doi: 10.1126/science.aaa3870.
- Bae, S., Kim, S.Y., Jung, J.H., Yoon, Y., Cha, H.J., Lee, H., et al. (2012). Akt is negatively regulated by the MULAN E3 ligase. *Cell Res* 22(5), 873-885. doi: 10.1038/cr.2012.38.
- Bagh, M.B., Peng, S., Chandra, G., Zhang, Z., Singh, S.P., Pattabiraman, N., et al. (2017). Misrouting of v-ATPase subunit V0a1 dysregulates lysosomal acidification in a neurodegenerative lysosomal storage disease model. *Nat Commun* 8, 14612. doi: 10.1038/ncomms14612.
- Bai, L., and Li, H. (2019). Cryo-EM is uncovering the mechanism of eukaryotic protein N-glycosylation. *FEBS J* 286(9), 1638-1644. doi: 10.1111/febs.14705.
- Bajaj, L., Lotfi, P., Pal, R., Ronza, A.D., Sharma, J., and Sardiello, M. (2019). Lysosome biogenesis in health and disease. *J Neurochem* 148(5), 573-589. doi: 10.1111/jnc.14564.
- Bajaj, L., Sharma, J., di Ronza, A., Zhang, P., Eblimit, A., Pal, R., et al. (2020). A CLN6-CLN8 complex recruits lysosomal enzymes at the ER for Golgi transfer. *J Clin Invest* 130(8), 4118-4132. doi: 10.1172/JCI130955.
- Ballabio, A., and Bonifacino, J.S. (2020). Lysosomes as dynamic regulators of cell and organismal homeostasis. *Nat Rev Mol Cell Biol* 21(2), 101-118. doi: 10.1038/s41580-019-0185-4.
- Bar-Peled, L., Chantranupong, L., Cherniack, A.D., Chen, W.W., Ottina, K.A., Grabiner, B.C., et al. (2013). A Tumor Suppressor Complex with GAP Activity for the Rag GTPases That Signal Amino Acid Sufficiency to mTORC1. *Science* 340(6136), 1100-1106. doi: 10.1126/science.1232044.
- Bar-Peled, L., Schweitzer, L.D., Zoncu, R., and Sabatini, D.M. (2012). Ragulator Is a GEF for the Rag GTPases that Signal Amino Acid Levels to mTORC1. *Cell* 150(6), 1196-1208. doi: 10.1016/j.cell.2012.07.032.
- Belova, L., Sharma, S., Brickley, D.R., Nicolarsen, J.R., Patterson, C., and Conzen, S.D. (2006). Ubiquitin-proteasome degradation of serum- and glucocorticoid-regulated kinase-1 (SGK-1) is mediated by the chaperone-dependent E3 ligase CHIP. *Biochem J* 400(2), 235-244. doi: 10.1042/BJ20060905.
- Benvenuto, G., Li, S., Brown, S.J., Braverman, R., Vass, W.C., Cheadle, J.P., et al. (2000). The tuberous sclerosis-1 (TSC1) gene product hamartin suppresses cell growth and augments the expression of the TSC2 product tuberin by inhibiting its ubiquitination. *Oncogene* 19(54), 6306-6316. doi: 10.1038/sj.onc.1204009.
- Bernfeld, E., Menon, D., Vaghela, V., Zerlin, I., Faruque, P., Frias, M.A., et al. (2018). Phospholipase D-dependent mTOR complex 1 (mTORC1) activation by glutamine. *J Biol Chem* 293(42), 16390-16401. doi: 10.1074/jbc.RA118.004972.

- Bertrand, M.J., Milutinovic, S., Dickson, K.M., Ho, W.C., Boudreault, A., Durkin, J., et al. (2008). cIAP1 and cIAP2 facilitate cancer cell survival by functioning as E3 ligases that promote RIP1 ubiquitination. *Mol Cell* 30(6), 689-700. doi: 10.1016/j.molcel.2008.05.014.
- Betz, C., and Hall, M.N. (2013). Where is mTOR and what is it doing there? *Journal of Cell Biology* 203(4), 563-574. doi: 10.1083/jcb.201306041.
- Bignell, G.R., Warren, W., Seal, S., Takahashi, M., Rapley, E., Barfoot, R., et al. (2000). Identification of the familial cylindromatosis tumour-suppressor gene. *Nat Genet* 25(2), 160-165. doi: 10.1038/76006.
- Blommaart, E.F.C., Luiken, J.J.F.P., Blommaart, P.J.E., Vanwoerkom, G.M., and Meijer, A.J. (1995). Phosphorylation of Ribosomal-Protein S6 Is Inhibitory for Autophagy in Isolated Rat Hepatocytes. *Journal of Biological Chemistry* 270(5), 2320-2326. doi: DOI 10.1074/jbc.270.5.2320.
- Bohlen, J., Roiuk, M., and Teleman, A.A. (2021). Phosphorylation of ribosomal protein S6 differentially affects mRNA translation based on ORF length. *Nucleic Acids Res* 49(22), 13062-13074. doi: 10.1093/nar/gkab1157.
- Bohm, R., Imseng, S., Jakob, R.P., Hall, M.N., Maier, T., and Hiller, S. (2021). The dynamic mechanism of 4E-BP1 recognition and phosphorylation by mTORC1. *Mol Cell*. doi: 10.1016/j.molcel.2021.03.031.
- Bonifacino, J.S., and Rojas, R. (2006). Retrograde transport from endosomes to the trans-Golgi network. *Nat Rev Mol Cell Biol* 7(8), 568-579. doi: 10.1038/nrm1985.
- Braulke, T., and Bonifacino, J.S. (2009). Sorting of lysosomal proteins. *Biochim Biophys Acta* 1793(4), 605-614. doi: 10.1016/j.bbamcr.2008.10.016.
- Broer, S., and Broer, A. (2017). Amino acid homeostasis and signalling in mammalian cells and organisms. *Biochem J* 474(12), 1935-1963. doi: 10.1042/BCJ20160822.
- Brummelkamp, T.R., Nijman, S.M., Dirac, A.M., and Bernards, R. (2003). Loss of the cylindromatosis tumour suppressor inhibits apoptosis by activating NF-kappaB. *Nature* 424(6950), 797-801. doi: 10.1038/nature01811.
- Budanov, A.V., and Karin, M. (2008). p53 target genes Sestrin1 and Sestrin2 connect genotoxic stress and mTOR signaling. *Cell* 134(3), 451-460. doi: 10.1016/j.cell.2008.06.028.
- Budanov, A.V., Shoshani, T., Faerman, A., Zelin, E., Kamer, I., Kalinski, H., et al. (2002). Identification of a novel stress-responsive gene Hi95 involved in regulation of cell viability. *Oncogene* 21(39), 6017-6031. doi: 10.1038/sj.onc.1205877.
- Buerger, C., DeVries, B., and Stambolic, V. (2006). Localization of Rheb to the endomembrane is critical for its signaling function. *Biochem Biophys Res Commun* 344(3), 869-880. doi: 10.1016/j.bbrc.2006.03.220.
- Burda, P., and Aebi, M. (1999). The dolichol pathway of N-linked glycosylation. *Biochim Biophys Acta* 1426(2), 239-257. doi: 10.1016/s0304-4165(98)00127-5.
- Burnett, P.E., Barrow, R.K., Cohen, N.A., Snyder, S.H., and Sabatini, D.M. (1998). RAFT1 phosphorylation of the translational regulators p70 S6 kinase and 4E-BP1. *Proceedings of the National Academy of Sciences of the United States of America* 95(4), 1432-1437. doi: DOI 10.1073/pnas.95.4.1432.
- Chan, C.H., Li, C.F., Yang, W.L., Gao, Y., Lee, S.W., Feng, Z., et al. (2012). The Skp2-SCF E3 ligase regulates Akt ubiquitination, glycolysis, herceptin sensitivity, and tumorigenesis. *Cell* 149(5), 1098-1111. doi: 10.1016/j.cell.2012.02.065.

- Chantranupong, L., Scaria, S.M., Saxton, R.A., Gygi, M.P., Shen, K., Wyant, G.A., et al. (2016). The CASTOR Proteins Are Arginine Sensors for the mTORC1 Pathway. *Cell* 165(1), 153-164. doi: 10.1016/j.cell.2016.02.035.
- Chantranupong, L., Wolfson, R.L., Orozco, J.M., Saxton, R.A., Scaria, S.M., Bar-Peled, L., et al. (2014). The Sestrins Interact with GATOR2 to Negatively Regulate the Amino-Acid-Sensing Pathway Upstream of mTORC1. *Cell Reports* 9(1), 1-8. doi: 10.1016/j.celrep.2014.09.014.
- Chauvin, C., Koka, V., Nouschi, A., Mieulet, V., Hoareau-Aveilla, C., Dreazen, A., et al. (2014). Ribosomal protein S6 kinase activity controls the ribosome biogenesis transcriptional program. *Oncogene* 33(4), 474-483. doi: 10.1038/onc.2012.606.
- Chen, J., Ou, Y., Luo, R., Wang, J., Wang, D., Guan, J., et al. (2021). SAR1B senses leucine levels to regulate mTORC1 signalling. *Nature*. doi: 10.1038/s41586-021-03768-w.
- Chen, J., Ou, Y., Yang, Y., Li, W., Xu, Y., Xie, Y., et al. (2018a). KLHL22 activates amino-acid-dependent mTORC1 signalling to promote tumorigenesis and ageing. *Nature* 557(7706), 585-589. doi: 10.1038/s41586-018-0128-9.
- Chen, X., Liu, M., Tian, Y., Li, J., Qi, Y., Zhao, D., et al. (2018b). Cryo-EM structure of human mTOR complex 2. *Cell Res* 28(5), 518-528. doi: 10.1038/s41422-018-0029-3.
- Chen, Z.J., and Sun, L.J. (2009). Nonproteolytic functions of ubiquitin in cell signaling. *Mol Cell* 33(3), 275-286. doi: 10.1016/j.molcel.2009.01.014.
- Chiang, G.G., and Abraham, R.T. (2005). Phosphorylation of mammalian target of rapamycin (mTOR) at Ser-2448 is mediated by p70S6 kinase. *J Biol Chem* 280(27), 25485-25490. doi: 10.1074/jbc.M501707200.
- Cho, S., Lee, G., Pickering, B.F., Jang, C., Park, J.H., He, L., et al. (2021). mTORC1 promotes cell growth via m(6)A-dependent mRNA degradation. *Mol Cell*. doi: 10.1016/j.molcel.2021.03.010.
- Chong-Kopera, H., Inoki, K., Li, Y., Zhu, T., Garcia-Gonzalo, F.R., Rosa, J.L., et al. (2006). TSC1 stabilizes TSC2 by inhibiting the interaction between TSC2 and the HERC1 ubiquitin ligase. *J Biol Chem* 281(13), 8313-8316. doi: 10.1074/jbc.C500451200.
- Chu, N., Salguero, A.L., Liu, A.Z., Chen, Z., Dempsey, D.R., Ficarro, S.B., et al. (2018). Akt Kinase Activation Mechanisms Revealed Using Protein Semisynthesis. *Cell* 174(4), 897-907 e814. doi: 10.1016/j.cell.2018.07.003.
- Colacurcio, D.J., and Nixon, R.A. (2016). Disorders of lysosomal acidification-The emerging role of v-ATPase in aging and neurodegenerative disease. *Ageing Res Rev* 32, 75-88. doi: 10.1016/j.arr.2016.05.004.
- Colombo, E., Horta, G., Roesler, M.K., Ihbe, N., Chhabra, S., Radyushkin, K., et al. (2021). The K63 deubiquitinase CYLD modulates autism-like behaviors and hippocampal plasticity by regulating autophagy and mTOR signaling. *Proc Natl Acad Sci U S A* 118(47). doi: 10.1073/pnas.2110755118.
- Costes, S.V., Daelemans, D., Cho, E.H., Dobbin, Z., Pavlakis, G., and Lockett, S. (2004). Automatic and quantitative measurement of protein-protein colocalization in live cells. *Biophys J* 86(6), 3993-4003. doi: 10.1529/biophysj.103.038422.
- Cui, Z., Napolitano, G., de Araujo, M.E.G., Esposito, A., Monfregola, J., Huber, L.A., et al. (2023). Structure of the lysosomal mTORC1-TFEB-Rag-Ragulator megacomplex. *Nature* 614(7948), 572-579. doi: 10.1038/s41586-022-05652-7.

- Dai, X., Jiang, C., Jiang, Q., Fang, L., Yu, H., Guo, J., et al. (2023). AMPK-dependent phosphorylation of the GATOR2 component WDR24 suppresses glucose-mediated mTORC1 activation. *Nat Metab*. doi: 10.1038/s42255-022-00732-4.
- Danyukova, T., Ludwig, N.F., Velho, R.V., Harms, F.L., Gunes, N., Tidow, H., et al. (2020). Combined in vitro and in silico analyses of missense mutations in GNPTAB provide new insights into the molecular bases of mucopolidosis II and III alpha/beta. *Hum Mutat* 41(1), 133-139. doi: 10.1002/humu.23928.
- de Araujo, M.E., Stasyk, T., Taub, N., Ebner, H.L., Furst, B., Filipek, P., et al. (2013). Stability of the endosomal scaffold protein LAMTOR3 depends on heterodimer assembly and proteasomal degradation. *J Biol Chem* 288(25), 18228-18242. doi: 10.1074/jbc.M112.349480.
- Demetriades, C., Doumpas, N., and Teleman, A.A. (2014). Regulation of TORC1 in response to amino acid starvation via lysosomal recruitment of TSC2. *Cell* 156(4), 786-799. doi: 10.1016/j.cell.2014.01.024.
- Demetriades, C., Plescher, M., and Teleman, A.A. (2016a). Lysosomal recruitment of TSC2 is a universal response to cellular stress. *Nature Communications* 7. doi: ARTN 10662 10.1038/ncomms10662.
- Demetriades, C., Plescher, M., and Teleman, A.A. (2016b). Lysosomal recruitment of TSC2 is a universal response to cellular stress. *Nat Commun* 7, 10662. doi: 10.1038/ncomms10662.
- Deng, L., Chen, L., Zhao, L., Xu, Y., Peng, X., Wang, X., et al. (2019). Ubiquitination of Rheb governs growth factor-induced mTORC1 activation. *Cell Res* 29(2), 136-150. doi: 10.1038/s41422-018-0120-9.
- Deng, L., Jiang, C., Chen, L., Jin, J., Wei, J., Zhao, L., et al. (2015). The ubiquitination of rag A GTPase by RNF152 negatively regulates mTORC1 activation. *Mol Cell* 58(5), 804-818. doi: 10.1016/j.molcel.2015.03.033.
- Desforges, M., and Sibley, C.P. (2010). Placental nutrient supply and fetal growth. *Int J Dev Biol* 54(2-3), 377-390. doi: 10.1387/ijdb.082765md.
- Di Malta, C., Siciliano, D., Calcagni, A., Monfregola, J., Punzi, S., Pastore, N., et al. (2017). Transcriptional activation of RagD GTPase controls mTORC1 and promotes cancer growth. *Science* 356(6343), 1188-1192. doi: 10.1126/science.aag2553.
- di Ronza, A., Bajaj, L., Sharma, J., Sanagasetti, D., Lotfi, P., Adamski, C.J., et al. (2018). CLN8 is an endoplasmic reticulum cargo receptor that regulates lysosome biogenesis. *Nat Cell Biol* 20(12), 1370-1377. doi: 10.1038/s41556-018-0228-7.
- Dibble, C.C., Elis, W., Menon, S., Qin, W., Klekota, J., Asara, J.M., et al. (2012). TBC1D7 is a third subunit of the TSC1-TSC2 complex upstream of mTORC1. *Mol Cell* 47(4), 535-546. doi: 10.1016/j.molcel.2012.06.009.
- Dikic, I., and Elazar, Z. (2018). Mechanism and medical implications of mammalian autophagy. *Nat Rev Mol Cell Biol* 19(6), 349-364. doi: 10.1038/s41580-018-0003-4.
- Ding, X., Bloch, W., Iden, S., Ruegg, M.A., Hall, M.N., Leptin, M., et al. (2016). mTORC1 and mTORC2 regulate skin morphogenesis and epidermal barrier formation. *Nat Commun* 7, 13226. doi: 10.1038/ncomms13226.
- Dooley, H.C., Razi, M., Polson, H.E., Girardin, S.E., Wilson, M.I., and Tooze, S.A. (2014). WIPI2 links LC3 conjugation with PI3P, autophagosome formation, and pathogen clearance by recruiting Atg12-5-16L1. *Mol Cell* 55(2), 238-252. doi: 10.1016/j.molcel.2014.05.021.

- Dorrello, N.V., Peschiaroli, A., Guardavaccaro, D., Colburn, N.H., Sherman, N.E., and Pagano, M. (2006). S6K1- and betaTRCP-mediated degradation of PDCD4 promotes protein translation and cell growth. *Science* 314(5798), 467-471. doi: 10.1126/science.1130276.
- Drenan, R.M., Liu, X., Bertram, P.G., and Zheng, X.F. (2004). FKBP12-rapamycin-associated protein or mammalian target of rapamycin (FRAP/mTOR) localization in the endoplasmic reticulum and the Golgi apparatus. *J Biol Chem* 279(1), 772-778. doi: 10.1074/jbc.M305912200.
- Duan, S., Skaar, J.R., Kuchay, S., Toschi, A., Kanarek, N., Ben-Neriah, Y., et al. (2011). mTOR generates an auto-amplification loop by triggering the betaTrCP- and CK1alpha-dependent degradation of DEPTOR. *Mol Cell* 44(2), 317-324. doi: 10.1016/j.molcel.2011.09.005.
- Dunn, K.W., Kamocka, M.M., and McDonald, J.H. (2011). A practical guide to evaluating colocalization in biological microscopy. *Am J Physiol Cell Physiol* 300(4), C723-742. doi: 10.1152/ajpcell.00462.2010.
- Duran, R.V., Oppliger, W., Robitaille, A.M., Heiserich, L., Skendaj, R., Gottlieb, E., et al. (2012). Glutaminolysis activates Rag-mTORC1 signaling. *Mol Cell* 47(3), 349-358. doi: 10.1016/j.molcel.2012.05.043.
- Dyachok, J., Earnest, S., Iturraran, E.N., Cobb, M.H., and Ross, E.M. (2016). Amino Acids Regulate mTORC1 by an Obligate Two-step Mechanism. *J Biol Chem* 291(43), 22414-22426. doi: 10.1074/jbc.M116.732511.
- Ea, C.K., Deng, L., Xia, Z.P., Pineda, G., and Chen, Z.J. (2006). Activation of IKK by TNFalpha requires site-specific ubiquitination of RIP1 and polyubiquitin binding by NEMO. *Mol Cell* 22(2), 245-257. doi: 10.1016/j.molcel.2006.03.026.
- Ebner, M., Sinkovics, B., Szczygiel, M., Ribeiro, D.W., and Yudushkin, I. (2017). Localization of mTORC2 activity inside cells. *J Cell Biol* 216(2), 343-353. doi: 10.1083/jcb.201610060.
- Efeyan, A., Schweitzer, L.D., Bilate, A.M., Chang, S., Kirak, O., Lamming, D.W., et al. (2014). RagA, but not RagB, is essential for embryonic development and adult mice. *Dev Cell* 29(3), 321-329. doi: 10.1016/j.devcel.2014.03.017.
- Efeyan, A., Zoncu, R., Chang, S., Gumper, I., Snitkin, H., Wolfson, R.L., et al. (2013). Regulation of mTORC1 by the Rag GTPases is necessary for neonatal autophagy and survival. *Nature* 493(7434), 679-683. doi: 10.1038/nature11745.
- Ekim, B., Magnuson, B., Acosta-Jaquez, H.A., Keller, J.A., Feener, E.P., and Fingar, D.C. (2011). mTOR kinase domain phosphorylation promotes mTORC1 signaling, cell growth, and cell cycle progression. *Mol Cell Biol* 31(14), 2787-2801. doi: 10.1128/MCB.05437-11.
- Faesen, A.C., Luna-Vargas, M.P., Geurink, P.P., Clerici, M., Merks, R., van Dijk, W.J., et al. (2011). The differential modulation of USP activity by internal regulatory domains, interactors and eight ubiquitin chain types. *Chem Biol* 18(12), 1550-1561. doi: 10.1016/j.chembiol.2011.10.017.
- Fan, C.D., Lum, M.A., Xu, C., Black, J.D., and Wang, X. (2013). Ubiquitin-dependent regulation of phospho-AKT dynamics by the ubiquitin E3 ligase, NEDD4-1, in the insulin-like growth factor-1 response. *J Biol Chem* 288(3), 1674-1684. doi: 10.1074/jbc.M112.416339.
- Fedele, A.O., and Proud, C.G. (2020). Chloroquine and bafilomycin A mimic lysosomal storage disorders and impair mTORC1 signalling. *Biosci Rep* 40(4). doi: 10.1042/BSR20200905.

- Felig, P., Owen, O.E., Wahren, J., and Cahill, G.F., Jr. (1969). Amino acid metabolism during prolonged starvation. *J Clin Invest* 48(3), 584-594. doi: 10.1172/JCI106017.
- Felig, P., Wahren, J., and Raf, L. (1973). Evidence of inter-organ amino-acid transport by blood cells in humans. *Proc Natl Acad Sci U S A* 70(6), 1775-1779. doi: 10.1073/pnas.70.6.1775.
- Fernandes, S.A., and Demetriades, C. (2021). The Multifaceted Role of Nutrient Sensing and mTORC1 Signaling in Physiology and Aging. *Front Aging* 2, 707372. doi: 10.3389/fragi.2021.707372.
- Fernandez-Majada, V., Welz, P.S., Ermolaeva, M.A., Schell, M., Adam, A., Dietlein, F., et al. (2016). The tumour suppressor CYLD regulates the p53 DNA damage response. *Nat Commun* 7, 12508. doi: 10.1038/ncomms12508.
- Fitzian, K., Bruckner, A., Brohee, L., Zech, R., Antoni, C., Kiontke, S., et al. (2021). TSC1 binding to lysosomal PIPs is required for TSC complex translocation and mTORC1 regulation. *Mol Cell* 81(13), 2705-2721 e2708. doi: 10.1016/j.molcel.2021.04.019.
- Frias, M.A., Thoreen, C.C., Jaffe, J.D., Schroder, W., Sculley, T., Carr, S.A., et al. (2006). mSin1 is necessary for Akt/PKB phosphorylation, and its isoforms define three distinct mTORC2s. *Curr Biol* 16(18), 1865-1870. doi: 10.1016/j.cub.2006.08.001.
- Fromm, S.A., Lawrence, R.E., and Hurley, J.H. (2020). Structural mechanism for amino acid-dependent Rag GTPase nucleotide state switching by SLC38A9. *Nature Structural & Molecular Biology* 27(11), 1017-+. doi: 10.1038/s41594-020-0490-9.
- Fu, W., and Hall, M.N. (2020). Regulation of mTORC2 Signaling. *Genes (Basel)* 11(9). doi: 10.3390/genes11091045.
- Fumagalli, S., and Pende, M. (2022). S6 kinase 1 at the central node of cell size and ageing. *Front Cell Dev Biol* 10, 949196. doi: 10.3389/fcell.2022.949196.
- Gan, X., Wang, J., Su, B., and Wu, D. (2011). Evidence for direct activation of mTORC2 kinase activity by phosphatidylinositol 3,4,5-trisphosphate. *J Biol Chem* 286(13), 10998-11002. doi: 10.1074/jbc.M110.195016.
- Gangloff, Y.G., Mueller, M., Dann, S.G., Svoboda, P., Sticker, M., Spetz, J.F., et al. (2004). Disruption of the mouse mTOR gene leads to early postimplantation lethality and prohibits embryonic stem cell development. *Mol Cell Biol* 24(21), 9508-9516. doi: 10.1128/MCB.24.21.9508-9516.2004.
- Ganley, I.G., Lam, D.H., Wang, J.R., Ding, X.J., Chen, S., and Jiang, X.J. (2009). ULK1 center dot ATG13 center dot FIP200 Complex Mediates mTOR Signaling and Is Essential for Autophagy. *Journal of Biological Chemistry* 284(18), 12297-12305. doi: 10.1074/jbc.M900573200.
- Gao, D., Inuzuka, H., Tan, M.K., Fukushima, H., Locasale, J.W., Liu, P., et al. (2011). mTOR drives its own activation via SCF(betaTrCP)-dependent degradation of the mTOR inhibitor DEPTOR. *Mol Cell* 44(2), 290-303. doi: 10.1016/j.molcel.2011.08.030.
- Gao, D., Wan, L., Inuzuka, H., Berg, A.H., Tseng, A., Zhai, B., et al. (2010). Rictor forms a complex with Cullin-1 to promote SGK1 ubiquitination and destruction. *Mol Cell* 39(5), 797-808. doi: 10.1016/j.molcel.2010.08.016.
- Garami, A., Zwartkruis, F.J., Nobukuni, T., Joaquin, M., Rocco, M., Stocker, H., et al. (2003). Insulin activation of Rheb, a mediator of mTOR/S6K/4E-BP signaling, is inhibited by TSC1 and 2. *Mol Cell* 11(6), 1457-1466. doi: 10.1016/s1097-2765(03)00220-x.

- Garcia-Martinez, J.M., and Alessi, D.R. (2008). mTOR complex 2 (mTORC2) controls hydrophobic motif phosphorylation and activation of serum- and glucocorticoid-induced protein kinase 1 (SGK1). *Biochem J* 416(3), 375-385. doi: 10.1042/BJ20081668.
- Gatto, F., Rossi, B., Tarallo, A., Polishchuk, E., Polishchuk, R., Carrella, A., et al. (2017). AAV-mediated transcription factor EB (TFEB) gene delivery ameliorates muscle pathology and function in the murine model of Pompe Disease. *Sci Rep* 7(1), 15089. doi: 10.1038/s41598-017-15352-2.
- Ghosh, P., Dahms, N.M., and Kornfeld, S. (2003). Mannose 6-phosphate receptors: new twists in the tale. *Nat Rev Mol Cell Biol* 4(3), 202-212. doi: 10.1038/nrm1050.
- Gieselmann, V., Pohlmann, R., Hasilik, A., and Von Figura, K. (1983). Biosynthesis and transport of cathepsin D in cultured human fibroblasts. *J Cell Biol* 97(1), 1-5. doi: 10.1083/jcb.97.1.1.
- Gingras, A.C., Gygi, S.P., Raught, B., Polakiewicz, R.D., Abraham, R.T., Hoekstra, M.F., et al. (1999). Regulation of 4E-BP1 phosphorylation: a novel two-step mechanism. *Genes Dev* 13(11), 1422-1437. doi: 10.1101/gad.13.11.1422.
- Goldbraikh, D., Neufeld, D., Eid-Mutlak, Y., Lasry, I., Gilda, J.E., Parnis, A., et al. (2020). USP1 deubiquitinates Akt to inhibit PI3K-Akt-FoxO signaling in muscle during prolonged starvation. *EMBO Rep* 21(4), e48791. doi: 10.15252/embr.201948791.
- Gollwitzer, P., Grutzmacher, N., Wilhelm, S., Kummel, D., and Demetriades, C. (2022). A Rag GTPase dimer code defines the regulation of mTORC1 by amino acids. *Nat Cell Biol* 24(9), 1394-1406. doi: 10.1038/s41556-022-00976-y.
- Gosavi, P., Houghton, F.J., McMillan, P.J., Hanssen, E., and Gleeson, P.A. (2018). The Golgi ribbon in mammalian cells negatively regulates autophagy by modulating mTOR activity. *Journal of Cell Science* 131(3). doi: ARTN jcs211987 10.1242/jcs.211987.
- Gu, X., Orozco, J.M., Saxton, R.A., Condon, K.J., Liu, G.Y., Krawczyk, P.A., et al. (2017). SAMTOR is an S-adenosylmethionine sensor for the mTORC1 pathway. *Science* 358(6364), 813-818. doi: 10.1126/science.aao3265.
- Guertin, D.A., Stevens, D.M., Thoreen, C.C., Burds, A.A., Kalaany, N.Y., Moffat, J., et al. (2006). Ablation in mice of the mTORC components raptor, rictor, or mLST8 reveals that mTORC2 is required for signaling to Akt-FOXO and PKC alpha but not S6K1. *Developmental Cell* 11(6), 859-871. doi: 10.1016/j.devcel.2006.10.007.
- Guo, P., Ma, X., Zhao, W., Huai, W., Li, T., Qiu, Y., et al. (2018). TRIM31 is upregulated in hepatocellular carcinoma and promotes disease progression by inducing ubiquitination of TSC1-TSC2 complex. *Oncogene* 37(4), 478-488. doi: 10.1038/onc.2017.349.
- Gwinn, D.M., Shackelford, D.B., Egan, D.F., Mihaylova, M.M., Mery, A., Vasquez, D.S., et al. (2008). AMPK phosphorylation of raptor mediates a metabolic checkpoint. *Mol Cell* 30(2), 214-226. doi: 10.1016/j.molcel.2008.03.003.
- Hagiwara, A., Cornu, M., Cybulski, N., Polak, P., Betz, C., Trapani, F., et al. (2012). Hepatic mTORC2 activates glycolysis and lipogenesis through Akt, glucokinase, and SREBP1c. *Cell Metab* 15(5), 725-738. doi: 10.1016/j.cmet.2012.03.015.
- Hamidi, A., Song, J., Thakur, N., Itoh, S., Marcusson, A., Bergh, A., et al. (2017). TGF-beta promotes PI3K-AKT signaling and prostate cancer cell migration through the TRAF6-mediated ubiquitylation of p85alpha. *Sci Signal* 10(486). doi: 10.1126/scisignal.aal4186.

- Han, J.M., Jeong, S.J., Park, M.C., Kim, G., Kwon, N.H., Kim, H.K., et al. (2012). Leucyl-tRNA Synthetase Is an Intracellular Leucine Sensor for the mTORC1-Signaling Pathway. *Cell* 149(2), 410-424. doi: 10.1016/j.cell.2012.02.044.
- Han, S., Witt, R.M., Santos, T.M., Polizzano, C., Sabatini, B.L., and Ramesh, V. (2008). Pam (Protein associated with Myc) functions as an E3 ubiquitin ligase and regulates TSC/mTOR signaling. *Cell Signal* 20(6), 1084-1091. doi: 10.1016/j.cellsig.2008.01.020.
- Hanker, A.B., Mitin, N., Wilder, R.S., Henske, E.P., Tamanoi, F., Cox, A.D., et al. (2010). Differential requirement of CAAX-mediated posttranslational processing for Rheb localization and signaling. *Oncogene* 29(3), 380-391. doi: 10.1038/onc.2009.336.
- Hannan, K.M., Brandenburger, Y., Jenkins, A., Sharkey, K., Cavanaugh, A., Rothblum, L., et al. (2003). mTOR-dependent regulation of ribosomal gene transcription requires S6K1 and is mediated by phosphorylation of the carboxy-terminal activation domain of the nucleolar transcription factor UBF. *Mol Cell Biol* 23(23), 8862-8877. doi: 10.1128/mcb.23.23.8862-8877.2003.
- Hao, F., Kondo, K., Itoh, T., Ikari, S., Nada, S., Okada, M., et al. (2018). Rheb localized on the Golgi membrane activates lysosome-localized mTORC1 at the Golgi-lysosome contact site. *J Cell Sci* 131(3). doi: 10.1242/jcs.208017.
- Hara, K., Maruki, Y., Long, X.M., Yoshino, K., Oshiro, N., Hidayat, S., et al. (2002). Raptor, a binding partner of target of rapamycin (TOR), mediates TOR action. *Cell* 110(2), 177-189. doi: 10.1016/S0092-8674(02)00833-4.
- Hara, K., Yonezawa, K., Kozlowski, M.T., Sugimoto, T., Andrabi, K., Weng, Q.P., et al. (1997). Regulation of eIF-4E BP1 phosphorylation by mTOR. *J Biol Chem* 272(42), 26457-26463. doi: 10.1074/jbc.272.42.26457.
- Hara, K., Yonezawa, K., Weng, Q.P., Kozlowski, M.T., Belham, C., and Avruch, J. (1998). Amino acid sufficiency and mTOR regulate p70 S6 kinase and eIF-4E BP1 through a common effector mechanism. *Journal of Biological Chemistry* 273(23), 14484-14494. doi: 10.1074/jbc.273.23.14484.
- Harhaj, E.W., and Dixit, V.M. (2012). Regulation of NF-kappaB by deubiquitinases. *Immunol Rev* 246(1), 107-124. doi: 10.1111/j.1600-065X.2012.01100.x.
- Harrington, L.S., Findlay, G.M., Gray, A., Tolkacheva, T., Wigfield, S., Rebholz, H., et al. (2004). The TSC1-2 tumor suppressor controls insulin-PI3K signaling via regulation of IRS proteins. *J Cell Biol* 166(2), 213-223. doi: 10.1083/jcb.200403069.
- Hasegawa, M., Fujimoto, Y., Lucas, P.C., Nakano, H., Fukase, K., Nunez, G., et al. (2008). A critical role of RICK/RIP2 polyubiquitination in Nod-induced NF-kappaB activation. *EMBO J* 27(2), 373-383. doi: 10.1038/sj.emboj.7601962.
- Hasilik, A., and Neufeld, E.F. (1980). Biosynthesis of lysosomal enzymes in fibroblasts. Synthesis as precursors of higher molecular weight. *J Biol Chem* 255(10), 4937-4945.
- Hatakeyama, R., Peli-Gulli, M.P., Hu, Z., Jaquenoud, M., Garcia Osuna, G.M., Sardu, A., et al. (2019). Spatially Distinct Pools of TORC1 Balance Protein Homeostasis. *Mol Cell* 73(2), 325-338 e328. doi: 10.1016/j.molcel.2018.10.040.
- Hemberger, M., Hanna, C.W., and Dean, W. (2020). Mechanisms of early placental development in mouse and humans. *Nat Rev Genet* 21(1), 27-43. doi: 10.1038/s41576-019-0169-4.

- Hertel, A., Alves, L.M., Dutz, H., Tascher, G., Bonn, F., Kaulich, M., et al. (2022). USP32-regulated LAMTOR1 ubiquitination impacts mTORC1 activation and autophagy induction. *Cell Rep* 41(10), 111653. doi: 10.1016/j.celrep.2022.111653.
- Herzig, S., and Shaw, R.J. (2018). AMPK: guardian of metabolism and mitochondrial homeostasis. *Nat Rev Mol Cell Biol* 19(2), 121-135. doi: 10.1038/nrm.2017.95.
- Holz, M.K., Ballif, B.A., Gygi, S.P., and Blenis, J. (2005). mTOR and S6K1 mediate assembly of the translation preinitiation complex through dynamic protein interchange and ordered phosphorylation events. *Cell* 123(4), 569-580. doi: 10.1016/j.cell.2005.10.024.
- Hosokawa, N., Hara, T., Kaizuka, T., Kishi, C., Takamura, A., Miura, Y., et al. (2009). Nutrient-dependent mTORC1 association with the ULK1-Atg13-FIP200 complex required for autophagy. *Mol Biol Cell* 20(7), 1981-1991. doi: 10.1091/mbc.E08-12-1248.
- Hoxhaj, G., and Manning, B.D. (2020). The PI3K-AKT network at the interface of oncogenic signalling and cancer metabolism. *Nat Rev Cancer* 20(2), 74-88. doi: 10.1038/s41568-019-0216-7.
- Hsieh, A.C., Liu, Y., Edlind, M.P., Ingolia, N.T., Janes, M.R., Sher, A., et al. (2012). The translational landscape of mTOR signalling steers cancer initiation and metastasis. *Nature* 485(7396), 55-U196. doi: 10.1038/nature10912.
- Hu, J., Zacharek, S., He, Y.J., Lee, H., Shumway, S., Duronio, R.J., et al. (2008). WD40 protein FBW5 promotes ubiquitination of tumor suppressor TSC2 by DDB1-CUL4-ROC1 ligase. *Genes Dev* 22(7), 866-871. doi: 10.1101/gad.1624008.
- Huang, J., and Manning, B.D. (2008). The TSC1-TSC2 complex: a molecular switchboard controlling cell growth. *Biochem J* 412(2), 179-190. doi: 10.1042/BJ20080281.
- Huang, Y., Hu, K., Zhang, S., Dong, X., Yin, Z., Meng, R., et al. (2018). S6K1 phosphorylation-dependent degradation of Mxi1 by beta-Trcp ubiquitin ligase promotes Myc activation and radioresistance in lung cancer. *Theranostics* 8(5), 1286-1300. doi: 10.7150/thno.22552.
- Hussain, S., Feldman, A.L., Das, C., Ziesmer, S.C., Ansell, S.M., and Galardy, P.J. (2013). Ubiquitin hydrolase UCH-L1 destabilizes mTOR complex 1 by antagonizing DDB1-CUL4-mediated ubiquitination of raptor. *Mol Cell Biol* 33(6), 1188-1197. doi: 10.1128/MCB.01389-12.
- Ichimura, Y., Kirisako, T., Takao, T., Satomi, Y., Shimonishi, Y., Ishihara, N., et al. (2000). A ubiquitin-like system mediates protein lipitation. *Nature* 408(6811), 488-492. doi: 10.1038/35044114.
- Inoki, K., Li, Y., Zhu, T., Wu, J., and Guan, K.L. (2002). TSC2 is phosphorylated and inhibited by Akt and suppresses mTOR signalling. *Nat Cell Biol* 4(9), 648-657. doi: 10.1038/ncb839.
- Inoki, K., Ouyang, H., Zhu, T., Lindvall, C., Wang, Y., Zhang, X., et al. (2006). TSC2 integrates Wnt and energy signals via a coordinated phosphorylation by AMPK and GSK3 to regulate cell growth. *Cell* 126(5), 955-968. doi: 10.1016/j.cell.2006.06.055.
- Inoki, K., Zhu, T., and Guan, K.L. (2003). TSC2 mediates cellular energy response to control cell growth and survival. *Cell* 115(5), 577-590. doi: 10.1016/s0092-8674(03)00929-2.
- Jacinto, E., Facchinetti, V., Liu, D., Soto, N., Wei, S., Jung, S.Y., et al. (2006). SIN1/MIP1 maintains rictor-mTOR complex integrity and regulates Akt phosphorylation and substrate specificity. *Cell* 127(1), 125-137. doi: 10.1016/j.cell.2006.08.033.

- Jacinto, E., Loewith, R., Schmidt, A., Lin, S., Ruegg, M.A., Hall, A., et al. (2004). Mammalian TOR complex 2 controls the actin cytoskeleton and is rapamycin insensitive. *Nat Cell Biol* 6(11), 1122-1128. doi: 10.1038/ncb1183.
- Jain, A., Arauz, E., Aggarwal, V., Ikon, N., Chen, J., and Ha, T. (2014). Stoichiometry and assembly of mTOR complexes revealed by single-molecule pulldown. *Proc Natl Acad Sci U S A* 111(50), 17833-17838. doi: 10.1073/pnas.1419425111.
- Jewell, J.L., Kim, Y.C., Russell, R.C., Yu, F.X., Park, H.W., Plouffe, S.W., et al. (2015). Metabolism. Differential regulation of mTORC1 by leucine and glutamine. *Science* 347(6218), 194-198. doi: 10.1126/science.1259472.
- Jia, J.J., Lahr, R.M., Solgaard, M.T., Moraes, B.J., Pointet, R., Yang, A.D., et al. (2021). mTORC1 promotes TOP mRNA translation through site-specific phosphorylation of LARP1. *Nucleic Acids Res* 49(6), 3461-3489. doi: 10.1093/nar/gkaa1239.
- Jiang, C., Dai, X., He, S., Zhou, H., Fang, L., Guo, J., et al. (2023). Ring domains are essential for GATOR2-dependent mTORC1 activation. *Mol Cell* 83(1), 74-89 e79. doi: 10.1016/j.molcel.2022.11.021.
- Jiang, Y., Su, S., Zhang, Y., Qian, J., and Liu, P. (2019). Control of mTOR signaling by ubiquitin. *Oncogene* 38(21), 3989-4001. doi: 10.1038/s41388-019-0713-x.
- Jin, G., Lee, S.W., Zhang, X., Cai, Z., Gao, Y., Chou, P.C., et al. (2015). Skp2-Mediated RagA Ubiquitination Elicits a Negative Feedback to Prevent Amino-Acid-Dependent mTORC1 Hyperactivation by Recruiting GATOR1. *Mol Cell* 58(6), 989-1000. doi: 10.1016/j.molcel.2015.05.010.
- Joo, H.M., Kim, J.Y., Jeong, J.B., Seong, K.M., Nam, S.Y., Yang, K.H., et al. (2011). Ret finger protein 2 enhances ionizing radiation-induced apoptosis via degradation of AKT and MDM2. *Eur J Cell Biol* 90(5), 420-431. doi: 10.1016/j.ejcb.2010.12.001.
- Jung, J., Genau, H.M., and Behrends, C. (2015). Amino Acid-Dependent mTORC1 Regulation by the Lysosomal Membrane Protein SLC38A9. *Molecular and Cellular Biology* 35(14), 2479-2494. doi: 10.1128/Mcb.00125-15.
- Kabeya, Y., Mizushima, N., Yamamoto, A., Oshitani-Okamoto, S., Ohsumi, Y., and Yoshimori, T. (2004). LC3, GABARAP and GATE16 localize to autophagosomal membrane depending on form-II formation. *J Cell Sci* 117(Pt 13), 2805-2812. doi: 10.1242/jcs.01131.
- Kaesler-Pebernard, S., Vionnet, C., Mari, M., Sankar, D.S., Hu, Z., Roubaty, C., et al. (2022). mTORC1 controls Golgi architecture and vesicle secretion by phosphorylation of SCYL1. *Nat Commun* 13(1), 4685. doi: 10.1038/s41467-022-32487-7.
- Kanayama, A., Seth, R.B., Sun, L., Ea, C.K., Hong, M., Shaito, A., et al. (2004). TAB2 and TAB3 activate the NF-kappaB pathway through binding to polyubiquitin chains. *Mol Cell* 15(4), 535-548. doi: 10.1016/j.molcel.2004.08.008.
- Kim, D.H., Sarbassov, D.D., Ali, S.M., King, J.E., Latek, R.R., Erdjument-Bromage, H., et al. (2002). MTOR interacts with Raptor to form a nutrient-sensitive complex that signals to the cell growth machinery. *Cell* 110(2), 163-175. doi: 10.1016/S0092-8674(02)00808-5.
- Kim, D.H., Sarbassov, D.D., Ali, S.M., Latek, R.R., Guntur, K.V.P., Erdjument-Bromage, H., et al. (2003). G beta L, a positive regulator of the rapamycin-sensitive pathway required for the nutrient-sensitive interaction between raptor and mTOR. *Molecular Cell* 11(4), 895-904. doi: 10.1016/S1097-2765(03)00114-X.

- Kim, E., Goraksha-Hicks, P., Li, L., Neufeld, T.P., and Guan, K.L. (2008). Regulation of TORC1 by Rag GTPases in nutrient response. *Nature Cell Biology* 10(8), 935-945. doi: 10.1038/ncb1753.
- Kim, J., Kundu, M., Viollet, B., and Guan, K.L. (2011). AMPK and mTOR regulate autophagy through direct phosphorylation of Ulk1. *Nat Cell Biol* 13(2), 132-141. doi: 10.1038/ncb2152.
- Kim, J.H., Seo, D., Kim, S.J., Choi, D.W., Park, J.S., Ha, J., et al. (2018). The deubiquitinating enzyme USP20 stabilizes ULK1 and promotes autophagy initiation. *EMBO Rep* 19(4). doi: 10.15252/embr.201744378.
- Kim, L.C., Cook, R.S., and Chen, J. (2017). mTORC1 and mTORC2 in cancer and the tumor microenvironment. *Oncogene* 36(16), 2191-2201. doi: 10.1038/onc.2016.363.
- Kim, S.H., Choi, J.H., Wang, P., Go, C.D., Hesketh, G.G., Gingras, A.C., et al. (2021). Mitochondrial Threonyl-tRNA Synthetase TARS2 Is Required for Threonine-Sensitive mTORC1 Activation. *Mol Cell* 81(2), 398-407 e394. doi: 10.1016/j.molcel.2020.11.036.
- Kim, Y.C., Park, H.W., Sciarretta, S., Mo, J.S., Jewell, J.L., Russell, R.C., et al. (2014). Rag GTPases are cardioprotective by regulating lysosomal function. *Nat Commun* 5, 4241. doi: 10.1038/ncomms5241.
- Kim, Y.M., Stone, M., Hwang, T.H., Kim, Y.G., Dunlevy, J.R., Griffin, T.J., et al. (2012). SH3BP4 Is a Negative Regulator of Amino Acid-Rag GTPase-mTORC1 Signaling. *Molecular Cell* 46(6), 833-846. doi: 10.1016/j.molcel.2012.04.007.
- Kirkin, V., and Rogov, V.V. (2019). A Diversity of Selective Autophagy Receptors Determines the Specificity of the Autophagy Pathway. *Mol Cell* 76(2), 268-285. doi: 10.1016/j.molcel.2019.09.005.
- Kliza, K., and Husnjak, K. (2020). Resolving the Complexity of Ubiquitin Networks. *Front Mol Biosci* 7, 21. doi: 10.3389/fmolb.2020.00021.
- Ko, C.J., Zhang, L., Jie, Z., Zhu, L., Zhou, X., Xie, X., et al. (2021). The E3 ubiquitin ligase Peli1 regulates the metabolic actions of mTORC1 to suppress antitumor T cell responses. *EMBO J* 40(2), e104532. doi: 10.15252/embj.2020104532.
- Ko, H.R., Kim, C.K., Lee, S.B., Song, J., Lee, K.H., Kim, K.K., et al. (2014). P42 Ebp1 regulates the proteasomal degradation of the p85 regulatory subunit of PI3K by recruiting a chaperone-E3 ligase complex HSP70/CHIP. *Cell Death Dis* 5(3), e1131. doi: 10.1038/cddis.2014.79.
- Kobayashi, T., Shimabukuro-Demoto, S., Yoshida-Sugitani, R., Furuyama-Tanaka, K., Karyu, H., Sugiura, Y., et al. (2014). The histidine transporter SLC15A4 coordinates mTOR-dependent inflammatory responses and pathogenic antibody production. *Immunity* 41(3), 375-388. doi: 10.1016/j.immuni.2014.08.011.
- Komander, D., Lord, C.J., Scheel, H., Swift, S., Hofmann, K., Ashworth, A., et al. (2008). The structure of the CYLD USP domain explains its specificity for Lys63-linked polyubiquitin and reveals a B box module. *Mol Cell* 29(4), 451-464. doi: 10.1016/j.molcel.2007.12.018.
- Komander, D., and Rape, M. (2012). The ubiquitin code. *Annu Rev Biochem* 81, 203-229. doi: 10.1146/annurev-biochem-060310-170328.
- Komander, D., Reyes-Turcu, F., Licchesi, J.D., Odenwaelder, P., Wilkinson, K.D., and Barford, D. (2009). Molecular discrimination of structurally equivalent Lys 63-linked and linear polyubiquitin chains. *EMBO Rep* 10(5), 466-473. doi: 10.1038/embor.2009.55.

- Koo, J., Wu, X., Mao, Z., Khuri, F.R., and Sun, S.Y. (2015). Rictor Undergoes Glycogen Synthase Kinase 3 (GSK3)-dependent, FBXW7-mediated Ubiquitination and Proteasomal Degradation. *J Biol Chem* 290(22), 14120-14129. doi: 10.1074/jbc.M114.633057.
- Kovalenko, A., Chable-Bessia, C., Cantarella, G., Israel, A., Wallach, D., and Courtois, G. (2003). The tumour suppressor CYLD negatively regulates NF-kappaB signalling by deubiquitination. *Nature* 424(6950), 801-805. doi: 10.1038/nature01802.
- Kowarz, E., Loscher, D., and Marschalek, R. (2015). Optimized Sleeping Beauty transposons rapidly generate stable transgenic cell lines. *Biotechnol J* 10(4), 647-653. doi: 10.1002/biot.201400821.
- Kuchay, S., Duan, S., Schenkein, E., Peschiaroli, A., Saraf, A., Florens, L., et al. (2013). FBXL2- and PTPL1-mediated degradation of p110-free p85beta regulatory subunit controls the PI(3)K signalling cascade. *Nat Cell Biol* 15(5), 472-480. doi: 10.1038/ncb2731.
- Kudo, M., Bao, M., D'Souza, A., Ying, F., Pan, H., Roe, B.A., et al. (2005). The alpha- and beta-subunits of the human UDP-N-acetylglucosamine:lysosomal enzyme N-acetylglucosamine-1-phosphotransferase [corrected] are encoded by a single cDNA. *J Biol Chem* 280(43), 36141-36149. doi: 10.1074/jbc.M509008200.
- Kuma, A., Hatano, M., Matsui, M., Yamamoto, A., Nakaya, H., Yoshimori, T., et al. (2004). The role of autophagy during the early neonatal starvation period. *Nature* 432(7020), 1032-1036. doi: 10.1038/nature03029.
- Lapierre, L.R., De Magalhaes, C.D., McQuary, P.R., Chu, C.C., Visvikis, O., Chang, J.T., et al. (2013). The TFEB orthologue HLH-30 regulates autophagy and modulates longevity in *Caenorhabditis elegans*. *Nature Communications* 4. doi: ARTN 2267 10.1038/ncomms3267.
- Laurent-Matha, V., Derocq, D., Prebois, C., Katunuma, N., and Liaudet-Coopman, E. (2006). Processing of human cathepsin D is independent of its catalytic function and auto-activation: involvement of cathepsins L and B. *J Biochem* 139(3), 363-371. doi: 10.1093/jb/mvj037.
- Lawrence, R.E., Cho, K.F., Rappold, R., Thrun, A., Tofaute, M., Kim, D.J., et al. (2018). A nutrient-induced affinity switch controls mTORC1 activation by its Rag GTPase-Ragulator lysosomal scaffold. *Nat Cell Biol* 20(9), 1052-1063. doi: 10.1038/s41556-018-0148-6.
- Lawrence, R.E., Fromm, S.A., Fu, Y.X., Yokom, A.L., Kim, D., Thelen, A.M., et al. (2019). Structural mechanism of a Rag GTPase activation checkpoint by the lysosomal folliculin complex. *Science* 366(6468), 971-+. doi: 10.1126/science.aax0364.
- Lear, T.B., Lockwood, K.C., Ouyang, Y., Evankovich, J.W., Larsen, M.B., Lin, B., et al. (2019). The RING-type E3 ligase RNF186 ubiquitinates Sestrin-2 and thereby controls nutrient sensing. *J Biol Chem* 294(45), 16527-16534. doi: 10.1074/jbc.AC119.010671.
- Lee, D.F., Kuo, H.P., Chen, C.T., Hsu, J.M., Chou, C.K., Wei, Y., et al. (2007). IKK beta suppression of TSC1 links inflammation and tumor angiogenesis via the mTOR pathway. *Cell* 130(3), 440-455. doi: 10.1016/j.cell.2007.05.058.
- Lee, D.F., Kuo, H.P., Chen, C.T., Wei, Y., Chou, C.K., Hung, J.Y., et al. (2008). IKKbeta suppression of TSC1 function links the mTOR pathway with insulin resistance. *Int J Mol Med* 22(5), 633-638. doi: 10.3892/ijmm_00000065.
- Leidal, A.M., Levine, B., and Debnath, J. (2018). Autophagy and the cell biology of age-related disease. *Nature Cell Biology* 20(12), 1338-1348. doi: 10.1038/s41556-018-0235-8.

- Leprivier, G., Remke, M., Rotblat, B., Dubuc, A., Mateo, A.R., Kool, M., et al. (2013). The eEF2 kinase confers resistance to nutrient deprivation by blocking translation elongation. *Cell* 153(5), 1064-1079. doi: 10.1016/j.cell.2013.04.055.
- Levy, S., Avni, D., Hariharan, N., Perry, R.P., and Meyuhas, O. (1991). Oligopyrimidine Tract at the 5' End of Mammalian Ribosomal-Protein Messenger-Rnas Is Required for Their Translational Control. *Proceedings of the National Academy of Sciences of the United States of America* 88(8), 3319-3323. doi: DOI 10.1073/pnas.88.8.3319.
- Li, H., Lee, W.S., Feng, X., Bai, L., Jennings, B.C., Liu, L., et al. (2022). Structure of the human GlcNAc-1-phosphotransferase alphabeta subunits reveals regulatory mechanism for lysosomal enzyme glycan phosphorylation. *Nat Struct Mol Biol* 29(4), 348-356. doi: 10.1038/s41594-022-00748-0.
- Li, J., Kim, S.G., and Blenis, J. (2014). Rapamycin: one drug, many effects. *Cell Metab* 19(3), 373-379. doi: 10.1016/j.cmet.2014.01.001.
- Li, T., Wang, X., Ju, E., da Silva, S.R., Chen, L., Zhang, X., et al. (2021). RNF167 activates mTORC1 and promotes tumorigenesis by targeting CASTOR1 for ubiquitination and degradation. *Nat Commun* 12(1), 1055. doi: 10.1038/s41467-021-21206-3.
- Li, W., Peng, C., Lee, M.H., Lim, D., Zhu, F., Fu, Y., et al. (2013). TRAF4 is a critical molecule for Akt activation in lung cancer. *Cancer Res* 73(23), 6938-6950. doi: 10.1158/0008-5472.CAN-13-0913.
- Lim, J.H., Jono, H., Komatsu, K., Woo, C.H., Lee, J., Miyata, M., et al. (2012). CYLD negatively regulates transforming growth factor-beta-signalling via deubiquitinating Akt. *Nat Commun* 3, 771. doi: 10.1038/ncomms1776.
- Lim, K.L., Chew, K.C., Tan, J.M., Wang, C., Chung, K.K., Zhang, Y., et al. (2005). Parkin mediates nonclassical, proteasomal-independent ubiquitination of synphilin-1: implications for Lewy body formation. *J Neurosci* 25(8), 2002-2009. doi: 10.1523/JNEUROSCI.4474-04.2005.
- Lin, Y.T., Yu, C.L., Tu, Y.K., and Chi, C.C. (2022). Efficacy and Safety of Topical Mechanistic Target of Rapamycin Inhibitors for Facial Angiofibromas in Patients with Tuberous Sclerosis Complex: A Systematic Review and Network Meta-Analysis. *Biomedicines* 10(4). doi: 10.3390/biomedicines10040826.
- Linares, J.F., Duran, A., Yajima, T., Pasparakis, M., Moscat, J., and Diaz-Meco, M.T. (2013a). K63 Polyubiquitination and Activation of mTOR by the p62-TRAF6 Complex in Nutrient-Activated Cells. *Molecular Cell* 51(3), 283-296. doi: 10.1016/j.molcel.2013.06.020.
- Linares, J.F., Duran, A., Yajima, T., Pasparakis, M., Moscat, J., and Diaz-Meco, M.T. (2013b). K63 polyubiquitination and activation of mTOR by the p62-TRAF6 complex in nutrient-activated cells. *Mol Cell* 51(3), 283-296. doi: 10.1016/j.molcel.2013.06.020.
- Liu, C.C., Lin, Y.C., Chen, Y.H., Chen, C.M., Pang, L.Y., Chen, H.A., et al. (2016). Cul3-KLHL20 Ubiquitin Ligase Governs the Turnover of ULK1 and VPS34 Complexes to Control Autophagy Termination. *Mol Cell* 61(1), 84-97. doi: 10.1016/j.molcel.2015.11.001.
- Liu, G.Y., and Sabatini, D.M. (2020). mTOR at the nexus of nutrition, growth, ageing and disease. *Nat Rev Mol Cell Biol* 21(4), 183-203. doi: 10.1038/s41580-019-0199-y.
- Liu, P., Gan, W., Chin, Y.R., Ogura, K., Guo, J., Zhang, J., et al. (2015). PtdIns(3,4,5)P3-Dependent Activation of the mTORC2 Kinase Complex. *Cancer Discov* 5(11), 1194-1209. doi: 10.1158/2159-8290.CD-15-0460.

- Liu, W., Yi, Y., Zhang, C., Zhou, B., Liao, L., Liu, W., et al. (2020). The Expression of TRIM6 Activates the mTORC1 Pathway by Regulating the Ubiquitination of TSC1-TSC2 to Promote Renal Fibrosis. *Front Cell Dev Biol* 8, 616747. doi: 10.3389/fcell.2020.616747.
- Liu, X., and Zheng, X.F. (2007). Endoplasmic reticulum and Golgi localization sequences for mammalian target of rapamycin. *Mol Biol Cell* 18(3), 1073-1082. doi: 10.1091/mbc.e06-05-0406.
- Ma, L., Chen, Z., Erdjument-Bromage, H., Tempst, P., and Pandolfi, P.P. (2005). Phosphorylation and functional inactivation of TSC2 by Erk implications for tuberous sclerosis and cancer pathogenesis. *Cell* 121(2), 179-193. doi: 10.1016/j.cell.2005.02.031.
- Ma, X.M., Yoon, S.O., Richardson, C.J., Julich, K., and Blenis, J. (2008). SKAR links pre-mRNA splicing to mTOR/S6K1-mediated enhanced translation efficiency of spliced mRNAs. *Cell* 133(2), 303-313. doi: 10.1016/j.cell.2008.02.031.
- Mace, P.D., Smits, C., Vaux, D.L., Silke, J., and Day, C.L. (2010). Asymmetric recruitment of cIAPs by TRAF2. *J Mol Biol* 400(1), 8-15. doi: 10.1016/j.jmb.2010.04.055.
- Madigan, J.P., Hou, F., Ye, L., Hu, J., Dong, A., Tempel, W., et al. (2018). The tuberous sclerosis complex subunit TBC1D7 is stabilized by Akt phosphorylation-mediated 14-3-3 binding. *J Biol Chem* 293(42), 16142-16159. doi: 10.1074/jbc.RA118.003525.
- Mahoney, S.J., Narayan, S., Molz, L., Berstler, L.A., Kang, S.A., Vlasuk, G.P., et al. (2018). A small molecule inhibitor of Rheb selectively targets mTORC1 signaling. *Nat Commun* 9(1), 548. doi: 10.1038/s41467-018-03035-z.
- Manders, E.M.M., Verbeek, F.J., and Aten, J.A. (1993). Measurement of co-localization of objects in dual-colour confocal images. *J Microsc* 169(3), 375-382. doi: 10.1111/j.1365-2818.1993.tb03313.x.
- Manifava, M., Smith, M., Rotondo, S., Walker, S., Niewczasz, I., Zoncu, R., et al. (2016). Dynamics of mTORC1 activation in response to amino acids. *Elife* 5. doi: 10.7554/eLife.19960.
- Manning, B.D., Tee, A.R., Logsdon, M.N., Blenis, J., and Cantley, L.C. (2002). Identification of the tuberous sclerosis complex-2 tumor suppressor gene product tuberlin as a target of the phosphoinositide 3-kinase/akt pathway. *Mol Cell* 10(1), 151-162. doi: 10.1016/s1097-2765(02)00568-3.
- Manning, B.D., and Toker, A. (2017). AKT/PKB Signaling: Navigating the Network. *Cell* 169(3), 381-405. doi: 10.1016/j.cell.2017.04.001.
- Mao, J.H., Kim, I.J., Wu, D., Climent, J., Kang, H.C., DelRosario, R., et al. (2008). FBXW7 targets mTOR for degradation and cooperates with PTEN in tumor suppression. *Science* 321(5895), 1499-1502. doi: 10.1126/science.1162981.
- Martina, J.A., Chen, Y., Gucek, M., and Puertollano, R. (2012). MTORC1 functions as a transcriptional regulator of autophagy by preventing nuclear transport of TFEB. *Autophagy* 8(6), 903-914. doi: 10.4161/auto.19653.
- Martina, J.A., and Puertollano, R. (2013). Rag GTPases mediate amino acid-dependent recruitment of TFEB and MITF to lysosomes. *Journal of Cell Biology* 200(4), 475-491. doi: 10.1083/jcb.201209135.
- Mayer, C., Zhao, J., Yuan, X., and Grummt, I. (2004). mTOR-dependent activation of the transcription factor TIF-IA links rRNA synthesis to nutrient availability. *Genes Dev* 18(4), 423-434. doi: 10.1101/gad.285504.

- Medina, D.L., Di Paola, S., Peluso, I., Armani, A., De Stefani, D., Venditti, R., et al. (2015). Lysosomal calcium signalling regulates autophagy through calcineurin and TFEB. *Nature Cell Biology* 17(3), 288-+. doi: 10.1038/ncb3114.
- Medina, D.L., Fraldi, A., Bouche, V., Annunziata, F., Mansueto, G., Spampinato, C., et al. (2011). Transcriptional activation of lysosomal exocytosis promotes cellular clearance. *Dev Cell* 21(3), 421-430. doi: 10.1016/j.devcel.2011.07.016.
- Meng, D., Yang, Q., Wang, H., Melick, C.H., Navlani, R., Frank, A.R., et al. (2020). Glutamine and asparagine activate mTORC1 independently of Rag GTPases. *J Biol Chem* 295(10), 2890-2899. doi: 10.1074/jbc.AC119.011578.
- Menon, S., Dibble, C.C., Talbott, G., Hoxhaj, G., Valvezan, A.J., Takahashi, H., et al. (2014). Spatial control of the TSC complex integrates insulin and nutrient regulation of mTORC1 at the lysosome. *Cell* 156(4), 771-785. doi: 10.1016/j.cell.2013.11.049.
- Merrick, W.C., and Pavitt, G.D. (2018). Protein Synthesis Initiation in Eukaryotic Cells. *Cold Spring Harb Perspect Biol* 10(12). doi: 10.1101/cshperspect.a033092.
- Mevissen, T.E.T., and Komander, D. (2017). Mechanisms of Deubiquitinase Specificity and Regulation. *Annu Rev Biochem* 86, 159-192. doi: 10.1146/annurev-biochem-061516-044916.
- Michels, A.A., Robitaille, A.M., Buczynski-Ruchonnet, D., Hodroj, W., Reina, J.H., Hall, M.N., et al. (2010). mTORC1 directly phosphorylates and regulates human MAF1. *Mol Cell Biol* 30(15), 3749-3757. doi: 10.1128/MCB.00319-10.
- Mindell, J.A. (2012). Lysosomal acidification mechanisms. *Annu Rev Physiol* 74, 69-86. doi: 10.1146/annurev-physiol-012110-142317.
- Mitchell, T., and Sugden, B. (1995). Stimulation of NF-kappa B-mediated transcription by mutant derivatives of the latent membrane protein of Epstein-Barr virus. *J Virol* 69(5), 2968-2976. doi: 10.1128/JVI.69.5.2968-2976.1995.
- Mohan, N., Shen, Y., Dokmanovic, M., Endo, Y., Hirsch, D.S., and Wu, W.J. (2016). VPS34 regulates TSC1/TSC2 heterodimer to mediate RheB and mTORC1/S6K1 activation and cellular transformation. *Oncotarget* 7(32), 52239-52254. doi: 10.18632/oncotarget.10469.
- Moore, S.F., Hunter, R.W., and Hers, I. (2011). mTORC2 protein complex-mediated Akt (Protein Kinase B) Serine 473 Phosphorylation is not required for Akt1 activity in human platelets [corrected]. *J Biol Chem* 286(28), 24553-24560. doi: 10.1074/jbc.M110.202341.
- Murakami, M., Ichisaka, T., Maeda, M., Oshiro, N., Hara, K., Edenhofer, F., et al. (2004). mTOR is essential for growth and proliferation in early mouse embryos and embryonic stem cells. *Mol Cell Biol* 24(15), 6710-6718. doi: 10.1128/MCB.24.15.6710-6718.2004.
- Musiwaro, P., Smith, M., Manifava, M., Walker, S.A., and Ktistakis, N.T. (2013). Characteristics and requirements of basal autophagy in HEK 293 cells. *Autophagy* 9(9), 1407-1417. doi: 10.4161/auto.25455.
- Nakatogawa, H. (2020). Mechanisms governing autophagosome biogenesis. *Nat Rev Mol Cell Biol* 21(8), 439-458. doi: 10.1038/s41580-020-0241-0.
- Nakatogawa, H., Ichimura, Y., and Ohsumi, Y. (2007). Atg8, a ubiquitin-like protein required for autophagosome formation, mediates membrane tethering and hemifusion. *Cell* 130(1), 165-178. doi: 10.1016/j.cell.2007.05.021.

- Napolitano, G., Di Malta, C., Esposito, A., de Araujo, M.E.G., Pece, S., Bertalot, G., et al. (2020). A substrate-specific mTORC1 pathway underlies Birt-Hogg-Dube syndrome. *Nature* 585(7826), 597-+. doi: 10.1038/s41586-020-2444-0.
- Nascimbeni, A.C., Codogno, P., and Morel, E. (2017). Phosphatidylinositol-3-phosphate in the regulation of autophagy membrane dynamics. *FEBS J* 284(9), 1267-1278. doi: 10.1111/febs.13987.
- Nazio, F., Strappazzon, F., Antonioli, M., Bielli, P., Cianfanelli, V., Bordi, M., et al. (2013). mTOR inhibits autophagy by controlling ULK1 ubiquitylation, self-association and function through AMBRA1 and TRAF6. *Nat Cell Biol* 15(4), 406-416. doi: 10.1038/ncb2708.
- Nellist, M., van Slegtenhorst, M.A., Goedbloed, M., van den Ouweland, A.M., Halley, D.J., and van der Sluijs, P. (1999). Characterization of the cytosolic tuberlin-hamartin complex. Tuberlin is a cytosolic chaperone for hamartin. *J Biol Chem* 274(50), 35647-35652. doi: 10.1074/jbc.274.50.35647.
- Nishimura, T., Tamura, N., Kono, N., Shimanaka, Y., Arai, H., Yamamoto, H., et al. (2017). Autophagosome formation is initiated at phosphatidylinositol synthase-enriched ER subdomains. *EMBO J* 36(12), 1719-1735. doi: 10.15252/embj.201695189.
- Nixon, R.A. (2013). The role of autophagy in neurodegenerative disease. *Nat Med* 19(8), 983-997. doi: 10.1038/nm.3232.
- Nojima, H., Tokunaga, C., Eguchi, S., Oshiro, N., Hidayat, S., Yoshino, K., et al. (2003). The mammalian target of rapamycin (mTOR) partner, raptor, binds the mTOR substrates p70 S6 kinase and 4E-BP1 through their TOR signaling (TOS) motif. *Journal of Biological Chemistry* 278(18), 15461-15464. doi: 10.1074/jbc.C200665200.
- Nuchel, J., Tauber, M., Nolte, J.L., Morgelin, M., Turk, C., Eckes, B., et al. (2021). An mTORC1-GRASP55 signaling axis controls unconventional secretion to reshape the extracellular proteome upon stress. *Mol Cell*. doi: 10.1016/j.molcel.2021.06.017.
- Ohanna, M., Sobering, A.K., Lapointe, T., Lorenzo, L., Praud, C., Petroulakis, E., et al. (2005). Atrophy of S6K1(-/-) skeletal muscle cells reveals distinct mTOR effectors for cell cycle and size control. *Nat Cell Biol* 7(3), 286-294. doi: 10.1038/ncb1231.
- Ohtake, F., Saeki, Y., Ishido, S., Kanno, J., and Tanaka, K. (2016). The K48-K63 Branched Ubiquitin Chain Regulates NF-kappaB Signaling. *Mol Cell* 64(2), 251-266. doi: 10.1016/j.molcel.2016.09.014.
- Orozco, J.M., Krawczyk, P.A., Scaria, S.M., Cangelosi, A.L., Chan, S.H., Kunchok, T., et al. (2020). Dihydroxyacetone phosphate signals glucose availability to mTORC1. *Nat Metab* 2(9), 893-901. doi: 10.1038/s42255-020-0250-5.
- Palmieri, M., Impey, S., Kang, H.J., di Ronza, A., Pelz, C., Sardiello, M., et al. (2011). Characterization of the CLEAR network reveals an integrated control of cellular clearance pathways. *Human Molecular Genetics* 20(19), 3852-3866. doi: 10.1093/hmg/ddr306.
- Pan, M., Zorbas, C., Sugaya, M., Ishiguro, K., Kato, M., Nishida, M., et al. (2022). Glutamine deficiency in solid tumor cells confers resistance to ribosomal RNA synthesis inhibitors. *Nat Commun* 13(1), 3706. doi: 10.1038/s41467-022-31418-w.
- Park, D., Lee, M.N., Jeong, H., Koh, A., Yang, Y.R., Suh, P.G., et al. (2014). Parkin ubiquitinates mTOR to regulate mTORC1 activity under mitochondrial stress. *Cell Signal* 26(10), 2122-2130. doi: 10.1016/j.cellsig.2014.06.010.

- Park, J.M., Jung, C.H., Seo, M., Otto, N.M., Grunwald, D., Kim, K.H., et al. (2016). The ULK1 complex mediates MTORC1 signaling to the autophagy initiation machinery via binding and phosphorylating ATG14. *Autophagy* 12(3), 547-564. doi: 10.1080/15548627.2016.1140293.
- Parmigiani, A., Nourbakhsh, A., Ding, B.X., Wang, W., Kim, Y.C., Akopiants, K., et al. (2014). Sestrins Inhibit mTORC1 Kinase Activation through the GATOR Complex. *Cell Reports* 9(4), 1281-1291. doi: 10.1016/j.celrep.2014.10.019.
- Pearce, L.R., Huang, X., Boudeau, J., Pawlowski, R., Wullschleger, S., Deak, M., et al. (2007). Identification of Protor as a novel Rictor-binding component of mTOR complex-2. *Biochem J* 405(3), 513-522. doi: 10.1042/BJ20070540.
- Pende, M., Kozma, S.C., Jaquet, M., Oorschot, V., Burcelin, R., Le Marchand-Brustel, Y., et al. (2000). Hypoinsulinaemia, glucose intolerance and diminished beta-cell size in S6K1-deficient mice. *Nature* 408(6815), 994-997. doi: 10.1038/35050135.
- Pende, M., Um, S.H., Mieulet, V., Sticker, M., Goss, V.L., Mestan, J., et al. (2004). S6K1(-/-)/S6K2(-/-) mice exhibit perinatal lethality and rapamycin-sensitive 5'-terminal oligopyrimidine mRNA translation and reveal a mitogen-activated protein kinase-dependent S6 kinase pathway. *Mol Cell Biol* 24(8), 3112-3124. doi: 10.1128/MCB.24.8.3112-3124.2004.
- Peng, M., Yin, N., and Li, M.O. (2017). SZT2 dictates GATOR control of mTORC1 signalling. *Nature* 543(7645), 433-+. doi: 10.1038/nature21378.
- Peterson, T.R., Laplante, M., Thoreen, C.C., Sancak, Y., Kang, S.A., Kuehl, W.M., et al. (2009). DEPTOR Is an mTOR Inhibitor Frequently Overexpressed in Multiple Myeloma Cells and Required for Their Survival. *Cell* 137(5), 873-886. doi: 10.1016/j.cell.2009.03.046.
- Petit, C.S., Rocznik-Ferguson, A., and Ferguson, S.M. (2013). Recruitment of folliculin to lysosomes supports the amino acid-dependent activation of Rag GTPases. *Journal of Cell Biology* 202(7), 1107-1122. doi: 10.1083/jcb.201307084.
- Platt, F.M., d'Azzo, A., Davidson, B.L., Neufeld, E.F., and Tifft, C.J. (2018). Lysosomal storage diseases. *Nat Rev Dis Primers* 4(1), 27. doi: 10.1038/s41572-018-0025-4.
- Prentzell, M.T., Rehbein, U., Sandoval, M.C., De Meulemeester, A.S., Baumeister, R., Brohee, L., et al. (2021). G3BPs tether the TSC complex to lysosomes and suppress mTORC1 signaling. *Cell* 184(3), 655-+. doi: 10.1016/j.cell.2020.12.024.
- Pullen, N., Dennis, P.B., Andjelkovic, M., Dufner, A., Kozma, S.C., Hemmings, B.A., et al. (1998). Phosphorylation and activation of p70s6k by PDK1. *Science* 279(5351), 707-710. doi: 10.1126/science.279.5351.707.
- Qi, L., Zang, H., Wu, W., Nagarkatti, P., Nagarkatti, M., Liu, Q., et al. (2020). CYLD exaggerates pressure overload-induced cardiomyopathy via suppressing autolysosome efflux in cardiomyocytes. *J Mol Cell Cardiol* 145, 59-73. doi: 10.1016/j.yjmcc.2020.06.004.
- Querfurth, H., and Lee, H.K. (2021). Mammalian/mechanistic target of rapamycin (mTOR) complexes in neurodegeneration. *Mol Neurodegener* 16(1), 44. doi: 10.1186/s13024-021-00428-5.
- Raas-Rothschild, A., Cormier-Daire, V., Bao, M., Genin, E., Salomon, R., Brewer, K., et al. (2000). Molecular basis of variant pseudo-hurler polydystrophy (mucopolidosis IIIC). *J Clin Invest* 105(5), 673-681. doi: 10.1172/JCI5826.

- Rabanal-Ruiz, Y., Byron, A., Wirth, A., Madsen, R., Sedlackova, L., Hewitt, G., et al. (2021). mTORC1 activity is supported by spatial association with focal adhesions. *J Cell Biol* 220(5). doi: 10.1083/jcb.202004010.
- Rabanal-Ruiz, Y., Otten, E.G., and Korolchuk, V.I. (2017). mTORC1 as the main gateway to autophagy. *Essays Biochem* 61(6), 565-584. doi: 10.1042/EBC20170027.
- Ramanathan, A., and Schreiber, S.L. (2009). Direct control of mitochondrial function by mTOR. *Proc Natl Acad Sci U S A* 106(52), 22229-22232. doi: 10.1073/pnas.0912074106.
- Ran, F.A., Hsu, P.D., Wright, J., Agarwala, V., Scott, D.A., and Zhang, F. (2013). Genome engineering using the CRISPR-Cas9 system. *Nat Protoc* 8(11), 2281-2308. doi: 10.1038/nprot.2013.143.
- Ratto, E., Chowdhury, S.R., Siefert, N.S., Schneider, M., Wittmann, M., Helm, D., et al. (2022). Direct control of lysosomal catabolic activity by mTORC1 through regulation of V-ATPase assembly. *Nat Commun* 13(1), 4848. doi: 10.1038/s41467-022-32515-6.
- Rebsamen, M., Pochini, L., Stasyk, T., de Araujo, M.E.G., Galluccio, M., Kandasamy, R.K., et al. (2015). SLC38A9 is a component of the lysosomal amino acid sensing machinery that controls mTORC1. *Nature* 519(7544), 477-+. doi: 10.1038/nature14107.
- Rega, L.R., Polishchuk, E., Montefusco, S., Napolitano, G., Tozzi, G., Zhang, J., et al. (2016). Activation of the transcription factor EB rescues lysosomal abnormalities in cystinotic kidney cells. *Kidney Int* 89(4), 862-873. doi: 10.1016/j.kint.2015.12.045.
- Remesar, X., Arola, L., Palou, A., and Alemany, M. (1980). Plasma amino-acid concentrations during development in the rat. *Arch Int Physiol Biochim* 88(5), 443-452. doi: 10.3109/13813458009092918.
- Richardson, C.J., Broenstrup, M., Fingar, D.C., Julich, K., Ballif, B.A., Gygi, S., et al. (2004a). SKAR is a specific target of S6 kinase 1 in cell growth control. *Current Biology* 14(17), 1540-1549. doi: 10.1016/j.cub.2004.08.061.
- Richardson, C.J., Schalm, S.S., and Blenis, J. (2004b). PI3-kinase and TOR: PIKTORing cell growth. *Seminars in Cell & Developmental Biology* 15(2), 147-159. doi: 10.1016/j.semcd.2003.12.023.
- Richo, G., and Conner, G.E. (1991). Proteolytic activation of human procathepsin D. *Adv Exp Med Biol* 306, 289-296. doi: 10.1007/978-1-4684-6012-4_35.
- Roberts, D.J., Tan-Sah, V.P., Ding, E.Y., Smith, J.M., and Miyamoto, S. (2014). Hexokinase-II positively regulates glucose starvation-induced autophagy through TORC1 inhibition. *Mol Cell* 53(4), 521-533. doi: 10.1016/j.molcel.2013.12.019.
- Roczniak-Ferguson, A., Petit, C.S., Froehlich, F., Qian, S., Ky, J., Angarola, B., et al. (2012). The Transcription Factor TFEB Links mTORC1 Signaling to Transcriptional Control of Lysosome Homeostasis. *Science Signaling* 5(228). doi: ARTN ra42 10.1126/scisignal.2002790.
- Rogala, K.B., Gu, X., Kadir, J.F., Abu-Remaileh, M., Bianchi, L.F., Bottino, A.M.S., et al. (2019). Structural basis for the docking of mTORC1 on the lysosomal surface. *Science* 366(6464), 468-+. doi: 10.1126/science.aay0166.
- Roux, P.P., Ballif, B.A., Anjum, R., Gygi, S.P., and Blenis, J. (2004). Tumor-promoting phorbol esters and activated Ras inactivate the tuberous sclerosis tumor suppressor complex via p90 ribosomal S6 kinase. *Proc Natl Acad Sci U S A* 101(37), 13489-13494. doi: 10.1073/pnas.0405659101.

- Roux, P.P., Shahbazian, D., Vu, H., Holz, M.K., Cohen, M.S., Taunton, J., et al. (2007). RAS/ERK signaling promotes site-specific ribosomal protein S6 phosphorylation via RSK and stimulates cap-dependent translation. *J Biol Chem* 282(19), 14056-14064. doi: 10.1074/jbc.M700906200.
- Rudnik, S., and Damme, M. (2021). The lysosomal membrane-export of metabolites and beyond. *FEBS J* 288(14), 4168-4182. doi: 10.1111/febs.15602.
- Ruiz-Blazquez, P., Pistorio, V., Fernandez-Fernandez, M., and Moles, A. (2021). The multifaceted role of cathepsins in liver disease. *J Hepatol* 75(5), 1192-1202. doi: 10.1016/j.jhep.2021.06.031.
- Russell, R.C., Tian, Y., Yuan, H., Park, H.W., Chang, Y.Y., Kim, J., et al. (2013). ULK1 induces autophagy by phosphorylating Beclin-1 and activating VPS34 lipid kinase. *Nat Cell Biol* 15(7), 741-750. doi: 10.1038/ncb2757.
- Ruvinsky, I., Sharon, N., Lerer, T., Cohen, H., Stolovich-Rain, M., Nir, T., et al. (2005). Ribosomal protein S6 phosphorylation is a determinant of cell size and glucose homeostasis. *Genes Dev* 19(18), 2199-2211. doi: 10.1101/gad.351605.
- Sagar, G.D., Gereben, B., Callebaut, I., Mornon, J.P., Zeold, A., da Silva, W.S., et al. (2007). Ubiquitination-induced conformational change within the deiodinase dimer is a switch regulating enzyme activity. *Mol Cell Biol* 27(13), 4774-4783. doi: 10.1128/MCB.00283-07.
- Saito, K., Kigawa, T., Koshiba, S., Sato, K., Matsuo, Y., Sakamoto, A., et al. (2004). The CAP-Gly Domain of CYLD Associates with the Proline-Rich Sequence in NEMO/IKK γ . *Structure* 12(9), 1719-1728. doi: 10.1016/j.str.2004.07.012.
- Sancak, Y., Bar-Peled, L., Zoncu, R., Markhard, A.L., Nada, S., and Sabatini, D.M. (2010). Regulator-Rag Complex Targets mTORC1 to the Lysosomal Surface and Is Necessary for Its Activation by Amino Acids. *Cell* 141(2), 290-303. doi: 10.1016/j.cell.2010.02.024.
- Sancak, Y., Peterson, T.R., Shaul, Y.D., Lindquist, R.A., Thoreen, C.C., Bar-Peled, L., et al. (2008). The Rag GTPases bind raptor and mediate amino acid signaling to mTORC1. *Science* 320(5882), 1496-1501. doi: 10.1126/science.1157535.
- Sancak, Y., Thoreen, C.C., Peterson, T.R., Lindquist, R.A., Kang, S.A., Spooner, E., et al. (2007). PRAS40 is an insulin-regulated inhibitor of the mTORC1 protein kinase. *Molecular Cell* 25(6), 903-915. doi: 10.1016/j.molcel.2007.03.003.
- Sarbassov, D.D., Ali, S.M., Kim, D.H., Guertin, D.A., Latek, R.R., Erdjument-Bromage, H., et al. (2004). Rictor, a novel binding partner of mTOR, defines a rapamycin-insensitive and raptor-independent pathway that regulates the cytoskeleton. *Curr Biol* 14(14), 1296-1302. doi: 10.1016/j.cub.2004.06.054.
- Sarbassov, D.D., Guertin, D.A., Ali, S.M., and Sabatini, D.M. (2005). Phosphorylation and regulation of Akt/PKB by the rictor-mTOR complex. *Science* 307(5712), 1098-1101. doi: 10.1126/science.1106148.
- Sardiello, M., Palmieri, M., di Ronza, A., Medina, D.L., Valenza, M., Gennarino, V.A., et al. (2009). A Gene Network Regulating Lysosomal Biogenesis and Function. *Science* 325(5939), 473-477. doi: 10.1126/science.1174447.
- Saxton, R.A., Chantranupong, L., Knockenhauer, K.E., Schwartz, T.U., and Sabatini, D.M. (2016a). Mechanism of arginine sensing by CASTOR1 upstream of mTORC1. *Nature* 536(7615), 229-+. doi: 10.1038/nature19079.

- Saxton, R.A., Knockenhauer, K.E., Wolfson, R.L., Chantranupong, L., Pacold, M.E., Wang, T., et al. (2016b). METABOLISM Structural basis for leucine sensing by the Sestrin2-mTORC1 pathway. *Science* 351(6268), 53-58. doi: 10.1126/science.aad2087.
- Schaim, S.S., Fingar, D.C., Sabatini, D.M., and Blenis, J. (2003). TOS motif-mediated raptor binding regulates 4E-BP1 multisite phosphorylation and function. *Current Biology* 13(10), 797-806. doi: 10.1016/S0960-9822(03)00329-4.
- Schieke, S.M., Phillips, D., McCoy, J.P., Jr., Aponte, A.M., Shen, R.F., Balaban, R.S., et al. (2006). The mammalian target of rapamycin (mTOR) pathway regulates mitochondrial oxygen consumption and oxidative capacity. *J Biol Chem* 281(37), 27643-27652. doi: 10.1074/jbc.M603536200.
- Schindelin, J., Arganda-Carreras, I., Frise, E., Kaynig, V., Longair, M., Pietzsch, T., et al. (2012). Fiji: an open-source platform for biological-image analysis. *Nat Methods* 9(7), 676-682. doi: 10.1038/nmeth.2019.
- Sekiguchi, T., Hirose, E., Nakashima, N., Li, M., and Nishimoto, T. (2001). Novel G proteins, Rag C and Rag D, interact with GTP-binding proteins, Rag A and Rag B. *J Biol Chem* 276(10), 7246-7257. doi: 10.1074/jbc.M004389200.
- Settembre, C., Di Malta, C., Polito, V.A., Garcia Arencibia, M., Vetrini, F., Erdin, S., et al. (2011). TFEB links autophagy to lysosomal biogenesis. *Science* 332(6036), 1429-1433. doi: 10.1126/science.1204592.
- Settembre, C., Zoncu, R., Medina, D.L., Vetrini, F., Erdin, S., Erdin, S., et al. (2012). A lysosome-to-nucleus signalling mechanism senses and regulates the lysosome via mTOR and TFEB. *Embo Journal* 31(5), 1095-1108. doi: 10.1038/emboj.2012.32.
- Sha, Y., Rao, L., Settembre, C., Ballabio, A., and Eissa, N.T. (2017). STUB1 regulates TFEB-induced autophagy-lysosome pathway. *EMBO J* 36(17), 2544-2552. doi: 10.15252/emboj.201796699.
- Shah, O.J., Wang, Z., and Hunter, T. (2004). Inappropriate activation of the TSC/Rheb/mTOR/S6K cassette induces IRS1/2 depletion, insulin resistance, and cell survival deficiencies. *Curr Biol* 14(18), 1650-1656. doi: 10.1016/j.cub.2004.08.026.
- Shen, K., Choe, A., and Sabatini, D.M. (2017). Intersubunit Crosstalk in the Rag GTPase Heterodimer Enables mTORC1 to Respond Rapidly to Amino Acid Availability. *Molecular Cell* 68(3), 552-+. doi: 10.1016/j.molcel.2017.09.026.
- Shen, K., Huang, R.K., Brignole, E.J., Condon, K.J., Valenstein, M.L., Chantranupong, L., et al. (2018). Architecture of the human GATOR1 and GATOR1-Rag GTPases complexes. *Nature* 556(7699), 64-+. doi: 10.1038/nature26158.
- Shen, K., and Sabatini, D.M. (2018). Ragulator and SLC38A9 activate the Rag GTPases through noncanonical GEF mechanisms. *Proceedings of the National Academy of Sciences of the United States of America* 115(38), 9545-9550. doi: 10.1073/pnas.1811727115.
- Shen, K., Sidik, H., and Talbot, W.S. (2016). The Rag-Ragulator Complex Regulates Lysosome Function and Phagocytic Flux in Microglia. *Cell Reports* 14(3), 547-559. doi: 10.1016/j.celrep.2015.12.055.
- Shor, B., Wu, J., Shakey, Q., Toral-Barza, L., Shi, C., Follettie, M., et al. (2010). Requirement of the mTOR kinase for the regulation of Maf1 phosphorylation and control of RNA polymerase III-dependent transcription in cancer cells. *J Biol Chem* 285(20), 15380-15392. doi: 10.1074/jbc.M109.071639.

- Silvestrini, M.J., Johnson, J.R., Kumar, A.V., Thakurta, T.G., Blais, K., Neill, Z.A., et al. (2018). Nuclear Export Inhibition Enhances HLH-30/TFEB Activity, Autophagy, and Lifespan. *Cell Reports* 23(7), 1915-1921. doi: 10.1016/j.celrep.2018.04.063.
- Son, S.M., Park, S.J., Lee, H., Siddiqi, F., Lee, J.E., Menzies, F.M., et al. (2019). Leucine Signals to mTORC1 via Its Metabolite Acetyl-Coenzyme A. *Cell Metab* 29(1), 192-201 e197. doi: 10.1016/j.cmet.2018.08.013.
- Song, Q., Meng, B., Xu, H., and Mao, Z. (2020). The emerging roles of vacuolar-type ATPase-dependent Lysosomal acidification in neurodegenerative diseases. *Transl Neurodegener* 9(1), 17. doi: 10.1186/s40035-020-00196-0.
- Sou, Y.S., Waguri, S., Iwata, J., Ueno, T., Fujimura, T., Hara, T., et al. (2008). The Atg8 conjugation system is indispensable for proper development of autophagic isolation membranes in mice. *Mol Biol Cell* 19(11), 4762-4775. doi: 10.1091/mbc.e08-03-0309.
- Spampanato, C., Feeney, E., Li, L., Cardone, M., Lim, J.A., Annunziata, F., et al. (2013). Transcription factor EB (TFEB) is a new therapeutic target for Pompe disease. *EMBO Mol Med* 5(5), 691-706. doi: 10.1002/emmm.201202176.
- Steingrimsdottir, E., Copeland, N.G., and Jenkins, N.A. (2004). Melanocytes and the microphthalmia transcription factor network. *Annu Rev Genet* 38, 365-411. doi: 10.1146/annurev.genet.38.072902.092717.
- Stracka, D., Jozefczuk, S., Rudroff, F., Sauer, U., and Hall, M.N. (2014). Nitrogen source activates TOR (target of rapamycin) complex 1 via glutamine and independently of Gtr/Rag proteins. *J Biol Chem* 289(36), 25010-25020. doi: 10.1074/jbc.M114.574335.
- Stuttfield, E., Aylett, C.H., Imseng, S., Boehringer, D., Scaiola, A., Sauer, E., et al. (2018). Architecture of the human mTORC2 core complex. *Elife* 7. doi: 10.7554/eLife.33101.
- Su, C.H., Wang, C.Y., Lan, K.H., Li, C.P., Chao, Y., Lin, H.C., et al. (2011). Akt phosphorylation at Thr308 and Ser473 is required for CHIP-mediated ubiquitination of the kinase. *Cell Signal* 23(11), 1824-1830. doi: 10.1016/j.cellsig.2011.06.018.
- Suizu, F., Hiramaki, Y., Okumura, F., Matsuda, M., Okumura, A.J., Hirata, N., et al. (2009). The E3 ligase TTC3 facilitates ubiquitination and degradation of phosphorylated Akt. *Dev Cell* 17(6), 800-810. doi: 10.1016/j.devcel.2009.09.007.
- Sun, J., Liu, Y., Jia, Y., Hao, X., Lin, W.J., Tran, J., et al. (2018). UBE3A-mediated p18/LAMTOR1 ubiquitination and degradation regulate mTORC1 activity and synaptic plasticity. *Elife* 7. doi: 10.7554/eLife.37993.
- Sun, S.C. (2010). CYLD: a tumor suppressor deubiquitinase regulating NF-kappaB activation and diverse biological processes. *Cell Death Differ* 17(1), 25-34. doi: 10.1038/cdd.2009.43.
- Sun, T., Liu, Z., and Yang, Q. (2020). The role of ubiquitination and deubiquitination in cancer metabolism. *Mol Cancer* 19(1), 146. doi: 10.1186/s12943-020-01262-x.
- Sutherland, R.M. (1988). Cell and environment interactions in tumor microregions: the multicell spheroid model. *Science* 240(4849), 177-184. doi: 10.1126/science.2451290.
- Swatek, K.N., and Komander, D. (2016). Ubiquitin modifications. *Cell Res* 26(4), 399-422. doi: 10.1038/cr.2016.39.
- Takahara, T., Hara, K., Yonezawa, K., Sorimachi, H., and Maeda, T. (2006). Nutrient-dependent multimerization of the mammalian target of rapamycin through the N-terminal HEAT repeat region. *J Biol Chem* 281(39), 28605-28614. doi: 10.1074/jbc.M606087200.

- Tan, M., Xu, J., Siddiqui, J., Feng, F., and Sun, Y. (2016). Depletion of SAG/RBX2 E3 ubiquitin ligase suppresses prostate tumorigenesis via inactivation of the PI3K/AKT/mTOR axis. *Mol Cancer* 15(1), 81. doi: 10.1186/s12943-016-0567-6.
- Tauriello, D.V., Haegebarth, A., Kuper, I., Edelmann, M.J., Henraat, M., Canninga-van Dijk, M.R., et al. (2010). Loss of the tumor suppressor CYLD enhances Wnt/beta-catenin signaling through K63-linked ubiquitination of Dvl. *Mol Cell* 37(5), 607-619. doi: 10.1016/j.molcel.2010.01.035.
- Tee, A.R., Anjum, R., and Blenis, J. (2003a). Inactivation of the tuberous sclerosis complex-1 and -2 gene products occurs by phosphoinositide 3-kinase/Akt-dependent and -independent phosphorylation of tuberin. *J Biol Chem* 278(39), 37288-37296. doi: 10.1074/jbc.M303257200.
- Tee, A.R., Fingar, D.C., Manning, B.D., Kwiatkowski, D.J., Cantley, L.C., and Blenis, J. (2002). Tuberous sclerosis complex-1 and -2 gene products function together to inhibit mammalian target of rapamycin (mTOR)-mediated downstream signaling. *Proc Natl Acad Sci U S A* 99(21), 13571-13576. doi: 10.1073/pnas.202476899.
- Tee, A.R., Manning, B.D., Roux, P.P., Cantley, L.C., and Blenis, J. (2003b). Tuberous sclerosis complex gene products, Tuberin and Hamartin, control mTOR signaling by acting as a GTPase-activating protein complex toward Rheb. *Curr Biol* 13(15), 1259-1268. doi: 10.1016/s0960-9822(03)00506-2.
- Teis, D., Taub, N., Kurzbaue, R., Hilber, D., de Araujo, M.E., Erlacher, M., et al. (2006). p14-MP1-MEK1 signaling regulates endosomal traffic and cellular proliferation during tissue homeostasis. *J Cell Biol* 175(6), 861-868. doi: 10.1083/jcb.200607025.
- Thomas, J.D., Zhang, Y.J., Wei, Y.H., Cho, J.H., Morris, L.E., Wang, H.Y., et al. (2014). Rab1A Is an mTORC1 Activator and a Colorectal Oncogene. *Cancer Cell* 26(5), 754-769. doi: 10.1016/j.ccell.2014.09.008.
- Thoreen, C.C., Chantranupong, L., Keys, H.R., Wang, T., Gray, N.S., and Sabatini, D.M. (2012). A unifying model for mTORC1-mediated regulation of mRNA translation. *Nature* 485(7396), 109-U142. doi: 10.1038/nature11083.
- Tiede, S., Storch, S., Lubke, T., Henrissat, B., Bargal, R., Raas-Rothschild, A., et al. (2005). Mucopolidiosis II is caused by mutations in GNPTA encoding the alpha/beta GlcNAc-1-phosphotransferase. *Nat Med* 11(10), 1109-1112. doi: 10.1038/nm1305.
- Toschi, A., Lee, E., Xu, L.M., Garcia, A., Gadir, N., and Foster, D.A. (2009). Regulation of mTORC1 and mTORC2 Complex Assembly by Phosphatidic Acid: Competition with Rapamycin. *Molecular and Cellular Biology* 29(6), 1411-1420. doi: 10.1128/Mcb.00782-08.
- Trompouki, E., Hatzivassiliou, E., Tschritzis, T., Farmer, H., Ashworth, A., and Mosialos, G. (2003). CYLD is a deubiquitinating enzyme that negatively regulates NF-kappaB activation by TNFR family members. *Nature* 424(6950), 793-796. doi: 10.1038/nature01803.
- Tsun, Z.Y., Bar-Peled, L., Chantranupong, L., Zoncu, R., Wang, T., Kim, C., et al. (2013). The Folliculin Tumor Suppressor Is a GAP for the RagC/D GTPases That Signal Amino Acid Levels to mTORC1. *Molecular Cell* 52(4), 495-505. doi: 10.1016/j.molcel.2013.09.016.
- Ukai, H., Araki, Y., Kira, S., Oikawa, Y., May, A.I., and Noda, T. (2018). Gtr/Ego-independent TORC1 activation is achieved through a glutamine-sensitive interaction with Pib2 on the vacuolar membrane. *Plos Genetics* 14(4). doi: ARTN e1007334 10.1371/journal.pgen.1007334.

- van der Welle, R.E.N., Jobling, R., Burns, C., Sanza, P., van der Beek, J.A., Fasano, A., et al. (2021). Neurodegenerative VPS41 variants inhibit HOPS function and mTORC1-dependent TFEB/TFE3 regulation. *EMBO Mol Med* 13(5), e13258. doi: 10.15252/emmm.202013258.
- van Slegtenhorst, M., Nellist, M., Nagelkerken, B., Cheadle, J., Snell, R., van den Ouweland, A., et al. (1998). Interaction between hamartin and tuberlin, the TSC1 and TSC2 gene products. *Hum Mol Genet* 7(6), 1053-1057. doi: 10.1093/hmg/7.6.1053.
- Vander Haar, E., Lee, S., Bandhakavi, S., Griffin, T.J., and Kim, D.H. (2007). Insulin signalling to mTOR mediated by the Akt/PKB substrate PRAS40. *Nature Cell Biology* 9(3), 316-U126. doi: 10.1038/ncb1547.
- Vargas, J.N.S., Hamasaki, M., Kawabata, T., Youle, R.J., and Yoshimori, T. (2023). The mechanisms and roles of selective autophagy in mammals. *Nat Rev Mol Cell Biol* 24(3), 167-185. doi: 10.1038/s41580-022-00542-2.
- Vilella-Bach, M., Nuzzi, P., Fang, Y., and Chen, J. (1999). The FKBP12-rapamycin-binding domain is required for FKBP12-rapamycin-associated protein kinase activity and G1 progression. *J Biol Chem* 274(7), 4266-4272. doi: 10.1074/jbc.274.7.4266.
- Villa, E., Sahu, U., O'Hara, B.P., Ali, E.S., Helmin, K.A., Asara, J.M., et al. (2021). mTORC1 stimulates cell growth through SAM synthesis and m(6)A mRNA-dependent control of protein synthesis. *Mol Cell*. doi: 10.1016/j.molcel.2021.03.009.
- Wakatsuki, S., Saitoh, F., and Araki, T. (2011). ZNRF1 promotes Wallerian degeneration by degrading AKT to induce GSK3B-dependent CRMP2 phosphorylation. *Nat Cell Biol* 13(12), 1415-1423. doi: 10.1038/ncb2373.
- Wan, W., You, Z., Zhou, L., Xu, Y., Peng, C., Zhou, T., et al. (2018). mTORC1-Regulated and HUWE1-Mediated WIPI2 Degradation Controls Autophagy Flux. *Mol Cell* 72(2), 303-315 e306. doi: 10.1016/j.molcel.2018.09.017.
- Wang, B., Jie, Z., Joo, D., Ordureau, A., Liu, P., Gan, W., et al. (2017a). TRAF2 and OTUD7B govern a ubiquitin-dependent switch that regulates mTORC2 signalling. *Nature* 545(7654), 365-369. doi: 10.1038/nature22344.
- Wang, C., Deng, L., Hong, M., Akkaraju, G.R., Inoue, J., and Chen, Z.J. (2001). TAK1 is a ubiquitin-dependent kinase of MKK and IKK. *Nature* 412(6844), 346-351. doi: 10.1038/35085597.
- Wang, D., Xu, C., Yang, W., Chen, J., Ou, Y., Guan, Y., et al. (2022). E3 ligase RNF167 and deubiquitinase STAMBPL1 modulate mTOR and cancer progression. *Mol Cell* 82(4), 770-784 e779. doi: 10.1016/j.molcel.2022.01.002.
- Wang, F.F., Zhang, X.J., Yan, Y.R., Zhu, X.H., Yu, J., Ding, Y., et al. (2017b). FBX8 is a metastasis suppressor downstream of miR-223 and targeting mTOR for degradation in colorectal carcinoma. *Cancer Lett* 388, 85-95. doi: 10.1016/j.canlet.2016.11.031.
- Wang, G., Gao, Y., Li, L., Jin, G., Cai, Z., Chao, J.I., et al. (2012). K63-linked ubiquitination in kinase activation and cancer. *Front Oncol* 2, 5. doi: 10.3389/fonc.2012.00005.
- Wang, S.Y., Tsun, Z.Y., Wolfson, R.L., Shen, K., Wyant, G.A., Plovianich, M.E., et al. (2015). Lysosomal amino acid transporter SLC38A9 signals arginine sufficiency to mTORC1. *Science* 347(6218), 188-194. doi: 10.1126/science.1257132.

- Wang, Z., Dang, T., Liu, T., Chen, S., Li, L., Huang, S., et al. (2016). NEDD4L Protein Catalyzes Ubiquitination of PIK3CA Protein and Regulates PI3K-AKT Signaling. *J Biol Chem* 291(33), 17467-17477. doi: 10.1074/jbc.M116.726083.
- Welz, P.S., Wullaert, A., Vlantis, K., Kondylis, V., Fernandez-Majada, V., Ermolaeva, M., et al. (2011). FADD prevents RIP3-mediated epithelial cell necrosis and chronic intestinal inflammation. *Nature* 477(7364), 330-334. doi: 10.1038/nature10273.
- Wolfson, R.L., Chantranupong, L., Saxton, R.A., Shen, K., Scaria, S.M., Cantor, J.R., et al. (2016). METABOLISM Sestrin2 is a leucine sensor for the mTORC1 pathway. *Science* 351(6268), 43-48. doi: 10.1126/science.aab2674.
- Wolfson, R.L., Chantranupong, L., Wyant, G.A., Gu, X., Orozco, J.M., Shen, K., et al. (2017). KICSTOR recruits GATOR1 to the lysosome and is necessary for nutrients to regulate mTORC1. *Nature* 543(7645), 438-+. doi: 10.1038/nature21423.
- Woo, S.Y., Kim, D.H., Jun, C.B., Kim, Y.M., Haar, E.V., Lee, S.I., et al. (2007). PRR5, a novel component of mTOR complex 2, regulates platelet-derived growth factor receptor beta expression and signaling. *J Biol Chem* 282(35), 25604-25612. doi: 10.1074/jbc.M704343200.
- Wrobel, L., Siddiqi, F.H., Hill, S.M., Son, S.M., Karabiyik, C., Kim, H., et al. (2020). mTORC2 Assembly Is Regulated by USP9X-Mediated Deubiquitination of RICTOR. *Cell Rep* 33(13), 108564. doi: 10.1016/j.celrep.2020.108564.
- Wrobel, M., Cendrowski, J., Szymanska, E., Grebowicz-Maciukiewicz, M., Budick-Harmelin, N., Macias, M., et al. (2022). ESCRT-I fuels lysosomal degradation to restrict TFEB/TFE3 signaling via the Rag-mTORC1 pathway. *Life Sci Alliance* 5(7). doi: 10.26508/lsa.202101239.
- Wyant, G.A., Abu-Remaileh, M., Wolfson, R.L., Chen, W.W., Freinkman, E., Danai, L.V., et al. (2017a). mTORC1 Activator SLC38A9 Is Required to Efflux Essential Amino Acids from Lysosomes and Use Protein as a Nutrient. *Cell* 171(3), 642-+. doi: 10.1016/j.cell.2017.09.046.
- Wyant, G.A., Abu-Remaileh, M., Wolfson, R.L., Chen, W.W., Freinkman, E., Danai, L.V., et al. (2017b). mTORC1 Activator SLC38A9 Is Required to Efflux Essential Amino Acids from Lysosomes and Use Protein as a Nutrient. *Cell* 171(3), 642-654 e612. doi: 10.1016/j.cell.2017.09.046.
- Xiang, T., Ohashi, A., Huang, Y., Pandita, T.K., Ludwig, T., Powell, S.N., et al. (2008). Negative Regulation of AKT Activation by BRCA1. *Cancer Res* 68(24), 10040-10044. doi: 10.1158/0008-5472.CAN-08-3009.
- Xu, H., and Ren, D. (2015). Lysosomal physiology. *Annu Rev Physiol* 77, 57-80. doi: 10.1146/annurev-physiol-021014-071649.
- Xu, Y., Lai, E., Liu, J., Lin, J., Yang, C., Jia, C., et al. (2013). IKK interacts with rictor and regulates mTORC2. *Cell Signal* 25(11), 2239-2245. doi: 10.1016/j.cellsig.2013.07.008.
- Yadav, R.B., Burgos, P., Parker, A.W., Iadevaia, V., Proud, C.G., Allen, R.A., et al. (2013). mTOR direct interactions with Rheb-GTPase and raptor: sub-cellular localization using fluorescence lifetime imaging. *BMC Cell Biol* 14, 3. doi: 10.1186/1471-2121-14-3.
- Yang, G., Humphrey, S.J., Murashige, D.S., Francis, D., Wang, Q.P., Cooke, K.C., et al. (2019). RagC phosphorylation autoregulates mTOR complex 1. *EMBO J* 38(3). doi: 10.15252/embj.201899548.

- Yang, G., Murashige, D.S., Humphrey, S.J., and James, D.E. (2015). A Positive Feedback Loop between Akt and mTORC2 via SIN1 Phosphorylation. *Cell Rep* 12(6), 937-943. doi: 10.1016/j.celrep.2015.07.016.
- Yang, H., Jiang, X., Li, B., Yang, H.J., Miller, M., Yang, A., et al. (2017). Mechanisms of mTORC1 activation by RHEB and inhibition by PRAS40. *Nature* 552(7685), 368-373. doi: 10.1038/nature25023.
- Yang, H., Yu, Z., Chen, X., Li, J., Li, N., Cheng, J., et al. (2021). Structural insights into TSC complex assembly and GAP activity on Rheb. *Nat Commun* 12(1), 339. doi: 10.1038/s41467-020-20522-4.
- Yang, H.J., Rudge, D.G., Koos, J.D., Vaidialingam, B., Yang, H.J., and Pavletich, N.P. (2013a). mTOR kinase structure, mechanism and regulation. *Nature* 497(7448), 217-+. doi: 10.1038/nature12122.
- Yang, Q., Inoki, K., Ikenoue, T., and Guan, K.L. (2006). Identification of Sin1 as an essential TORC2 component required for complex formation and kinase activity. *Genes Dev* 20(20), 2820-2832. doi: 10.1101/gad.1461206.
- Yang, W.L., Jin, G., Li, C.F., Jeong, Y.S., Moten, A., Xu, D., et al. (2013b). Cycles of ubiquitination and deubiquitination critically regulate growth factor-mediated activation of Akt signaling. *Sci Signal* 6(257), ra3. doi: 10.1126/scisignal.2003197.
- Yang, W.L., Wang, J., Chan, C.H., Lee, S.W., Campos, A.D., Lamothe, B., et al. (2009). The E3 ligase TRAF6 regulates Akt ubiquitination and activation. *Science* 325(5944), 1134-1138. doi: 10.1126/science.1175065.
- Yang, Y., Sun, L., Tala, Gao, J., Li, D., Zhou, J., et al. (2013c). CYLD regulates RhoA activity by modulating LARG ubiquitination. *PLoS One* 8(2), e55833. doi: 10.1371/journal.pone.0055833.
- Yao, Y., Hong, S., Ikeda, T., Mori, H., MacDougald, O.A., Nada, S., et al. (2020). Amino Acids Enhance Polyubiquitination of Rheb and Its Binding to mTORC1 by Blocking Lysosomal ATXN3 Deubiquitinase Activity. *Mol Cell* 80(3), 437-451 e436. doi: 10.1016/j.molcel.2020.10.004.
- Ye, M., Huang, J., Mou, Q., Luo, J., Hu, Y., Lou, X., et al. (2021). CD82 protects against glaucomatous axonal transport deficits via mTORC1 activation in mice. *Cell Death Dis* 12(12), 1149. doi: 10.1038/s41419-021-04445-6.
- Yim, W.W., and Mizushima, N. (2020). Lysosome biology in autophagy. *Cell Discov* 6, 6. doi: 10.1038/s41421-020-0141-7.
- Yin, F., He, H., Zhang, B., Zheng, J., Wang, M., Zhang, M., et al. (2019). Effect of Deubiquitinase Ovarian Tumor Domain-Containing Protein 5 (OTUD5) on Radiosensitivity of Cervical Cancer by Regulating the Ubiquitination of Akt and its Mechanism. *Med Sci Monit* 25, 3469-3475. doi: 10.12659/MSM.912904.
- Yin, S., Liu, L., and Gan, W. (2021). The Roles of Post-Translational Modifications on mTOR Signaling. *Int J Mol Sci* 22(4). doi: 10.3390/ijms22041784.
- Yip, C.K., Murata, K., Walz, T., Sabatini, D.M., and Kang, S.A. (2010). Structure of the human mTOR complex I and its implications for rapamycin inhibition. *Mol Cell* 38(5), 768-774. doi: 10.1016/j.molcel.2010.05.017.

- Yoon, M.S., Du, G.W., Backer, J.M., Frohman, M.A., and Chen, J. (2011). Class III PI-3-kinase activates phospholipase D in an amino acid-sensing mTORC1 pathway. *Journal of Cell Biology* 195(3), 435-447. doi: 10.1083/jcb.201107033.
- Yu, L., McPhee, C.K., Zheng, L.X., Mardones, G.A., Rong, Y.G., Peng, J.Y., et al. (2010). Termination of autophagy and reformation of lysosomes regulated by mTOR. *Nature* 465(7300), 942-U911. doi: 10.1038/nature09076.
- Yu, Y., Yoon, S.O., Poulogiannis, G., Yang, Q., Ma, X.M., Villen, J., et al. (2011). Phosphoproteomic analysis identifies Grb10 as an mTORC1 substrate that negatively regulates insulin signaling. *Science* 332(6035), 1322-1326. doi: 10.1126/science.1199484.
- Yu, Z., Chen, J., Takagi, E., Wang, F., Saha, B., Liu, X., et al. (2022). Interactions between mTORC2 core subunits Rictor and mSin1 dictate selective and context-dependent phosphorylation of substrate kinases SGK1 and Akt. *J Biol Chem* 298(9), 102288. doi: 10.1016/j.jbc.2022.102288.
- Yuan, H.X., Russell, R.C., and Guan, K.L. (2013). Regulation of PIK3C3/VPS34 complexes by MTOR in nutrient stress-induced autophagy. *Autophagy* 9(12), 1983-1995. doi: 10.4161/auto.26058.
- Zaidi, N., Maurer, A., Nieke, S., and Kalbacher, H. (2008). Cathepsin D: a cellular roadmap. *Biochem Biophys Res Commun* 376(1), 5-9. doi: 10.1016/j.bbrc.2008.08.099.
- Zhang, J., Yang, Z., Ou, J., Xia, X., Zhi, F., and Cui, J. (2017). The F-box protein FBXL18 promotes glioma progression by promoting K63-linked ubiquitination of Akt. *FEBS Lett* 591(1), 145-154. doi: 10.1002/1873-3468.12521.
- Zhang, J.W., Kim, J., Alexander, A., Cai, S.L., Tripathi, D.N., Dere, R., et al. (2013). A tuberous sclerosis complex signalling node at the peroxisome regulates mTORC1 and autophagy in response to ROS. *Nature Cell Biology* 15(10), 1186-U1145. doi: 10.1038/ncb2822.
- Zhao, L., Wang, X., Yu, Y., Deng, L., Chen, L., Peng, X., et al. (2018). OTUB1 protein suppresses mTOR complex 1 (mTORC1) activity by deubiquitinating the mTORC1 inhibitor DEPTOR. *J Biol Chem* 293(13), 4883-4892. doi: 10.1074/jbc.M117.809533.
- Zhao, Y., Xiong, X., and Sun, Y. (2011). DEPTOR, an mTOR inhibitor, is a physiological substrate of SCF(betaTrCP) E3 ubiquitin ligase and regulates survival and autophagy. *Mol Cell* 44(2), 304-316. doi: 10.1016/j.molcel.2011.08.029.
- Zheng, C., Kabaleeswaran, V., Wang, Y., Cheng, G., and Wu, H. (2010). Crystal structures of the TRAF2: cIAP2 and the TRAF1: TRAF2: cIAP2 complexes: affinity, specificity, and regulation. *Mol Cell* 38(1), 101-113. doi: 10.1016/j.molcel.2010.03.009.
- Zheng, L., Ding, H., Lu, Z., Li, Y., Pan, Y., Ning, T., et al. (2008). E3 ubiquitin ligase E6AP-mediated TSC2 turnover in the presence and absence of HPV16 E6. *Genes Cells* 13(3), 285-294. doi: 10.1111/j.1365-2443.2008.01162.x.
- Zhou, R., and Snyder, P.M. (2005). Nedd4-2 phosphorylation induces serum and glucocorticoid-regulated kinase (SGK) ubiquitination and degradation. *J Biol Chem* 280(6), 4518-4523. doi: 10.1074/jbc.M411053200.
- Zhou, X., Clister, T.L., Lowry, P.R., Seldin, M.M., Wong, G.W., and Zhang, J. (2015). Dynamic Visualization of mTORC1 Activity in Living Cells. *Cell Reports* 10(10), 1767-1777. doi: 10.1016/j.celrep.2015.02.031.

- Zhu, G., Herlyn, M., and Yang, X. (2021). TRIM15 and CYLD regulate ERK activation via lysine-63-linked polyubiquitination. *Nat Cell Biol* 23(9), 978-991. doi: 10.1038/s41556-021-00732-8.
- Zoncu, R., Bar-Peled, L., Efeyan, A., Wang, S.Y., Sancak, Y., and Sabatini, D.M. (2011). mTORC1 Senses Lysosomal Amino Acids Through an Inside-Out Mechanism That Requires the Vacuolar H⁺-ATPase. *Science* 334(6056), 678-683. doi: 10.1126/science.1207056.

Appendix

Contributions

Table 8 Experimental work contributions.

Table of contributions			
Figure 2.1	SAF	Figure 2.19	SAF
Figure 2.2	SAF	Figure 2.20	DDA
Figure 2.3	SAF	Figure 2.21	SAF
Figure 2.4	SAF	Figure 2.22	DDA; SAF
Figure 2.5	SAF	Figure 2.23	DDA; SW
Figure 2.6	SAF	Figure 2.24	DDA; SAF
Figure 2.7	SAF	Figure 2.25	SAF
Figure 2.8	SAF	Figure 2.26	SAF
Figure 2.9	DDA	Figure 2.27	SAF
Figure 2.10	SAF	Figure 2.28	SAF
Figure 2.11	DDA; SAF	Figure 2.29	SAF
Figure 2.12	SAF	Figure 2.30	SAF
Figure 2.13	DDA	Figure 2.31	SAF; JP
Figure 2.14	DDA	Figure 2.32	SAF; JP
Figure 2.15	SAF	Figure 2.33	SAF
Figure 2.16	DDA; SAF	Figure 2.34	SAF
Figure 2.17	DDA	Figure 2.35	SAF
Figure 2.18	SAF; DDA	Figure 2.36	SAF; JP

SAF: Stephanie de Alcantara Fernandes

DDA: Danai-Dimitra Angelidaki

SW: Sabine Wilhelm

JP: Jiyoung Pan

Erklärung

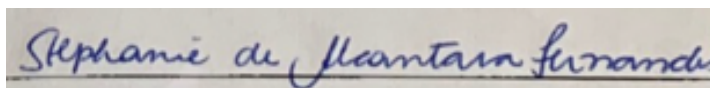
Erklärung zur Dissertation gemäß der Promotionsordnung vom 12. März 2020

Hiermit versichere ich an Eides statt, dass ich die vorliegende Dissertation selbstständig und ohne die Benutzung anderer als der angegebenen Hilfsmittel und Literatur angefertigt habe. Alle Stellen, die wörtlich oder sinngemäß aus veröffentlichten und nicht veröffentlichten Werken dem Wortlaut oder dem Sinn nach entnommen wurden, sind als solche kenntlich gemacht. Ich versichere an Eides statt, dass diese Dissertation noch keiner anderen Fakultät oder Universität zur Prüfung vorgelegen hat; dass sie - abgesehen von unten angegebenen Teilpublikationen und eingebundenen Artikeln und Manuskripten - noch nicht veröffentlicht worden ist sowie, dass ich eine Veröffentlichung der Dissertation vor Abschluss der Promotion nicht ohne Genehmigung des Promotionsausschusses vornehmen werde. Die Bestimmungen dieser Ordnung sind mir bekannt. Darüber hinaus erkläre ich hiermit, dass ich die Ordnung zur Sicherung guter wissenschaftlicher Praxis und zum Umgang mit wissenschaftlichem Fehlverhalten der Universität zu Köln gelesen und sie bei der Durchführung der Dissertation zugrundeliegenden Arbeiten und der schriftlich verfassten Dissertation beachtet habe und verpflichte mich hiermit, die dort genannten Vorgaben bei allen wissenschaftlichen Tätigkeiten zu beachten und umzusetzen. Ich versichere, dass die eingereichte elektronische Fassung der eingereichten Druckfassung vollständig entspricht.

Teilpublikationen:

Fernandes S.A. and Demetriades C. (2021) The Multifaceted Role of Nutrient Sensing and mTORC1 Signaling in Physiology and Aging. *Front. Aging* 2:707372. doi: 10.3389/fragi.2021.707372

Köln, den 20. März 2023



Stephanie de Alcantara Fernandes